Université de Montréal

MÉCANISMES D'ACTION DES ANTIOESTROGÈNES TOTAUX

par

Khalid Hilmi

Département de biochimie

Faculté de Médecine

Thèse présentée à la Faculté des études supérieures
en vue de l'obtention du grade de Philosophiae Doctor (Ph .D)
en biochimie

Avril 2012

Université de Montréal
Faculté des études supérieures et postdoctorales

Cette thèse intitulée :

MÉCANISMES D'ACTION DES ANTIOESTROGÈNES TOTAUX

Présentée par :
Khalid Hilmi

a été évaluée par un jury composé des personnes suivantes :

Muriel Aubry, Ph.D., président-rapporteur
Sylvie Mader, Ph.D., directeur de recherche
Alain Verreault, Ph.D., membre du jury
Nicolas Gérvy, Ph.D., examinateur externe
Mohamed Benderdour, Ph.D., représentant du doyen de la FES

Résumé

Le cancer du sein est le cancer qui a la plus forte fréquence au Canada. En 2012, on estime que 23 200 nouveaux cas de cancer du sein seront diagnostiqués. Deux tiers des tumeurs mammaires expriment ou surexpriment le récepteur des oestrogènes α (ERα). De même, les oestrogènes sont importants pour la croissance de ces tumeurs.

La présence des récepteurs hormonaux est un critère qui détermine le choix de la thérapie; à cet égard, le ciblage des récepteurs des oestrogènes par les antioestrogènes a pour but d'inactiver ces récepteurs et diminuer leur contribution à la croissance tumorale.

Les antioestrogènes sont des inhibiteurs compétitifs de ERα. Tamoxifene est le médicament le plus utilisé pour traiter les tumeurs mammaires ER+ de tous les stades, avant ou après la ménopause. Tamoxifene est antioestrogène partiel ou SERM qui a un profile mixte d'activités agonistes et antagonistes. Fulvestrant ou ICI 182, 780 est un antioestrogène de type total ou SERD dépourvu de toute activité agoniste. Ce composé est utilisé en clinique chez les femmes après la ménopause ayant des tumeurs mammaires avancées. Fulvestrant constitue, donc, une deuxième ligne thérapeutique en cas de rechute après à un traitement par Tamoxifene.

Afin de comprendre le potentiel thérapeutique de Fulvestrant, il est primordial d'étudier son impact sur ERα. Actuellement, la polyubiquitination et la dégradation de ERα sont les mécanismes les plus connus pour expliquer l'inactivation de ERα par Fulvestrant. Par ailleurs, en utilisant des modèles cellulaires ER+ et ER-; nous avons montré que les antioestrogènes totaux induisent une insolubilité de ERα indépendamment de leur capacité à induire sa dégradation. L'insolubilité corrèle avec l'association de ERα avec la matrice nucléaire et avec l'inhibition de sa transactivation. L'hélice H12 du domaine de liaison du ligand joue un rôle important dans l'insolubilité et l'inactivation de ERα par les antioestrogènes totaux.

Par ailleurs, les antioestrogènes totaux se distinguent par leur capacité à induire la SUMOylation de ERα par SUMO1 et SUMO2/3. La SUMOylation est rapide et précède la dégradation de ERα dans cellules ER+.

À l'aide de dérivés de l'antioestrogène total ICI 164, 384, nous avons montré que la chaine latérale des antioestrogènes totaux est à la base de l'induction de la SUMOylation et de l'inactivation de ERα. De plus, la SUMOylation semble être une marque d'inhibition, car la déSUMOylation restaure une activité de ERα en présence des antioestrogènes totaux. L'hélice H12 du LBD et le domaine de liaison à l'ADN sont requis pour l'induction de la SUMOylation.

La recherche de protéines impliquées dans l'inactivation et dans la SUMOylation a permis d'identifier le facteur de remodelage de la chromatine ACF dans le même complexe que ERα. De manière similaire à la SUMOylation, le recrutement de ACF est précoce et constitue une propriété spécifique des antioestrogènes totaux. D'autre part, Fulvestrant induit le recrutement de ACF au niveau du promoteur du gène cible des oestrogènes pS2, ce qui suggère une contribution du remodelage de la chromatine dans les mécanismes d'action des antioestrogènes totaux. La surexpression de la DéSUMOylase SENP1 abolit le recrutement de ACF ce qui indique un rôle de la SUMOylation dans le recrutement de ACF. De même, l'hélice H12 du LBD de ERα constitue un lien entre l'inactivation de ERα et le recrutement de ACF.

L'insolubilité, la SUMOylation et l'interaction du complexe ACF sont le reflet des mécanismes d'action des antioestrogènes totaux. Ces observations peuvent être utilisées comme des critères fonctionnels pour identifier d'autres composés avec de meilleures propriétés pharmacologiques que Fulvestrant.

Mots-clés : cancer du sein; récepteur des oestrogènes α; antioestrogènes; fulvestrant; SUMOylation; remodelage de la chromatine, complexe ACF.

Abstract

Approximately 70% of breast tumors express or overexpress estrogen receptor alpha (ERα) and are treated with antiestrogens (AEs), which act as competitive inhibitors of this receptor. Tamoxifen has been widely used for the treatment of ERα-positive tumors, but intrinsic or acquired resistance can lead to tumor recurrence. Full AEs such as Fulvestrant (ICI182, 780) are currently used to treat postmenopausal women with ERα-positive breast cancers with disease progression following Tamoxifen therapy. Unlike Tamoxifen and other Selective estrogen receptor modulators (SERMs), full AEs (SERDs) are devoid of any agonistic activity. It is currently thought that the capacity of full AEs to induce rapid polyubiquitination and degradation of ERα underlies their complete suppression of ERα signalling.

On the one hand, we show a correlation between ICI 182, 780 induced ERα inhibition and its association with the insoluble fraction. This insolubility corresponds to an immobilization within the nuclear matrix and takes place in the absence of an accelerated turn over. The helix 12 in the ligand binding domain is important in the induction of insolubility and inactivation.

On the other hand, we identify ERα as a target for Small Ubiquitin-like Modifier (SUMO) posttranslational modification by SUMO1 and SUMO2/3 specifically when liganded with full AEs. Induction of SUMOylation is rapid and precedes receptor degradation in ERα-positive breast cancer cells. On the other hand, the SERMs do not induce SUMOylation. The helix 12 in the ligand binding domain and the DNA binding domain play a role in the induction of SUMOylation in the presence of full AEs. Structure activity relationship experiments with full AE derivatives showed that the induction of SUMOylation is correlated with the degree of inhibition of ERα-mediated transcription. In addition, preventing SUMOylation by overexpression of a SENP1 deSUMOylase abolished the inverse agonist properties of full AEs without increasing activity in the presence of agonists or of Tamoxifen.

In our attempt to screen for factors with a possible role in SUMOylation and inactivation, we show that the treatment with SERDs but not SERMs, induces a rapid interaction between ERα and the human ATP-utilizing chromatin assembly and remodeling factor (ACF) in ERα-negative and ERα-positive cell lines. The helix 12 is important since introducing single point mutations in this helix lead to an increased solubility and abrogate ACF recruitment. Using ChIP, we find an increase of ACF1 subunit association with proximal promoter of estrogen target gene pS2 suggesting a possible role of ACF in remodeling in this promoter. ACF recruitment is SUMOylation dependant since the overexpression of DeSUMOylase SENP1 abolishes the interaction between ERα and ACF.

Together, induction of insolubility, SUMOylation and ACF recruitment are characteristic properties of full antiestrogens that contribute to their specific activity profile. They can be used to screen for new compounds with an improved therapeutic potential.

Keywords : breast cancer; estrogen receptor α; antiestrogens; Fulvestrant;SUMOylation; chromatin remodeling; ACF complex.

Table des matières

Liste des sigles et des abréviations

A	Alanine
ACF	ATP utilizing chromatin assembly and remodeling factor
ADNc	Acide désoxyrobonucléique complémentaire
AF-1	Activation function 1
AF-2	Activation function 2
AIB1	Amplified in breast cancer 1
AP-1	Acivator protein 1
AR	Androgenes receptor
ARNm	Acide ribonucléique messager
ATP	Adenosine triphosphate
BAF57	Brg-1 associated factor 57
BAZ1A	bromodomain adjacent to zinc finger domain 1A
bHLH	Basic Helix-loop-Hélix
BPTF	Bromodomain PHD finger Transcription Factor
BRG1	Brahma related gene 1
BSA	Bovin Serum Albumin
CARM1	coactivator-associated arginine methyltransferase 1
CBP	coactivator binding protein
Cdk	Cyclin dependent kinase
CHD1	chromatin-helicase-DNA binding protein 1
CHRAC	chromatin accessibility complexe
CYP19	Cytochrome P450 aromatase 19
DAXX	death-domain associated protein
DBD	DNA binding domain
DDM1	Decreased DNA methylation 1
DMEM	Dulbecco's Modified Eagle Medium

E2	17β-estradiol
EDTA	Ethylene diamine tetra acetic acid
EGF	Epithelial growth factor
EGFP	Enhanced green fluoresecent protein
eNOS	Nitric oxyde synthase
ErbB2	epithelial growth factor 2 (HER-2)
ERE	Estrogen response element
ERR	Estrogen related receptor
FSH	Follicle stimulating hormone
GRIP-1	Clucocorticoid receptor interacting protein 1
HAT	Histone acétyl-transférase
HDAC	Histone déacétylase
HEG0	Récepteur des oestrogènes alpha
HP	Heterochromatin protein
HRE	hormone response element
HRP	horseradish peroxidase
HSB	high salt buffer
HSP70	Heat shok protein 70
IB	immunobuvardage
ICI	ICI 182,780
IGF	Insuline like growth factor
IL2	interleukine 2
INO80	inositol80
ISWI	imitation switch
LBD	ligand binding domain
LH	luteinizing hormone
MAPK	Mitogen activated protein kinase
MCF7	Michigan Cancer Foundation 7
MNAR	modulator of non-genomic action of estrogen receptor

MR	Mineralocorticoid receptor
NCoA	Nuclear receptor coactivator
NcoR	Nuclear receptor corepressor
NFKB	Nuclear Factor kappa bêta
NEM	N-ethylmalemeid
NO	Nitric oxyde
NoRc	Nucleolar remodeling complex
NP40	Nonidet P 40
NuRD	nucleosome remodeling and deacetylase
NURF	Nucleosome remodeling factor
OHT	4-hydroxytamoxifen
P/CAF	p300/CBP associated factor
PAS	Per/ARNT/Sim
PBS	Phosphate buffer salin
PHD	Plant homeodomain
PIAS	Protein inhibitor of activated STAT
PI3-kinase	Phosphatidyl-Inositol-3 Kinase
PML	Promyelocytic leukemia protein
PPAR	peroxisomal proliferator-activated receptor
PR	progesterone receptor
PRE	Polycomb response element
PRMT1	protein arginine methyltransferase1
Pu	Purine
Py	Pyrimidine
Q	Glutamine
R	Arginine
Ral	Raloxifen
RAR	Retinoid acid receptor
RNF4	Ring finger protein 4

RSF	remodeling and spacing factor
RXR	Retinoid X receptor
S	Serine
SATB1	Special AT rich binding protein1
SAE	SUMO activating enzyme
SDS	sodium dodecyl sulfate
SDS PAGE	SDS-polyacrylamide gel electrophoresis
SENP	SUMO/sentin specific peptidase
SERM	Selective estrogen receptor modulator
SERD	Selective estrogen receptor downregulator
SIM	SUMO interacting motif
SLIDE	SANT like domaine
SMARCA1	SWI/SNF related, matrix associated, actin dependent regulator of chromatin, subfamily a, member 1
SMARCA5	SWI/SNF related, matrix associated, actin dependent regulator of chromatin, subfamily a, member 5
SRC-2	Steroid receptor coactivator 2
SRC-3	Steroid receptor coactivator 3
SUMO	Small ubiquitin like modifier
STAT5	Signal transducers and activator of transcriptions 5
SWI/SNF	switch/sucrose non fermenting
TFIIA	Transcription factor IIA
TFIIB	Transcription factor IIB
TFIID	Transcription factor IID
TFIIE	Transcription factor IIE
TFIIH	Transcription factor IIH
TIF-2	Transciption intermediary factor 2
TR	Thyroid hormone receptor
TRAP220	Thyroid hormone receptor-associated protein complex

	component
TRIP1	thyroid receptor interacting protein 1
Ubc9	Ubiquitine conjugating enzyme 9
UFD	Ubiquitine fold domain
UIM	Ubiquitin interacting motif
V	Valine
VDR	Vitamin D3 Receptor
WSTF	Willams syndrome transcription factor
WT	wild-type
X	Acide aminé quelconque
Y	Tyrosine

Liste des figures

Introduction

Article 1

Article 2

Remerciements

J’aimerais tout d’abord remercier mon directeur de recherche le Dr Sylvie Mader. Sylvie est un exemple de motivation et de rigueur, elle a su me transmettre sa passion pour la science. Tout au long de ces années, elle était toujours disponible pour m’apprendre le métier de chercheur et pour m’encourager. Merci Sylvie!

Je tiens à remercier le Dr Nader Hussein, mon principal collaborateur avec qui j’ai partagé les succès et les revers. Merci à : Martine Bail, Slim Fourati, Mohamed El Ezzy, Houssam Ismail, David Cotnoir-White. Également, Tous mes collègues de laboratoire sans exception pour leur aide inestimable et pour l’ambiance amicale qui règne au laboratoire.

Bien entendu, je ne saurais exprimer ma gratitude envers mes parents, mes sœurs et Christine pour le support inconditionnel pendant toutes ces années.

Finalement, je voudrais remercier l’université de Montréal et plus particulièrement la FES, le GRUM et les IRSC pour le financement.

Introduction

1-Physiologie des oestrogènes

1-1-Synthèse des oestrogènes

Les oestrogènes, aussi connus comme étant les hormones sexuelles femelles, sont des hormones stéroïdiennes. Bien qu'ils soient présents dans les deux sexes, on en trouve une quantité significativement plus importante chez la femme que chez l'homme. On distingue trois formes d'oestrogènes : l'estrone (E1), l'oestriol (E3) et le 17β-estradiol (E2), ce dernier étant le principal oestrogène circulant avec la plus grande activité biologique.

Chez la femme avant la ménopause, la biosynthèse des oestrogènes s'effectue principalement dans les ovaires par les cellules de la granulosa. La production des oestrogènes est stimulée par les hormones de la glande pituitaire, la FSH et la LH. La voie de biosynthèse des oestrogènes est initiée à partir du cholestérol et passe par la formation de la progestérone puis d'androgènes. Le précurseur androgénique subit une aromatisation par l'enzyme CYP19 afin de produire les oestrogènes. Le 17β-estradiol est produit également à partir de l'estrone par l'enzyme hydroxystéroïde déshydrogénase [1-3]. Chez l'homme, la synthèse des oestrogènes s'effectue dans les testicules et dans les glandes corticosurrénales. Dans les testicules la synthèse des oestrogènes est amorcée dans les cellules de Leydig et les androgènes sont aromatisés en oestrogènes dans les cellules de Sertoli.

Après la ménopause la synthèse des oestrogènes s'effectue à l'extérieur des gonades, au niveau du tissu adipeux, des os, du cerveau, et dans les cellules du muscle squelettique [4].

Les niveaux des oestrogènes circulants chez la femme avant la ménopause se situent entre 40 et 400 pg/ml [5, 6]. Chez la femme après la ménopause, les concentrations plasmatiques de E2 sont inférieures à 37pg/ml et chez l'homme les concentrations plasmatiques sont d'environ 25-50 pg/ml. Les oestrogènes sont des molécules lipophiles

impliquées dans un large éventail de mécanismes physiologiques et agissent de façon paracrine, autocrine et intracrine [3].

1-2-Effets des oestrogènes sur le système reproducteur

Chez les mammifères, les oestrogènes ne sont pas nécessaires au développement prénatal [7]. Par contre, ils exercent un rôle important dans le développement postnatal. Les oestrogènes sont au cœur de toutes les fonctions du système reproducteur chez le sexe féminin. Ils permettent le développement et le maintien des caractères sexuels secondaires lors de la puberté en stimulant la maturation des ovaires [7]. Lors de chaque cycle menstruel, les oestrogènes participent à la maturation de la muqueuse utérine et à la mise en place de la nidation en cas de fécondation. Ils permettent également de maintenir la grossesse et activent la lactogénèse [8].

1-3-Effets des oestrogènes sur le système nerveux

Les oestrogènes exercent des effets rapides sur la connectivité des neurones et la transmission synaptique en modifiant la conductance des ions au sein des cellules neuronales [9].

Les oestrogènes circulants induisent des changements morphologiques et fonctionnels au niveau du néocortex et de l'hippocampe [10]. Une synthèse locale des oestrogènes par l'aromatase située au niveau de l'hippocampe permet de compenser pour la diminution des oestrogènes circulants chez la femme après la ménopause [11, 12].

Les oestrogènes exercent un rôle neuroprotecteur contre les accidents cérébraux et les processus dégénératifs ils améliorent les performances qui impliquent la mémoire verbale et les fonctions cognitives dans les maladies d'Alzheimer et de Parkinson [13-15].

1-4-Effets des oestrogènes sur le système cardiovasculaire

Les oestrogènes jouent un rôle antiathérosclerotique en réduisant la densité des lipoprotéines (LDL) et en favorisant la fibrinolyse. Ils ralentissent la progression des lésions et permettent la relaxation et la vasodilatation des petites et des grandes artères [16-

18]. L'effet protecteur des oestrogènes au niveau du système cardiovasculaire repose sur le fait que l'incidence des maladies cardiovasculaires est plus faible chez les femmes avant la ménopause comparativement aux hommes. Cependant, les études clinique de l'effet de la thérapie de substitution hormonale sur le système cardiovasculaire chez les femmes après la ménopause (HERS) ne montrent pas un effet concluant des oestrogènes sur la mortalité ou la morbidité cardiovasculaire [18].

1-5-Effets des oestrogènes sur le tissu osseux

Les oestrogènes jouent un rôle important dans la maturation du squelette. D'une part, la sécrétion des gonadotrophines à la puberté augmente la synthèse des oestrogènes qui induisent une croissance rapide des os pendant une période de 3 à 4 ans [19]. D'autre part, les oestrogènes participent à la préservation de la densité osseuse. Les oestrogènes contrôlent la formation et la résorption des os. Ils constituent un signal proapoptotique au niveau des ostéoclastes et stimulent la prolifération et la différenciation des ostéoblastes [3]. L'administration des oestrogènes atténue la résorption des os et améliore le bilan calcique [20]. La déficience en oestrogènes après la ménopause est bien reliée à l'ostéoporose. Ceci est en accord avec les phénotypes observés chez des souris ovarictomisées [21].

1-6- Les oestrogènes dans la tumorigénèse mammaire

En 1896, Beaston et Boyd établirent le lien entre les hormones ovariennes et le cancer du sein par le fait que l'ablation des ovaires permet la régression des tumeurs chez les femmes pré ménopausées. Plus tard, en 2002, les oestrogènes ont été classés comme carcinogènes par le US National Toxicology Programme and Cancer [22]. L'exposition aux oestrogènes est un facteur déterminant dans l'initiation, la promotion et la progression du cancer du sein. Une puberté précoce et une ménopause tardive augmentent la durée d'exposition aux oestrogènes. Les jeunes filles qui entreprennent la puberté une année plus tard par rapport à la moyenne ont jusqu'à 20 % de réduction du risque du cancer du sein.

D'autre part, une ménopause avant l'âge de 45 ans réduit de 50 % le risque de la maladie par rapport à une ménopause tardive après 55 ans [23, 24].

Il existe une corrélation positive entre l'augmentation des niveaux des oestrogènes circulants et le risque de développer le cancer du sein. Des études épidémiologiques prospectives ont permis de détecter des niveaux élevés d'oestrogènes au niveau du plasma des femmes qui ont pu développer des tumeurs mammaires 5 ans plus tard [25-27] alors que des niveaux faibles des oestrogènes plasmatiques sont habituellement détectés au niveau des populations à faible risque [28].

L'incidence du cancer du sein demeure élevée chez des femmes ménopausées après le déclin de la production des oestrogènes par les ovaires. L'incidence est d'autant plus forte quand il s'agit de groupe de femmes avec un excès de poids [27]. En fait, une synthèse locale des oestrogènes continue à s'effectuer au niveau de plusieurs autres tissus dont le tissu adipeux périphérique et au niveau de la glande mammaire par les cellules épithéliales. Cette production *in situ* est due à une forte expression de l'enzyme aromatase qui synthétise les oestrogènes à partir de leurs précurseurs androgéniques [29]. L'expression de cette enzyme au niveau des tumeurs mammaires est significativement plus grande que dans les lésions bénignes et permet d'atteindre des niveaux locaux très élevés en oestrogènes [30, 31]. Il a été suggéré que le microenvironnement formé par les tumeurs et leur stroma stimule l'expression de l'aromatase par les fibroblastes du stroma via la production de plusieurs facteurs comme la prostaglandine E2, TNFα, IL 6 et IL11 [32]. Ces facteurs activent également le recrutement des cellules du système immunitaire et influencent l'expansion et la progression des tumeurs mammaires [33].

Plusieurs mécanismes non exclusifs peuvent expliquer l'effet carcinogénique des oestrogènes. Ces molécules induisent la prolifération des cellules épithéliales mammaires à travers des récepteurs nucléaires appelés récepteurs aux oestrogènes. Ces récepteurs agissent comme des facteurs de transcription dépendants des hormones et régulent l'expression de gènes cibles jouant un rôle dans le contrôle du cycle cellulaire. D'autre part, une surexpression de ces récepteurs est caractéristique des deux tiers de tumeurs mammaires [34]. La prolifération rapide est en corrélation avec une accélération du cycle

cellulaire, elle réduit le temps nécessaire pour les mécanismes de réparation de l'ADN et augmente les niveaux de l'ADN endommagé et les risques de mutations [35].

Il existe d'autres mécanismes qui n'impliquent pas nécessairement les récepteurs des oestrogènes traditionnels. Les modèles animaux montrent que l'administration des oestrogènes à des souris qui n'expriment pas le récepteur des oestrogènes et qui expriment l'oncogène Wnt peut développer des tumeurs mammaires [36]. Ces observations ont été appuyées par le fait que 17β-estradiol ou son métabolite 4-hydroxycatechols induisent la formation des adénocarcinomes mammaires dans les modèles animaux et cellulaires [37, 38]. Le métabolisme des oestrogènes génère des 3,4 oestrogènes quinones. Ces métabolites électrophiles forment des adduits avec les adénines et guanines menant à une dépurination de l'ADN et peuvent également causer des dommages oxydatifs aux protéines [39, 40]. La réaction d'hydroxylation du 17β-estradiol est catalysée par les 4-hydoxylases P4501B1 et P4501A1 qui sont fortement exprimés dans les tumeurs mammaires. Des études épidémiologiques relient l'augmentation du risque du cancer du sein avec un polymorphisme des 4-hydroxylases [41].

2-Les récepteurs des oestrogènes

2-1-La superfamille des récepteurs nucléaires

En 1962, Jensen et Jacobsen ont observé la présence de sites de liaison du 17β - estradiol au niveau de l'utérus et ont conclu que l'action des oestrogènes passe par une protéine réceptrice. En 1986, deux groupes rapportent le clonage de l'ADN complémentaire du récepteur des oestrogènes α (ERα) à partir de cellules MCF7 [42, 43]. Ce récepteur est devenu, avec celui des glucocorticoïdes, un prototype de la superfamille des récepteurs nucléaires. Plus tard en, 1996, l'ADN du récepteur des oestrogènes bêta (ERβ) a été cloné à partir de la prostate du rat [44]. La super famille des récepteurs nucléaires compte 48 membres qui jouent de nombreux rôles dans le développement, le métabolisme, la différenciation et la reproduction. Les récepteurs nucléaires se caractérisent par la présence d'un domaine central appelé domaine de liaison à l'ADN (DBD), qui permet de lier des

séquences spécifiques au niveau de l'ADN appelées éléments de réponses aux hormones (HRE) et une région carboxy-terminale qui possède l'essentiel de la propriété de reconnaissance et de liaison des ligands [45].

La superfamille des récepteurs nucléaires peut être divisée en 4 familles selon les propriétés de dimérisation et de liaison à l'ADN [46]. La classe I inclut les récepteurs des hormones stéroïdiennes: les récepteurs des oestrogènes (ER), le récepteur des glucocorticoïdes (GR), le récepteur des androgènes (AR), le récepteur de la progestérone (PR) et le récepteur des minéralcorticoïdes (MR). Ces récepteurs une fois activés par les ligands, se dissocient des complexes formés de protéines chaperonnes et se lient à leur HRE respectif sous forme d'homodimères, Les HREs de cette classe sont sous forme de palindromes (→←) de manière à ce que chaque monomère de récepteur se fixe sur un demi-site.

La classe II des récepteurs nucléaires lie des éléments de réponse en répétition directe (→→) ou en palindromes inversés (←→) sous forme d'hétéro dimères obligatoires avec RXR et ce en absence du ligand. Cette classe inclut le récepteur de l'hormone thyroïdienne (TR), le récepteur de l'acide rétinoïque *tout-trans* (RAR), les récepteurs des eicosenoids (PPAR) et le récepteur de la vitamine D3 (VDR).

Les classes III et IV contiennent des récepteurs orphelins. Ils peuvent lier l'ADN sous forme de monomère tel que NGFI-B, sous forme d'homodimère ou d'hétérodimère avec RXR tel que HNF4 [45].

2-2-Les récepteurs des oestrogènes: structure et fonction

Les récepteurs des oestrogènes (ERs) sont codés par deux gènes différents, le gène ERα sur le locus chromosomique 6q25.1 chez l'homme, alors que celui de ERβ se trouve sur le locus 14q23.2 [47]. Les patrons d'expression des deux récepteurs varient dans le temps et selon les tissus ce qui suggère des fonctions biologiques différentes [44, 48]. Les deux récepteurs présentent six régions d'identité de séquence, caractérisées d'après leurs

degrés de conservation au sein de la superfamille des récepteurs nucléaires. Les six régions sont nommées de A à F à partir de l'extrémité aminoterminale (Fig 1**)**. La région A/B a une identité de séquence de 27 % dans les deux récepteurs. Elle contient une fonction d'activation indépendante de l'hormone (AF-1) dont l'activité est variable selon le contexte du promoteur et selon le type cellulaire [49, 50]. La région C présente 97 % d'identité dans ERα et ERβ. Elle constitue le domaine de la liaison à l'ADN (DBD). Le DBD contient deux doigts de zinc de type C4 et un signal de localisation nucléaire.

Le récepteur est capable de lier avec une forte affinité une séquence consensus de 15 pb appelée élément de réponse aux oestrogènes (ERE 5'-PuGGTCAnnnTGACCPy-3') [51]. D'autres séquences qui ressemblent au consensus peuvent être liées avec des affinités variables. Les EREs peuvent se situer à de longues distances du site d'initiation de la transcription [52]. La région D est une région charnière avec une portion qui interagit avec les HSP90. Cette région peu structurée possède aussi un signal de localisation nucléaire du récepteur. Finalement, les régions E et F sont identiques à 60 % à ceux du ERβ, elles constituent le domaine de la liaison du ligand (LBD) qui contient une fonction d'activation dépendante du ligand (AF-2), des interfaces de dimérisation et d'interaction avec les HSP90 [53, 54].

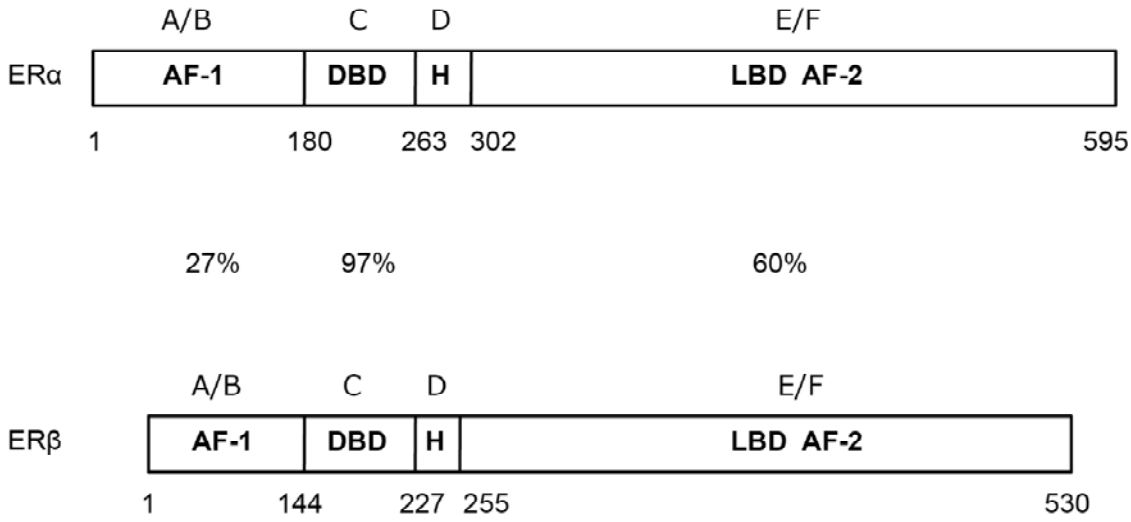

Figure 1.Représentation schématique des récepteurs des oestrogènes α et β. Adapté de [55].

2-3-Activation de la transcription par le récepteur des oestrogènes α

2-3-1-Voie génomique ERE dépendante.

Contrairement aux hormones et aux facteurs de croissance hydrophiles qui lient des récepteurs situés au niveau de la surface cellulaire, les oestrogènes, de par leur nature lipophile, diffusent passivement à travers la bicouche lipidique et se rendent au noyau par des mécanismes encore mal caractérisés. ERα est un facteur de transcription dépendant de l'hormone. En absence du ligand, ERα est majoritairement nucléaire, une petite fraction étant membranaire et cytoplasmique [56]. Il se trouve associé à l'état monomérique à un complexe inactivant formé des protéines chaperonnes HSP70 et HSP90, la cochaperonne p23 et des immunophilines mais peut se trouver aussi sous forme de dimère libre [57, 58]. Globalement, 17β-estradiol se lie à ERα avec une affinité de moyenne de 0,3 nM [59, 60] et entraîne un changement de conformation qui permet au récepteur de se dissocier de son complexe inactivant, de se dimériser ou hétérodimériser avec ERβ et de fixer les ERE situées dans les promoteurs des gènes cibles des oestrogènes [61].

Le dimère active la transcription via les fonctions de transactivation AF-1 et AF-2, qui interagissent avec des cofacteurs impliqués dans le remodelage de la chromatine et l'activation transcriptionnelle[62].

Le complexe SWI/SNF humain BRG1/BRM est le premier cofacteur recruté par le biais sous unité BAF57 [63]. Ensuite le complexe des coactivateurs de la famille p160/SRC-1 et des cointégrateurs CBP/P300 et p/CAFest recruté [64]. Ces complexes possèdent une activité histone acétyltransférase intrinsèque. Ensuite, CARM1 et PRMT sont aussi recrutés par les coactivateurs de la famille p160. Ces cofacteurs possèdent une activité de type histone méthyltransférase. Ensemble, ces complexes déstabilisent les nucléosomes par des mécanismes ATP-dépendant dans le cas de SWI/SNF ou par des modifications des queues des histones sur des résidus lysines ou arginines spécifiques. Le

résultat est l'affaiblissement des interactions entre l'ADN et les histones et l'ouverture des nucléosomes.

Par ailleurs, au niveau du site d'initiation de la transcription, il y a assemblage du complexe de pré initiation qui compte la polymérase II et les facteurs de transcription généraux (TFIIA, TFIIB, TFIID, TFIIE, TFIIF et TFIIH). Finalement, le complexe médiateur TRAP/DRIPα interagit avec ERα faisant le lien entre le complexe coactivateur et la machinerie basale de transcription [65].

Il existe des mécanismes d'activation du récepteur qui ne nécessitent pas la liaison du ligand. En effet ERα peut être activé par les voies de signalisation impliquant les facteurs de croissance. La voie des MAPK kinase est en grande partie responsable de la phosphorylation des sérines de la région A/B du récepteur. Il a été démontré que les sérines 118 et 167 sont des résidus cibles des MAPK suite à l'activation par EGF et IGF [66, 67]. La sérine 167 de ERα peut aussi être la cible de la kinase AKT, un effecteur de la voie des PI3 kinase jouant un rôle dans la survie cellulaire [66, 68]. De leur côté, les sérines 104 et 106 sont plutôt la cible du complexe cycline A/cdk2 en l'absence de l' hormone [69]. Les phosphorylations de la région A/B favorisent le recrutement de coactivateurs transcriptionnels capables de remodeler la chromatine et d'augmenter l'efficacité de l'initiation de la transcription des gènes ciblés [70].

2-3-2-Voie génomique ERE indépendante.

La présence des ERE dans un promoteur donné n'est pas une condition *sine qua non* de la régulation du gène par les oestrogènes puisque de nombreux gènes cibles des oestrogènes ne contiennent pas d'ERE de haute affinité. En fait, d'autres séquences d'ADN peuvent être impliquées dans les effets transcriptionnels des oestrogènes sans qu'elles soient liées directement par les récepteurs des oestrogènes. Au niveau de ces séquences les récepteurs sont recrutés par des facteurs de transcription déjà fixés sur leurs propres éléments de réponse et peuvent activer ou réprimer les gènes cibles des oestrogènes.

L'exemple le mieux connu est celui des sites AP-1 qui sont liés par le complexe Fos-Jun. Ce type de régulation est observé au niveau des promoteurs de l'ovalbumine, de la

collagénase et de la Cyclin D1 [71-73]. La fonction AF-2 et le DBD jouent un rôle dans l'interaction avec AP-1 [74, 75]. Au niveau des promoteurs riches en GC, le récepteur est recruté par le facteur SP-1 comme dans le cas de E2F1ou par un ½ ERE adjacent au site de SP-1, tel que le promoteur de la cathepsine D1 [76, 77].

Également, le récepteur est recruté par NFκB, GATA1, STAT5 et par Runx1 [78-82]. Ainsi Il peut exercer un rôle activateur ou inhibiteur dépendamment du contexte du promoteur et la nature des cofacteurs recrutés.

2-3-3-Voie non génomique de la signalisation par les oestrogènes

De nombreuses observations montrent que les oestrogènes exercent des effets très rapides ne pouvant être expliqués par l'activation de la transcription et la synthèse de protéines. Ces effets non transcriptionnels incluent: la mobilisation du calcium intracellulaire, la stimulation des adénylates cyclases et l'activation des voies de signalisation des MAPK kinases [83-85]. Les effets non transcriptionnels des oestrogènes ont été attribués à une fraction de récepteur des oestrogènes localisée au niveau de la membrane plasmique [86-88]. Cette localisation membranaire a été attribuée à une palmitolylation de la cystéine 447 [89, 90]. Le mécanisme des effets non transcriptionnels des oestrogènes est mis en évidence dans le système cardiovasculaire. Les oestrogènes permettent la vasodilatation en l'espace de quelques secondes [91] et ce, en induisant la synthèse de l'oxyde nitrique (NO) au niveau des cellules endothéliales par l'acide nitrique synthétase (eNOS) [16, 17].

Au niveau des cellules MCF7, des récepteurs des oestrogènes traditionnels ont été détectés au niveau de la membrane plasmique. Ils mettent en place des complexes de protéines d'échafaudage caveoline-1, MNAR, les sous unités activatrices de la protéine G et de la PI3kinase [85, 92-94]. Ces complexes activent les voies MAPK et AKT qui sont impliquées dans la prolifération et dans la survie cellulaire au niveau des cellules MCF7. Les récepteurs des oestrogènes membranaires interagissent directement avec ErbB2 et avec les récepteurs des facteurs de croissance IGF-1 et EGF et activent ces récepteurs

membranaires à activité tyrosine kinase. [95, 96]. Au niveau des cellules hépatiques HepG2 un mécanisme semblable qui implique l'induction de la cycline D1 a été observé [97].

2-4-Mécanismes moléculaires de l'activation du récepteur des oestrogènes α

2-4-1-Mode de liaison du ligand

La structure cristallographique du récepteur des oestrogènes alpha avec le 17 β-estradiol montre que le domaine de liaison du ligand (LBD) est formé de trois couches d'hélice alpha. Au centre se trouvent trois hélices, H5/H6, H9 et H10. Des deux côtés se trouvent les hélices H1 à H4 et les hélices H7, H8 et H11 (Fig 2**)**. Le restant du LBD est composé de deux feuillets antiparallèles S1 et S2 et finalement une hélice H12 essentielle pour l'activation du récepteur [98]. Cet arrangement aménage une cavité hydrophobe ellipsoïdale qui peut accueillir une variété de ligands hydrophobes ayant un anneau phénolique [59].

Le 17β-estradiol se lie en diagonale au niveau de la cavité du LBD et établit des liens par ponts hydrogènes avec le groupe carboxylé de la glutamine 353. Le guanidinium de l'arginine 394 et une molécule d'H_2O, le reste de la molécule participe à des interactions hydrophobes. L'hélice H12 est très mobile en absence du ligand et la présence de E2 stabilise sa conformation. Elle se replie sur le LBD et s'accote sur les hélices H3, H5/H6 et H11. Ce repliement lui permet de projeter son côté hydrophobe vers le ligand sans établir des contacts et d'exposer son côté chargé. Ce côté comprend les résidus aspartates 538 et 545 et le glutamate 542, vers le solvant. Cette conformation de l'hélice H12 est définie comme la conformation agoniste de la fonction d'activation AF-2. L'hélice H12 constitue, avec les hélices H3, H4 et H5, une surface en sillon nécessaire pour la reconnaissance et l'interaction avec les protéines corégulatrices [99, 100].

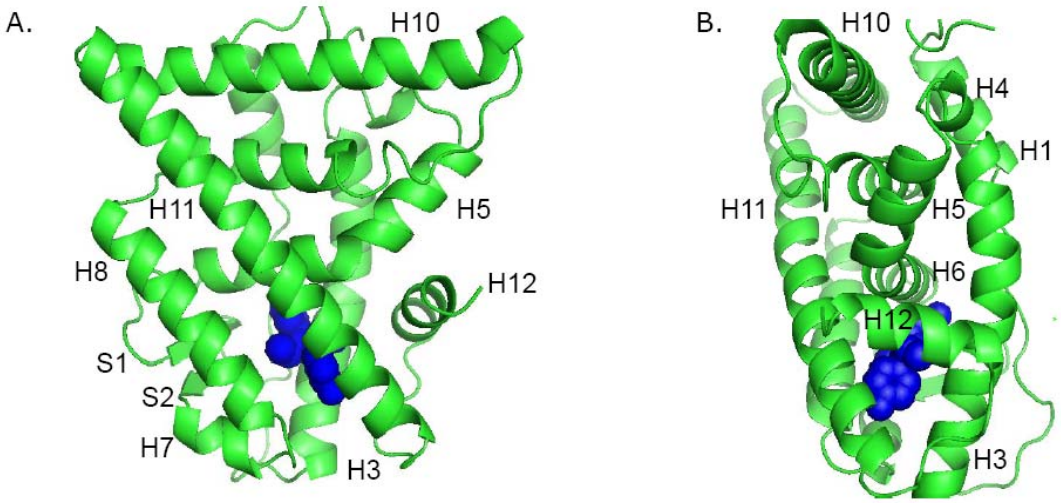

Figure 2. Représentation en ruban du domaine de liaison du ligand de ERα en présence de 17β-estradiol.

A. Vue perpendiculaire à la surface de dimérisation **B.** Vue parallèle avec la surface de dimérisation. Adapté de [98].

2-4-2-recrutement des corégulateurs

Des protéines interagissant avec le récepteur des oestrogènes de manière ligand dépendante furent identifiées la première fois lors d'expériences de *GST pull down* et ont été nommées ensuite P160 à cause de leur poids moléculaire [101]. Cette famille contient trois membres: SRC1 (p160-NCoA-1) est le premier coactivateur des récepteurs nucléaires à avoir été cloné; SRC-2 (TIF-2, GRIP1, NCoA2) et SRC-3 (ACTR, AIB1, RAC3, TRAM1, NCoA3) qui est amplifié dans le cancer du sein [53]. La famille des p160/SRC exerce un effet stimulant sur l'activité de ERα et ERβ et cette activité peut être inhibée par des inhibiteurs compétitifs des récepteurs [102]. Le recrutement des coactivateurs nécessite la fonction AF-2 du LBD. Cependant, la fonction AF-1 a ses propres coactivateurs comme p69 RNA hélicase et peut avoir une synergie avec la fonction AF-2 pour le recrutement des coactivateurs [103].

Les coactivateurs de la famille des p160/SRC contiennent trois domaines caractéristiques: un domaine aminoterminal bHLH, un domaine PAS impliqué dans les interactions protéiques et un domaine carboxyle terminal munit d'une activité enzymatique histone acétyltransférase et qui permet l'interaction avec CBP/p300. Le domaine central contient une signature moléculaire qui consiste en trois motifs conservés LXXLL (L: leucine et X: n'importe quel acide aminé) et permet l'interaction avec la fonction AF-2 des récepteurs nucléaires dans sa conformation agoniste [104]. L'affinité et la sélectivité de liaison des motifs LXXLL varient au sein d'un même coactivateur et d'un membre à l'autre au sein de la famille p160/SRC. De même, les régions qui flanquent les motifs LXXLL joue un rôle dans ces deux processus [105, 106].

La structure cristallographique du deuxième motif de type LXXLL du coactivateur GRIP-1 en interaction avec le LBD du ERα ayant une AF-2 en conformation agoniste montre que le motif LXXLL adopte une conformation en hélice. La glutamine 542 conservée au niveau de l'hélice H12 crée un pont hydrogène avec l'amide de l'acide aminé qui se trouve en aminoterminal du peptide LXXLL alors que la lysine K362 conservée au niveau de l'hélice H3 fait un pont hydrogène avec la fonction carboxyle terminale du

peptide LXXLL. Ce positionnement permet de bien diriger le côté hydrophobe du peptide vers la cavité du LBD et la mise en place d'interactions hydrophobes [100].

2-4-3-recrutement des corégulateurs: le complexe médiateur

Le complexe médiateur TRAP/SMCC/DRIP/ARC permet le recrutement du complexe de la machinerie basale de la transcription par divers facteurs de transcription [107, 108]. La sous unité TRAP220 interagit avec ERα et TR de manière en présence du ligand. Cette interaction est attribuée à des motifs de type LXXLL situés au niveau de la région aminoterminale de TRAP220 [109]. ERα est moins efficace que ERβ en terme du recrutement du complexe TRAP/DRIP *in vitro*, ce qui peut justifier les différences physiologiques entre les deux récepteurs [110]. Il a été suggéré que l'acétylation de la fonction AF-2 des récepteurs nucléaires induit la dissociation de coactivateurs de la famille p160 /SRC-1. Ceci permet le recrutement cyclique d'autres complexes coactivateurs TRAP/DRIP [111].

2-5-Rôle du récepteur des oestrogènes α dans la tumorigenèse mammaire.

2-5-1-ERα et la classification des tumeurs mammaires

La glande mammaire est une structure ramifiée de tubules se terminant par des lobules. Typiquement, un tubule contient une couche de cellules épithéliales luminales entourées par des cellules myoépithéliales le tubule est séparé du stroma par une membrane basale. Le stroma contient la matrice extracellulaire, les fibroblastes, les cellules immunitaires et les adipocytes ainsi que les vaisseaux sanguins.

Le cancer du sein est une maladie hétérogène qui englobe une multitude de tumeurs qui varient dans leur biologie et leur réponse aux traitements. Il est possible de classer les tumeurs mammaires en se basant sur l'expression des marqueurs moléculaires et les profils d'expression des gènes. Les marqueurs clés utilisés pour la classification sont l'expression des récepteurs nucléaires ERα, PgR et le récepteur membranaire HER2. Le statut de PgR

est positivement corrélé avec celui de ERα toutefois, son utilisation comme marqueur indépendant de ERα est sujette à controverse [112].

Par immunohistochimie, le statut ER+ est établi quand il y a au moins 1% des cellules qui expriment ERα dans le noyau. Quant au statut de HER2, il est établi par immunohistochimie et par hybridation *in situ* et son seuil est fixé à 10% des cellules [113].

En se basant sur ces trois marqueurs, il est possible de distinguer trois classes de tumeurs, les tumeurs ER+/PR+ (HER2-), les tumeurs HER2+ (ER-/PR-) et les tumeurs ER-/PR-/HER2. Les travaux de Perou CM. et coll. ont montré qu'il était possible de récapituler ses classes de tumeurs par la nature des transcriptomes des tumeurs. Trois classes de tumeurs ont ainsi été définies : les classes luminales, HER2-*like* et Basal-*like*. 70% des tumeurs HER2+ sont classées dans la classes HER2-*like*, 75% des tumeurs ER+ se trouve dans le groupe luminales et 88% des tumeurs ER-/PR-/HER- sont classes dans le groupe Basal-*like* [114].

2-5-2- ERα et les cancers hormono-dépendant

Avant l'introduction de divers agents pharmacologiques, la thérapie du cancer du sein fut essentiellement ablative. À l'époque, les chirurgies visaient à éliminer toutes les sources directes ou indirectes d'oestrogènes (ovaire, hypophyse). Les travaux de Jensen au début des années 1970 ont mené au concept selon lequel la présence des récepteurs des oestrogènes dans les tumeurs du sein serait une indication pour une réponse à la thérapie endocrinienne ablative [115-117]. Dès lors, la détection du récepteur des oestrogènes par le test de liaison du ligand ou par immunohistochimie fut le test de base pour la prédiction de la sensibilité à la thérapie endocrinienne.

Les observations cliniques et épidémiologiques montrent que les oestrogènes sont nécessaires pour le développement normal des glandes mammaires et jouent un rôle la formation des tumeurs. L'expression du récepteur est plus élevée dans le tissu mammaire des femmes issues de populations à haut risque (BRCA1/2 mutation, histoire familiale de cancers du sein, âge) par rapport à des femmes issues de populations à faible risque.

L'ablation du gène de ERα (ESR1) chez la souris rend le développement de la glande mammaire impossible même après la stimulation avec les oestrogènes. Cette ablation permet aussi d'avoir une résistance à la transformation maligne et ce même après la transduction avec un oncogène [36]. Dans un tissu mammaire sain, ERα est exclusivement exprimé dans 15 à 30 % des cellules épithéliales luminales [118]. Approximativement 70 % des carcinomes mammaires humains expriment ERα [119]. L'amplification du gène ESR1 qui code pour ERα est corrélée avec une augmentation l'expression de la protéine et ces changements se produisent très tôt lors du processus de la tumorigenèse [34, 120]. Les forts niveaux de ERα au sein des cellules tumorales les rendent plus sensibles aux effets prolifératifs des oestrogènes et leur procurent un avantage sélectif. Cependant, le statut ER+ de ces tumeurs est indicateur de la sensibilité à la thérapie endocrine et améliore les pronostics de survie par rapport aux tumeurs négatives pour l'expression des récepteurs.

3-Ciblage du récepteur des oestrogènes α dans les cancers hormono-dépendant

3-1-Développement des antioestrogènes partiels de type SERM

Les observations de Jensen ont fourni le fondement des stratégies thérapeutiques visant l'inhibition de la signalisation par les oestrogènes. Deux approches majeures ont découlé de ces travaux: Diminuer l'apport en oestrogènes par des inhibiteurs de l'aromatase et inhiber la liaison des oestrogènes avec les récepteurs par les antioestrogènes. Les antioestrogènes ont été développés dans les années 1950 dans le cadre de la recherche sur la contraception. Des composés antioestrogènes non stéroïdiens de type triphenylethylène comme Ethamoxytriphol (MER-25) et chlomiphene (MRL41) étaient de puissants agents contraceptifs dans les modèles animaux mais leur usage à long terme fut restreint à cause d'une toxicité significative [121, 122]. Ces deux composés montraient, cependant, des

effets inhibiteurs considérables sur les tumeurs du cancer du sein [121, 123]. Au début des années 1970, Tamoxifène (ICI 46,474, Nolvadex) fut introduit comme agent contraceptif ayant un potentiel thérapeutique dans le traitement du cancer du sein [124]. Depuis, il constitue l'antioestrogène de choix pour traiter les tumeurs ER+ de tous les stages aussi bien chez la femme avant ou après la ménopause [125]. Tamoxifène est utilisé comme traitement adjuvant dans les stades précoces de la maladie où il permet de réduire le risque du développement de tumeurs primaires contralatérales [126] et également lors de la prévention chez les femmes issues de groupes à haut risque [127].

Dans les années 1990 Eli Lilly introduit l'acronyme SERM pour (Modulateurs Sélectifs du Récepteur des oestrogènes) pour décrire une propriété longtemps associée aux antioestrogènes de type triphenylethylène, ces composés ont des actions mixtes qui varient selon les espèces et les tissus [49]. Chez la souris, tamoxifène est un agoniste dans l'utérus et le vagin alors qu'il est un antioestrogène dans la glande mammaire [128, 129]. Raloxifène (Ral), un autre antioestrogène de type SERM, c'est un agoniste dans le tissu osseux de la souris ovariectomisée et exerçe un effet antioestrogénique dans l'utérus et la glande mammaire [130, 131]. Ces observations ont été extrapolées au niveau clinique. Chez l'humain, Tamoxifène exerce un effet antioestrogénique au niveau de la glande mammaire, alors qu'il présente un effet oestrogénique partiel au niveau du tissu osseux et au niveau de l'utérus où son administration corrèle avec 3 à 4 fois d'augmentation du risque du cancer de l'endomètre [127, 132]. L'activité oestrogénique de Tamoxifène est une activité de type agoniste partielle qui peut s'expliquer par le fait que les antioestrogènes de type SERMs, dans certains contextes cellulaires et sur certains promoteurs, permettent d'activer la transcription par ERα. Il a été suggéré que le ratio entre les niveaux de coactivateurs et les corépresseurs dans un type cellulaire donné serait déterminant du type de la réponse. La surexpression des coactivateurs dans les cellules d'adénocarcinome mammaire favorise une réponse de type oestrogénique de tamoxifène [133]. Dans les cellules d'hépatocarcinome, la surexpression du corépresseur SMRT diminue la réponse de tamoxifène par contre la surexpression du coactivateur SRC1 inverse le phénomène [134].

La fonction d'activation AF-1 est importante dans la réponse sélective des antioestrogènes SERM. Ces composés inactivent la fonction AF-2 alors que la fonction AF-1 intègre les signaux qui proviennent de la voie des kinases MAPK [135] et la phosphorylation de la sérine S118 située au sein de AF-1 induit l'expression des gènes cibles des oestrogènes [136]. Une autre étude décrit une synergie entre la AF-2 et un domaine hélical situé au niveau de la AF-1. Les deux fonctions coopèrent pour l'interaction avec le coactivateur SRC-1 ce qui permet d'activer un promoteur sensible à tamoxifène [103, 137].

Le développement de résistances aux antioestrogènes de type SERMs a été observé cliniquement. En fait, l'usage de Raloxifène pour maintenir une bonne densité osseuse a un effet négatif quand vient le temps de traiter un cancer du sein [138]. Un long traitement avec le tamoxifène permet aux cellules MCF7 implantées dans des souris athymiques de recommencer à croître de manière tamoxifène dépendante [139]. Les mécanismes de résistance aux SERMs peuvent être d'ordre métabolique. Le tamoxifène a besoin d'être transformé par l'enzyme CYP2d6 en un métabolite actif de forte affinité, 4-hydroxytamoxifen (4-OHT) (endoxifène) et des mutations de cette enzyme sont responsables de la réduction de l'efficacité du traitement [140, 141]. Une mutation ponctuelle D351Y au niveau du récepteur des oestrogènes a été isolée à partir des tumeurs de MCF7 qui croissent en présence de tamoxifène [131]. Un autre mécanisme de résistance implique une surexpression des récepteurs à EGF, HER-2/*neu* et les coactivateurs de ERα [142, 143]. Plus récemment, Il a été montré que la phosphorylation de la sérine 305 du ERα par la Protéine kinase A (PKA) en présence de tamoxifène favorise l'adoption d'une conformation favorable à l'activation de la transcription [144].

3-2-Mécanisme d'action des antioestrogènes de type SERM

Les antioestrogènes partiels sont des inhibiteurs compétitifs du récepteur des oestrogènes α. Tamoxifène et Raloxifène exercent leur effet antagoniste par le biais de leur chaîne latérale (Fig.3) [145, 146]. Du point de vue structural, ils se lient à la cavité de liaison du ligand au sein du LBD. La reconnaissance du ligand se fait par la

complémentation de charge entre l'amine tertiaire de sa chaîne latérale et l'aspartate 351 du LBD, l'hydroxyle phénolique établissant des ponts hydrogène avec la glutamate 353, l'arginine 394 et une molécule d'eau [98, 147]. À l'exception de l'hélice H12, la structure du LBD est identique dans le cas des complexes ERα-E2 et ERα-4OHT (Fig.4).

En fait, 4-OHT projette sa chaîne latérale vers l'extérieur du LBD entre les hélices H3, H4 et H5. Les diméthyles de l'amine tertiaire créent blocage avec la leucine 540 de l'hélice H12 dans sa conformation agoniste. Ceci dicte à l'hélice une nouvelle conformation de faible énergie dite antagoniste. Au lieu de se replier sur la cavité de liaison du ligand comme dans le cas du complexe ERalpha–E2 [148], l'hélice H12 est repositionnée entre les hélices H3 et H5 au niveau du sillon de recrutement des coactivateurs de manière à mimer ces coactivateurs [147]. D'autres part, l'hélice H12 contient un motif de type LXXML semblable à la signature moléculaire des coactivateurs de la famille P160/SRC [104, 149].

La conformation antagoniste de l'hélice H12 est stabilisée par complémentation de charge avec la lysine 362 et la glutamate 380 et l'hélice dirige son côté hydrophobe vers l'intérieur du LBD. Le résultat est une inhibition du recrutement des coactivateurs et une inactivation complète de la fonction d'activation AF-2. [147, 148]. Même si le complexe ERalpha-4OHT est capable de se fixer sur l'ADN avec la même affinité que le complexe ERalpha–E2, un recrutement restreint des coactivateurs par la fonction AF-2 et un recrutement des corépresseurs NcoR et SMRT associés avec une activité HDAC qui condense la chromatine, seraient à la base de l'antagonisme du tamoxifène [150-153]. En conclusion, le développement de nouvelles molécules SERM nécessite une meilleure compréhension des effets moléculaires et cellulaires des oestrogènes, afin de proposer de nouveaux composés pour la prévention des complications liées à la ménopause (maladie cardiovasculaires, bouffées de chaleur) et dans le traitement du cancer su sein.

–

•Antioestrogènes de types SERM

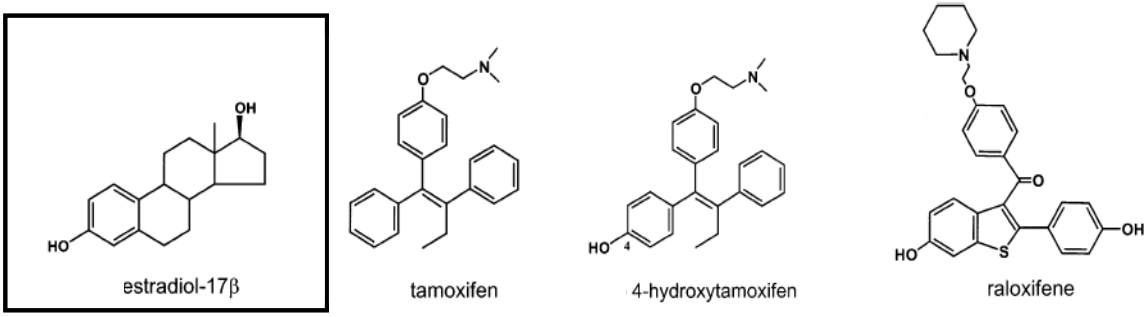

•Antioestrogènes Totaux

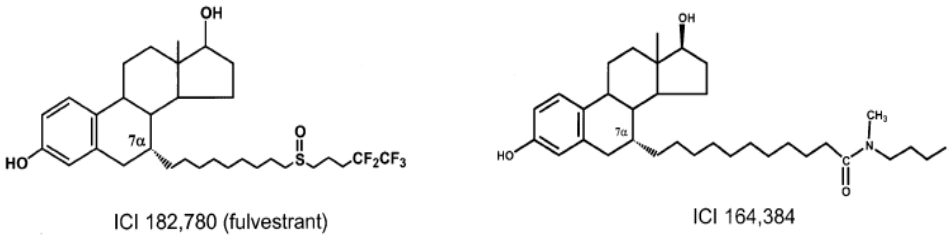

Figure 3. Les antioestrogènes de type SERM et SERD en comparaison avec 17β-estradiol et genistein.

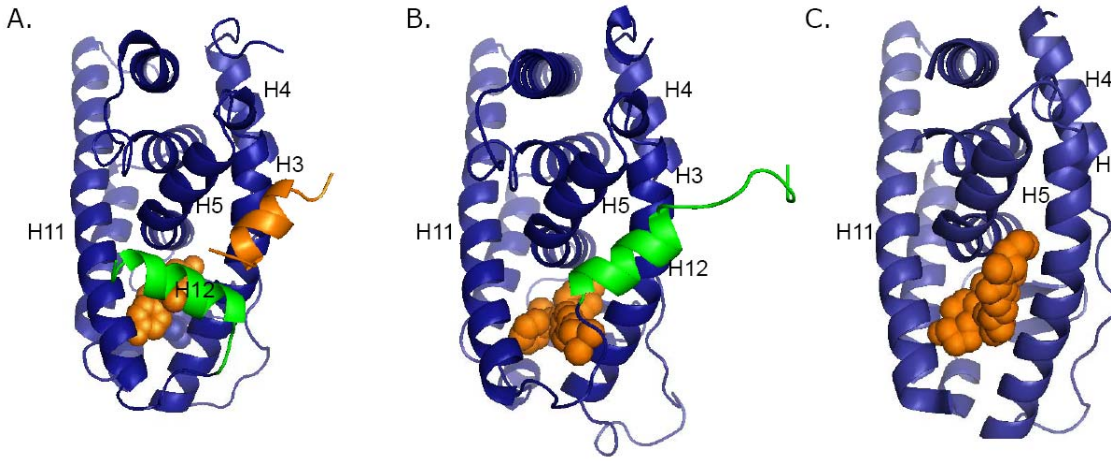

Figure 4. Représentation en ruban du LBD en complexe avec E2, OHT et ICI164, 384.

A: La conformation de l'hélice H12 au niveau du complexe (LBD-E2) [98]. B: L'hélice H12 au niveau du complexe (LBD-4OHT) occupe le sillon du recrutement des co-activateurs formé par H3/H4 et H5 [147]. C: conformation du complexe en présence de (LBD-ICI 164 384), la structure de [154].

3-3-Développement des antioestrogènes totaux SERD

Les antioestrogènes totaux ont été développés à fin d'avoir des inhibiteurs compétitifs de la liaison des oestrogènes avec. Ces composés ont une réponse biologique qui contraste avec celle des SERMs. Ils exercent un effet homogène en agissant comme des antagonistes des récepteurs des oestrogènes indépendamment du contexte du tissu ou du promoteur. Cette classe inclut ICI 164, 384, ICI 182, 780 (Faslodex, Fulvestrant) **(**Fig 3), RU48668, RU39416, EM 139 et EM800. À l'opposé des antioestrogènes de type SERMs qui ont une structure à base de triphenylethylène, les antioestrogènes totaux sont des analogues du 17β-estradiol auquel on a greffé une longue chaîne latérale. ICI 164, 384, un

analogue 7-α-alkylamide du 17β -estradiol fut le premier composé de cette classe. Il ne montre aucun effet oestrogénique. Il bloque l'effet utéro trophique du 17β-estradiol et du tamoxifène et bloque les cellules MCF7 dans de la phase G1 du cycle cellulaire [155]. Ces effets ont été attribués à la capacité de ce composé à inhiber la liaison du ERα à l'ADN *in vitro* et par l'induction des gènes qui bloquent la progression du cycle cellulaire comme p21 ^{Waf1}[156, 157].

ICI 182, 780 (Faslodex, Fulvestrant) a été développé à partir du ICI 164, 384. Pour augmenter la biodisponibilité et l'affinité. L'amide tertiaire a été remplacée par un groupe polaire et l'alkyle terminal a été remplacé par une fluorine; le résultat est une affinité qui équivaut à 89% de celle du 17β-estradiol, une inhibition de 10 fois supérieure de l'effet utéro trophique par rapport à ICI 164, 384 et une inhibition de la croissance des cellules MCF7 deux fois meilleure par rapport à Tamoxifène [158].

Les antioestrogènes totaux sont importants en clinique. ICI182, 780 est utilisé en deuxième ligne pour traiter les tumeurs avancées exprimant ER+ et PR+ chez les femmes après la ménopause ayant progressé dans la thérapie conventionnelle à base de antioestrogènes de type SERM. Cependant, il n'offre pas l'effet bénéfique que les SERMs exercent sur la densité osseuse [6, 159, 160].

3-4-Mécanisme d'action des antioestrogènes totaux SERD

La structure cristallographique du récepteur des oestrogènes alpha avec ICI 182, 780 n'est pas résolue et les informations dont on dispose proviennent de la structure cristallographique du récepteur ERβ avec ICI 164,384. Le mode de liaison du ligand est entièrement dicté par sa longue chaîne 7-α-alkylamide qui impose une rotation de 180^{o} du noyau stéroïdien de l'antioestrogène [154]. L'hydroxyle de l'anneau phénolique fait des ponts hydrogènes avec la glutamate 260, l'arginine 301 et avec une molécule d'eau alors que le 17β hydroxyle maintient son interaction avec l'histidine 430. La chaîne latérale de ICI164, 384 est projetée à l'extérieur du LBD et la structure de l'hélice H12 n'étant pas résolue, suggérant une grande mobilité (Fig 4). Des expériences de mutagenèse au niveau de l'hélice H12 montrent son importance dans l'antagonisme de ICI164, 384 [161, 162]. Il

a été suggéré que le non-repliement de l'hélice H12 peut provoquer l'exposition de surfaces hydrophobes au niveau de la cavité de liaison du ligand, comme dans le cas du complexe ERα-GW5638 ce qui peut affecter la stabilité de la protéine et restreindre le recrutement des coactivateurs [163, 164].

Les antioestrogènes totaux exercent leur action principalement sur la protéine sans affecter les niveaux de l'ARNm de ERα [165-167]. ICI182, 780, diminue la présence du récepteur dans le noyau en inhibant son import nucléaire [168] et il déstabilise la dimérisation du récepteur provoquant une réduction de sa demie vie [169] [170]. Bien qu'ICI 182, 780 se lie à ERα et ERβ, il n'affecte pas les niveaux de ERβ[171]. En fait, ERα est rapidement polyubiquitiné et dégradé par le proteasome 26S alors que les niveaux de ERβ demeurent stables même après 24 h de traitement. Les résidus lysines 302 et 303 semblent jouer un rôle dans l'ubiquitination de ERα en présence de ICI182, 780 [172]. Cependant, les résidus clés qui subissent cette modification demeurent inconnus. La dégradation du récepteur s'effectue dans un compartiment nucléaire par une activité protéase associée au noyau et implique une interaction avec des composantes de la matrice nucléaire [173-176]. D'autres observations montrent que ICI182, 780 agit sur la dynamique du récepteur au sein du noyau car il induit une immobilisation rapide [177-180]. Cette immobilisation corrèle avec un changement des propriétés d'extraction de la protéine [181-183].

4-Les complexes de remodelage de la chromatine

4-1-Organisation de la chromatine chez les eucaryotes :un aperçu

Chez les eucaryotes l'ADN est compacté dans le noyau sous forme de fibres de chromatine avec plusieurs degrés d'organisation dans le temps et l'espace. Cette structure complexe contrôle l'accessibilité de l'ADN aux protéines impliquées dans des processus cellulaires tels que la transcription. Le nucléosome est la forme de base de l'organisation de la chromatine et consiste en un octamère de protéines histones canoniques ou leurs variantes [184]. Classiquement, deux exemplaires des sous-unités H2A, H2B, H3 et H4 autour desquelles environ 146pb d'ADN super enroulé font 1.75 tour [185]. On distingue les variantes de H2A (H2A.Z, MacroH2A, H2AX et H2ABBD) et les variantes de H3 (H3.1, H3.2, H3.3 et CENPA) L'incorporation des variantes des histones agit somme un signal d'activation, d'inhibition ou une réponse au dommage de l'ADN [186]. À cet égard, il a été démontré que l'incorporation des H2A.Z induit un positionnement préférentiel des nucléosomes menant à l'activation [187].

Chaque histone présente un domaine central structuré suffisant aux interactions histone-histone et histone-ADN. De plus, les histones présentent une région queue qui joue un rôle important dans la formation des structures de chromatine d'ordre supérieur. Les régions aminoterminales des histones sont le lieu de nombreuses modifications post-traductionnelles, telles que l'acétylation, la méthylation, l'ubiquitination et la phosphorylation. L'acétylation et la méthylation sont contrôlées respectivement par des enzymes de type histones acétyltransférases et méthyltransférase comme CARM1 et PRMT. Ces modifications permettent de neutraliser les charges positives des résidus arginines et lysines ce qui diminue l'affinité des histones pour l'ADN et ultimement améliore son accessibilité aux facteurs de transcription [188, 189].

Cependant, de la méthylation pourrait aussi bien corréler avec l'activation et avec l'inhibition de la transcription. On distingue les marques de l'euchromatine : la méthylation des lysines 4, 36 et 79 de l'histone H3 et les marques de l'hétérochromatine : la dimétylation et la trimétylation de la lysine 27 de l'histone H3 et la méthylation de la lysine 20 de l'histone H4 [186].

4-2-Les facteurs de remodelage de la chromatine ATP dépendant

4-2-1-Les complexes de types SWI/SNF

Le complexe SWI/SNF (switch/succrose non-fermenting) a été découvert initialement lors d'un criblage au niveau de la levure à la recherche des mutations qui causent un défaut au niveau du gène SUC2 codant pour une invertase impliquée dans le métabolisme des glucides [190, 191]. Les complexes SWI/SNF de la drosophile, *Brahma*, son homologue humain, hBRM/BRG1 et celui de la levure, RSC, partagent la même sous unité ATPasique homologue à Snf2 du complexe Swi2/Snf2 de la levure en plus d'un bromodomaine [192]. Ensemble, ils forment la sous-famille SNF2 au sein de la famille des SWI2/SNF2 [193]. D'autres sous unités ATPasiques homologues à la sous unité SNF2 sont impliquées dans la formation d'autres complexes de la famille SWI2/SNF2, qui comprend six autres sous-familles: ISWI, CHD1, INO80, CSB, RAD54, DDM1.

Les complexes SWI/SNF humains de la sous-famille SNF2 demeurent les plus étudiés. Ils peuvent atteindre 2MDa de taille et peuvent contenir entre 8 et 16 sous unités dont une seule à activité ATPasique [194-196]. Leurs composantes actives sont très conservées de la levure à l'humain. Ces complexes sont recrutés aux régions régulatrices par des facteurs qui lient l'ADN [197]. Ils se lient à la chromatine avec une affinité nanomolaire et utilisent l'énergie de l'hydrolyse de l'ATP pour affaiblir les contacts ADN–histones. Ceci peut augmenter jusqu'à 30 fois l'affinité d'un coactivateur pour un site donné [198]. *In vitro*, la sous unité SWI a une activité ATPasique avec l'ADN nu mais son activité est maximale est atteinte en présence de nucléosomes intacts [199].

4-2-2-Les complexes de type ISWI

Le groupe des complexes ISWI s'appelle aussi le groupe SNF2L [200]. Il se classe au sein de la sous-famille ISWI et partage la sous unité ATPase SNF2 caractéristique de la superfamille des SWI2/SNF2. Les complexes ISWI exercent un large éventail de fonctions au sein de la cellule, incluant l'activation et la répression de la transcription, l'assemblage de la chromatine, le glissement des nucléosomes, la réplication de l'hétérochromatine, et sont aussi impliqués dans la cohésion des chromatides sœurs [200]. Les premiers complexes ISWI, purifiés chez la drosophile furent nommés NURF, ACF et CHRAC [201] (Fig 5). Ensuite, des homologues furent identifiés dans de nombreuses espèces. Chez l'humain, la sous-unité ATPasique est SNF2H dans les complexes de type ACF/WCRF, CHRAC, WICH, NoRC, NuRD et RSF. Seul le complexe NURF présente une sous unité ATPasique SNF2L.

Même s'ils sont de composition similaire, les complexes ISWI montrent des activités différentes, CHRAC et ACF ont tendance à compacter la chromatine et permettre l'assemblage des nucléosomes *in vitro* et *in vivo* [202, 203]. Quant au complexe NURF, il agit de manière similaire au complexe de type SWI/SNF en déstabilisant le nucléosome [204-206]. Contrairement à l'activité ATPasique des complexes SWI/SNF, celle des complexes ISWI est stimulée par des nucléosomes intacts contenant une queue hypoacétylée de l'histone H4 [198, 207].

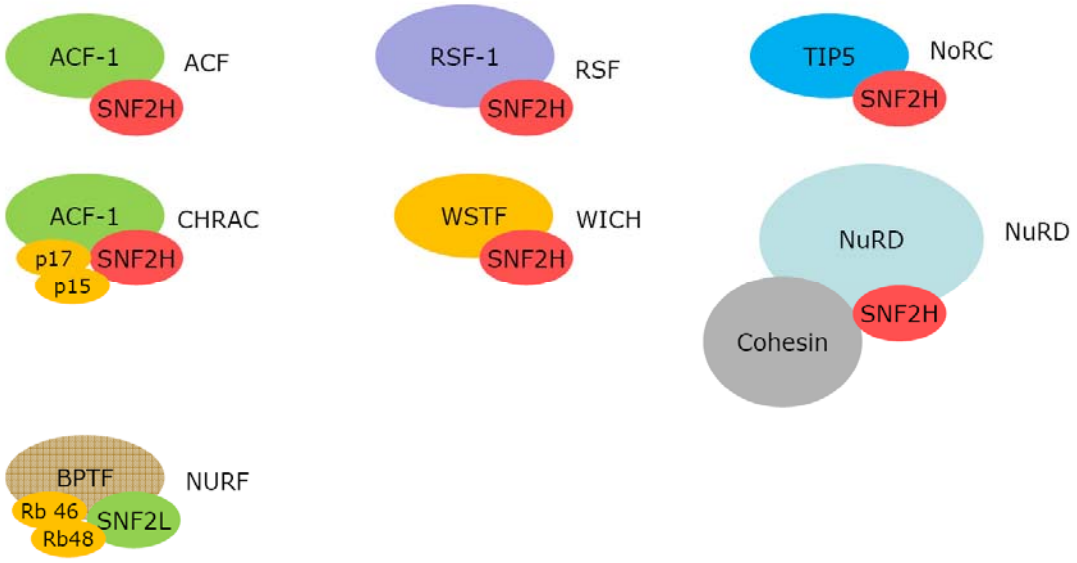

Figure 5. Représentation schématique des complexes de remodelage de la chromatine ISWI humain.

Adapté de [200].

4-2-3- Anatomie moléculaire du complexe ACF

Le complexe ACF est formé d'une sous unité ATPasique SNF2H et une sous unité non catalytique ACF1 (Fig 6). SNF2H présente un domaine aminoterminal de 691 acides aminés qui contient l'essentielle de l'activité catalytique car ce domaine est capable de se lier à l'ADN et au nucléosome. L'ADN seul n'est pas suffisant pour l'activité ATPasique de SNF2H ce qui suggère un rôle important des histones [207-209]. La région carboxyle-terminal se replie en 12 hélices et présente un domaine replié en quatre hélices et appelé HAND [210], situé entre les résidus 697 et 795. Le domaine HAND est suivi immédiatement par le domaine SANT, qui est organisé en trois hélices entre les résidus 796 à 850 et s'apparente au domaine de liaison à l'ADN de c-myb. Il a été suggéré que ce domaine aurait une fonction de liaison de l'ADN [211]. Cependant, la présence des résidus hydrophobes au niveau de l'hélice 3 et le caractère acide du domaine SANT est incompatible avec la fonction de liaison de l'ADN [199].

Il existe un troisième domaine, entre les résidus 886 et 977, qui se replie en trois hélices et ne présente pas la séquence canonique du domaine SANT. Pour le distinguer du domaine SANT, il a été appelé SLIDE pour SANT *like domain*e. Ce domaine contient des résidus conservés qui se trouvent au niveau du DBD de c-myb et présente une charge nette positive. L'activité de remodelage maximale de SNF2H nécessite une séquence à caractère basique (Arginine17 Histidine18 Arginine19) située au niveau de la région aminoterminale de l'histone H4. En absence de cette région, il ya perte de la reconnaissance du nucléosome et une inhibition de l'activité ATPasique. La liaison au nucléosome peut être aussi altérée par l'acétylation des lysines adjacentes K12 et K16 [209, 212]. La délétion du domaine SLIDE abolit la liaison à l'ADN et rend SNF2H inactif même en présence des nucléosomes intacts. Par contre, la délétion du domaine SANT n'affecte pas la liaison à l'ADN mais l'activité ATPasique est nulle même en présence des nucléosomes intacts. Ceci suggère un mécanisme où la reconnaissance de l'ADN est assurée par le domaine SLIDE alors que le domaine SANT constitue le module de reconnaissance de l'histone H4 [199, 210].

La sous-unité non catalytique du complexe ACF est ACF1, aussi appelée WCRF180 et BAZ1A. Le gène BAZ1A code pour une protéine d'environ 180 kDa qui a plusieurs

motifs conservés : WAC, BAZ, DDT, bromodomaine et des doigts PHD [107, 202, 203] (Fig 6). Le complexe formé d'ACF1 et de SNF2H nécessite une interaction entre une région carboxyle-terminal de SNF2H située entre les acides aminés 962 et 991 et les motifs DDT et bromodomaine de ACF1 [213]. Le domaine PHD pourrait aussi jouer un rôle dans cette interaction [203].

D'un point de vue mécanistique, les études in *vitro* ont démontré que ACF1 exerce un effet allostérique sur SNF2H et permet d'augmenter l'efficacité de sa translocation de l'ADN vers les octamères d'histones sans augmenter la quantité d'ATP hydrolysée par SNF2H. Le modèle actuel suggère que ACF1 interagit avec les octamères d'histone et constitue un point d'ancrage pour SNF2H. Ce dernier se lie à l'ADN par son domaine SLIDE et à l'histone H4 par son domaine SANT. L'énergie de l'hydrolyse de l'ATP est convertie en un mouvement de torsion qui est propagé autour du nucléosome par la sous unité ACF1. Ainsi, le complexe peut catalyser la mobilisation des nucléosomes et la l'enroulement de l'ADN autour des histones [214].

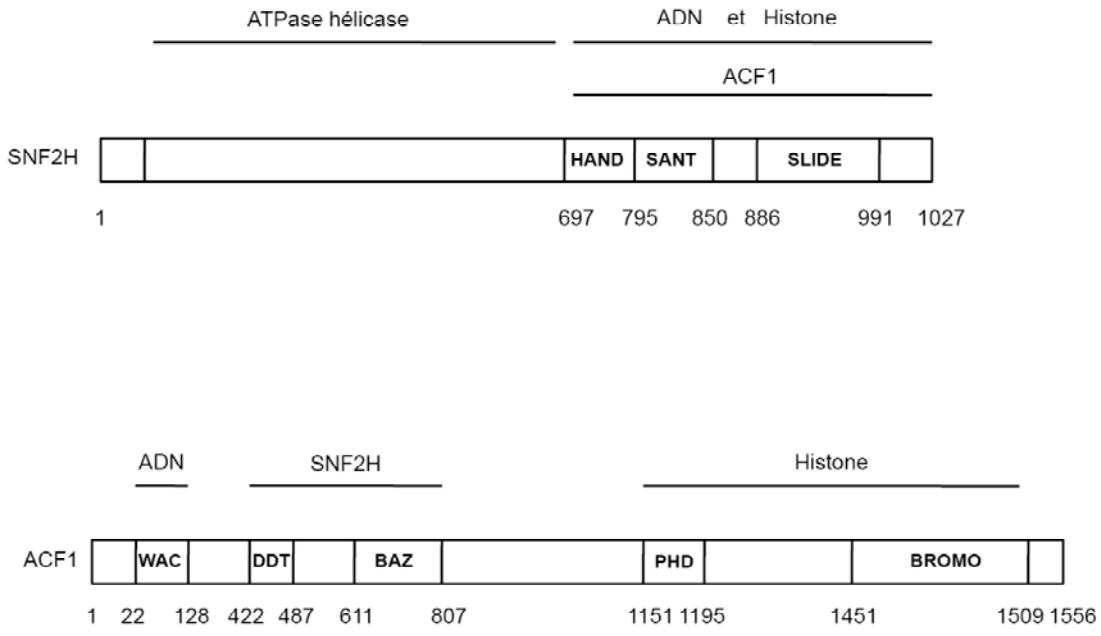

Figure 6. Représentation schématique de ACF1 et SNF2H et les fonctions de leurs domaines.

Adapté de [213, 215].

4-2-4- Conséquences biologiques de la suppression de ACF1et SNF2H

La sous-unité catalytique du complexe ACF joue un rôle important dans le développement. Chez la souris, la suppression du gène SNF2H induit la mortalité des embryons avant l'implantation et l'inactivation du gène au niveau des cellules souches hématopoïétiques inhibe la capacité des progéniteurs CD34+ à activer l'érythropoïèse [216]. SNF2H constitue une cible des facteurs de transcription E2F suggérant un rôle dans le cycle cellulaire [217, 218]. Contrairement à la sous unité SNF2H, la délétion de acf1 chez la drosophile génère des embryons semi-létaux qui n'exhibent pas d'anormalités morphologiques. Ces embryons se caractérisent par une diminution de la périodicité des nucléosomes mais pas une perte totale ce qui suggère que le rôle de acf peut être compensé par autres facteurs de remodelage de la chromatine ATP dépendant.

4-2-5- Rôle de ACF dans l'inhibition de la transcription

Les gènes du groupe polycombe PcG sont impliqués dans l'inactivation transcriptionnelle via les éléments PRE. Chez la drosophile, le phénotype *white* est une cible bien connue de la répression par PcG. Il a été démontré que la suppression de acf1 conduit à une activation partielle de rapporteur PRE *white* [219].

Dans les thymocytes, il a été démontré que ACF1, SNF2H et HDAC1sont recrutés par SATB1, une protéine de la matrice nucléaire, des expériences d'immunoprécipitation de la chromatine ont indiqué que ces protéines sont recrutées au locus *IL2Rα* afin d'inhiber sont expression. De plus, l'absence de SATB1 altère le positionnement des nucléosomes au niveau de ce locus, cet effet a été attribué à l'absence de recrutement de ACF [220].

Le complexe ACF permet de stabiliser le complexe répresseur formé par NCOR-HDAC et le récepteur de la vitamine D3. Ce complexe est recruté au niveau des promoteurs de RANKL et IGFBP3 en absence du ligand. En présence de la vitamine D3, le complexe répresseur est relâché. De plus, la suppression de ACF1augmente l'accessibilité de la nucléase micrococale au promoteur de RANKL ce qui suggère un rôle de ACF dans la mobilisation des nucléosomes [215]. Également dans le contexte des récepteurs nucléaires,

il a été démontré que SNF2H joue un rôle important dans la répression par le récepteur de l'hormone thyroïdienne (TR). Le complexe N-CoR/HDAC3 s'associe avec TR et recrute SNF2H en absence du ligand. Dans ce contexte, la désacétylation est cruciale car le ciblage de HDAC3 par des siRNA inhibe le recrutement de SNF2H [221].

4-2-6- Rôle de ACF dans la réplication de l'hétérochromatine

L'hétérochromatine centromérique est répliqué tard dans la phase S, il a été démontré que la suppression de acf 1 au niveau des neuroblastes de la drosophile raccourcie la durée de la phase S [219]. Ceci ne concorde pas avec les résultats obtenus dans les cellules HeLa où la supression de ACF1 augmente la durée de la phase S [217].

4-2-7- Rôle de ACF dans la réparation des dommages à l'ADN

ACF joue un rôle dans la réparation des dommages de l'ADN**.** Il a été démontré que l'irradiation ou le traitement par la Bléomycine induit une accumulation du complexe ACF aux sites des dommages de l'ADN double brin (DSB). De plus, quand ACF1 et SNF2H sont supprimés, les cellules deviennent sensibles aux traitements qui induisent les dommages de l'ADN. KU 70/80 sont des facteurs requis pour la réparation par recombinaison homologue (HR) et pour la réparation de type NHEJ *(nonhomologous end joining*). Il a été démontré que ACF interagit avec KU 70/80 et sa suppression diminue ces deux types de réparation [222, 223]. Le rôle de ACF a été mis en évidence par une deuxième étude; la suppression de ACF1 augmente l'apoptose et la proportion des cellules qui traversent le point de contrôle G2/M et ce malgré de nombreux dommages à l'ADN [224].

5-La SUMOylation

5-1-Définition

La SUMOylation est une modification posttraductionnelle par la liaison covalente de protéines SUMO aux résidus lysines. Initialement, SUMO1 fut identifiée comme une protéine qui se replie de manière similaire à l'ubiquitine et qui interagit avec PML [225]. Les eucaryotes supérieurs expriment une famille de 4 membres codés par quatre gènes différents. SUMO2 et SUMO3 ont 95 % d'identité de séquence et ne diffèrent que par trois acides aminés; ils constituent une sous-famille appelée SUMO2/3 qui partage une identité de séquence de 50 % avec SUMO1 et 86 % avec SUMO4 [226-228]. La distribution cellulaire des trois paralogues est variable, SUMO1 se trouve au niveau du nucléole, l'enveloppe nucléaire et au niveau des foci cytoplasmique. SUMO2/3 sont associés avec les chromosomes, ils s'accumulent graduellement pendant la télophase. La proportion non conjuguée de SUMO2/3 est plus grande que celle de SUMO1[227].

La SUMOylation est le processus qui permet la formation d'un lien isopeptidique entre le groupement carboxyle du dernier résidu du peptide SUMO et le groupement amine ε de la lysine au niveau de la protéine cible. Typiquement, la lysine ciblée par la SUMOylation se trouve dans un consensus ψKXE/D où ψ est un acide aminé hydrophobe et X est n'importe quel acide aminé [229]. Le consensus de SUMOylation peut inclure un site de phosphorylation ψKXEXXSP ou des acides aminés acides ψKXEXXEEEE [230, 231]. La SUMOylation peut s'effectuer en absence d'une séquence consensus et la présence d'une séquence consensus n'est pas toujours corrélée avec la SUMOylation [232].

De manière similaire à l'ubiquitin, les protéines SUMO2/3/4 peuvent former des chaines polymériques grâce à la lysine 11 située dans un consensus de SUMOylation. Par opposition, SUMO1 ne contient pas un tel site et peut se lier sous forme monomérique à la protéine cible ou terminer une chaine polymérique de SUMO2/3 [232].

5-2-le cycle de la SUMOylation

La SUMOylation utilise une cascade enzymatique analogue à celle de l'ubiquitination mais avec des composantes différentes (Fig 7)

5-2-1-Maturation de SUMO

Les protéines SUMO sont traduites sous forme de précurseurs immatures, des protéases spécifiques à SUMO appelées déSUMOylases induisent un clivage catalytique qui expose deux glycines terminales.

5-2-2-L'hétéro dimère d'activation (E1)

Une fois mature, SUMO est transféré à un complexe hétérodimérique formé par SAE1et SAE2. SAE1 contient trois domaines, une cystéine catalytique, un domaine d'adénylation et un domaine *ubiquitin fold domain* UFD. En utilisant de l'ATP, SAE1 catalyse la formation d'une SUMO adénylée. Le clivage du lien AMP-SUMO est suivi de la formation d'un intermédiaire covalent dans lequel il existe un lien thioester entre la SUMO et la cystéine catalytique de SAE2 [233].

5-2-3-L'enzyme de conjugaison (E2)

La SUMO est transférée à l'enzyme de conjugaison E2 (UBC9) au niveau de la cystéine 93. UBC9 se distingue par la capacité à reconnaitre le substrat et à catalyser la formation d'un lien isopeptidique entre la SUMO est la protéine cible [229, 234]. Contrairement à l'ubiquitination, Il existe une seule enzyme E2 chez les mammifères et sa délétion induit la mortalité à l'état embryonnaire chez la souris [235].

5-2-4-Ligase de SUMO (E3)

Les enzymes E3 facilitent l'attachement de la SUMO à la protéine cible. La nécessité d'une E3 est un sujet de débat car la SUMOylation peut s'effectuer *In vitro* en absence d'une E3. À l'opposé de l'ubiquitination pour laquelle il existe des centaines d'enzymes E3, il n'existe que peu de ligases de SUMO. Les enzymes PIAS humains sont

les ligases de SUMO les mieux connues. Initialement, les PIAS ont été identifiées comme des inhibiteurs de STAT1 et STAT3 [236]. On distingue 4 enzymes PIAS qui proviennent des gènes différents, PIAS1, PIASxα, PIASxβ et PIAS4 (PIASy). D'autres protéines qui n'appartiennent pas à la famille des PIAS peuvent exhiber une activité SUMO ligase parmi lesquelles il y a RanBP2, PML, polycombe pc2, TOPORS, HDAC 4 et HDAC7 [237, 238].

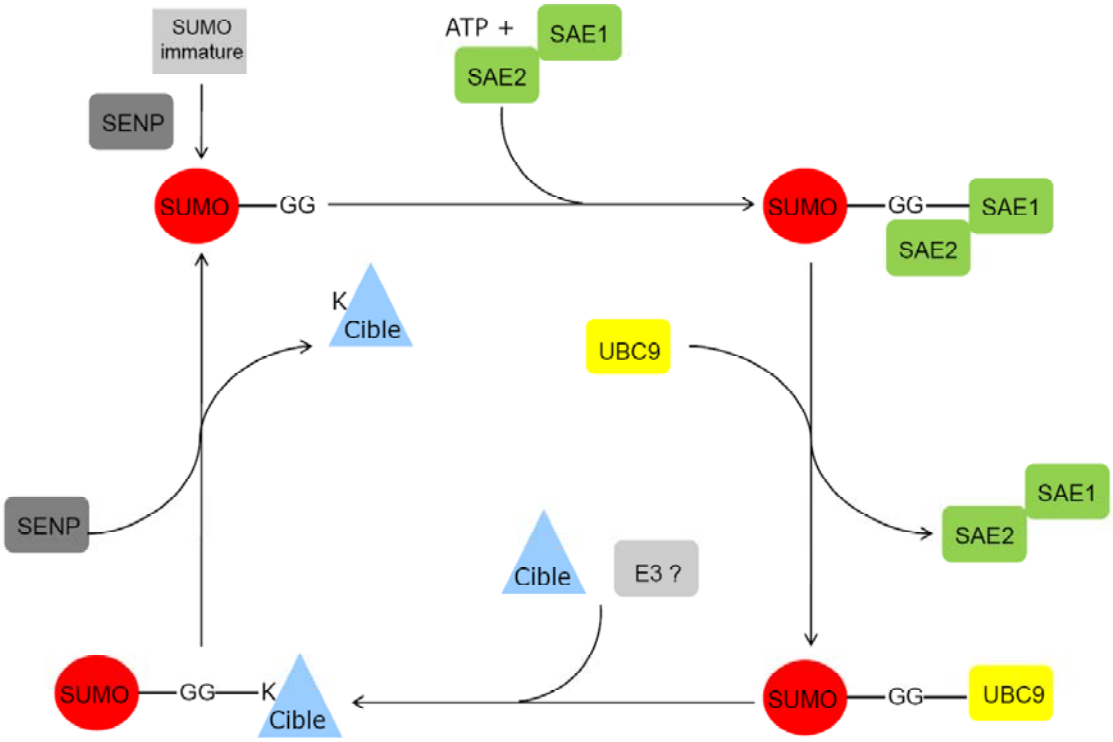

Figure 7. Représentation schématique du cycle de la SUMOylation

5-3-Les protéases spécifiques à SUMO (SENPs)

La SUMOylation est un processus dynamique et réversible. Il existe une famille de protéases spécifiques à SUMO qui sont SENP1, 2, 3, 5, 6, 7 et 8. Les SENPs font partie du clan CE des protéases à cystéine, ils se caractérisent pas une triade catalytique formée par les résidus Histidine, asparagine et cystéine. Les SENPs contiennent un tunnel qui accommode les deux glycines situées au niveau de la région carboxyle-terminal de la SUMO. Globalement, les SENPs jouent deux rôles dans la cascade de la SUMOylation; ils permettent la maturation des précurseurs SUMO en catalysant un clivage peptidique et catalysent la dissociation entre SUMO et les protéines cibles [238].

Les enzymes SENPs exhibent des préférences dans leurs activités isodopeptidase. SENP1 et SENP2 peuvent déconjuger les trois isoformes de SUMO, SENP3 et SENP5 expriment une activité envers SUMO 2 et SUMO3 alors que SENP6 et SENP7 ne possèdent pas d'activité de maturation du pro-SUMO. Finalement, SENP8 exhibe une activité envers Nedd8 mais pas envers SUMO ou ubiquitin.

La balance entre la SUMOylation et DéSUMOylation est altérée dans certains cancers. Les niveaux de SENP3 sont élevés dans les cancers de la prostate, de l'ovaire, du rectum et du côlon. Également, Il a été démontré que SENP6 est régulée à la baisse dans le cancer du sein comparativement à un tissu sain. Des niveaux plus élevés de SENP1 ont été observés dans d'adénocarcinomes thyroïdiens [239].

5-4-Les motifs SIM

La modification d'une protéine par la SUMOylation constitue un signal pour des interactions non covalentes. L'exemple le mieux connu est celui des protéines qui contiennent des séquences en acides aminés appelés SIM. On distingue les motifs suivants :

- hydrophobe-hydrophobe-X-S-X-(S/T)-acide-acide-acide,
- (V/I/L)-X-(V/I/L)-(V/I/L) [240],
- K-X3-5-(I/V)-(I/L)-(I/L)-X3-(D/E/Q/N)-(D/E)-(D/E) [241].

Les acides aminés acides qui entourent ce consensus ou la présence d'une sérine phosphorylable jouent un rôle dans la spécificité de la liaison du motif SIM [242, 243]. Parmi les protéines qui présentent des SIM, il y a les SUMO ligase PIAS1,2,3, RanBP2, et les composantes des corps PML : PML, SP100 et Daxx [244, 245].

5-5-Mode d'interaction de SUMO avec SIM

Même si le repliement de la SUMO est similaire à celui de l'ubiquitine, le recrutement des SIM par SUMO utilise des surfaces différentes de celles que l'ubiquitine utilise pour recruter les UIM (ubiquitin interacting motif) [246].

Le noyau hydrophobe du SIM forme un brin β qui peut s'insérer entre l'hélice α et le deuxième feuillet β de la protéine SUMO. La phénylalanine 36 et la tyrosine 51 de la protéine SUMO forment un amas hydrophobe qui accommode les chaines latérales hydrophobes du SIM [247].

Dans le cas du SIM de PIAS2, la valine 4, l'isoleucine 5 et la leucine 7 sont cruciales pour l'affinité de liaison. L'isoleucine 5 et la leucine 7 s'incrustent dans de la poche formée par la phénylalanine 36 et la tyrosine 51 de SUMO1. Les peptides SIM inversés (V/I) X (V/I) (V/I) et (V/I) (V/I) X (V/I/L) peuvent adopter des orientations opposées à fin de lier le même site au niveau de SUMO [248].

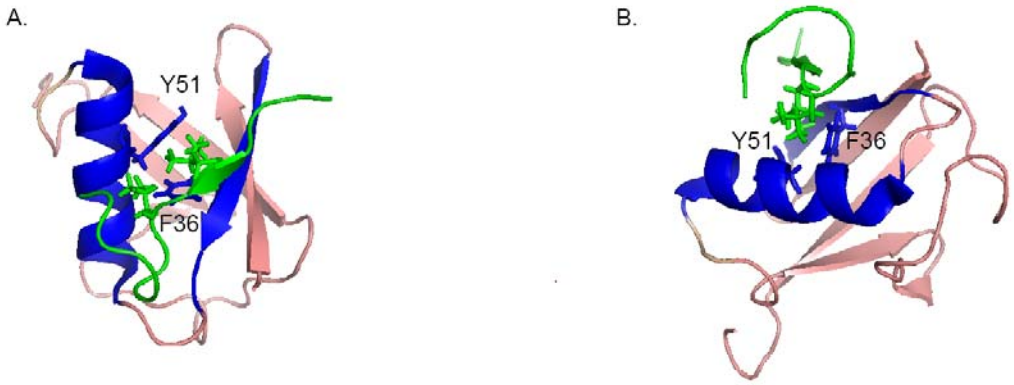

Figure 8. Représentation en ruban de l'interaction de SUMO1 avec peptide SIM de PIAS2. A. vue perpendiculaire avec l'axe l'hélice, en vert le peptide SIM. B. rotation de 90^{o} par rapport à l'axe vertical adapté de [248].

5-5-La SUMOylation et les corps PML

Les corps PML se trouvent dans la majorité des types cellulaires. Le nombre des corps PML varie entre 1 et 30 selon le type cellulaire, l'état de différenciation et la phase du cycle cellulaire. En microscopie électronique, Les corps PML apparaissent sous forme de structures sphériques et denses d'un diamètre qui varie entre 0,1 et 1µm Également, une certaine localisation à la matrice nucléaire a été observée pour les corps PML [249, 250]. La principale composante des corps PML est la protéine PML (TRIM19) [251]. La séquestration des protéines mal repliées fut parmi les premiers rôles des corps PML, cependant les corps PML sont impliqués dans de plusieurs processus cellulaires incluant la réponse aux dommages de l'ADN, l'apoptose, et la sénescence.

Plusieurs observations relient la SUMOylation aux corps PML. Les études d'hybridation *in situ* ont démontré que les corps PML sont les principaux sites de la SUMOylation dans la cellule et l'ablation de l'enzyme de conjugaison de la SUMOylation (UBC9) conduit à une diminution du nombre des corps PML [235, 252]. La protéine PML est SUMOylée au niveau des lysines 65, 160 et 490 et contient un motif SIM, de plus la SUMOylation de PML est importante pour la formation des corps PML [253-256]. Le rôle des motifs SIM dans la formation des corps PML a été remis en question car la délétion du motif SIM n'empêche pas de former des corps PML.

La SUMOylation de PML aux lysines 65 et 160 est suivie par un transfert de PML à la matrice nucléaire et le recrutement des composantes des corps, PML DAXX et SP100 [257]. Finalement, Il a été démontré que PML peut fonctionner comme une SUMO E3 ligase car sa surexpression augmente les niveaux de SUMOylation chez la levure [258].

5-6-La SUMOylation et le concept STUBL

Initialement, RNF4 a été identifié comme un coactivateur des récepteurs aux oestrogènes et aux androgènes [259]. RNF4 possède un domaine RING caractéristique des E3 ligases de l'ubiquitin et possède également la capacité de lier SUMO1 *in vitro*. RNF4 se localise au niveau des corps PML avec SUMO1 [260]. Chez la levure, RNF4 compense la perte du complexe formé par les *rfp1 rfp2* (deux protéines qui contiennent un domaine SIM) *et slx8* (activité E3 ligase) [261].d'où le nom *SUMO Targeted Ubiquitin Ligase*

La capacité de RNF4 de se lier à SUMO découle du fait qu'il contient 4 SIM potentiel localisé au niveau de sa région aminoterminale. PML est le premier substrat pour lequel le rôle de RNF4 a été bien décris [262] et [263].

Le traitement à l'arsenic induit une forte modification de PML par la SUMOylation et l'ubiquitination suivies d'une dégradation, la délétion de RNF4 ou l'inhibition du proteasome 26 S conduisent à l'accumulation des formes SUMOylées de PML, en présence de l'arsenic. *In vitro*, RNF4 se lie de manière plus efficace aux formes poly SUMO par rapport aux formes mono et di SUMO. La liaison aux chaines polySUMO est compromise en absence des domaines SIM. De plus, les mutations des cystéines du doigt de zinc du domaine RING de RNF4 inhibent la polyubiquitination de SUMO2 au niveau des résidus 11, 32 et 41.

5-7-Rôle de la SUMOylation dans l'inhibition transcriptionnelle

Les données actuelles indiquent que la conjugaison avec SUMO constitue une surface d'interaction avec les corépresseurs. Au cœur de ce modèle se trouvent les interactions non covalentes via les SIM [264, 265]. Dans le paragraphe qui suit nous allons passer en revue les exemples les mieux connus.

5-7-1-Recrutement des HDAC

La SUMOylation du facteur de transcription elk1 permet l'interaction avec HDAC2 [266]. De la même manière, La SUMOylation de CBP est importante pour le recrutement de HDAC2 et DAXX et la SUMOylation du correpresseur Groucho induit le recrutement de HDAC1 [243, 267].

Le recrutement des HDAC ne justifie pas tous les effets répressifs de la SUMOylation, car l'inhibition de l'activité HDAC par TSA ne permet pas de lever l'inhibition les facteurs elk1 et SP3 [268].

5-7-2-Recrutement de LSD1

La répression des gènes SCN1A et SCN3A par le complexe LSD1/CoREST/HDAC est due à la SUMOylation, l'interaction de CoREST 1 avec SUMO2/3 requiert un motif SIM non consensuel. Ceci permet à la dé-méthylase LDS1 d'enlever les marques de la chromatine active [269].

5-7-3-Recrutement du facteur de remodelage de la chromatine Mi-2 et de HP1

Il a été démontré que Mi-2 est un effecteur de la SUMOylation chez la drosophile et chez les mammifères. Le recrutement de Mi-2 est due de la SUMOylation du facteur SP3 et sa déplétion permet de lever l'inhibition de certains gènes cibles de SP3 [268].

Par ailleurs, une autre étude du même groupe a démontré que la SUMOylation permet de recruter les protéines de l'hétérochromatine HP1α HP1β etHP1γ. La SUMOylation de SP100 favorise le recrutement HP1α et la mutation des sites de SUMOylation au niveau de SP3 abolit le recrutement de HP1α HP1β et HP1γ [265].

5-7-4-Recrutement de SETDB1

SETDB1 est une méthlytransferase qui catalyse la tri méthylation de l'histone H3 à lysine K9 ce qui corrèle avec la répression transcriptionnelle. Des observations récentes démontrent que SETDB1 et CHD3 se lient à SUMO par des motifs SIM consensuels de manière dépendante de la SUMOylation de KAP1 [264].

5-8-Rôle de la SUMOylation dans l'activation de la transcription

La SUMOylation est généralement reliée avec l'inactivation de la transcription cependant, il existe des cas où la SUMOylation active la transcription des gènes. Le cas le mieux connu est celui de la SUMOylation de p53. La SUMOylation de p53 à la lysine 368 stimule sa capacité à transactiver, Une des explications probables fut la compétition avec l'ubiquitination de p53 par MDM2, cette ubiquitination conduisant à une dégradation de p53 [270, 271].

La SUMOylation de l'enzyme dnmt3a perturbe son interaction avec HDAC1 et HDAC2 ce qui inhibe sa capacité à inhiber la transcription [272]. Également, la SUMOylation de ikaros inhibe son interaction avec Sin3 et le complexe NuRD ce permet la levée de l'inhibition de Ikaros [273].

5-9-SUMOylation des récepteurs nucléaires des hormones stéroïdiennes

5-9-1-Récepteur des androgènes

Les lysines 386 et 520 sont modifiées par SUMO1 en présence de la testostérone. La double mutation de ces sites ou la surexpression de SENP1 conduisent à une hausse de l'activité transcriptionnelle d'AR sur un vecteur rapporteur [274, 275]. La SUMOylation de AR permet de recruter DAXX [276]. La surexpression de HDAC4 augmente les niveaux de la SUMOylation et d'inhibition de AR ce qui suggère un rôle SUMO E3 ligase de HDAC4 [277].

5-9-2-Récepteur des glucocorticoides

Les sites de SUMOylation en présence du ligand sont les lysines 277, 293 et 703 [275, 278]. Cette SUMOylation est corrélée avec la translocation de GR dans le noyau et une diminution de ses niveaux de transactivation avec le ligand. Les sites de SUMOylation chevauchent avec les motifs de contrôle de la synergie transcriptionnelle de GR sur les promoteurs multiplex [279]. La SUMOylation de GR permet de recruter DAXX par les motifs SIM et l'inhibition exercée par DAXX dépend du contexte du promoteur [280, 281].

5-9-3-Récepteur de la progesterone

La SUMOylation est dépendante de l'hormone est s'effectue au niveau de la lysine 388 localisée dans la région N-terminale, cette SUMOylation inhibe l'activité transcriptionnelle [282, 283]. La phosphorylation de la sérine 294 diminue la SUMOylation de lysine 388 en réponse aux signaux mitogéniques et augmente la transactivation de PR-B de manière semblable à la DéSUMOylation par SENP1 [284].

5-9-4-Récepteur des minéralocorticoides

MR possède cinq consensus de SUMOylation. Sa SUMOylation implique les PIAS1xα, PIASy et s'effectue en présence du ligand au niveau des lysines 89, 399, 428, 494 et 953. La mutation des sites de SUMOylation engendre un faible regain d'activité. En présence de l'agoniste, MR recrute Ubc9 et PIAS1 dont la surexpression exerce une action répressive qui dépend du contexte du promoteur. La répression par PIAS1 n'est pas due à son rôle dans la SUMOylation car les mutants de SUMOylation sont inhibés en présence de PIAS1 [285, 286].

5-9-5-ERR

L'inactivation de la région aminoterminale de ERRγ implique la SUMOylation des lysines 14 et 40. Les mutations de ces sites augmentent la transactivation de ERRγ. La SUMOylation des lysines 14 et 40 dépend de la phosphorylation des sérines 19 et 45. Quand les sites de phosphorylation sont mutés en alanine, ERRγ perd sa SUMOylation et regagne une activité transcriptionnelle. Par contre, quand les sites de phosphorylation sont remplacés par un phosphomimétique, cela conduit à une augmentation de la de SUMOylation et une à une inhibition de la transactivation de ERRγ [230].

Problématique

Tamoxifène est le médicament de choix pour le traitement des tumeurs ER+ de tous les stades avant ou après la ménopause. Cependant, le succès de cette thérapie peut se heurter à une résistance *de novo* ou à une résistance acquise due à l'exposition au tamoxifène. Afin de se doter de stratégies alternatives, le développement de nouveaux composés a conduit à une deuxième génération de composés antioestrogéniques appelés antioestrogènes. Fulvestrant ou ICI 182, 780 est le seul antioestrogène total approuvé en clinique. Des doses de 500 mg sont administrées mensuellement aux patientes après la ménopause advenant la résistance à tamoxifène. Les inhibiteurs de l''aromatase sont une bonne alternative, il peuvent également être administré dans le contexte de récidive après la thérapie antioestrogénique.

Un fort potentiel antiprolifératif et proapoptotique de Fulvestrant est observé dans les modèles cellulaires et animaux de plus, Fulvestrant n'a pas de résistance croisée avec tamoxifène. Cependant, les essais cliniques n'indiquent qu'un taux de réponse de 10 % quand Fulvestrant est utilisé en deuxième ligne thérapeutique. Il a été suggéré que ce sont les propriétés pharmacologiques de Fulvestrant qui limitent son usage car des concentrations bien en deçà des doses utilisées *in vitro* sont détectées dans les biopsies de tumeurs.

Notre compréhension des mécanismes d'action des antioestrogènes a été stimulée par la résolution des structures cristallographiques du LBD de ERα avec son ligand naturel et avec les antioestrogènes. Deux observations majeures ont découlé de ces travaux. Tout d'abord, les hélices H3, H4, H5, et H12 du LBD constituent une interface pour le recrutement des Co activateurs transcriptionnels. Deuxièmement, l'interaction de la chaine latérale des antioestrogènes avec l'hélice H12 serait à la base de l'inactivation de ERα. Ce mécanisme est commun aux deux types d'antioestrogènes, bien que la structure résultante soit différente. En même temps, il a été démontré que Fulvestrant induit une forte polyubiquitylation de ERα suivie de sa dégradation. Dès lors, l'inactivation des gènes cibles des oestrogènes par Fulvestrant fut attribuée en majeure partie à sa capacité à réduire les niveaux de ERα. Néanmoins, les facteurs impliqués dans la polyubiquitination et la dégradation de ERα sont toujours inconnus et la séquence des événements entre la liaison

de Fulvestrant et la dégradation de ERα par le proteasome 26S restent à déterminer. En nous basant sur les éléments ci-dessus nous avons émis l'hypothèse suivante;

L’inactivation de ERα en présence des antioestrogènes stotaux implique des modifications post-traductionnelles et des interactions protéiques

Pour tester l'hypothèse suivante nous nous sommes fixés les objectifs suivants;

Objectif 1: Identifier les partenaires protéiques et les modifications pos traductionnelles qui jouent un rôle dans l'inactivation et la dégradation de ERα en présence des AEs totaux.

Objectif 2: Définir l'anti-oestrogénicité totale et la caractérisation du rôle de l'hélice H12 du LBD de ERα.

Résultats

1 er Article : Role of SUMOylation in full antioestrogenicity

(publié dans *Molecular and cell biology* Journal le 05 juillet 2012)

Role of SUMOylation in full antiestrogenicity

Khalid Hilmi[1,2,*], Nader Hussein[1,2,*], Rodrigo Mendoza-Sanchez[3], Mohamed El-Ezzy[2], Houssam Ismail[2], Chantal Durette[2,4], Maria Johanna Rozendaal[1,§], Martine Bail[1], Michel Bouvier[1,2], Pierre Thibault[2,4], James L. Gleason[3] and Sylvie Mader[1,2,#]

* co-first authors.

[1] Biochemistry Department, Université de Montréal, Montréal, Québec, H3C 3J7 Canada.

[2] Institute for Research in Immunology and Cancer, Université de Montréal, Montréal, Québec, H3C 3J7 Canada.

[3] Chemistry Department, McGill University, Montreal, Québec, H3A 2K6 Canada

[4] Chemistry Department, Université de Montréal, Montréal, Québec, H3C 3J7 Canada.

[#] Corresponding author

Materials and methods: 2382 words

Introduction, Results, Discussion: 5066 words

[§] Now at Biochemistry Department, Stanford University, Stanford, California, 94305, USA.

ABSTRACT

The selective estrogen receptor downregulator (SERD) fulvestrant can be used as second line treatment in patients having relapsed after treatment with tamoxifen, a selective estrogen receptor modulator (SERM), suggesting different mechanisms of action. Unlike tamoxifen, SERDs are devoid of partial agonist activity. While the full antiestrogenicity of SERDs may result in part from their capacity to down-regulate levels of estrogen receptor alpha (ERα) through proteasome-mediated degradation, SERDs are also fully antiestrogenic in the absence of increased receptor turnover in HepG2 cells. Here we report that SERDs induce a rapid and strong SUMOylation of ERα in ERα-positive and -negative cell lines including in HepG2 cells. In derivatives of the SERD ICI164,384, SUMOylation was dependent on the length of the side chain and correlated with the degree of antiestrogenicity. Four sites of SUMOylation were identified by mass spectrometry analysis in HEK293 cells. Preventing SUMOylation by overexpression of a SENP desumoylase partially derepressed transcription in the presence of full antiestrogens in HepG2 cells without increasing activity in the presence of agonists or of the SERM tamoxifen. Our results reveal that ERα SUMOylation contributes to full antiestrogenicity in the absence of accelerated receptor turnover.

INTRODUCTION

Estrogens, mainly 17beta-estradiol (E2), play a crucial role in normal breast development, but also contribute to mammary tumorigenesis. Antiestrogens (AEs) used for breast cancer treatment and prevention, such as tamoxifen (Tam), raloxifene (Ral) or fulvestrant (9, 17, 52, 63), block the proliferative effects of estrogens on breast epithelial and carcinoma cells by competing for estrogen receptors (ERα and ERβ). Similar to other nuclear receptors, ERs activate gene transcription by binding to specific DNA sites and recruiting transcriptional coactivators in a ligand-dependent manner (13, 40, 41, 70, 85).

AEs prevent ER activation through induction of an altered conformation of receptor ligand binding domain that suppresses recruitment of coactivators (8, 66, 79) and/or increases recruitment of co-repressors (23, 34, 45, 61, 77, 83, 94). However, selective ER modulators (SERMs, which include Tam and Ral) have partial agonist activity in a tissue- and gene-specific manner. For example, both have estrogenic effects on bone mass (6), and Tam has estrogenic effects on the uterus (2, 5, 21, 88, 90), while Ral does not cause uterine hypertrophy (6). Tam and to a lesser extent Ral also have partial agonist activity in breast cancer cells in a gene-specific manner (22). Tissue-specific recruitment of coactivators and co-repressors is thought to underlie selective partial agonist activity and alterations in these expression patterns in breast could contribute to development of resistance to AE-based therapy (23, 37, 38, 45, 77, 81, 82).

Other AEs such as ICI164,384, ICI182,780 (Fulvestrant) or RU58,668 have no estrogenic activity in rodent uterotrophic assays (7, 89, 92) and can inhibit growth of cell

lines or tumors resistant to SERMs (9, 18, 59, 78). They are designated as full AEs or Selective Estrogen Receptor Downregulators (SERDs) due to their capacity to accelerate ERα turnover in expressing tissues and cells, while Tam stabilizes the receptor (15, 27, 28, 48, 50, 69, 95). ERα is ubiquitinated in the absence as well as in the presence of ligand, but full AEs increase the rate of ubiquitination by about 2-fold in HeLa cells, and proteasome inhibitors abrogate the enhanced receptor degradation induced by full antiestrogens in MCF7 cells (95). Nevertheless, the importance of accelerated ERα turnover to full antiestrogenicity is currently under debate; indeed, overexpression of ERα saturated the capacity of cells to degrade the receptor without loss of antiestrogenicity (93). In addition, accelerated ERα turn-over induced by full AEs is not observed in all cell models. For instance, ICI182,780 stabilizes the receptor to the same extent as Tam and Ral in HepG2 cells (50), yet while Tam displays partial agonist activity in this cell model, ICI182,780 and Ral have inverse agonist activity (10, 19, 50, 56, 62). Further, our observation that both ICI182,780 and Ral induce accumulation of the receptor in an insoluble fraction in HepG2 cells in a manner dependent on the conformation of helix 12 in the LBD suggested mechanisms of antiestrogenicity other than induced degradation (50).

Here, we explored the modifications of both endogenous and transiently expressed ERα forms in the presence of full AEs and observed that the receptor is SUMOylated. SUMOylation is a covalent modification regulating the subcellular localization, turnover or activity of target proteins (26, 29-31, 43, 74), often correlating with inactivation of transcription factors (25, 51, 91). SUMO proteins, which share structural similarities with

ubiquitin, are attached via an isopeptide linkage to lysine residues of target proteins. The SUMO conjugation pathway is similar to that of ubiquitin, but with distinct activating (SAE1-2), conjugating (Ubc9) and ligase (PIAS proteins, nucleoporin RanBP2, polycomb protein Pc2, TRIM proteins) enzymes (12, 14, 26, 36, 55). SUMO-specific proteases (SENPs) contribute both to SUMO activation by cleavage prior to ligation and to reversal of SUMOylation and are thus responsible for the rapid dynamics of SUMO modification (14, 55, 99).

Unlike other nuclear receptors (67), ERα does not contain the consensus SUMOylation sequence ΨKXE/D, where K is the targeted lysine, Ψ is a hydrophobic residue (usually I, L or V) and X is any amino acid (71). However, conjugation can also occur at Lys residues outside this motif (35), and SUMO-1 modification of ERα in the presence of estrogen was recently reported (76). We find that SERDs, and to a more limited and variable extent the SERM raloxifene, induce rapid and marked SUMOylation of ERα at multiple sites. ERα SUMOylation is dependent on the length of the AE side chains and correlates with full antiestrogenicity. Abrogation of SUMOylation increases transcriptional activity specifically in the presence of full AEs. These observations indicate that ERα SUMOylation contributes to the specific pharmacological profile of full AEs.

MATERIALS AND METHODS

Materials

Transfection reagent polyethlenimine PEI was purchased from Polysciences, Inc. Proteasome inhibitor (MG132) was from Calbiochem. N-ethylmaleimide (NEM) was from Thermo Scientific. Proteases and phosphatases inhibitors, Doxycyclin, 17β-estradiol (E2), 4-hydroxytamoxifene (OHT), Raloxifene (Ral), Fulvestrant (ICI 182,780) Coelenterazine H were from Sigma. RU58,668, RU39,411 were provided by Dr. Jack Michel Renoir (CNRS, France). Anti-Flag M2 Affinity Gel, mouse monoclonal anti-tubulin and mouse monoclonal anti-Flag M2 were purchased from Sigma. Mouse monoclonal anti-SUMO1 (anti-GMP-1) antibody was from Zymed and rabbit polyclonal anti-SUMO-2/3 antibody was purchased from Invitrogen. Rabbit monoclonal anti-ERα antibody (clone 60C) was from Upstate. Mouse monoclonal Anti-ERα MAB-463 antibody was from Chemicon. The rabbit polyclonal anti-ERα antibody (HC20), rabbit polyclonal anti-His-Tag antibody, mouse monoclonal anti-Pol II antibody, and mouse monoclonal anti-Cytokeratin 5/8 were purchased from Santa Cruz Biotechnology Inc. NiNTA agarose was from Qiagen. Horseradish peroxidase conjudated secondary antibodies were purchased from Jackson. Polyvinylidene difluoride (PVDF) membranes were from Millipore and ECL detection reagent was from PerkinElmer. Synthesis of ICI164,384-derived antiestrogens is described in the Supplementary Materials and Method section.

Constructs and expression vectors

pSG5-ERα expression vector was kind gift from Dr Chambon (IGBMC France). pcDNA3-EGFP-Flag, pTET-ON (rtTA) and pRevTRE-EGFP-Flag were kindly provided from Dr Sylvain Meloche (IRIC, Université de Montréal, Canada). pcDNA3-HA-Flag-SENP1 was a gift from Dr O'hare (Marie Curie Research Institute, UK). YFP SUMO3 and YFP SUMO1G were a kind gift from Mary Dasso (National Institutes of Health, Bethesda, MD). Mutations L539A, L540A, and L541A were generated by site-directed mutagenesis of the ERα cDNA (the sequence of oligonucleotides used for mutagenesis is available upon request). cDNAs encoding the ERα wild-type, ABCD, DEF, CDEF, ABDEF (delta-DBD) and EF were generated by PCR amplification of ERα cDNA. The PCR products were cloned between PacI and PmeI restriction sites, replacing EGFP in pCDNA3-EGFP-Flag. To construct pRevTRE-HEG0-Flag, PCR-amplified ERα was inserted between PacI and PmeI restriction sites in pRevTRE-EGFP-Flag with concomitant elimination of EGFP. All recombinant vectors were verified by DNA sequencing of inserted cDNAs, and western analysis of protein expression.

Cell culture and transient transfection

All cell lines were purchased from American Type Culture Collection (ATCC). HepG2 and HEK293 cells were maintained at 37ºC in Dulbecco's modified Eagle's medium (Wisent) supplemented with 10% fetal bovine serum (Sigma), 2mM L-glutamine and 100 U/ml penicillin-streptomycin (Wisent). MCF7 cells were maintained in α-MEM (alpha

Modification of Eagle's medium) supplemented with 10% FBS, 2mM L-glutamine and 100 U/ml penicillin-streptomycin. T47D and T47D-KBluc cells were maintained respectively in RPMI 10% fetal bovine serum100 U/ml penicillin-streptomycin. Three days before all experiments, cells were switched to phenol red-free DMEM containing 10% charcoal-stripped serum (FBS-T). MCF7 Tet-on ERα cells were generated by stable retroviral infection of the pTET ON rTTA expression vector followed by a second round of infection with pRevTRE-ERα-Flag. Cells were induced with doxycyclin 0.5μg/ml for 48 h prior to experiments. HEK 293 cells were seeded at a density of 3.5x 10^6 cells per 10 cm petri dish in phenol red-free DMEM containing 10% charcoal-stripped serum. 24 hours later, the cells were transfected using polyethylenimine (10 μg of PEI per μg DNA). HEK293 cells stably expressing a His_6-SUMO3 mutant (24) were cultured in DMEM High Glucose (Hyclone SH30081.02) supplemented with 10% FBS (Fisher), 1% L-glutamine and 1% Penicillin/Streptomycin (Fisher).

Immunoblotting and immunoprecipitation

Cells were washed with ice-cold PBS and harvested in PBS containing 10 mM N-ethylmaleimide. For the preparation of whole cell extracts, pellets were resuspended in buffer containing 50 mM Tris-Cl pH7.5, 150 mM NaCl, 2% SDS, 0.5% Triton X-100, 1% NP40, 20 mM N-ethylmaleimide and a mixture of proteases and phosphatases inhibitors. Samples were sonicated using a Bioruptor (Diagenode) for 16 min at medium power level and an interval of 30 seconds between pulses. Following sonication, samples were

centrifuged for 10 minutes at 12 000 x g and total proteins were quantified with a DC protein assay (Bio Rad). Aliquots standardized for protein contents were denatured in Laemmli sample buffer (2% SDS, 10% Glycerol, 60 mM Tris-Cl pH 6,8 0,01% Bromophenol blue, 100 mM DTT) for 5 min at 95 ^{0}C and resolved on 7% SDS-PAGE. After electrotransfer, the PVDF membrane was blocked by incubation at room temperature for 1h in PBS supplemented with 0.2% Tween 20 and 5% nonfat dry milk. ERα was detected with the rabbit monoclonal anti-ERα clone 60C antibody and HRP-conjugated anti-rabbit. Complexes were revealed by enhanced chemiluminescence (PerkinElmer Corp.) as recommended by the manufacturer. For solubility Assay, soluble fractions were prepared by three freeze-thaw cycles using high salt buffer (400 mM KCl, 20% Glycerol, 20 mM Tris-Cl, 2 mM EDTA) as previously described (58). For immunoprecipitation of ERα, cell lysates (in 50 mM Tris-Cl pH7.5, 150 mM NaCl, 2% SDS, 0.5% Triton X-100, 0.5% SDS, 1% NP40, 20 mM N-ethylmaleimide) were diluted to 0.02% SDS. After pre-clearing, immunoprecipitation was performed overnight at 4 C using a rabbit polyclonal anti-ERα antibody HC20 and protein A sepharose. Flagged ERα was immunoprecipitated in the same conditions using M2 Flag beads. Following immunopreciptation three washes in buffer containing 50 mM Tris-Cl pH7.5, 150 mM NaCl. 5mM EDTA were performed, protein complexes were denaturated in 1X Laemmli sample buffer described above.

Cell fractionation

Cell fractionation was prepared as described (20). Cells were washed twice with PBS at 4ºC and soluble proteins (cytoplasm-nucleoplasm fraction) were extracted by treatment for 10 min with ice-cold cytoskeleton (CSK) buffer (100 mM NaCl, 300 mM sucrose, 10 mM PIPES, 3 mM $MgCl_2$ and 0.5% Triton X-100, pH 6.8) containing protease inhibitors (pepstatin A, aprotinin, leupeptin, phenylmethylsulphonyl fluoride (PMSF)), phosphatase inhibitors (sodium fluoride, sodium orthovanadate, β-glycerol phosphate, sodium pyrophosphate) and ribonuclease inhibitor 20 units/ml. The salt–labile cytoskeleton and chromatin proteins were removed by treatment with extraction buffer 250 mM $((NH_4)_2SO_4$, 300 mM sucrose, 10 mM PIPES, 3 mM $MgCl_2$ and 0.5% Triton X-100, pH 6.8) containing protease and phosphatase inhibitors and ribonuclease inhibitor. The samples were incubated at 4°C for 5 minutes then centrifuged for 5 minutes at 500 x g. The supernatant is part of the Chromatin Bound (CB) fraction. The chromatin fraction was removed by digestion with RNAse-free DNAse I (100 μg/ml) in digestion buffer (CSK plus 50 mM NaCl) containing protease inhibitors and ribonuclease inhibitor for 30 min at room temperature. Digestion was stopped by gently adding extraction buffer as used before and incubated 5 min at 4ºC. Cells were centrifuged for 5 min at 15,000x g, 4ºC. Supernatants were added to the chromatin-bound fractions. The remaining pellet, essentially composed of nuclear matrix components, was ressupended using in in buffer containing 50 mM Tris-Cl pH7.5, 150 mM NaCl, 2% SDS, 0.5% Triton X-100, 1% NP40, and briefly sonicated. The samples of each fraction were quantified for protein content and subjected to SDS

PAGE and Western blotting. Tubulin, Pol II and cytokeratin 5/8 were used respectively as markers for the CN, CB and NM fractions.

Luciferase reporter assays

HepG2 cells (10^6 cells) were transiently transfected by electroporation with the expression vector of ERα (400 ng), the reporter vector ERE3-TATA-Luc or GREB1ERE-TATA-Luc (200 ng) and a CMV-β-galactosidase internal control expression vector (400 ng), complemented with salmon sperm DNA to 8 μg total DNA. Electroporated cells were seeded in 6-well plates (approximately 10^6 cells per well). 16 hours after transfection, cells were treated with E2 (25 nM), OHT (100 nM), ICI182,780 (100 nM), Ral (100 nM) or vehicle (ethanol). For structure activity relationship studies, cells were treated with ICI 164, 384 derivatives (5μM) alone or in combination with E2 (5nM). Cells were lysed after another 24 hours and aliquots of whole cell extracts were assayed for luciferase activity in the presence of luciferin with a Veritas Microplate luminometer (Turner Biosystems). Results were normalized for ß-galactosidase activity revealed with α- Nitrophenyl β-D-Galactopyronsiadse (ONPG) and measured at 420 nm with a Spectramax 190 plate reader (Molecular Devices).

T47D cells that stably express a luciferase reporter vector were treated with ICI164,384 derivatives (5 μM) alone or in combination with TSA (300 nM) for 16 h. The relative luciferase signal was obtained by normalizing the luciferase signals to that of the

vehicle treatment. Each experiment was carried in triplicate and repeated at least three times.

BRET

For BRET assays, HEK 293 cells were seeded in 24 well plates at a density of 2.10^5 cells per well. After 24 h, they were cotransfected with RLuc-ERα (RLuc tag added on the N-terminus of ERα) and plasmids encoding YFP-SUMO3, HA-Flag-SENP1 and YFP-SUMO1G (as a control). The following day cells were treated with vehicle (ethanol) and ICI 182 780 (100 nM).

Cells were washed twice in PBS 48 h later and harvested with in PBS containing 5 mM EDTA and supplemented with ICI182,780 (100 nM) or vehicle (ethanol). Aliquots containing 100,000 cells were distributed in 96-well microplates (white Optiplates, Packard Instruments). Coelenterazine H was added to a final concentration of 5 μM, and readings were immediately collected on a Mithras LB 940 (Berthold Technologies,) with sequential integration of signals detected at 485 nm (*Renilla* luciferase emission) and 530 nm (YFP emission). The Net BRET ratio was calculated as described (49) and YFP-SUMO to RLuc-ERα ratios were calculated for each amount of transfected YFP-SUMO expression vector in the presence of a fixed amount of the RLuc-ERα vector as the total YFP signal measured by direct YFP stimulation [YFP] minus the basal YFP signal from cells transfected with only RLuc-ERα [YFP0] divided by the RLuc signal [RLuc] in the cotransfected cells.

HEK293 SUMO3 mutant cell culture and purification of SUMOylated ERα

HEK293 cells stably expressing His_6-SUMO3Q92RQ93N mutant (10^6 cells/replicate) were cultured as reported previously (24) and were transfected with an expression vector for ERα wt. Cells were washed with ice cold PBS containing N-ethyl maleimide (NEM, 10 mM) and centrifuged at 1000 g for 5 min. Cells were lysed in buffer A (6 M Guanidine-HCl; 100 mM NaH_2PO_4; 5 mM imidazole; 10 mM Tris-HCl pH 8; 10 mM β-mercaptoethanol; 20 mM NEM supplemented with proteases and phosphatases inhibitors). Cell lysates were sonicated using an ice-water bath Bioruptor (Diagenode) at setting (medium power output) for 16 cycles of 30 s followed by 30 s cooling interval. The sonicated lysates were centrifuged for 10 minutes at 12 000 g. Following protein quantification with Bradford protein assay (BioRad), pull down of His-tagged protein was performed by Ni-NTA agarose beads (Qiagen) overnight at 4 ^oC. His-tagged proteins retained by Ni-NTA agarose beads were washed three times with 10 ml of the buffer A supplemented with 10 mM imidazole and then twice with 10 ml of buffer B (8 M urea, 100 mM NaH_2PO_4, 10 mM Tris-HCl pH 6.3) and once in ice cold PBS. Immobilized proteins in 50 mM ammonium bicarbonate were reduced with 5 mM tris(2-carboxyethyl)phosphine, TCEP (Pierce) for 20 min at 37°C and then alkylated with 50 mM chloroacetamide (Sigma-Aldrich) for 20 min at 37°C. Excess chloroacetamide was reacted with a solution of 50 mM dithiothreitol. The solution was digested overnight with modified trypsin (1:50, enzyme:substrate ratio) at 37 ºC under high agitation speed. The digest was acidified with

trifluoroacetic acid (TFA), desalted using an Oasis HLB cartridge (Waters) and dried in a speed vac concentrator.

Mass Spectrometry analysis of SUMOylated peptides

LC-MS/MS analyses were performed on a nano-LC 2D pump (Eksigent) coupled to a LTQ-Orbitrap Velos mass spectrometer via a nanoelectrospray ion source (Thermo Fisher Scientific). Peptides were loaded on an Optiguard SCX trap column (5 µm particle, 300Å, 0.5 ID x 23 mm, Optimize Technologies) and eluted on a 360 μm ID x 4 mm, C_{18} trap column prior to separation on a custom-made 150 µm ID x 10 cm nano-LC column (Jupiter C_{18}, 3 µm, 300 Å, Phenomenex). Tryptic digests were loaded on the SCX trap and sequentially eluted using salt plugs of 0, 250, 500, 750 mM, 1 and 2 M ammonium acetate, pH 3.5. Peptides were separated on the analytical column using a linear gradient of 5-40% acetonitrile (0.2% formic acid) in 53 min with a flow rate of 600 nL/min. The mass spectrometer was operated in data dependent mode to automatically switch between survey MS and MS/MS acquisitions. The conventional MS spectra (survey scan) were acquired in the Orbitrap at a resolution of 60 000 for *m*/*z* 400 after accumulation of 10^6 ions in the linear ion trap. Mass calibration used a lock mass from ambient air [protonated $(Si(CH_3)_2O))_6$; m/z 445.120029], and provided mass accuracy within 5 ppm for precursor and fragment ion mass measurements. MS/MS spectra were acquired in HCD activation mode using an isolation window of 2 Da. Precursor ions were accumulated to a target value of 30000 with a maximum injection time of 100 ms and fragment ions were

transferred to the Orbitrap analyzer operating at a resolution of 15000 at *m/z* 400. The dynamic exclusion of previously acquired precursor ions was enabled (repeat count 1, repeat duration: 30 s; exclusion duration 45 s).

MS data were acquired using the Xcalibur software (version 2.1 build1139). Peak lists were generated using Mascot distiller (version 2.3.2.0, Matrix science) and MS/MS spectra were searched against a concatenated target/decoy IPI human database containing 75429 forward sequences (version 3.54, released Jan 2009) using Mascot (version 2.3.2, Matrix Science) to achieve a false-positive rate of less than 2% ($p < 0.02$). MS/MS spectra were searched with a mass tolerance of 10 ppm for precursor ions and 0.05 Da for fragments. The number of allowed missed cleavage sites for trypsin was set to 3 and phosphorylation (STY), oxidation (M), deamidation (NQ), carbamidomethylation (C) and SUMOylation (K) (GGTQN: SUMO3) were selected as variable modifications. A software application was developed to search mascot generic files (mgf) for specific SUMO3 fragment ions (e.g. *m/z* 132.0768, 226.0822, 243.1088, 344.1565, 401.1779; and neutral losses of SUMO3 remnant) to produce a mgf file containing only MS/MS spectra of potential SUMOylated peptide candidates. SUMO fragment ions were removed from the corresponding mgf files and searched again using Mascot as indicated above. Manual inspection of all MS/MS spectra for modified peptides was performed to validate assignments.

Docking studies

Docking studies were performed using the default settings of Glide 5.5 (Maestro v2009 suite, Schrodinger). The pdb file of crystal structure of ERβ complexed to ICI164,384 (1HJ1) was prepared using the Protein Preparation Wizard and the ligands to be docked were prepared by LigPrep (both modules within the Maestro suite). The images were generated from the docking studies using a registered copy of the 'Educational-Use-Only' edition of PyMOL.

RESULTS

Fulvestrant induces resistance to extraction in detergent-free buffers and post-translational modifications of ERα prior to receptor degradation in MCF7 cells.

The full antiestrogen ICI182,780 (Fulvestrant) induces accelerated ERα degradation in the luminal breast cancer cell line MCF7 (27, 48, 50, 54, 95). However, this is not observed in HepG2 cells where ERα becomes resistant to extraction in detergent-free buffers (50). Accumulation of the receptor in an insoluble fraction was also reported as soon as 20 min after fulvestrant addition in MCF7 (27). To assess properties of ERα prior to receptor depletion, MCF7 cells were treated with or without ICI182,780 and the proteasome inhibitor MG132 for variable times and ERα levels were assessed by Western analysis in high-salt or total extracts (Fig. 1). ERα levels dropped rapidly (as soon as 10 min after ligand addition) in high salt buffer in the presence of ICI182,780, whether in the absence or presence of MG132 (Fig. 1A). On the other hand, this decline was more progressive in total extracts and was abrogated by treatment with the proteasome inhibitor MG132 (Fig. 1B).

Consistent with previous reports, these results indicate that insolubility precedes degradation in ER+ MCF7 cells.

Strikingly, modified forms of the receptor were observed in total extracts both in the absence and presence of MG132 (Fig. 1B, bottom panels). These forms peaked at 45 min in the absence of MG132, but continued to accumulate in its presence. In addition, a basal level of modified forms was observed only in the presence of MG132, possibly representing ubiquitinated forms of the receptor (Fig. 1B, bottom right panel). Modified forms induced in the presence of ICI182,780 were more discrete, consisting mainly of two relatively low molecular weight bands compared to the ladder observed with MG132 in the absence of ligand (Fig. 1B, bottom right panel). To investigate whether these modified forms are associated with a specific nuclear sub-fraction, we performed serial fractionation of MCF7 cells into cyto-nuclear, chromatin-bound and nuclear matrix fractions. Modified forms were detected in the chromatin-bound and nuclear matrix fractions, and more faintly in the cyto-nuclear fraction (Fig. S1), suggesting either that modification enzymes are present in all fractions or that the receptor rapidly equilibrates between these fractions. By contrast, a modified form of the receptor was observed in the absence of ligand only in the nuclear matrix fraction.

The full antiestrogen Fulvestrant induces rapid SUMOylation of ERα.

The molecular weight of modified receptor bands suggested addition of ubiquitin-like molecules. Interestingly, SUMOylation of ERα in the presence of estradiol was previously

reported in COS cells and MCF7 cells (76). SUMO molecules have a molecular weight similar to Ubi molecules and SUMOylation of transcription factors has been often, albeit not always, associated with transcriptional inactivation (25, 51, 91). To further investigate the nature of the observed fulvestrant-induced modifications, we immunoprecipitated an ERα-Flag fusion protein expressed in a doxycyclin-inducible manner in MCF7 cells. The ERα-Flag protein was detectable by western analysis using an anti-ERα antibody in cells expressing ERα-Flag, but not GFP-Flag, in the absence or presence of treatment with E2 or ICI182,780 for 1 h (Fig. 2A). Higher molecular weight bands recognized by the anti-ERα antibody accumulated in the presence of ICI182,780 in the immunoprecipitate with an anti-Flag antibody, whereas unmodified ERα was detected under all conditions (Fig. 2A). The modified forms, but not unmodified flagged ERα, were also recognized by an antibody directed against SUMO1 (Fig. 2A). In a similar experiment performed at different times after addition of ICI182,780, a SUMO2/3 antibody also revealed multiple modified forms of ERα, with an apparent shift to higher molecular weight forms at 2 h (Fig. 2B). Finally, immunoprecipitation of endogenous ERα in MCF7 cells after 2h treatment with ICI182,780 or vehicle also revealed SUMO1-modified forms that were more abundant in the presence of MG132 (Fig. 2C).

SUMOylation of ERα in the presence of ICI182,780 was not limited to ER-expressing breast cancer cells, as it was also observed in ER-negative HEK293 cells transiently transfected with an ERα-Flag expression vector. ERα bands modified by endogenous SUMO1 or SUMO2/3 were detected in the presence of ICI182,780 after anti-Flag

immunoprecipitation (Fig. 3A-B). Conversely, SUMOylation was not detected in the absence of treatment or in the presence of E2 in HEK293 cells.

We next turned to Bioluminescence Resonance Energy Transfer (BRET) to investigate the effect of ligands on SUMOylation in live cells. HEK293 cells were co-transfected with an expression vector for ERα fused to Renilla luciferase at its N-terminus together with an expression vector for SUMO1 or SUMO3 fused to an N-terminal YFP tag (64). SUMOylation of ERα should result in energy transfer between the luciferase and YFP tags (65). As a negative control, we used the SUMO1G mutant carrying a single C-terminal glycine that is refractory to conjugation (4). BRET titration curves performed with increasing concentrations of SUMO1 or SUMO3 and a fixed concentration of ERα in the presence of ICI182,780 for 2 h displayed typical hyperbolic curves indicative a specific interaction (65); net BRET ratios for SUMO3 in ICI182,780 treated cells is significantly different from those obtained for untreated cells or for the SUMO1G mutant in the absence or presence of ICI (p-value < 0.05, Dunn's Multiple Comparison Test). In contrast to ICI182,780, E2 induced SUMOylation to a much smaller but statistically significant extent compared to absence of treatment with SUMO1G. These results indicate that ERα is SUMOylated in a rapid manner both in ER+ MCF7 breast cancer and in transiently transfected HEK293 cells after addition of the SERD fulvestrant.

Induction of ERα SUMOylation is a general property of full antiestrogens.

We next examined whether all AEs induced SUMOylation comparable to that observed with ICI182,780. MCF7 cells were treated with different antiestrogens for 1 h (100 nM). Modified ERα bands were observed in a western analysis in the presence of full AEs ICI812,780, RU58,668 and ICI164,384, but not in the absence of treatment or in the presence of E2, OHT or RU39,411 (Fig. 4A). Faint modified forms were observed in the presence of Ral under longer exposures (data not shown). To confirm the identity of the modified forms, HEK293 cells transiently transfected with the ERα-Flag expression vector were subjected to immunoprecipitation with an anti-Flag antibody followed by western analysis with either an anti-ERα or an anti-SUMO2/3 antibody. Strong SUMOylated bands were observed after treatment with the three full AEs (ICI182,780, RU58,668 and ICI164,384). Only faint modified bands were observed with the SERMs Raloxifene and RU39,411, and none with OHT (Fig. 4B). These results were confirmed in a more quantitative manner using BRET, which indicated that SUMOylation levels induced by E2 and OHT were inferior to those seen in the presence of RU39,411 and Ral, which in turn were lower than those induced by ICI164,384, RU58,668 and ICI182,780 (Fig. S2).

Antiestrogen side chain length is critical for SUMOylation.

While all AEs prevent the agonist-induced conformation of helix H12 on top of the ligand-binding cavity due to steric hindrance with the antiestrogen side chains, alternative positioning of H12 in the coactivator-binding groove was observed only in the presence of

SERMs (8, 66, 79). In the crystal structure of ERβ complexed to the SERD ICI164,384, the side chain prevents the association of H12 with the coactivator binding groove. The structure of H12 is unresolved, suggesting that H12 is highly mobile (66). The length of the AE side chain may thus control the differential functional properties of SERMs and SERDs through differences in H12 positioning. To determine the impact of the size of the side chain on ERα SUMOylation and full antiestrogenicity, we synthesized a series of SERD derivatives of ICI164,384 with different side chain lengths. We also placed the amide in the side chain at position 5 (C4 linker) instead of 11 (C10 linker) in order to assess its importance in full antiestrogenicity. Molecules with side chains containing 16 (as in ICI164,384) or 19 (as in ICI182,780) atoms were synthesized, as well as shorter (13 or 15 atoms) and longer (22 atoms) side chains (Fig. 5A).

MCF7 cells were incubated with the different AEs (5 μM final) for 4 hours and levels of unmodified and modified receptors were determined by western analysis. Modified ERα forms were detected in the presence of AEs with 15, 16, or 19 atoms (Fig. 5B). Antiestrogens with a shorter side chain (13 or 14 atoms) failed to induce SUMOylation detectably in this assay. The position of the amide could be shifted from position 11 as in ICI164,384 (C10(16)) to position 5 (C4(16)) without loss in SUMOylation (Fig. 5B). BRET assays in HEK293 cells also revealed a correlation of SUMOylation with increasing chain length except for the C10(22) compound, with maximal SUMOylation induced by AEs with 15, 16, or 19 atom side chains (Fig. S2).

To assess antiestrogenicity, we examined effects of compounds on ERα transcriptional activity of in HepG2 cells, widely-used to distinguish between partial and full AEs (10, 19, 50, 56, 62). Ligand-induced patterns of SUMOylation were similar in HepG2 and MCF7 cells (Fig. S3). In HepG2 cells, ERα transcriptional activity measured using ERE3-TATA-Luciferase was induced by the SERMs RU39,411 and OHT (2-3 fold compared to 10-fold with E2), whereas full AEs RU58,668, ICI182,780 or ICI164,384 displayed inverse agonist activity, repressing the activity of the unliganded receptor to background levels (Fig. 5C). The SERM Ral also efficiently repressed basal activity, correlating with efficient induction of SUMOylation in HepG2 cells (data not shown, but see also Fig. 9). Interestingly, the ICI164,384 derivative with a 13 atom side chain (C10(13)), which did not induce SUMOylation, displayed partial agonist activity comparable to that of OHT and RU39,411. On the other hand, derivatives C10(15) and C10(19), which induce ERα SUMOylation, displayed inverse agonist activity like the parental ICI164,384 or other full AEs. Placing the amide group at position 5, which did not alter SUMOylation, also did not affect inverse agonist activity (see C4(16)). Derivatives C10(14) and C10(22), which induced poor SUMOylation (Fig. 5B and Fig. S3), repressed transcriptional activity only to basal levels. Note that all molecules repressed E2 agonist activity (Fig. 5C), indicating that they bound ERα at the concentrations used and that the activity observed reflects their degree of antagonism/agonism.

Finally, we assessed the activity of our AEs in the ER+ breast cancer cell line T47D-KBluc, which stably carries an estrogen-dependent reporter vector in which luciferase

expression is controlled by a minimal ERE3-TATA promoter (97). While transcriptional activity was very low in the presence of the SERD ICI164,384, partial agonist activity was detected with the C10(13), C10(14) and C10(22) compounds (Fig. S4B). However, the C10(15), C10(16) and C10(19) compounds did not induce any detectable transcriptional activity, similar to SERDs ICI164,384, fulvestrant and RU58,668. In addition, while SERMs also did not yield detectable transcriptional activity alone, treatment with the HDAC inhibitor TSA resulted in gain in agonist activity with SERMs OHT, Ral and RU39,411 as previously reported (53). No gain of activity was observed with SERDs or with compounds C15, C16 and C19, further demonstrating their SERD-like properties (Fig. S4B). Note that SUMOylation was also observed in the presence of compounds C10(15), C10(16) and C10(19) but not of the other derivatives in T47D cells (Fig. S4A)**.** These results indicate that SUMOylation of ERα is dependent on the length of the AE side chain, which in this series of ICI164,384 derivatives is optimal between 15-19 atoms, and correlates with full antiestrogenicity both in transiently transfected HepG2 cells and in ER-positive T47D cells.

Mutations in helix H12 affect both SUMOylation and antiestrogenicity.

Consistent with the hypothesis that positioning of helix 12 is an important discriminator between SERMs and SERDs, several point mutants in H12 have been previously described to result in increased partial transcriptional activity in the presence of SERDs (50). Mutation of long hydrophobic amino acids L539 and L540 into alanines

results in increased transcriptional activity in the presence of fulvestrant, while mutating amino acid L541 had not effect (50). Of interest, the two inactivating mutations also strongly reduced SUMOylation in HepG2 cells, while mutation L541 did not affect SUMOylation (Fig. 6). These results indicate that SUMOylation also correlates with full antiestrogenicity in ER mutants in the presence of fulvestrant.

ERα is SUMOylated at several residues in the presence of full antiestrogens.

In order to assess whether SUMOylation induced by full AEs affects one or several ERα domains, we first used a mutant where all Lys residues in the hinge region were mutated to Arg residues (Fig. S5, 5KR mutant). This mutant was previously reported to strongly reduce SUMOylation of ERα in the presence of E2 (76). Marked SUMOylation of ERα was still observed in the presence of ICI182,780 with this mutant, suggesting that other domains of ERα can be targeted by SUMOylation in the presence of full AEs. We next tested SUMOylation of mutants deleted for various regions. Exposure of these mutants to ICI182,780 for 1 h indicated that deletion of the AB domain (mutant CDEF) was tolerated, while deletion of the C (ΔC) and A-C (mutant DEF) domains abrogated SUMOylation (Fig. 7).

To assess SUMOylation sites of ERα in a more direct manner, we expressed the receptor in HEK293 cells stably expressing a His-Tagged mutant form of SUMO3 that allows immunopurification of SUMOylated forms (24). Cells were pretreated with MG132 for 2 h and then ICI182,780 was added for an additional 8 h before extraction in denaturing

buffer. SUMOylated proteins were purified on a His-affinity column and digested with trypsin. Modified tryptic peptides bearing the remnant side chain from the mutant SUMO3 were enriched by immunopurification and analyzed by LC-MS/MS. Independent mass spectrometry analyses performed on two independent protein extracts revealed SUMOylation of ERα at residues K171, K180, K299, and K472 (Fig. 8A). Confirmation of modified residues was obtained from the high resolution HCD MS/MS spectra of the corresponding tryptic peptides where specific SUMO3 reporter ions were observed at *m/z* 132.08, 243.11 (Fig. 8B-E). The first two sites (K171, K180) are located in the ERα N-terminal domain just before the DNA-binding domain, while K299 is in the hinge region and K472 in the steroid-binding domain. Interestingly, the tryptic peptide comprising the remnant SUMO3 chain at K171 was also identified with a phosphorylated S167 residue (Fig. 8B). This residue was previously reported as a major estrogen-induced phosphorylation site accounting for almost 50 % of the phosphorylation on ERα in human MCF-7 mammary carcinoma cells (3). Whether S167 phosphorylation regulates K171 SUMOylation is presently unknown, but we note that mutation of S167 to alanine did not abrogate fulvestrant-induced SUMOylation of ERα (Fig. S5). Our mass spectrometry analyses also revealed the phosphorylation of residues S282, S576 and S578 (data not shown). Recent reports have also identified S282 as a phosphorylation site (96). Finally, ICI182,780 still induced strong SUMOylation of a mutant of K171, K180 and all 5 hinge domain lysines including K299, indicating that additional sites can be SUMOylated (7KR

mutant, Fig. S5). These results reveal that AEs induce SUMOylation of ERα at multiple sites.

Induction of ERα SUMOylation contributes to full antiestrogenicity in HepG2 cells.

To investigate the role of sumoylation in full antiestrogenicity, we cotransfected HepG2 cells with an expression vector for the desumoylase SENP1 (Flag-SENP1). Expression of Flag-SENP1 (Fig. 9A) resulted in loss of the high molecular weight modified ERα forms. Note that we also observed a dose-dependent suppression of ERα SUMOylation in BRET experiments in HEK293 cells expressing Flag-SENP1 (Fig. S6). We then investigated the effect of SENP1 expression on transcriptional activity of ERα in the presence of different ligands using the reporter vector GREB1 ERE-TATA-Luc. Transfection of SENP1 did not affect basal or Tam-induced luciferase activity, but de-repressed ERα activity in the presence of full antiestrogens and Ral, leading to an ~4-fold increase in transcriptional activity that was highly statistically significant (Fig. 9B). Similar results were obtained with the ERE3-TATA-Luc construct (data not shown). In conclusion, induction of ERα SUMOylation contributes to suppression of ERα transcriptional activation properties in a cell model where full antiestrogens do not induce more rapid ERα degradation.

Role of antiestrogen side chain length in full antiestrogenicity.

To investigate how the side chain length may affect the structure of the ERα LBD, ICI164,384 was changed to our various derivatives by molecular replacement within the ERβ structure. In the active ER conformation (8), H12 folds on top of the binding pocket revealing a coactivator recognition surface involving also helices 3, 4, 5, which form a shallow pocket and a second deeper pocket connected by a hydrophobic groove, where the leucines from the NR-box of coactivators can interact. In the crystal structure of ICI164,384 complexed to ERβ (PDB code: 1HJ1, (66)), where H12 is not resolved, the long side chain of the ligand bends towards the coactivator binding surface where the butyl group of the amide directly interacts with the shallow pocket formed by residues Leu-261, Met-264, Ile-265, and Leu- 286 (corresponding to Leu-354, Met-357, Ile-258 and L379 in hERα) without extending into the deeper pocket.

We hypothesized that the length dependence in the side chain for SUMOylation may result from the ability to interact with the hydrophobic pockets and/or connecting groove. We assessed this possibility with molecular docking using Glide (Glide 5.0, Shrodinger LLC) to dock a library of 24 secondary amides with side chains ranging from 7 to 24 atoms in total, including our synthesized SERD derivatives, to the 1HJ1 protein crystal structure. Through a visual inspection of the poses that resulted from our docking experiment, we observed that side chains with lengths of 7 to 12 atoms were not sufficiently long to reach the coactivator binding groove (Fig. 10B). A chain length of 13 atoms was able to reach the edge of the first shallow pocket, but not sufficiently long to fill the space in the pocket (Fig.

10C). Molecules with a side-chain length of 14 atoms were sufficiently long to reach and fill the first shallow pocket. As the side chain increased in size, some were able to fill the pocket and also extend into the connecting hydrophobic groove (Fig. 10D-E). With side-chains of 20-atoms or longer, the docking results indicated an ability to bind in the first pocket but either with a bowed conformation in the center of the chain so that the end of the chain interacted with the first pocket or with a significant turn to put the middle of the chain in the pocket and the end of the chain pointing away from the hydrophobic groove (Fig. 10F). We interpret this as the molecules being too long to fit properly within the co-activator binding groove. The docking observations are consistent with the experimental results where the transition to gain in SUMOylation activity occurs at a chain length of 14 atoms, is significant for chain lengths of 15-19 atoms and then diminishes with longer chain lengths.

DISCUSSION

The effects of SUMOylation on transcriptional activity of nuclear receptors have been studied mostly in the presence of agonists and appear to be receptor-specific. One study reported that SUMOylation potentiates transcriptional activity of agonist-bound glucocorticoid receptor (GR) (46), whereas other studies concluded that SUMOylation represses transcription induced by GR, the progesterone receptor or the androgen receptor (1, 60, 68, 86). E2 was previously shown to induce SUMOylation of ERα in the hinge region, resulting in enhanced transcriptional activity (76). In addition, Ubc9 and PIAS1/3 proteins can act as ERα coactivators in a manner independent from their SUMOylation properties (42, 76). Our results indicate that full antiestrogens specifically induce a rapid and massive SUMOylation of ERα by SUMO1/2/3 in both ER-positive (MCF7 and T47D) and-negative (HEK293 and HepG2) cell lines. SUMOylation induced by full antiestrogens was observed under conditions where SUMO-modified forms are undetectable in the presence of E2 in MCF7 or HEK293 cells. Weaker E2-induced SUMOylation was however detected by BRET, possibly due to the overexpression of the YFP-SUMO fusion protein.

SUMOylation of ERα is highly induced by full antiestrogens such as ICI164,384, ICI182,780 or RU58,668, but to a much lesser extent or not detectably by SERMs such as OHT, Ral or RU39,411. Ral has a different pattern of partial agonist activity compared to Tam, and is known to behave as a full antiestrogen in HepG2 (16). Interestingly, this correlates with efficient induction of SUMOylation by Ral but not Tam in HepG2 cells. In

addition, inhibition of SUMOylation increased transcriptional activity of ERα complexed to Ral or to full antiestrogens, but not to Tam in these cells.

RU58,668 and RU39,411 share the same steroidal backbone but differ by their side chain. RU58,668, ICI182,780 and ICI164,384 have long side chains (16-19 atoms), whereas RU39,411 and other SERMs such as Tam and Ral have shorter side chains. We further demonstrated that side chain length is crucial for induction of ERα SUMOylation and correlates with full antiestrogenicity in variants of SERD ICI164,384. The interaction of the side chain of full AEs with the coactivator binding groove is thought to prevent H12 from associating with the groove, and thus stability of the helix, which may play a role in recruitment of the SUMOylation machinery. Hence, the gain of activity of H12 mutants (50) may be due to a stabilized association of the helix with the coactivator binding groove, or alternatively to interference of mutations in H12 with protein-protein interactions required for efficient SUMOylation and transcriptional inactivation of the receptor.

Although ligand-specific SUMOylation must result from conformational changes in the ligand binding domain induced by full AEs, domain deletion experiments indicated that the LBD alone is not detectably SUMOylated. Deletion of the AB region did not suppress SUMOylation, but region C appears to be necessary. While we have not detected SUMOylation sites in the DBD, this may be due to insufficient coverage in our mass spectrometry experiments. However, the DBD may alternatively play a role in recruitment of the SUMOylation machinery. Notably, a requirement for the C region for the estradiol-induced interaction between ER and Ubc9/PIAS1 was previously reported (42).

Mass spectrometry analysis of tryptic peptides from extracts enriched in His_6-SUMO3 modified proteins identified four SUMOylation sites. MS/MS spectra of the corresponding peptides showed specific fragment ions characteristic of the SUMO3 remnant side chains and confirmed the location of the modified residues. Of note, one the SUMOylation sites is located in the hinge region and is part of a group of 5 Lys residues found to be necessary for SUMOylation in the presence of E2 (76). Nevertheless, mutagenesis of these Lys residues combined to the three sites confirmed in our two mass spectrometry analyses did not detectably lower SUMOylation induced by full AEs. This could be due to compensation mechanisms, if secondary sites are SUMOylated in the absence of the main sites. However, it is also possible that a larger number of Lys residues are SUMOylated in wt ERα in the presence of full AEs (note that a coverage of 58% of the receptor sequence was attained in one of the two experiments after immunoprecipitation of SUMOylated peptides). Further studies will be needed to completely map the SUMO modification sites induced by full antiestrogens.

Significantly, inhibiting SUMOylation by overexpression of SENP proteins led to a ligand-specific gain in transcriptional activity that was not observed in the presence of E2 or Tam. Our results thus indicate that SUMOylation plays a role in full antiestrogenicity observed in the absence of induced receptor turnover. SUMOylation takes place more rapidly than receptor degradation in MCF7 cells, and hence may contribute to early transcriptional shut-off before receptor levels become limiting for transcriptional activation or when the degradation machinery is saturated (93).

The mechanisms by which SUMOylation suppresses ERα-dependent transcription in the presence of full AEs remain to be fully investigated. SUMOylation may alter several nuclear receptor properties, such as subcellular location, interaction with DNA or with cofactors, as observed for a variety of other proteins (26, 29-31, 43, 74). For instance, the corepressor DAXX1 has been found to contain a SUMO-interacting motif that mediates its corepressor role with glucocorticoid, mineralocorticoid and androgen receptors as well as with a series of other transcription factors (11, 47, 80). However, while an interaction between ERα and endogenous DAXX was detected in co-immunoprecipitation experiments in HEK293 cells it appeared not to be ligand-modulated (data not shown). In this respect, we note that SUMOylation was found to inhibit GR independently of DAXX (32). SUMOylated ERα complexed to full AEs may interact with other SIM domain-containing corepressors or chromatin remodeling enzymes (33, 57, 75). In addition, the nuclear matrix protein Sp100 as well as the nuclear body organizer PML also contain SIMs (39, 64) and may interact with SUMOylated ERα in the nuclear matrix fraction. Recruitment of SUMO ligases to ERα in the presence of full AEs may also result in the modification of ERα cofactors in addition to the receptor itself. SUMOylation of cofactors AIB1 and PGC1 was shown to attenuate their coactivating properties (72, 98) while the corepressor activities of NCoR and NRIP1 were potentiated by SUMOylation (73, 87). Future experiments will need to characterize protein complexes formed by ERα complexed to full antiestrogens and investigate the SUMOylation status of these proteins. Finally, the relationship between SUMOylation and other properties of full AEs such as insolubility and degradation needs to

be investigated. Insolubility appears early after ligand addition, preceding SUMOylation, and is not affected by loss of receptor SUMOylation due to cotransfection of SENP1 or deletion of the DNA binding domain (Fig. S7). On the other hand, all ligands inducing insolubility led to SUMOylation, suggesting that insolubility may be necessary for SUMOylation. In addition, it will be of interest to investigate a potential role of SUMOylation in degradation of the receptor by a mechanism similar to the SUMO-dependent ubiquitination of PML (44, 84).

Together, our results indicate that full AEs induce a major increase in the rate of SUMOylation of the receptor, and that SUMOylation contributes to full antiestrogenicity. in the absence of enhanced ERα degradation. Significantly, SUMOylation has the potential of inhibiting ERα transcription with faster kinetics than those expected simply from induced loss of ERα, resulting in transcriptional shut-off subsequently reinforced by loss of the receptor protein.

ACKNOWLEDGEMENTS

This work was supported by grants from the Canadian Breast Cancer Alliance and the Cancer Research Society, Inc. SM holds the CIBC breast cancer research chair at Université de Montréal. KH, MEE and HI have been recipient of awards from the Faculté des Études Supérieures de l'Université de Montréal and MEE and HI received Perseverance M. Sc. fellowships. NH was recipient of a fellowship from the Montreal Center for Experimental Therapeutics in Cancer. RMS was supported by a scholarship from CIHR (Strategic Training Initiative in Chemical Biology) and a CONACyT (Consejo Nacional de Ciencia y Tecnología) graduate studies scholarship.

We are grateful to Muriel LeRomancer, Laura Corbo, Mary Dasso, Sylvain Meloche, Justyna Kulpa and David Cotnoir for generous gifts of plasmids. We are indebted to Xavier Mascle and Muriel Aubry for expert advice with SUMOylation and BRET assays.

REFERENCES:

1. **Abdel-Hafiz, H., G. S. Takimoto, L. Tung, and K. B. Horwitz.** 2002. The inhibitory function in human progesterone receptor N termini binds SUMO-1 protein to regulate autoinhibition and transrepression. J Biol Chem **277:**33950-6.
2. **Anzai, Y., C. F. Holinka, H. Kuramoto, and E. Gurpide.** 1989. Stimulatory effects of 4-hydroxytamoxifen on proliferation of human endometrial adenocarcinoma cells (Ishikawa line). Cancer Research **49:**2362-5.
3. **Arnold, S. F., J. D. Obourn, H. Jaffe, and A. C. Notides.** 1994. Serine 167 is the major estradiol-induced phosphorylation site on the human estrogen receptor. Mol Endocrinol **8:**1208-14.
4. **Ayaydin, F., and M. Dasso.** 2004. Distinct in vivo dynamics of vertebrate SUMO paralogues. Mol Biol Cell **15:**5208-18.
5. **Barsalou, A., W. Gao, S. Anghel, J. Carriere, and S. Mader.** 1998. Estrogen response elements can mediate agonist activity of antiestrogens in human endometrial Ishikawa cells. J. Biol. Chem. **273:**17138-17146.
6. **Black, L. J., M. Sato, E. R. Rowley, D. E. Magee, A. Bekele, D. C. Williams, G. J. Cullinan, R. Bendele, R. F. Kauffman, W. R. Bensch, C. A. Frolik, J. D. Termine, and H. U. Bryant.** 1994. Raloxifene (LY139481 HCI) prevents bone loss and reduces serum cholesterol without causing uterine hypertrophy in ovariectomized rats. J. Clin. Invest. **93:**63-9.

7. **Bowler, J., T. J. Lilley, J. D. Pittam, and A. E. Wakeling.** 1989. Novel steroidal pure antiestrogens. Steroids **54:**71-99.

8. **Brzozowski, A. M., A. C. Pike, Z. Dauter, R. E. Hubbard, T. Bonn, O. Engstrom, L. Ohman, G. L. Greene, J. A. Gustafsson, and M. Carlquist.** 1997. Molecular basis of agonism and antagonism in the oestrogen receptor. Nature **389:**753-8.

9. **Bundred, N., and A. Howell.** 2002. Fulvestrant (Faslodex): current status in the therapy of breast cancer. Expert Rev Anticancer Ther **2:**151-60.

10. **Castro-Rivera, E., and S. Safe.** 2003. 17 beta-estradiol- and 4-hydroxytamoxifen-induced transactivation in breast, endometrial and liver cancer cells is dependent on ER-subtype, cell and promoter context. J Steroid Biochem Mol Biol **84:**23-31.

11. **Chang, C. C., M. T. Naik, Y. S. Huang, J. C. Jeng, P. H. Liao, H. Y. Kuo, C. C. Ho, Y. L. Hsieh, C. H. Lin, N. J. Huang, N. M. Naik, C. C. Kung, S. Y. Lin, R. H. Chen, K. S. Chang, T. H. Huang, and H. M. Shih.** 2011. Structural and functional roles of Daxx SIM phosphorylation in SUMO paralog-selective binding and apoptosis modulation. Mol Cell **42:**62-74.

12. **Chu, Y., and X. Yang.** 2011. SUMO E3 ligase activity of TRIM proteins. Oncogene **30:**1108-16.

13. **Claessens, F., and D. T. Gewirth.** 2004. DNA recognition by nuclear receptors. Essays Biochem **40:**59-72.

14. **Creton, S., and S. Jentsch.** 2010. SnapShot: The SUMO system. Cell **143:**848-848 e1.

15. **Dauvois, S., P. S. Danielian, R. White, and M. G. Parker.** 1992. Antiestrogen ICI 164,384 reduces cellular estrogen receptor content by increasing its turnover. Proc Natl Acad Sci U S A **89:**4037-41.

16. **Dayan, G., M. Lupien, A. Auger, S. I. Anghel, W. Rocha, S. Croisetiere, J. A. Katzenellenbogen, and S. Mader.** 2006. Tamoxifen and raloxifene differ in their functional interactions with aspartate 351 of estrogen receptor alpha. Mol Pharmacol **70:**579-88.

17. **Dunn, B. K., and L. G. Ford.** 2001. From adjuvant therapy to breast cancer prevention: bcpt and star. Breast J. **7:**144-147.

18. **England, G. M., and V. C. Jordan.** 1997. Pure antiestrogens as a new therapy for breast cancer. Oncol Res **9:**397-402.

19. **Fan, J. D., B. L. Wagner, and D. P. McDonnell.** 1996. Identification of the sequences within the human complement 3 promoter required for estrogen responsiveness provides insight into the mechanism of tamoxifen mixed agonist activity. Mol Endocrinol **10:**1605-16.

20. **Fey, E. G., K. M. Wan, and S. Penman.** 1984. Epithelial cytoskeletal framework and nuclear matrix-intermediate filament scaffold: three-dimensional organization and protein composition. J Cell Biol **98:**1973-84.

21. **Fisher, B., J. P. Costantino, C. K. Redmond, E. R. Fisher, D. L. Wickerham, and W. M. Cronin.** 1994. Endometrial cancer in tamoxifen-treated breast cancer patients: findings from the National Surgical Adjuvant Breast and Bowel Project (NSABP) B-14. J. Natl. Cancer Inst. **86:**527-37.

22. **Frasor, J., F. Stossi, J. M. Danes, B. Komm, C. R. Lyttle, and B. S. Katzenellenbogen.** 2004. Selective estrogen receptor modulators: discrimination of agonistic versus antagonistic activities by gene expression profiling in breast cancer cells. Cancer Res **64:**1522-33.

23. **Fujita, T., Y. Kobayashi, O. Wada, Y. Tateishi, L. Kitada, Y. Yamamoto, H. Takashima, A. Murayama, T. Yano, T. Baba, S. Kato, Y. Kawabe, and J. Yanagisawa.** 2003. Full activation of estrogen receptor alpha activation function-1 induces proliferation of breast cancer cells. J Biol Chem **278:**26704-14.

24. **Galisson, F., L. Mahrouche, M. Courcelles, E. Bonneil, S. Meloche, M. K. Chelbi-Alix, and P. Thibault.** 2011. A Novel Proteomics Approach to Identify SUMOylated Proteins and Their Modification Sites in Human Cells. Mol Cell Proteomics **10:**M110 004796.

25. **Garcia-Dominguez, M., and J. C. Reyes.** 2009. SUMO association with repressor complexes, emerging routes for transcriptional control. Biochim Biophys Acta **1789:**451-9.

26. **Gareau, J. R., and C. D. Lima.** 2010. The SUMO pathway: emerging mechanisms that shape specificity, conjugation and recognition. Nat Rev Mol Cell Biol **11:**861-71.

27. **Giamarchi, C., C. Chailleux, M. Callige, P. Rochaix, D. Trouche, and H. Richard-Foy.** 2002. Two antiestrogens affect differently chromatin remodeling of trefoil factor 1 (pS2) gene and the fate of estrogen receptor in MCF7 cells. Biochim Biophys Acta **1578:**12-20.

28. **Gibson, M. K., L. A. Nemmers, W. C. Beckman, Jr., V. L. Davis, S. W. Curtis, and K. S. Korach.** 1991. The mechanism of ICI 164,384 antiestrogenicity involves rapid loss of estrogen receptor in uterine tissue. Endocrinology **129:**2000-10.

29. **Gill, G.** 2004. SUMO and ubiquitin in the nucleus: different functions, similar mechanisms? Genes Dev **18:**2046-59.

30. **Gutierrez, G. J., and Z. Ronai.** 2006. Ubiquitin and SUMO systems in the regulation of mitotic checkpoints. Trends Biochem Sci **31:**324-32.

31. **Heun, P.** 2007. SUMOrganization of the nucleus. Curr Opin Cell Biol **19:**350-5.

32. **Holmstrom, S. R., S. Chupreta, A. Y. So, and J. A. Iniguez-Lluhi.** 2008. SUMO-mediated inhibition of glucocorticoid receptor synergistic activity depends on stable assembly at the promoter but not on DAXX. Mol Endocrinol **22:**2061-75.

33. **Ivanov, A. V., H. Peng, V. Yurchenko, K. L. Yap, D. G. Negorev, D. C. Schultz, E. Psulkowski, W. J. Fredericks, D. E. White, G. G. Maul, M. J. Sadofsky, M. M. Zhou, and F. J. Rauscher, 3rd.** 2007. PHD domain-mediated E3 ligase activity

directs intramolecular sumoylation of an adjacent bromodomain required for gene silencing. Mol Cell **28:**823-37.

34. **Jackson, T. A., J. K. Richer, D. L. Bain, G. S. Takimoto, L. Tung, and K. B. Horwitz.** 1997. The partial agonist activity of antagonist-occupied steroid receptors is controlled by a novel hinge domain-binding coactivator L7/SPA and the corepressors N-CoR or SMRT. Mol. Endocrinol. **11:**693-705.

35. **Jeram, S. M., T. Srikumar, P. G. Pedrioli, and B. Raught.** 2009. Using mass spectrometry to identify ubiquitin and ubiquitin-like protein conjugation sites. Proteomics **9:**922-34.

36. **Johnson, E. S.** 2004. Protein modification by SUMO. Annu Rev Biochem **73:**355-82.

37. **Johnston, S. R.** 1997. Acquired tamoxifen resistance in human breast cancer--potential mechanisms and clinical implications. Anticancer Drugs **8:**911-30.

38. **Keeton, E. K., and M. Brown.** 2005. Cell cycle progression stimulated by tamoxifen-bound estrogen receptor-alpha and promoter-specific effects in breast cancer cells deficient in N-CoR and SMRT. Mol Endocrinol **19:**1543-54.

39. **Kim, E. T., K. K. Kim, M. J. Matunis, and J. H. Ahn.** 2009. Enhanced SUMOylation of proteins containing a SUMO-interacting motif by SUMO-Ubc9 fusion. Biochem Biophys Res Commun **388:**41-5.

40. **Kininis, M., and W. L. Kraus.** 2008. A global view of transcriptional regulation by nuclear receptors: gene expression, factor localization, and DNA sequence analysis. Nucl Recept Signal **6:**e005.

41. **Kishimoto, M., R. Fujiki, S. Takezawa, Y. Sasaki, T. Nakamura, K. Yamaoka, H. Kitagawa, and S. Kato.** 2006. Nuclear receptor mediated gene regulation through chromatin remodeling and histone modifications. Endocr J **53:**157-72.

42. **Kobayashi, S., H. Shibata, K. Yokota, N. Suda, A. Murai, I. Kurihara, I. Saito, and T. Saruta.** 2004. FHL2, UBC9, and PIAS1 are novel estrogen receptor alpha-interacting proteins. Endocr Res **30:**617-21.

43. **Lallemand-Breitenbach, V., and H. de The.** 2010. PML nuclear bodies. Cold Spring Harb Perspect Biol **2:**a000661.

44. **Lallemand-Breitenbach, V., M. Jeanne, S. Benhenda, R. Nasr, M. Lei, L. Peres, J. Zhou, J. Zhu, B. Raught, and H. de The.** 2008. Arsenic degrades PML or PML-RARalpha through a SUMO-triggered RNF4/ubiquitin-mediated pathway. Nat Cell Biol **10:**547-55.

45. **Lavinsky, R. M., K. Jepsen, T. Heinzel, J. Torchia, T. M. Mullen, R. Schiff, A. L. Del-Rio, M. Ricote, S. Ngo, J. Gemsch, S. G. Hilsenbeck, C. K. Osborne, C. K. Glass, M. G. Rosenfeld, and D. W. Rose.** 1998. Diverse signaling pathways modulate nuclear receptor recruitment of N-CoR and SMRT complexes. Proc Natl Acad Sci U S A **95:**2920-5.

46. **Le Drean, Y., N. Mincheneau, P. Le Goff, and D. Michel.** 2002. Potentiation of glucocorticoid receptor transcriptional activity by sumoylation. Endocrinology **143:**3482-9.

47. **Lin, D. Y., Y. S. Huang, J. C. Jeng, H. Y. Kuo, C. C. Chang, T. T. Chao, C. C. Ho, Y. C. Chen, T. P. Lin, H. I. Fang, C. C. Hung, C. S. Suen, M. J. Hwang, K. S. Chang, G. G. Maul, and H. M. Shih.** 2006. Role of SUMO-interacting motif in Daxx SUMO modification, subnuclear localization, and repression of sumoylated transcription factors. Mol Cell **24:**341-54.

48. **Long, X., and K. P. Nephew.** 2006. Fulvestrant (ICI 182,780)-dependent interacting proteins mediate immobilization and degradation of estrogen receptor-alpha. J Biol Chem **281:**9607-15.

49. **Lupien, M., J. Eeckhoute, C. A. Meyer, Q. Wang, Y. Zhang, W. Li, J. S. Carroll, X. S. Liu, and M. Brown.** 2008. FoxA1 translates epigenetic signatures into enhancer-driven lineage-specific transcription. Cell **132:**958-70.

50. **Lupien, M., M. Jeyakumar, E. Hebert, K. Hilmi, D. Cotnoir-White, C. Loch, A. Auger, G. Dayan, G. A. Pinard, J. M. Wurtz, D. Moras, J. Katzenellenbogen, and S. Mader.** 2007. Raloxifene and ICI182,780 increase estrogen receptor-alpha association with a nuclear compartment via overlapping sets of hydrophobic amino acids in activation function 2 helix 12. Mol Endocrinol **21:**797-816.

51. **Lyst, M. J., and I. Stancheva.** 2007. A role for SUMO modification in transcriptional repression and activation. Biochem Soc Trans **35:**1389-92.

52. **MacGregor, J. I., and V. C. Jordan.** 1998. Basic guide to the mechanisms of antiestrogen action. Pharmacol Rev **50:**151-96.

53. **Margueron, R., V. Duong, S. Bonnet, A. Escande, F. Vignon, P. Balaguer, and V. Cavailles.** 2004. Histone deacetylase inhibition and estrogen receptor alpha levels modulate the transcriptional activity of partial antiestrogens. J Mol Endocrinol **32:**583-94.

54. **Marsaud, V., A. Gougelet, S. Maillard, and J. M. Renoir.** 2003. Various phosphorylation pathways, depending on agonist and antagonist binding to endogenous estrogen receptor alpha (ERalpha), differentially affect ERalpha extractability, proteasome-mediated stability, and transcriptional activity in human breast cancer cells. Mol Endocrinol **17:**2013-27.

55. **Melchior, F., M. Schergaut, and A. Pichler.** 2003. SUMO: ligases, isopeptidases and nuclear pores. Trends Biochem Sci **28:**612-8.

56. **Metivier, R., G. Penot, G. Flouriot, and F. Pakdel.** 2001. Synergism between ERalpha transactivation function 1 (AF-1) and AF-2 mediated by steroid receptor coactivator protein-1: requirement for the AF-1 alpha-helical core and for a direct interaction between the N- and C-terminal domains. Mol Endocrinol **15:**1953-70.

57. **Minty, A., X. Dumont, M. Kaghad, and D. Caput.** 2000. Covalent modification of p73alpha by SUMO-1. Two-hybrid screening with p73 identifies novel SUMO-1-interacting proteins and a SUMO-1 interaction motif. J Biol Chem **275:**36316-23.

58. **Nguyen, D., S. V. Steinberg, E. Rouault, S. Chagnon, B. Gottlieb, L. Pinsky, M. Trifiro, and S. Mader.** 2001. A G577R mutation in the human AR P box results in selective decreases in DNA binding and in partial androgen insensitivity syndrome. Mol Endocrinol **15:**1790-802.

59. **Nicholson, R. I., J. M. Gee, D. L. Manning, A. E. Wakeling, M. M. Montano, and B. S. Katzenellenbogen.** 1995. Responses to pure antiestrogens (ICI 164384, ICI 182780) in estrogen-sensitive and -resistant experimental and clinical breast cancer. Ann N Y Acad Sci **761:**148-63.

60. **Nishida, T., and H. Yasuda.** 2002. PIAS1 and PIASxalpha function as SUMO-E3 ligases toward androgen receptor and repress androgen receptor-dependent transcription. J Biol Chem **277:**41311-7.

61. **Norris, J. D., D. Fan, A. Sherk, and D. P. McDonnell.** 2002. A negative coregulator for the human ER. Mol Endocrinol **16:**459-68.

62. **Norris, J. D., D. Fan, M. R. Stallcup, and D. P. McDonnell.** 1998. Enhancement of estrogen receptor transcriptional activity by the coactivator GRIP-1 highlights the role of activation function 2 in determining estrogen receptor pharmacology. J Biol Chem **273:**6679-88.

63. **O'Regan, R. M., and V. C. Jordan.** 2001. Tamoxifen to raloxifene and beyond. Semin. Oncol. **28:**260-273.

64. **Percherancier, Y., D. Germain-Desprez, F. Galisson, X. H. Mascle, L. Dianoux, P. Estephan, M. K. Chelbi-Alix, and M. Aubry.** 2009. Role of SUMO in RNF4-

mediated promyelocytic leukemia protein (PML) degradation: sumoylation of PML and phospho-switch control of its SUMO binding domain dissected in living cells. J Biol Chem **284:**16595-608.

65. **Perroy, J., S. Pontier, P. G. Charest, M. Aubry, and M. Bouvier.** 2004. Real-time monitoring of ubiquitination in living cells by BRET. Nat Methods **1:**203-8.

66. **Pike, A. C., A. M. Brzozowski, J. Walton, R. E. Hubbard, A. G. Thorsell, Y. L. Li, J. A. Gustafsson, and M. Carlquist.** 2001. Structural insights into the mode of action of a pure antiestrogen. Structure (Camb) **9:**145-53.

67. **Poukka, H., P. Aarnisalo, U. Karvonen, J. J. Palvimo, and O. A. Janne.** 1999. Ubc9 interacts with the androgen receptor and activates receptor-dependent transcription. J Biol Chem **274:**19441-6.

68. **Poukka, H., U. Karvonen, O. A. Janne, and J. J. Palvimo.** 2000. Covalent modification of the androgen receptor by small ubiquitin-like modifier 1 (SUMO-1). Proc Natl Acad Sci U S A **97:**14145-50.

69. **Reid, G., M. R. Hubner, R. Metivier, H. Brand, S. Denger, D. Manu, J. Beaudouin, J. Ellenberg, and F. Gannon.** 2003. Cyclic, proteasome-mediated turnover of unliganded and liganded ERalpha on responsive promoters is an integral feature of estrogen signaling. Mol Cell **11:**695-707.

70. **Robinson-Rechavi, M., H. Escriva Garcia, and V. Laudet.** 2003. The nuclear receptor superfamily. J Cell Sci **116:**585-6.

71. **Rodriguez, M. S., C. Dargemont, and R. T. Hay.** 2001. SUMO-1 conjugation in vivo requires both a consensus modification motif and nuclear targeting. J Biol Chem **276:**12654-9.

72. **Rytinki, M. M., and J. J. Palvimo.** 2009. SUMOylation attenuates the function of PGC-1alpha. J Biol Chem **284:**26184-93.

73. **Rytinki, M. M., and J. J. Palvimo.** 2008. SUMOylation modulates the transcription repressor function of RIP140. J Biol Chem **283:**11586-95.

74. **Seeler, J. S., and A. Dejean.** 2003. Nuclear and unclear functions of SUMO. Nat Rev Mol Cell Biol **4:**690-9.

75. **Sekiyama, N., T. Ikegami, T. Yamane, M. Ikeguchi, Y. Uchimura, D. Baba, M. Ariyoshi, H. Tochio, H. Saitoh, and M. Shirakawa.** 2008. Structure of the small ubiquitin-like modifier (SUMO)-interacting motif of MBD1-containing chromatin-associated factor 1 bound to SUMO-3. J Biol Chem **283:**35966-75.

76. **Sentis, S., M. Le Romancer, C. Bianchin, M. C. Rostan, and L. Corbo.** 2005. Sumoylation of the estrogen receptor alpha hinge region regulates its transcriptional activity. Mol Endocrinol **19:**2671-84.

77. **Shang, Y., and M. Brown.** 2002. Molecular determinants for the tissue specificity of SERMs. Science **295:**2465-8.

78. **Shaw, L. E., A. J. Sadler, D. Pugazhendhi, and P. D. Darbre.** 2006. Changes in oestrogen receptor-alpha and -beta during progression to acquired resistance to

tamoxifen and fulvestrant (Faslodex, ICI 182,780) in MCF7 human breast cancer cells. J Steroid Biochem Mol Biol **99:**19-32.

79. **Shiau, A. K., D. Barstad, P. M. Loria, L. Cheng, P. J. Kushner, D. A. Agard, and G. L. Greene.** 1998. The structural basis of estrogen receptor/coactivator recognition and the antagonism of this interaction by tamoxifen. Cell **95:**927-37.

80. **Shih, H. M., C. C. Chang, H. Y. Kuo, and D. Y. Lin.** 2007. Daxx mediates SUMO-dependent transcriptional control and subnuclear compartmentalization. Biochem Soc Trans **35:**1397-400.

81. **Shou, J., S. Massarweh, C. K. Osborne, A. E. Wakeling, S. Ali, H. Weiss, and R. Schiff.** 2004. Mechanisms of tamoxifen resistance: increased estrogen receptor-HER2/neu cross-talk in ER/HER2-positive breast cancer. J Natl Cancer Inst **96:**926-35.

82. **Smith, C. L., Z. Nawaz, and B. W. O'Malley.** 1997. Coactivator and corepressor regulation of the agonist/antagonist activity of the mixed antiestrogen, 4-hydroxytamoxifen. Mol Endocrinol **11:**657-66.

83. **Takimoto, G. S., J. D. Graham, T. A. Jackson, L. Tung, R. L. Powell, L. D. Horwitz, and K. B. Horwitz.** 1999. Tamoxifen resistant breast cancer: coregulators determine the direction of transcription by antagonist-occupied steroid receptors. J Steroid Biochem Mol Biol **69:**45-50.

84. **Tatham, M. H., M. C. Geoffroy, L. Shen, A. Plechanovova, N. Hattersley, E. G. Jaffray, J. J. Palvimo, and R. T. Hay.** 2008. RNF4 is a poly-SUMO-specific E3

ubiquitin ligase required for arsenic-induced PML degradation. Nat Cell Biol **10:**538-46.

85. **Tavera-Mendoza, L. E., S. Mader, and J. H. White.** 2006. Genome-wide approaches for identification of nuclear receptor target genes. Nucl Recept Signal **4:**e018.

86. **Tian, S., H. Poukka, J. J. Palvimo, and O. A. Janne.** 2002. Small ubiquitin-related modifier-1 (SUMO-1) modification of the glucocorticoid receptor. Biochem J **367:**907-11.

87. **Tiefenbach, J., N. Novac, M. Ducasse, M. Eck, F. Melchior, and T. Heinzel.** 2006. SUMOylation of the corepressor N-CoR modulates its capacity to repress transcription. Mol Biol Cell **17:**1643-51.

88. **Tonetti, D. A., and V. C. Jordan.** 1996. Targeted anti-estrogens to treat and prevent diseases in women. Mol Med Today **2:**218-23.

89. **Van de Velde, P., F. Nique, F. Bouchoux, J. Bremaud, M. C. Hameau, D. Lucas, C. Moratille, S. Viet, D. Philibert, and G. Teutsch.** 1994. RU 58,668, a new pure antiestrogen inducing a regression of human mammary carcinoma implanted in nude mice. J Steroid Biochem Mol Biol **48:**187-96.

90. **Vanleeuwen, F. E.** 1994. Endometrial cancer during tamoxifen treatment. Lancet **343:**1048.

91. **Verger, A., J. Perdomo, and M. Crossley.** 2003. Modification with SUMO. A role in transcriptional regulation. EMBO Rep **4:**137-42.

92. **Wakeling, A. E., M. Dukes, and J. Bowler.** 1991. A potent specific pure antiestrogen with clinical potential. Cancer Res **51:**3867-73.

93. **Wardell, S. E., J. R. Marks, and D. P. McDonnell.** 2011. The turnover of estrogen receptor alpha by the selective estrogen receptor degrader (SERD) fulvestrant is a saturable process that is not required for antagonist efficacy. Biochem Pharmacol **82:**122-30.

94. **Webb, P., P. Nguyen, and P. J. Kushner.** 2003. Differential SERM effects on corepressor binding dictate ERalpha activity in vivo. J Biol Chem **278:**6912-20.

95. **Wijayaratne, A. L., and D. P. McDonnell.** 2001. The human estrogen receptor-alpha is a ubiquitinated protein whose stability is affected differentially by agonists, antagonists, and selective estrogen receptor modulators. J Biol Chem **276:**35684-92.

96. **Williams, C. C., A. Basu, A. El-Gharbawy, L. M. Carrier, C. L. Smith, and B. G. Rowan.** 2009. Identification of four novel phosphorylation sites in estrogen receptor alpha: impact on receptor-dependent gene expression and phosphorylation by protein kinase CK2. BMC Biochem **10:**36.

97. **Wilson, V. S., K. Bobseine, and L. E. Gray, Jr.** 2004. Development and characterization of a cell line that stably expresses an estrogen-responsive luciferase reporter for the detection of estrogen receptor agonist and antagonists. Toxicol Sci **81:**69-77.

98. **Wu, H., L. Sun, Y. Zhang, Y. Chen, B. Shi, R. Li, Y. Wang, J. Liang, D. Fan, G. Wu, D. Wang, S. Li, and Y. Shang.** 2006. Coordinated regulation of AIB1

transcriptional activity by sumoylation and phosphorylation. J Biol Chem **281:**21848-56.

99. **Yamaguchi, T., P. Sharma, M. Athanasiou, A. Kumar, S. Yamada, and M. R. Kuehn.** 2005. Mutation of SENP1/SuPr-2 reveals an essential role for desumoylation in mouse development. Mol Cell Biol **25:**5171-82.

FIGURE LEGENDS

Fig. 1: ICI 182,780 induces specific modifications of ERα in MCF7 cells.

MCF7 cells were pretreated or not with the proteasome inhibitor MG132 (10 μM) for 16 h, and then with or without ICI182,780 (100 nM) for indicated times. HSB soluble fraction (**A**) and whole cell extract (**B**) were resolved by SDS-PAGE, and ERα and tubulin levels were assessed by western blotting. Two different exposures are shown in **B.** to reveal both receptor degradation and modification.

Fig. 2: ICI 182, 780 induces SUMOylation of ERα in MCF7 cells.

A. and **B**. MCF7 cells expressing doxycyclin-inducible ERα-Flag or EGFP-Flag were treated with ICI182,780 (100 nM), E2 (25 nM) or vehicle for 1 h in **A** and with ICI182,780 or vehicle for 20 min or 2 h in **B**. ERα-Flag was immunoprecipitated from total cell extracts. After SDS–PAGE, SUMO1, SUMO2/3 and ERα levels were analyzed by western blotting. **C**. MCF7 cells were pretreated or not with the proteasome inhibitor MG132 (10 μM) for 3 h, then incubated with ICI182,780 (100 nM) or vehicle for 2h. Endogenous ERα was immunoprecipitated from total cell extracts. After SDS–PAGE, SUMO1 and ERα levels were assessed by western blotting.

Fig. 3: ICI 182, 780 induces ERα SUMOylation by SUMO1, 2, and 3 in transiently transfected HEK 293 cells.

A. and **B.** HEK 293 cells were transiently transfected with an expression vector for Flag-tagged ERα. 48 h later, cells were treated for 1 h with E2 (25 nM), ICI 182,780 (100 nM) or vehicle. ERα-Flag was immunoprecipitated from total cell extracts. Following SDS–PAGE, SUMO1, SUMO2/3 and ERα levels were analyzed by western blotting. **C.** BRET1 titration assay using HEK 293 cells cotransfected with a constant amount of RLuc-ERα wt and increasing amounts of YFP-SUMO3. As a control, the unprocessable form of SUMO1 (YFP-SUMO1G) was used to measure the BRET signal resulting from random collisions (BRET bystander effect). HEK 293 cells were treated with vehicle (0), E2 (25 nM) and ICI 182,780 (100 nM) for 2 h. The curves were fitted using nonlinear regression equation assuming a single binding site (GraphPad Prism). Standard deviation was calculated from triplicates of each condition.

Fig. 4: Full AEs, but not agonists or SERMs, induce efficient ERα SUMOylation.

A. MCF7 cells were treated for 1h with E2 (25 nM), OHT, RU39,411, Ral, ICI182,780 , RU 58,668, ICI 164, 384 (100 nM) or vehicle for 1h. Whole cell extracts were resolved on SDS-PAGE and ERα levels and tubulin levels were assessed by western blotting.

B. HEK293 were transiently transfected with the expression vectors for ERα-Flag or EGFP-Flag (0) for 48 h and treated with E2 (25 nM), antiestrogens OHT, RU39, 411, Ral, ICI182,780, ICI164,384, RU58,668 (100 nM) or vehicle for 1h. ERα-Flag was immunoprecipitated from total cell extracts. After SDS–PAGE, SUMO2/3 and ERα levels were assessed by western blotting.

Fig. 5: SUMOylation correlates with full antiestrogenicity in HepG2 cells.

A. The structures of derivatives of ICI164,384 with a carbone-sulfure bond at the begining of the AE side-chain. The steroid skeleton is identical in all ICI164,384 derivatives. **B.** Effects of derivatives on ERα SUMOylation in MCF7 cells. Cells were treated for 1 h with 5 nM E2 or 5 μM of antiestrogens including ICI164,384 derivatives. Whole cell extracts were resolved by SDS-PAGE and ERα levels were assessed by western blotting. **C.** HepG2 cells were transiently transfected with the expression vector for ERα, the reporter vector ERE3-TATA-Luc and the expression vector for CMV-β-galactosidase. Cells were treated 24 hours after transfection with 5 nM E2 and/or 5 μM of antiestrogens. Cells were lysed after another 24 h and aliquots of whole cell extracts were assayed for luciferase activity. The experiment was performed 2 times with similar results and a representative experiment is shown (mean values +/- SD from duplicates).

Fig. 6: Mutations in H12 that increase transcriptional activity in the presence of fulvestrant suppress SUMOylation of the receptor.

HepG2 cells were transiently transfected by electroporation with expression vectors for ERα wt or helix 12 mutants, or with the empty parental vector (0). Cells were treated 24 h after transfection with ICI182,780 (ICI) or vehicle (0). Cells were lysed after another 24 h and whole cell extracts were prepared. Following SDS-PAGE, ERα and tubulin levels were assessed by western blotting.

Fig. 7: Multiple domains of ERα are affected by SUMOylation

HEK 293 cells stably expressing His_6-SUMO3 mutant were transfected with the expression vectors for ERα full length (FL) or deletion mutants. 48h later, cells were treated for 1 h with ICI182,780 (100 nM) or vehicle (0). Flag-tagged proteins were immunoprecipitated from total cell extracts. Following SDS-PAGE, ERα truncated forms and His_6-SUMO3 modified proteins were assessed by western blotting using anti-Flag or anti-His tag antibodies. Arrow heads correspond to the non-modified forms of each construct at the expected molecular weight and stars indicate the lowest molecular weight His-SUMO modified form.

Fig. 8: Identification of SUMOylation sites by mass spectrometry. A. Distribution of SUMOylation and phosphorylation sites identified on ERα by mass spectrometry. **B.** High resolution tandem mass spectra of tryptic peptides corresponding to modified lysine residues at K171 (B), K180 (C), K299 (D) and K472 (E) acquired using HCD on the LTQ-Orbitrap Velos. Phosphorylated S167 is indicated by pS in panel (B). Mass accuracy of fragment ions was typically within 5 ppm of theoretical values.

Fig. 9: SUMOylation contributes to ICI182,780-induced ERα inactivation in HepG2 cells.

A. HepG2 cells were transfected with the expression vectors for ERα and the deSUMOylase SENP1 linked to a Flag epitope. The cells were treated for 24 h with E2 (25 nM), antiestrogens (100 nM) or vehicle alone. ERα and SENP1 levels were analyzed in whole cell extracts by SDS–PAGE and western blotting. **B**. HepG2 cells were transiently transfected with the expression vector for ERα alone or together with expression vectors for the deSUMOylase SENP1, with the GREB1 ERE-TATA-Luc reporter vector and the internal control CMV-β-galactosidase expression vector. Cells were treated as described above. Transcriptional activity of ERα was measured by luciferase activity normalized for β-galactosidase activity. The mean of six independent experiments ± SEM is represented on the graph. * p value < 0,01 (one-tailed t-test) between each individual treatment compared with or without SENP1 transfection.

Fig. 10: Representative docking solutions of ICI164,384 and derivatives in crystal structure of ERβ.

A. ICI164,384 and derivatives with **B.** a theoretical 9-atom long side-chain *N*-methyl-*N*-propyl 4-thiobutyramide, **C.** a 13-atom side chain C10(13), **D.** a 15-atom side chain C10(15), **E.** a 19-atom side chain C10(19) and **F.** a theoretical 21-atom side chain *N*-methyl-*N*-nonyl 10-thiodecanamide structures were modeled using Glide Software.

SUPPLEMENTAL FIGURES:LEGENDS

Fig. S1: ERα is modified in all nuclear sub-fractions in MCF7 cells treated with ICI182,780.

MCF7 cells were treated with E2 (25 nM), ICI 182,780 (100 nM) or vehicle for 1 h. Cytonuclear (CN), chromatin-bound (CB) and nuclear matrix (NM) fractions were prepared, aliquots containing equal amounts of total proteins were resolved by SDS-PAGE and ERα levels in each fraction were analyzed by western blot. Tubulin, PolII and CK5/8 were used as markers for fractionation.

Fig S2: SUMOylation is differentially induced by SERMs and full antiestrogens in a BRET assay.

HEK 293 cells were cotransfected with 20 ng of RLuc-ERα and 100 ng of YFP-SUMO3. HEK293 cells were treated 48 hours after transfection with 5 nM E2, 5 μM of antiestrogens including newly synthesized ICI164,384 derivatives. Interaction between RLuc-ERα and YFP-SUMO3 was measured in a BRET 1 assay. Standard deviation was calculated from triplicates of each condition and was added as error bars on the bar graph.

Fig. S3: Side-chain length-dependent SUMOylation in HepG2 cells.

HepG2 cells were transiently transfected with the expression vector for ERα. The cells were treated 24 h after transfection with E2 or antiestrogens (5 μM). Whole cell

extracts were prepared after another 24 h. Following SDS-PAGE, ERα and tubulin levels were assessed in each extract by western blotting.

Fig. S4: ERα is SUMOylated in T47D breast cancer cells following treatment with full antiestrogens.

A. T47D cells were treated with 5 μM of the designated compounds for 1 h. Whole cell extracts were resolved by SDS-PAGE and ERα protein levels were assessed by western blotting. **B.** T47D–KBluc cells were treated for 16 h with 5 μM of antiestrogens alone or with TSA (300 nM). Cells were then lysed and luciferase activity measured.

Fig. S5: Evidence for additional SUMOylation sites.

A. Schematic presentation of ERα SUMOylation mutants. **B**. HEK 293 were transiently transfected with the expression vectors of wild type ERα or lysine to arginine mutants. 36 h later, the cells were treated for 8 h with ICI 182, 780 (100 nM) or vehicle. Total cell extracts were prepared using 2% SDS containing buffer. ERα levels were assessed by western blotting.

Fig. S6: SENP1 overexpression suppresses ERα SUMOylation in BRET assay.

HEK 293 were cotransfected with of 20 ng RLuc-ERα, 10 ng YFP-SUMO3 or 10 ng YFP-SUMO1G and an increasing concentration of SENP1 expression vector. Cells were treated with vehicle and ICI 182, 780 (100 nM) for 2 h. Interaction between RLuc-ERα

with YFP-SUMO3 was measured by BRET 1 assay. Standard deviation was calculated from triplicates of each condition and was added as error bars on the bar graph.

Fig S7. DeSUMOylation does not prevent ERα association with the high-salt insoluble compartment.

A. HEK 293 were transiently transfected with expression vectors for wt or DBD-deleted ERα. **B.** Cells were transiently transfected with an expression vector for wt ERα combined with an expression vector for EGFP or the desumoylase SENP1. 48 h later, cells were treated for 1h with E2 (25 nM), ICI 182,780 (100 nM) or vehicle. HSB soluble fraction and whole cell extract were resolved by SDS-PAGE. Levels of wt ERα or its truncated form were analyzed by western blotting.

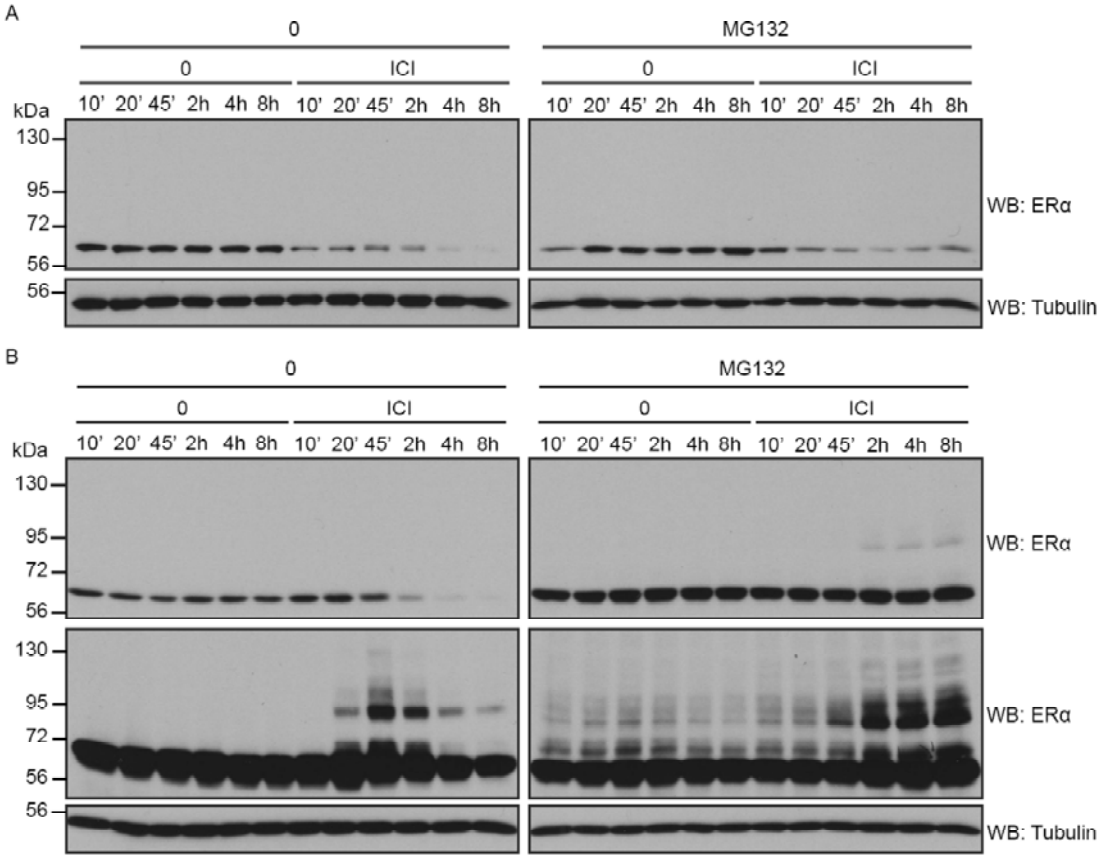

Fig. 1: ICI 182,780 induces specific modifications of ERα in MCF7 cells.

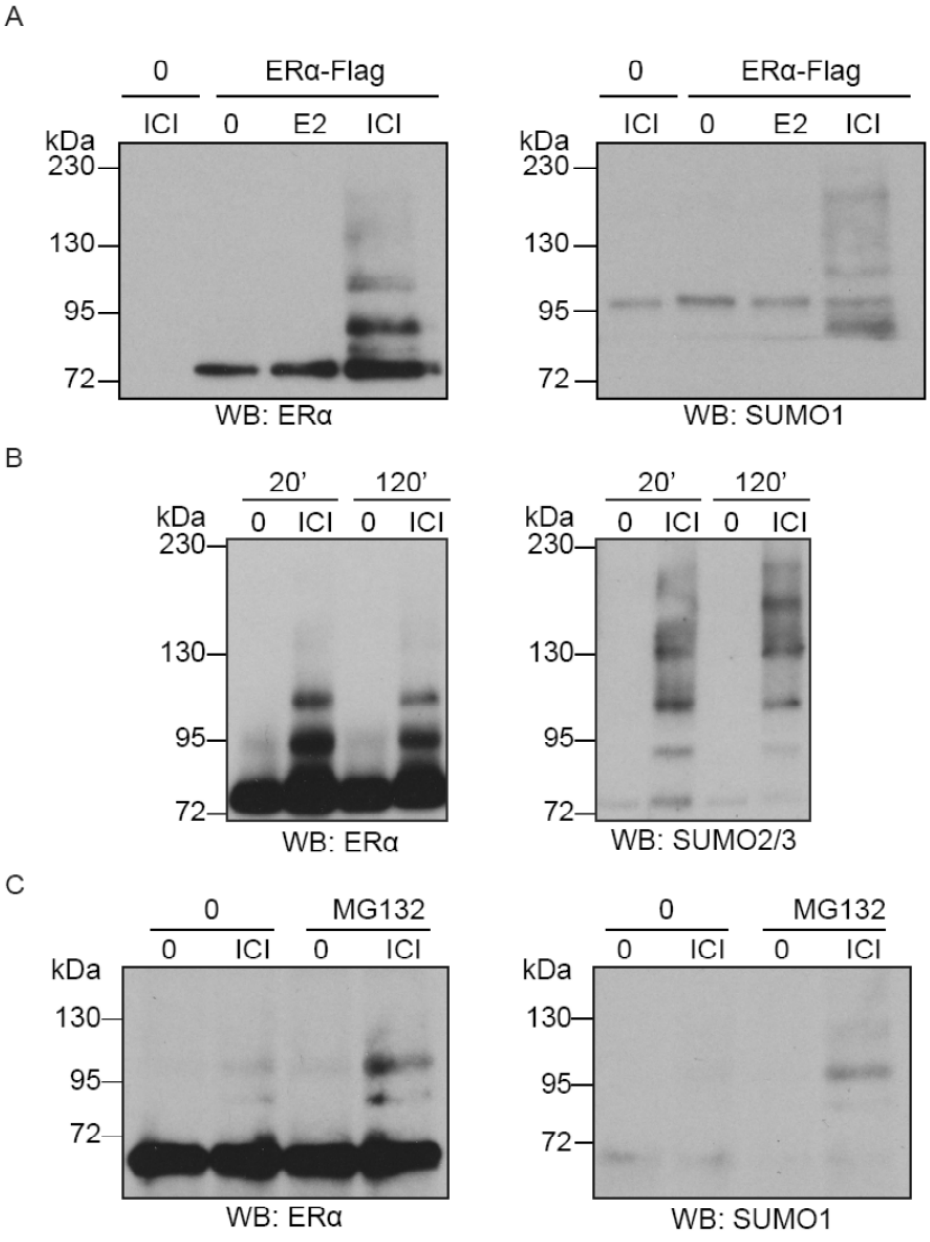

Fig. 2: ICI 182, 780 induces SUMOylation of ERα in MCF7 cells.

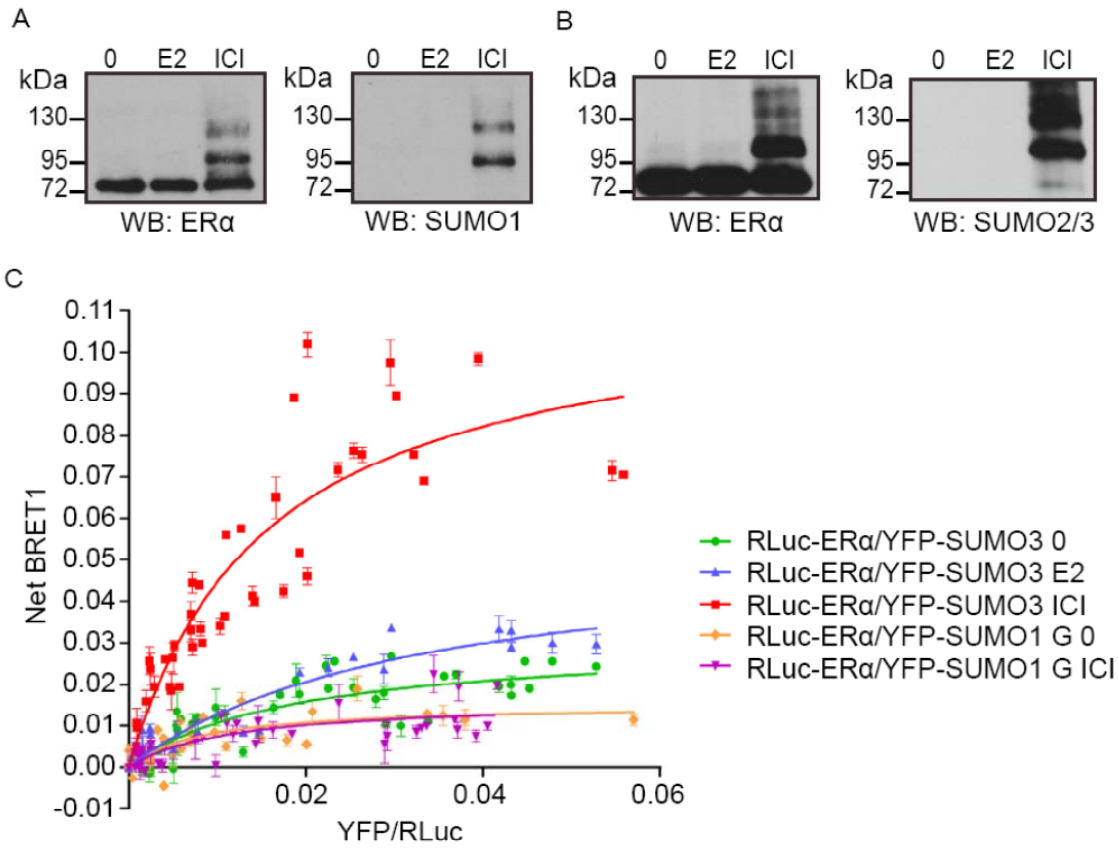

Fig. 3: ICI 182, 780 induces ERα SUMOylation by SUMO1, 2, and 3 in transiently

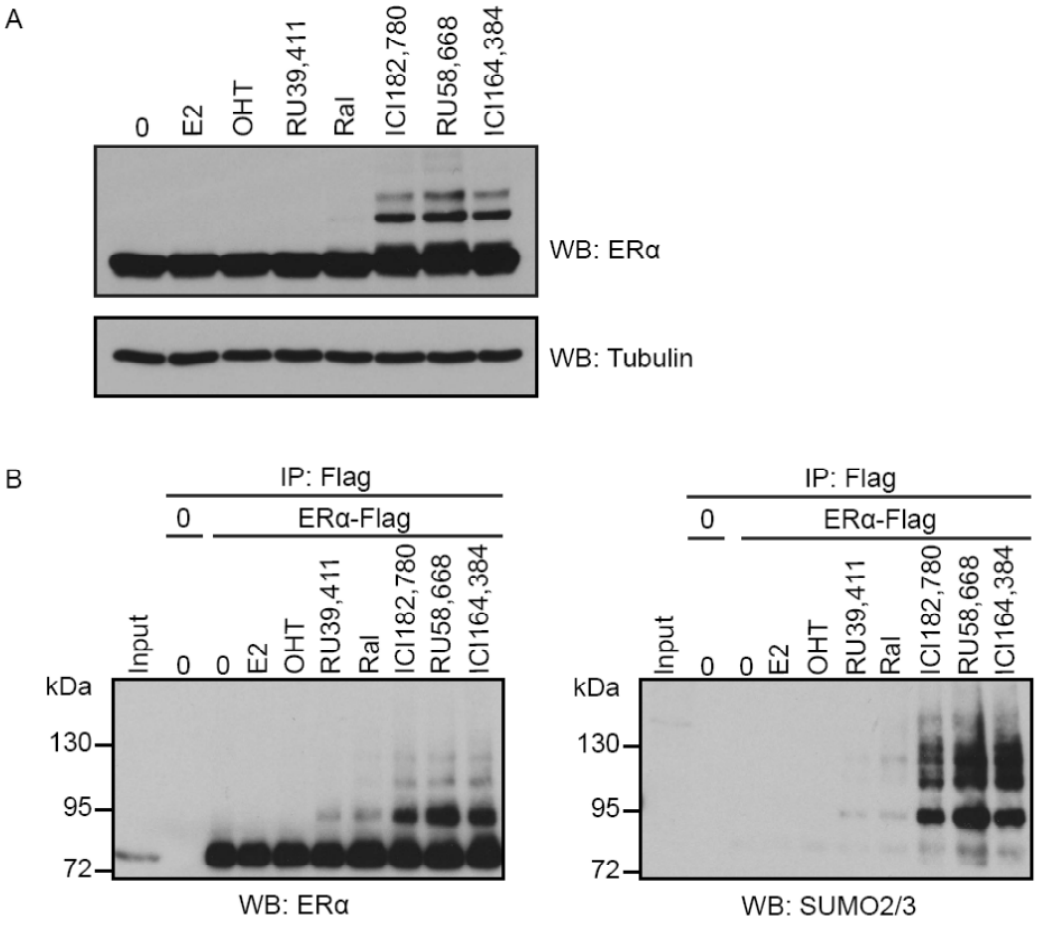

Fig. 4: Full AEs, but not agonists or SERMs, induce efficient ERα SUMOylation.

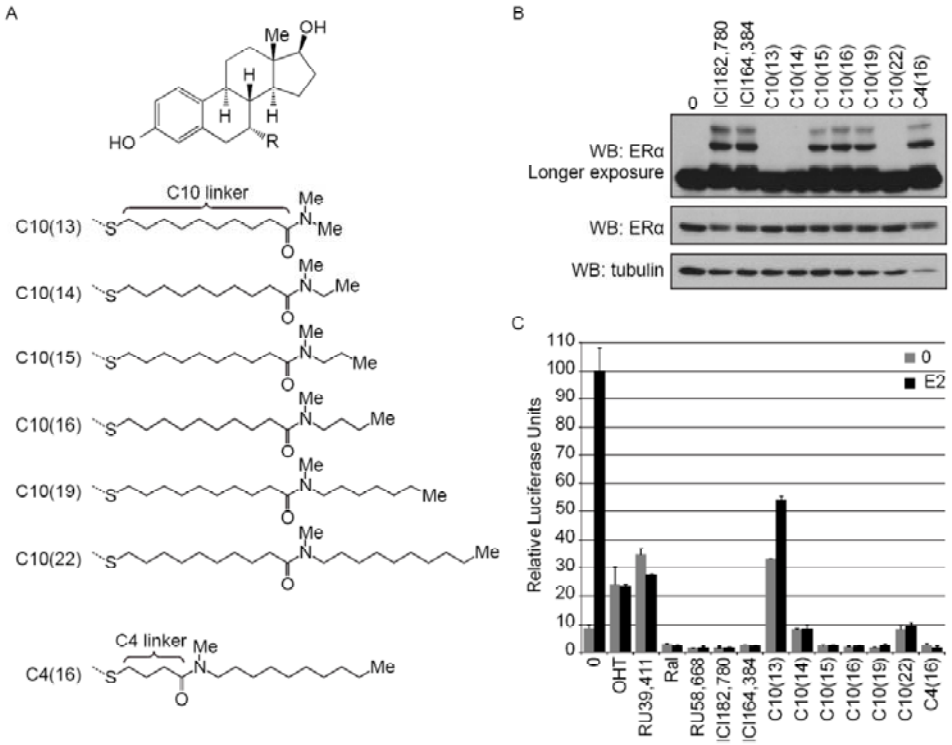

Fig. 5: SUMOylation correlates with full antiestrogenicity in HepG2 cells.

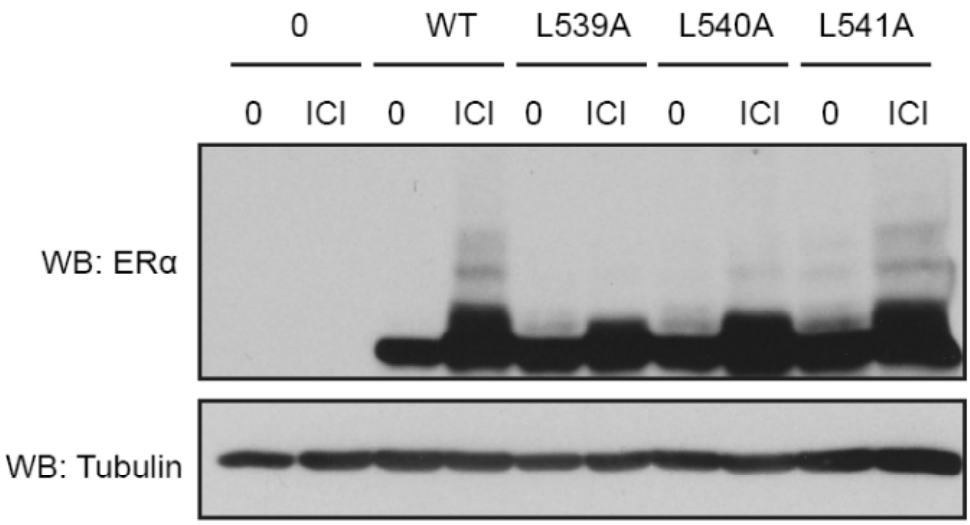

Fig. 6: Mutations in H12 that increase transcriptional activity in the presence of fulvestrant suppress SUMOylation of the receptor.

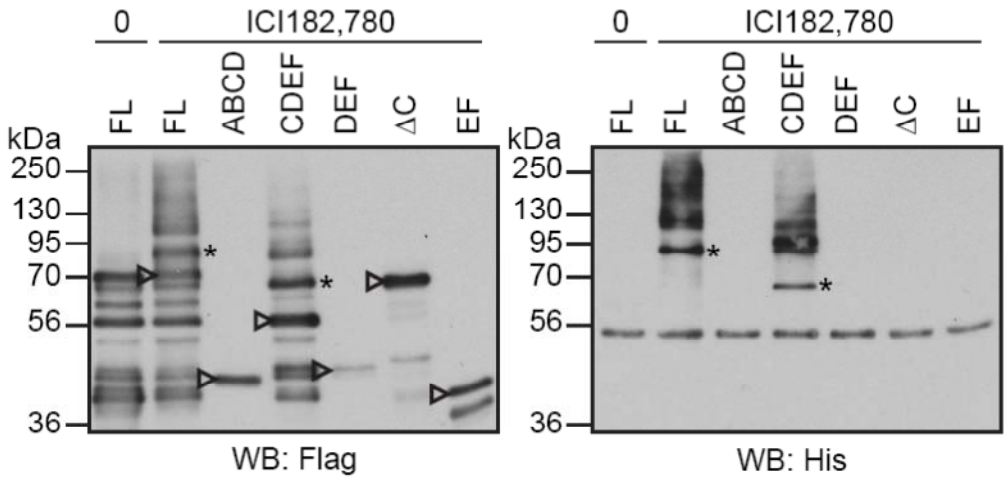

Fig. 7: Multiple domains of ERα are affected by SUMOylation

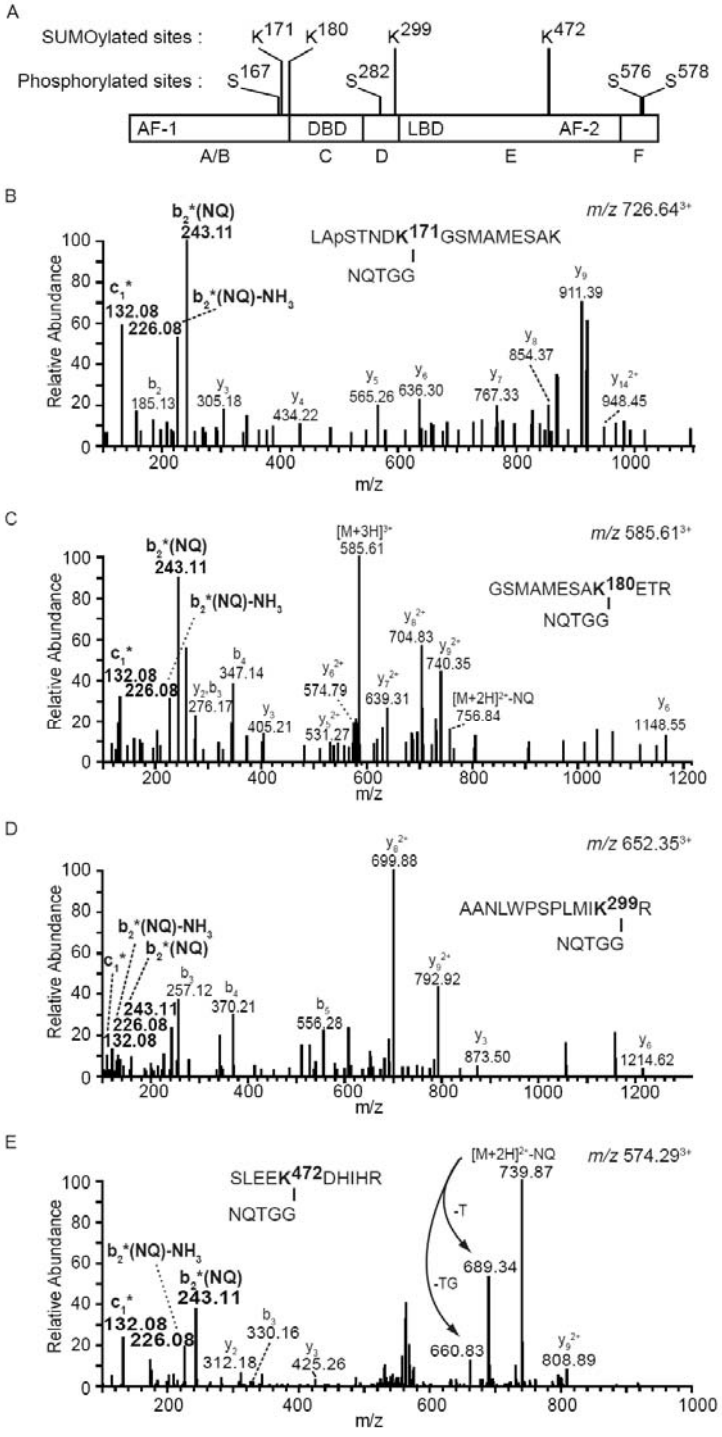

Fig. 8: Identification of SUMOylation sites by mass spectrometry

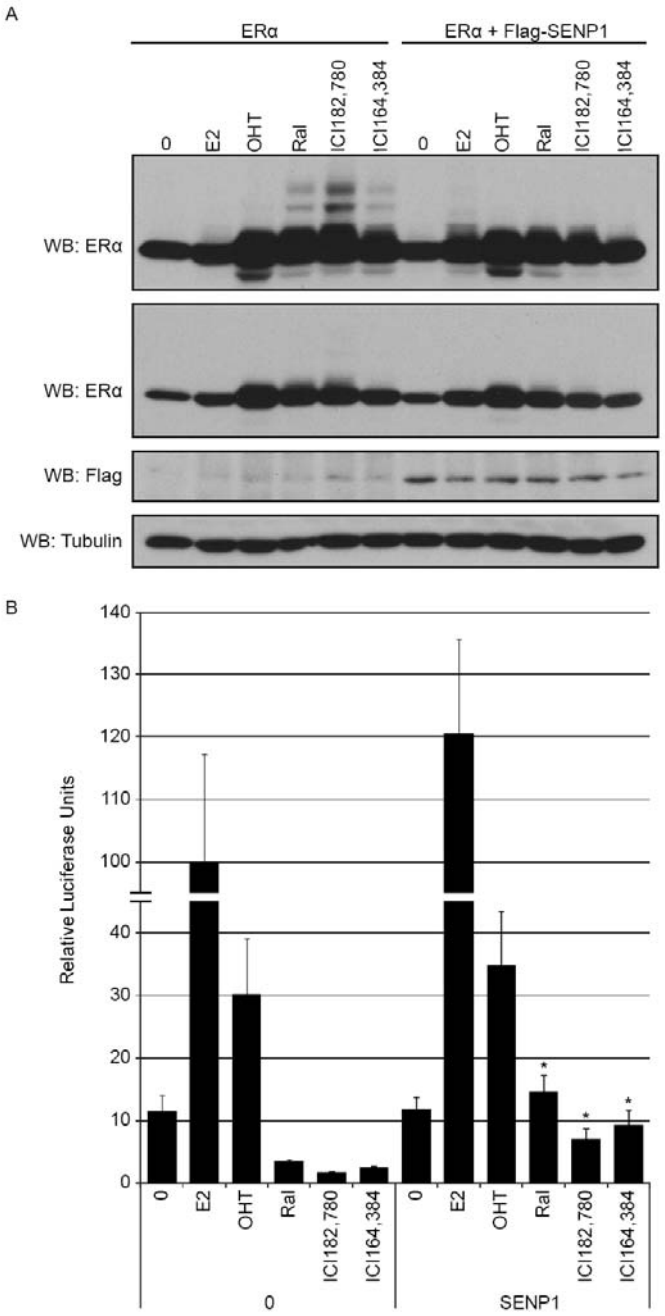

Fig. 9: SUMOylation contributes to ICI182,780-induced ERα inactivation in HepG2 cells.

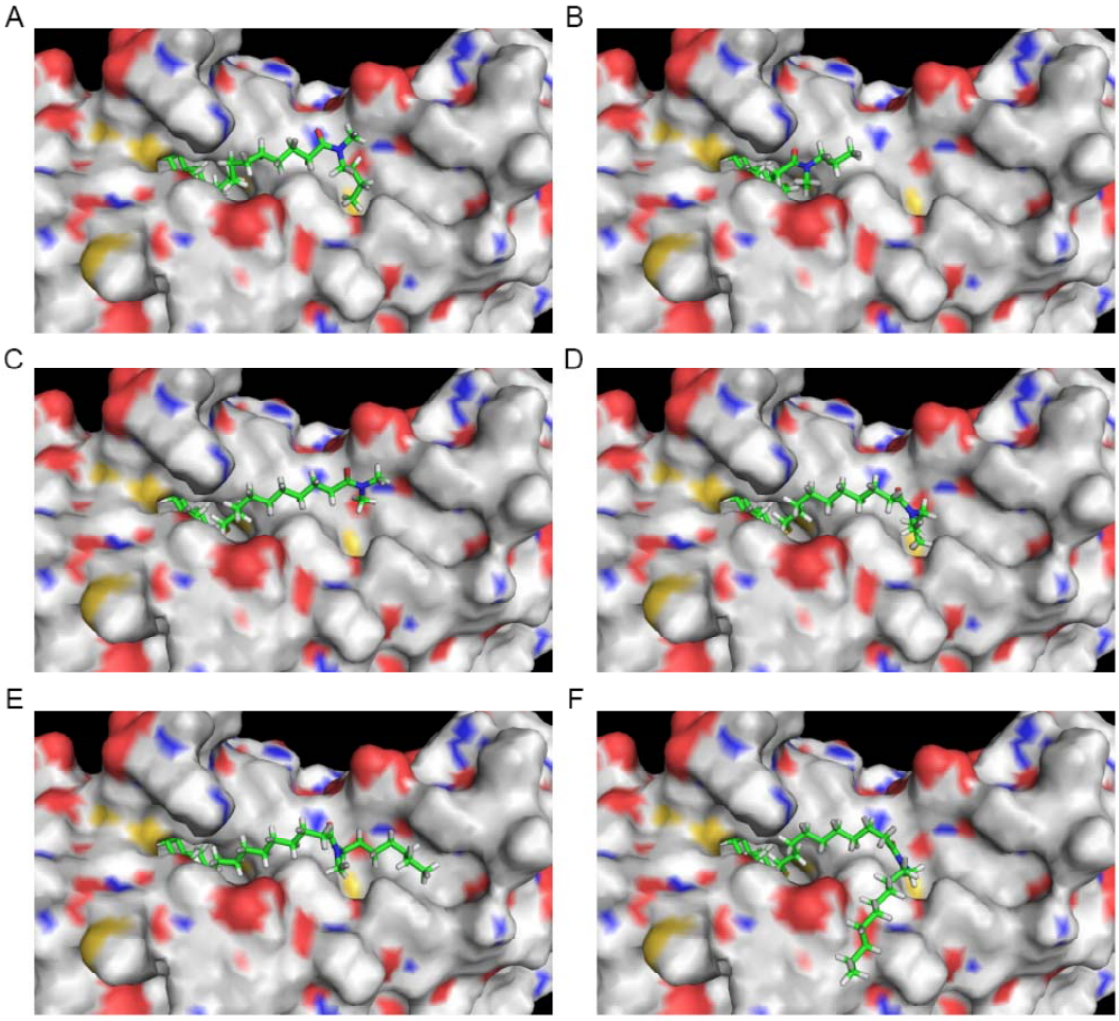

Fig. 10: Representative docking solutions of ICI164,384 and derivatives in crystal structure of ERβ.

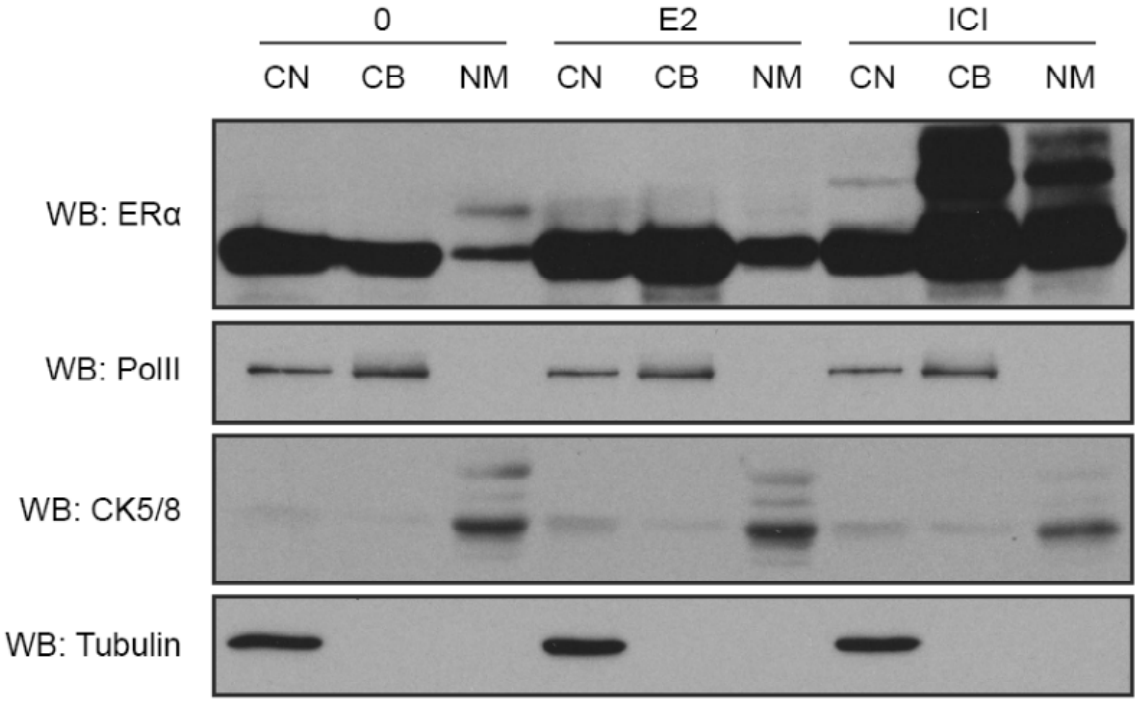

Fig. S1: ERα is modified in all nuclear sub-fractions in MCF7 cells treated with ICI182,780.

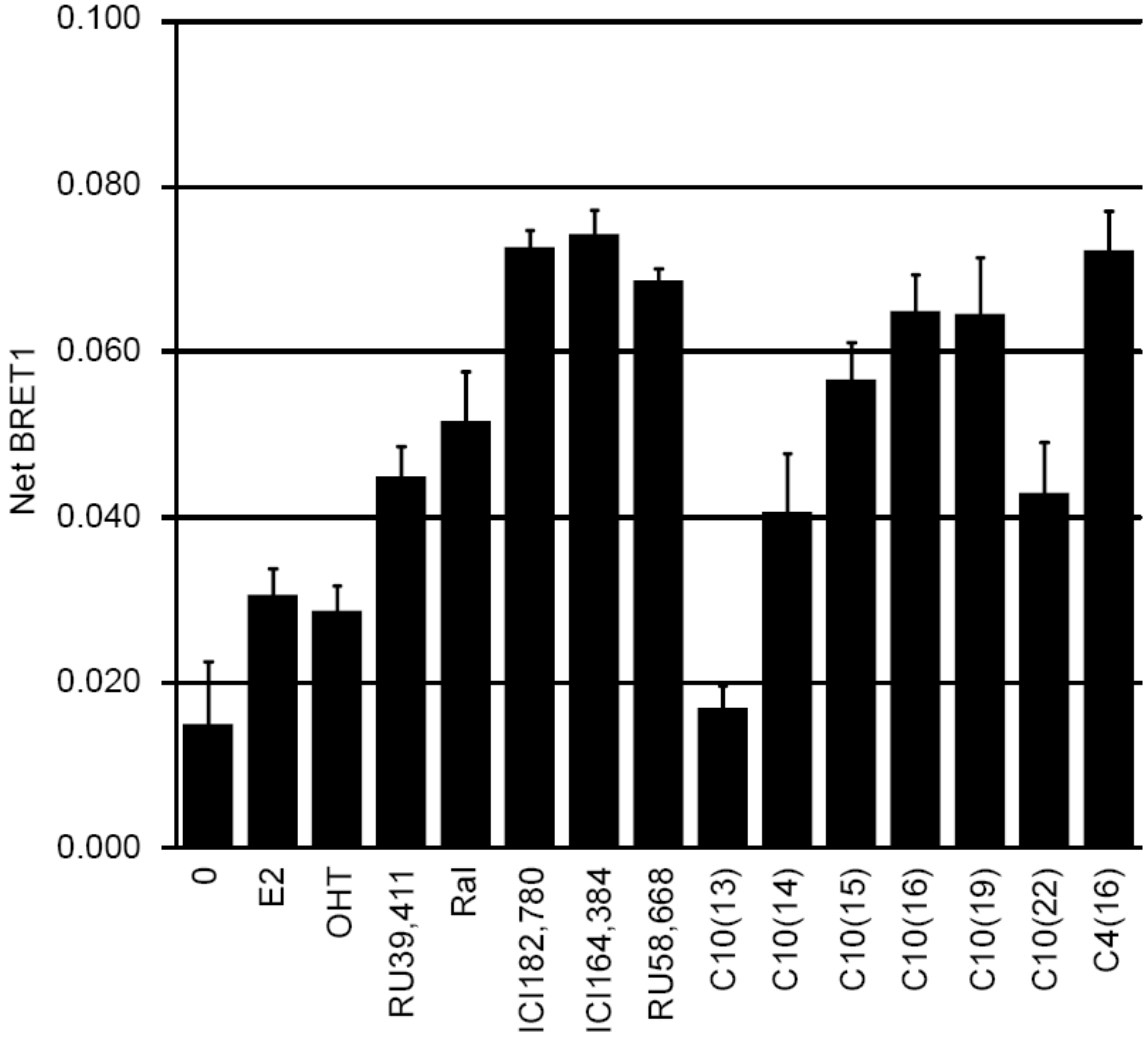

Fig S2: SUMOylation is differentially induced by SERMs and full antiestrogens in a BRET assay.

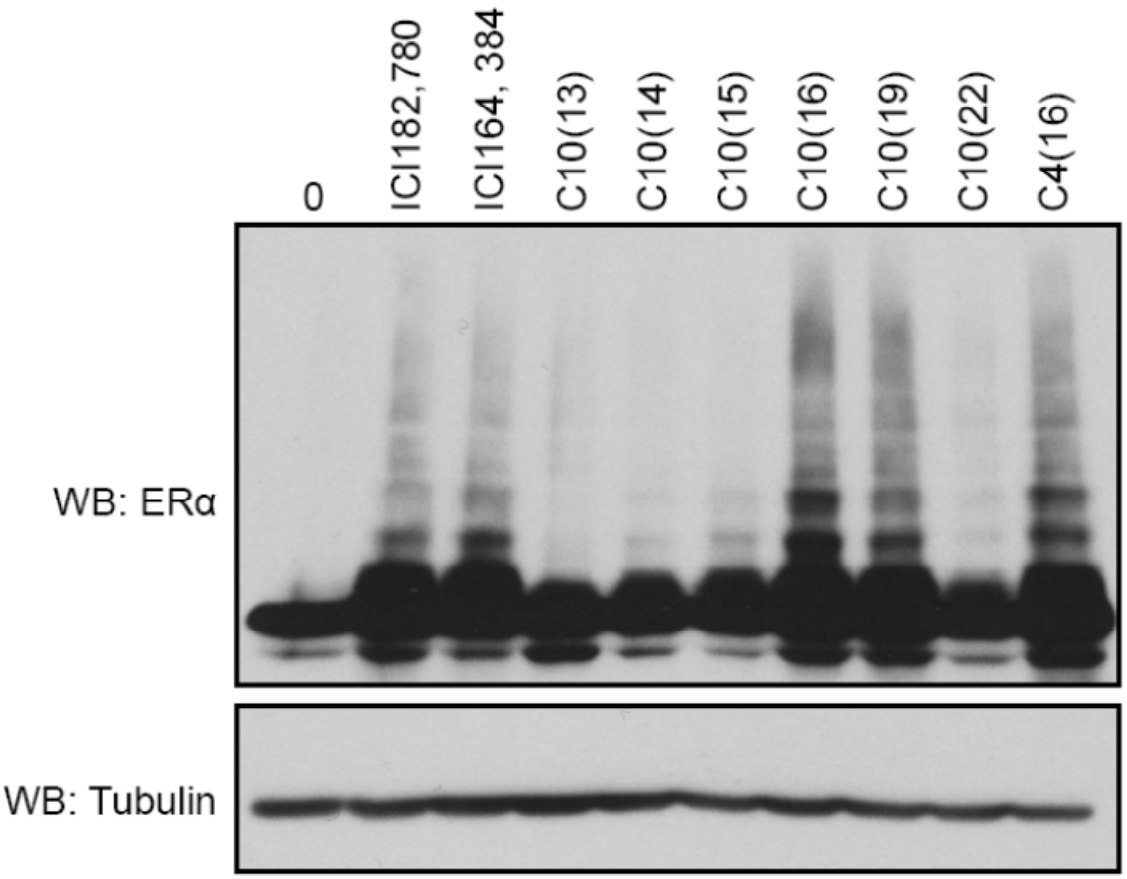

Fig. S3: Side-chain length-dependent SUMOylation in HepG2 cells.

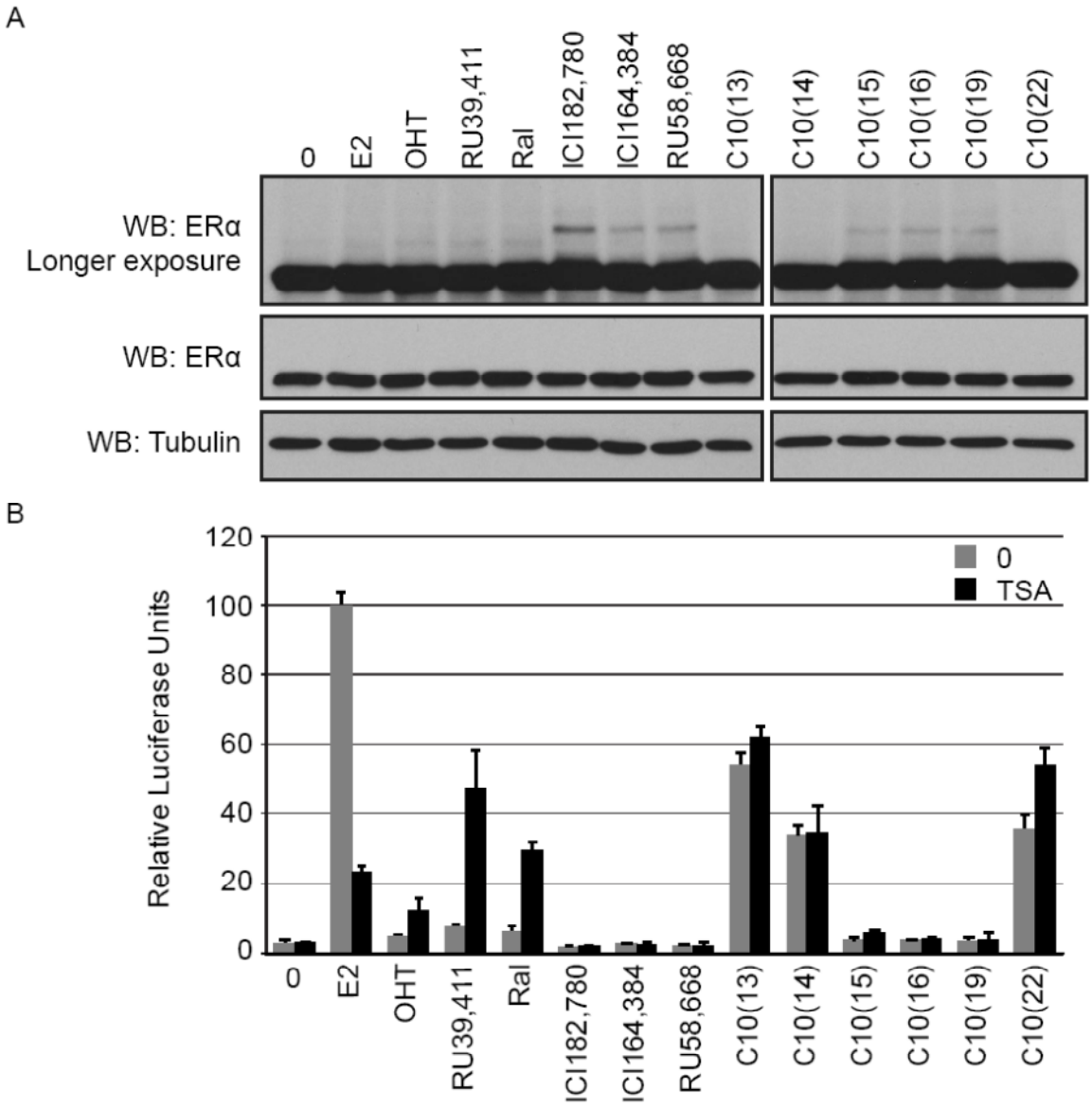

Fig. S4: ERα is SUMOylated in T47D breast cancer cells following treatment with full antiestrogens.

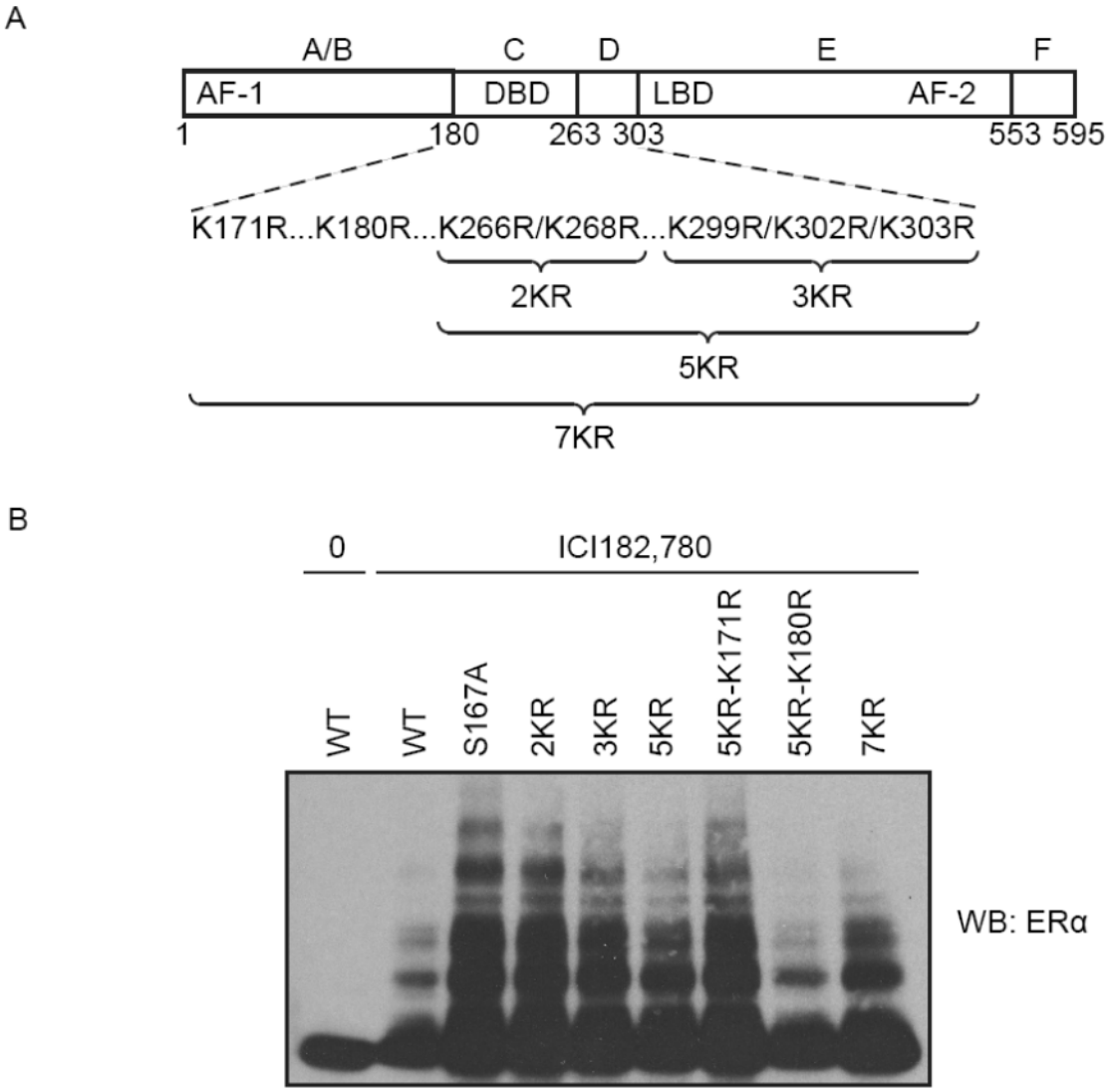

Fig. S5: Evidence for additional SUMOylation sites.

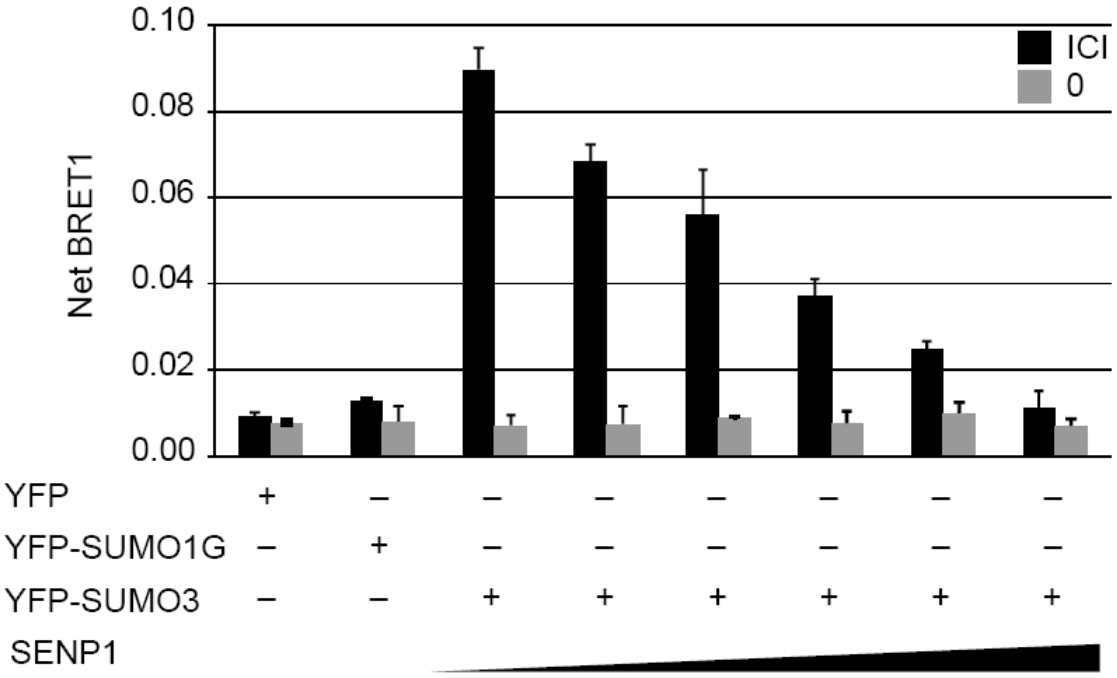

Fig. S6: SENP1 overexpression suppresses ERα SUMOylation in BRET assay.

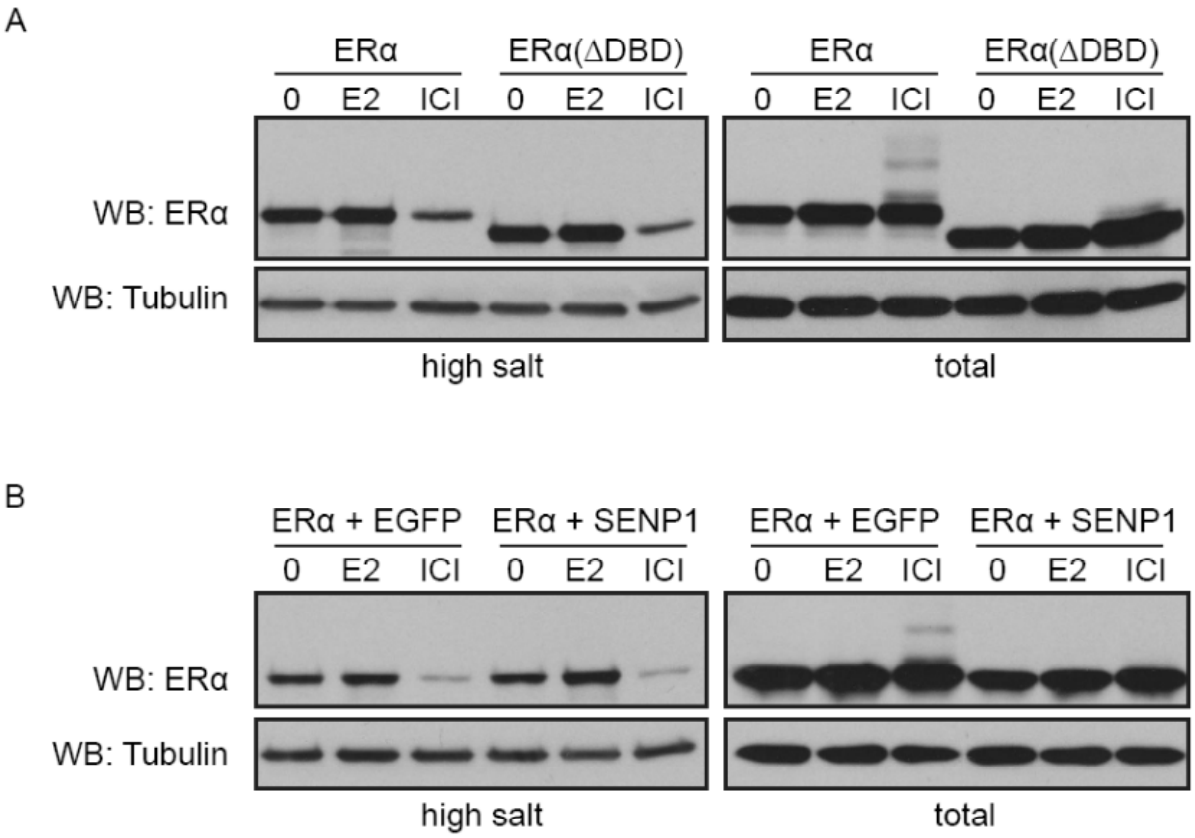

Fig S7. DeSUMOylation does not prevent ERα association with the high-salt insoluble compartment.

SUPPLEMENTARY METHODS

Synthesis of SERD derivatives of ICI164,384

The synthesis of the ICI164,384 derivatives uses 7α-mercapto-E2 (**9**) as a key intermediate. We performed a modification to Napolitano's synthesis of **9** (1) as shown in Figure 1. The thiol was used to attach the desired alkyl chains through thiol alkylation. This approach provides an efficient and convergent synthesis of our derivatives.

Synthetic scheme

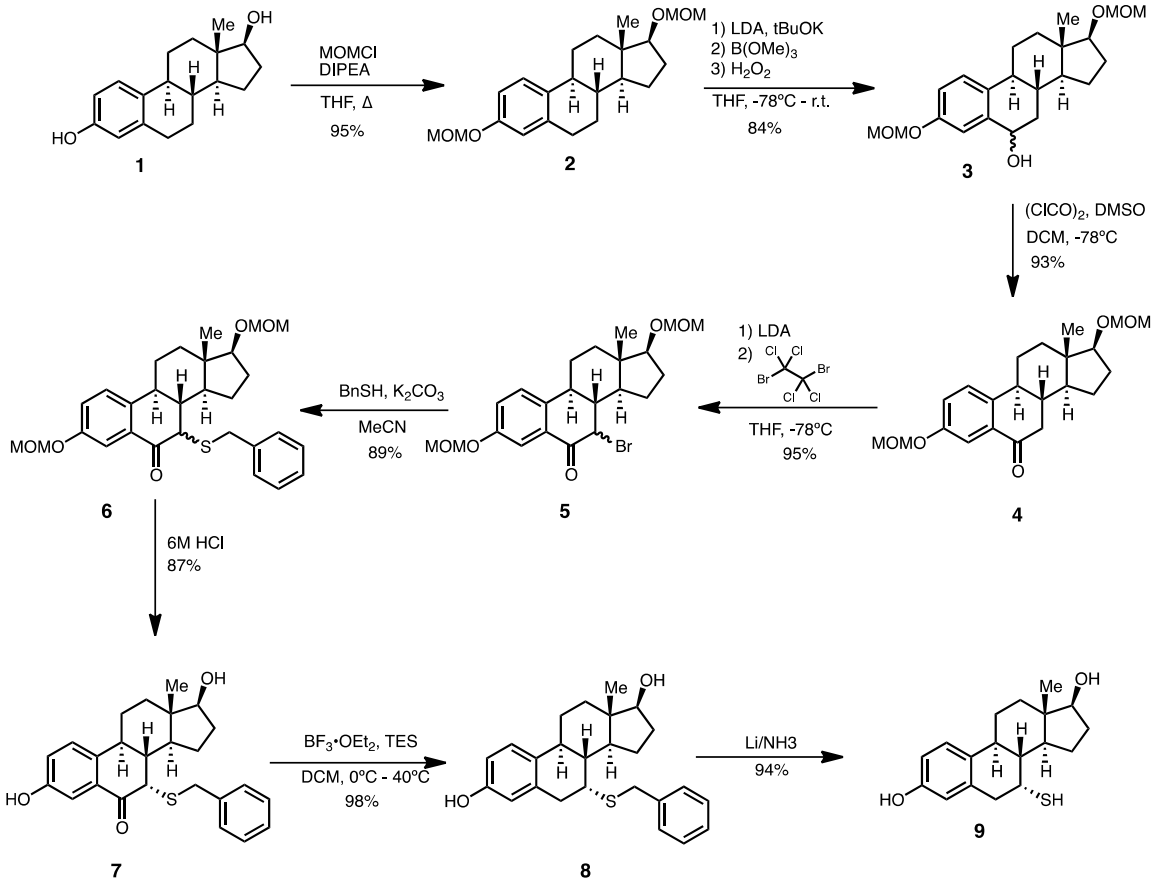

Figure 1. **Synthesis of 7α-mercapto-E2**

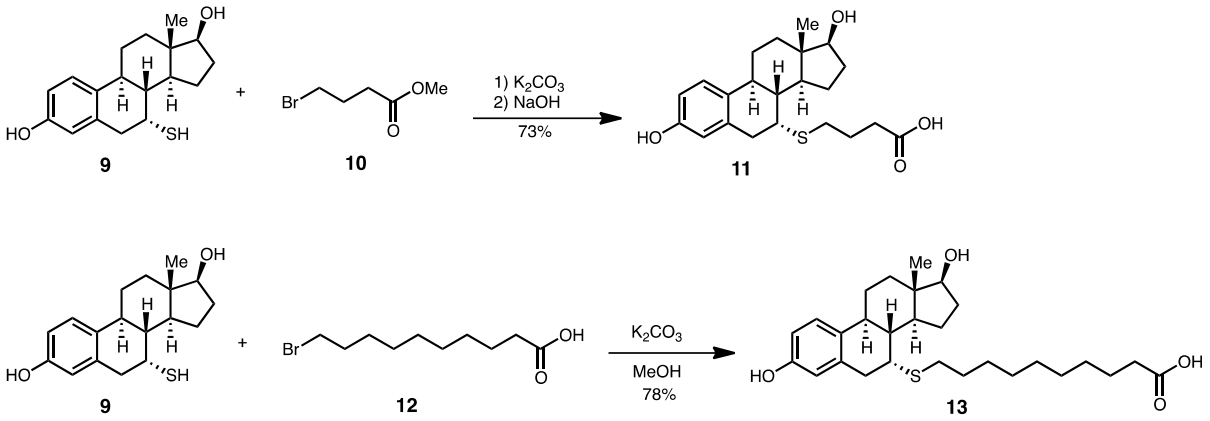

Figure 2. **Thiol ligation process with two different alkyl bromides**

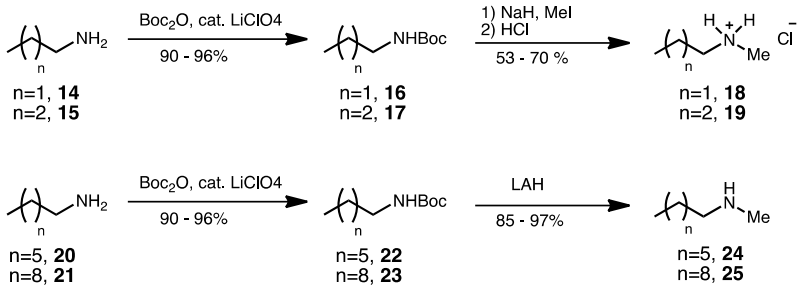

Figure 3. **Synthesis of secondary amines**

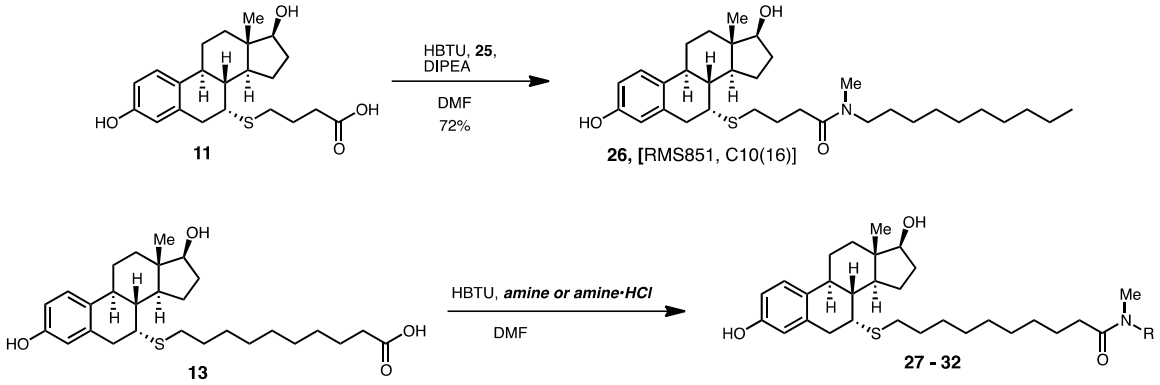

Entry	*Amine or amine•HCl*	R	Product
1	Me_2NH•HCl	Methyl	**27, [**RMS760, C10(13)]
2	MeNHEt	Ethyl	**28, [**RMS854, C10(14)]
3	**18**	Propyl	**29, [**RMS855, C10(15)]
4	**19**	Butyl	**30, [**RMS276, C10(16)]
5	**24**	Heptyl	**31, [**RMS762, C10(19)]
6	**25**	Decyl	**32, [**RMS856, C10(22)]

Figure 4. **Synthesis of SERD derivatives of ICI164,384**

General methods

MeCN and CH_2Cl_2 were distilled from CaH_2 under argon. THF was distilled from sodium metal/benzophenone ketyl under argon. All other commercial solvents and reagents were used as received from the Aldrich Chemical Company, Fischer Scientific, EMD

Chemicals or BDH. All glassware was flame dried and allowed to cool under a stream of dry argon.

Silica gel (60Å, 230–400 mesh) used in flash column chromatography was obtained from Silicycle and was used as received. Analytical TLC was performed on precoated silica gel plates (Ultra Pure Silica Gel Plates purchased from Silicycle), visualized with a Spectroline UV254 lamp, and stained with a 20% phosphomolybdic acid in ethanol solution, or a basic solution of KMnO4.

1H and 13C NMR, recorded at 300 MHz and 75 MHz, respectively, were performed on a Varian Mercury 300 spec- trometer. 1H and 13C NMR, recorded at 400 MHz and 100 MHz, respectively, were performed on a Varian Mercury 400 spectrometer. 1H and 13C NMR, recorded at 500 MHz and 126 MHz, respectively, were performed on a Varian Dante 500 spectrometer. Proton chemical shifts were internally referenced to the residual proton resonance in CDCl3 (∂ 7.26 ppm), CD3OD (∂ 3.31 ppm). Carbon chemical shifts were internally referenced to the deuterated solvent signals in CDCl3 (∂ 77.2 ppm) and CD_3OD (∂ 49.0 ppm).

General procedure A: Protection of amines with di-tert-butyl-dicarbonate (Boc_2O). A 0.1 M solution of amine (1.0 equiv.) and LiClO4 (0.2 equiv.) in dichloromethane was cooled down to 0ºC and Boc_2O (1.1 equiv.) was added dropwise. Upon addition, the reaction mixture was slowly warmed up to r.t. and stirred for 3 hours. The reaction mixture was concentrated and directly purified by chromatography on silica gel eluting 0 – 10% ethyl acetate in hexanes.

General procedure B: Amide formation between acid and amine with O-Benzotriazole-N,N,N',N'-tetramethyl uranium hexafluorophosphate (HBTU)

HBTU (1.3 equiv.) was added to a 0.5M – 1M solution of carboxylic acid (1.0 equiv.), amine (1.1 equiv.) and N,N-diisopropylethylamine (3.0 equiv.) in dimethylformamide. The reaction was stirred 2 h at room temperature and was quenched with 5 times the reaction volume of brine. The reaction was extracted with ethyl acetate (3x) and the combined organic layers were washed with a saturated solution of sodium bicarbonate, an aqueous 0.1M HCl and brine. The organic layer was dried over anhydrous sodium sulfate, filtered and concentrated.

General procedure C: Amide formation between acid and amine hydrochloride with O-Benzotriazole-N,N,N',N'-tetramethyl uranium hexafluorophosphate (HBTU)

HBTU (1.3 equiv.) was added to a 0.5M – 1M solution of carboxylic acid (1.0 equiv.), amine hydrochloride (1.1 equiv.) and N,N-diisopropylethylamine (4.0 equiv.) in dimethylformamide. The reaction was stirred 2 h at room temperature and was quenched with 5 times the reaction volume of brine. The reaction was extracted with ethyl acetate (3x) and the combined organic layers were washed with a saturated solution of sodium bicarbonate, an aqueous 0.1M HCl and brine. The organic layer was dried over anhydrous sodium sulfate, filtered and concentrated.

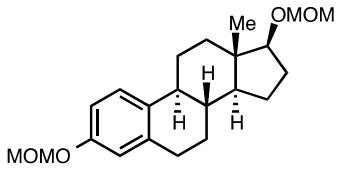

Chemical Formula: $C_{22}H_{32}O_4$
Molecular Weight: 360.49

(8*R*,9*S*,13*S*,14*S*,17*S*)-3,17-bis(methoxymethoxy)-13-methyl-7,8,9,11,12,13,14,15,16,17-decahydro-6*H*-cyclopenta[*a*]phenanthrene (2). Chloromethyl methyl ether (7.0 mL; 91.8 mmol; 5 equiv.) was added dropwise to a solution of 17β-

estradiol **1** (5.05 g; 18.36 mmol; 2.0 equiv.) and *N,N*-diisopropylethylamine (19.2mL; 110.16 mmol; 6.0 equiv.) in tetrahydrofuran (150 mL) at 0ºC. On completion of the addition, the reaction mixture was allowed to warm up to room temperature for 1h and then refluxed overnight. The reaction mixture was cooled to 0ºC and quenched with a saturated solution of aqueous ammonium chloride (80 mL). The aqueous phase was extracted with ethyl acetate (2 x 100 mL). The organic layers were combined, washed with a 0.1 M solution of hydrochloric acid (2 x 200 mL) and brine (200 mL), dried over anhydrous sodium sulfate, filtered and concentrated. The residue was purified by chromatography on silica gel eluting 10% ethyl acetate in hexanes to afford **2** as a colourless oil (6.32 g, 95%). $_1$H-NMR (400 MHz; $CDCl_3$): δ 7.22 (d, *J* = 8.4 Hz, 1H), 6.85 (dd, *J* = 8.5, 2.7 Hz, 1H), 6.79 (d, *J* = 2.6 Hz, 1H), 5.16 (s, 2H), 4.70-4.66 (m, 2H), 3.64 (t, *J* = 8.5 Hz, 1H), 3.49 (d, *J* = 3.5 Hz, 3H), 3.39 (d, *J* = 3.4 Hz, 3H), 2.87 (dt, *J* = 7.6, 4.0 Hz, 2H), 2.33-1.87 (m, 4H), 1.73-1.19 (m, 8H), 0.83 (s, 3H). ^{13}C-NMR (100 MHz; $CDCl_3$): δ 155.0, 138.1, 133.9, 126.3, 116.2, 113.7, 96.0, 94.4, 86.5, 55.9, 55.1, 49.9, 44.0, 43.0, 38.5, 37.2, 29.7, 28.0, 27.1, 26.3, 23.1, 11.7 HRMS (ESI): m/z calcd for [(M+H)+] =273.1776, found =273.1780.

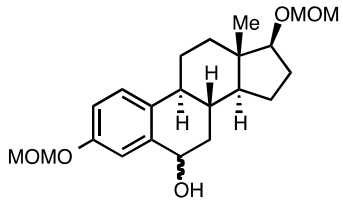

Chemical Formula: $C_{22}H_{32}O_5$
Molecular Weight: 376.49

(8*R*,9*S*,13*S*,14*S*,17*S*)-3,17-bis(methoxymethoxy)-13-methyl-7,8,9,11,12,13,14,15,16,17-decahydro-6*H*-cyclopenta[*a*]phenanthren-6-ol (3): A solution of n-butyllithium in hexanes (2.15 M; 28.8 mL; 61.8 mmol; 4.0 equiv.) was added to a solution of diisopropylamine (8.9 mL, 61.8 mmol; 1.20 equiv.) in tetrahydrofuran (35 mL) at -78ºC. The mixture was stirred at -78ºC for 15 min. and was slowly added via cannula to a solution of potassium tert-butoxide (6.94 g; 61.8 mmol; 4.0 equiv.) in

tetrahydrofuran (50 mL) at -78ºC and stirred 30 min at -78ºC upon addition. A solution of **2** (5.57g; 15.4 mmol; 1 equiv.) in tetrahydrofuran (20 mL) was added dropwise through a pressure equalizer addition funnel and stirred for 3 h at -78ºC resulting in a deep red colour solution. The reaction flask was switched to an ice bath and trimethyl borate (17.2 mL; 154.6 mmol; 10 equiv.) was added in one portion. The reaction was slowly warmed up and stirred for 2 h at 0ºC. Hydrogen peroxide (50% w in water; 26.7 mL; 463.8 mmol; 30 equiv.) was added slowly, in such a rate to avoid rapid precipitation. On completion of addition, the reaction was stirred and room temperature for 1h. The reaction mixture was cooled to 0ºC and quenched slowly with a 10% solution of sodium thiosulfate (85 mL). The reaction was extracted with ethyl acetate (300 mL), washed with water (3x200 mL) and brine (250 mL). The organic phase was dried under anhydrous sodium sulfate, filtered and concentrated. The residue was purified by chromatography on silica gel eluting a gradient of 10% to 30% of ethyl acetate in hexanes in 5% increments every column volume yielding **3** as an amorphous solid (3.89g, 84% yield). ^{1}H-NMR (400 MHz; $CDCl_3$): δ 7.24 (d, *J* = 2.3 Hz, 1H), 7.17 (d, *J* = 8.6 Hz, 1H), 6.89 (dd, *J* = 8.5, 2.6 Hz, 1H), 5.14 (q, *J* = 6.1 Hz, 2H), 4.78 (dd, *J* = 10.3, 6.6 Hz, 1H), 4.63 (q, *J* = 5.1 Hz, 2H), 3.59 (t, *J* = 8.4 Hz, 1H), 3.44 (s, 3H), 3.34 (s, 3H), 2.26-2.19 (m, 3H), 2.09-1.96 (m, 2H), 1.69-1.19 (m, 9H), 0.78 (s, 3H). ^{13}C-NMR (100 MHz; $CDCl_3$): δ 155.6, 140.9, 133.6, 126.4, 115.6, 114.6, 96.0, 94.4, 86.4, 69.9, 60.0, 55.1, 49.3, 44.3, 42.9, 38.1, 37.8, 37.1, 30.0, 26.2, 23.0, 11.7. HRMS (ESI): m/z calcd for [(M+H)+] =377.2250, found =377.2261.

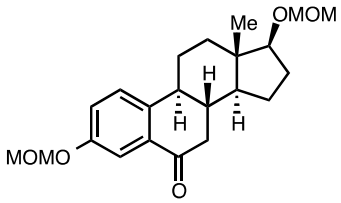

Chemical Formula: $C_{22}H_{30}O_5$
Molecular Weight: 374.47

(8*R*,9*S*,13*S*,14*S*,17*S*)-3,17-bis(methoxymethoxy)-13-methyl-7,8,9,11,12,13,14,15,16,17-decahydro-6*H*-cyclopenta[*a*]phenanthren-6-one (4): A solution of dimethylsulfoxide (1.26 mL; 17.76 mmol; 3.0 equiv.) in dichloromethane (40 mL) at -78ºC was slowly added via cannula over 10 min to a solution of oxalyl chloride (775 µL; 8.88 mmol; 1.5 equiv.) in dichloromethane (50 mL) at -78ºC. The reaction was stirred 15 min at -78ºC. A solution of **3** (2.23 g; 5.92 mmol; 1.0 equiv.) in dichloromethane (50 mL) was slowly added to the reaction mixture via cannula over 15 min and stirred 1 h at -78ºC. Triethylamine (4.13 mL; 29.6 mmol; 5.0 equiv.) was added to the reaction mixture in one portion and the mixture was allowed to warm up to room temperature for 15 min. Water (100 mL) was added and the aqueous phase was extracted with dichlorometane (150 mL). The organic phases were combined, concentrated and further dissolved in ethyl acetate (200 mL), washed with a 0.1 M solution of hydrochloric acid (100 mL) and brine (100 mL). The organic phase was dried under anhydrous sodium sulfate, filtered and concentrated. The residue was purified by chromatography on silica gel eluting 15% of ethyl acetate in hexanes yielding **4** as a colourless oil (2.06 g, 93%). ^{1}H-NMR (400 MHz; $CDCl_3$): δ 7.69 (d, *J* = 2.8 Hz, 1H), 7.35 (dd, *J* = 8.6, 0.6 Hz, 1H), 7.20 (dd, *J* = 8.6, 2.9 Hz, 1H), 5.19 (s, 2H), 4.67-4.63 (m, 2H), 3.62 (t, *J* = 8.5 Hz, 1H), 3.46 (s, 3H), 3.37 (s, 3H), 2.73 (dd, *J* = 16.9, 3.4 Hz, 1H), 2.48-1.92 (m, 5H), 1.69-1.23 (m, 7H), 0.81 (s, 3H). 13-C NMR (126 MHz; CDCl3): δ 197.5, 155.8, 140.7, 133.6, 126.8, 122.5, 113.6, 96.1, 94.5, 86.3, 56.2, 55.3, 50.0, 44.1, 43.06, 42.88, 39.9, 36.9, 28.1, 25.6, 23.0, 11.7. HRMS (ESI): m/z calcd for [(M+H)+] =375.2093, found =375.2083.

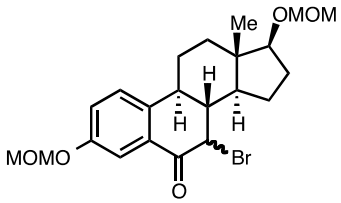

Chemical Formula: $C_{22}H_{29}BrO_5$
Molecular Weight: 453.37

(8*R*,9*S*,13*S*,14*S*,17*S*)-7-bromo-3,17-bis(methoxymethoxy)-13-methyl-7,8,9,11,12,13,14,15,16,17-decahydro-6*H*-cyclopenta[*a*]phenanthren-6-one (5): A solution of n-butyllithium in hexanes (2.56 M; 3.1 mL; 8.01 mmol; 1.5 equiv.) was added to a solution of diisopropylamine (1.1 mL, 8.01 mmol; 1.5 equiv.) in tetrahydrofuran (15 mL) at -78ºC. The mixture was stirred at -78ºC for 15 min. and was slowly added via cannula to a solution of **4** (2.00 g; 5.34 mmol; 1.0 equiv.) in tetrahydrofuran (40 mL) at -78ºC and stirred for 30 min at -78ºC upon addition of a solution of 1,2-dibromotetrachloroethane (2.6 g; 8.01 mmol; 1.5 equiv.) in tetrahydrofuran (15mL). The mixture was stirred at -78ºC for 1 h, quenched with 10 mL of water and warmed up to r.t. The reaction mixture was washed with 3 mL of water and the organic phase was extracted with ethyl acetate (3 x 70 mL) and washed with a saturated aqueous solution of ammonium chloride (100 mL) and brine (100 mL). The organic phase was dried under anhydrous sodium sulfate, filtered and concentrated. The residue was purified by chromatography on silica gel eluting 10% of ethyl acetate in hexanes yielding **5** as a viscous oil (2.3 g, 95%). 1H-NMR (400 MHz; CDCl3): δ 7.74 (d, *J* = 2.8 Hz, 1H), 7.36 (d, *J* = 8.7 Hz, 1H), 7.24 (dd, *J* = 8.7, 2.8 Hz, 1H), 5.20-5.17 (m, 2H), 4.66-4.62 (m, 2H), 4.49 (d, *J* = 2.5 Hz, 1H), 3.66 (t, *J* = 8.5 Hz, 1H), 3.45 (s, 3H), 3.35 (s, 3H), 2.79 (td, *J* = 10.8, 4.3 Hz, 1H), 2.45-2.41 (m, 1H), 2.16-2.00 (m, 2H), 1.82-1.28 (m, 7H), 0.82 (s, 3H). 13-C NMR (126 MHz; cdcl3): δ 190.3, 155.9, 139.5, 130.5, 127.1, 123.4, 114.8, 96.1, 94.4, 86.0, 56.1, 55.2, 55.0, 46.1, 43.5, 42.6, 37.2, 36.4, 27.8, 25.3, 21.7, 11.9. HRMS (ESI): m/z calcd for [(M+H)+] =453.1198, found =453.1205.

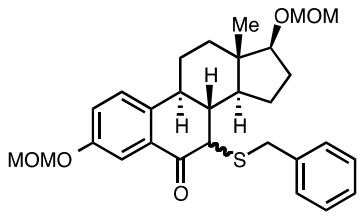

Chemical Formula: $C_{29}H_{36}O_5S$
Molecular Weight: 496.66

(8*R*,9*S*,13*S*,14*S*,17*S*)-7-(benzylthio)-3,17-bis(methoxymethoxy)-13-methyl-7,8,9,11,12,13,14,15,16,17-decahydro-6*H*-cyclopenta[*a*]phenanthren-6-one (6). Benzyl mercaptan (596 µL, 5.09 mmol, 1.1 equiv.) was added to a solution of **5** (2.10 g, 4.63 mmol, 1.0 equiv.) in deoxygenated acetonitrile (30 mL) at 0ºC. Upon the addition, potassium carbonate (1.92 g, 13.89 mmol, 3.0 equiv.) was added and the reaction mixture and the mixture was allowed to slowly warm up to r.t. and stirred for 7 h. The acetonitrile was evaporated out and the residual potassium carbonate was quenched with 1 M HCl until pH 2-4 was reached. The organic phase was extracted with ethyl acetate (40 mL x2) and the combined organic fractions were washed with water (60 mL) and brine (60 mL). The residue was purified by chromatography on silica gel eluting 10 - 15% ethyl acetate in hexanes to yield **7** as a solid (2.05 g, 89%). 1H-NMR (400 MHz; $CDCl_3$): δ 7.82 (d, *J* = 2.8 Hz, 1H), 7.41 (d, *J* = 7.2 Hz, 2H), 7.32-7.29 (m, 3H), 7.22 (ddd, *J* = 16.4, 9.9, 3.3 Hz, 2H), 5.21 (s, 2H), 4.62-4.59 (m, 2H), 3.70 (q, *J* = 14.8 Hz, 2H), 3.57 (t, *J* = 8.5 Hz, 1H), 3.48 (s, 3H), 3.33 (s, 3H), 3.21 (d, *J* = 3.2 Hz, 1H), 2.71-2.64 (m, 1H), 2.36-2.31 (m, 1H), 2.13 (td, *J* = 11.1, 3.2 Hz, 1H), 1.98-1.89 (m, 2H), 1.65-1.29 (m, 6H), 0.72 (s, 3H). 13-C NMR (126 MHz; cdcl3): δ 11.50, 21.04, 25.85, 27.77, 33.70, 36.48, 38.18, 41.99, 42.53, 45.02, 49.16, 55.16, 56.10, 86.17, 94.44, 96.06, 114.69, 122.37, 126.83, 127.12, 128.30, 129.62, 131.49, 137.65, 139.30, 155.89, 191.74. HRMS (ESI): m/z calcd for [(M+H)+] = 497.2283, found = 497.2272

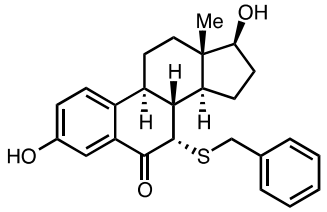

Chemical Formula: $C_{25}H_{28}O_3S$
Molecular Weight: 408.55

(7*S*,8*R*,9*S*,13*S*,14*S*,17*S*)-7-(benzylthio)-3,17-dihydroxy-13-methyl-7,8,9,11,12,13,14,15,16,17-decahydro-6*H*-cyclopenta[*a*]phenanthren-6-one (7): A 6M

HCl solution (20 mL) was added to a solution of **6** (1.60 g, 3.22 mmol) in tetrahydrofuran (20 mL) at 0ºC. The reaction mixture was allowed to warm up slowly to room temperature and stirred for 20 hr. The reaction was cooled to 0ºC and the acid was neutralized with a 6M aqueous solution of NaOH until pH 6 -7 was reached. The reaction was extracted with ethyl acetate (40 mLx2) and the mixed organic layers were washed with a saturated aqueous solution of ammonium chloride (40 mL) and brine (60 mL). The organic layer was dried over anhydrous sodium sulfate, filtered and concentrated. The residue was purified by chromatography on silica gel eluting 10 to 10 - 15% ethyl acetate in toluene to yield **7** as a solid (1.16g, 87%). ^{1}H-NMR (400 MHz; $CDCl_3$): δ 7.76 (d, *J* = 2.9 Hz, 1H), 7.42-7.40 (m, 2H), 7.34-7.24 (m, 4H), 7.09 (dd, *J* = 8.5, 2.9 Hz, 1H), 6.76 (s, 1H), 3.76-3.68 (m, 3H), 3.25 (d, *J* = 3.3 Hz, 1H), 2.70-2.64 (m, 1H), 2.40-1.81 (m, 6H), 1.66-1.25 (m, 4H), 0.72 (s, 3H). ^{13}C NMR (126 MHz; $CDCl_3$): δ 192.5, 154.8, 138.1, 137.5, 131.3, 129.6, 128.4, 127.20, 127.14, 121.5, 114.0, 81.4, 49.3, 45.1, 42.9, 42.3, 38.1, 36.0, 33.8, 30.2, 25.9, 21.1, 10.9. HRMS (ESI): m/z calcd for [(M+Na)+] =431.1657, found = 431.1659

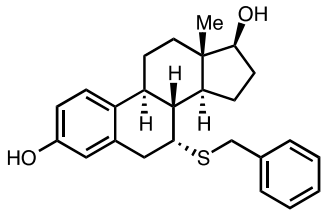

Chemical Formula: $C_{25}H_{30}O_2S$
Molecular Weight: 394.57

(7*R*,8*R*,9*S*,13*S*,14*S*,17*S*)-7-(benzylthio)-13-methyl-7,8,9,11,12,13,14,15,16,17-decahydro-6*H*-cyclopenta[*a*]phenanthrene-3,17-diol (8): Boron trifluoride diethyl ether (2.5 mL, 20.08 mmol, 8 equiv.) was added dropwise to a solution of **7** (1.03 g, 2.51 mmol, 1 equiv.) in dichloromethane (40 mL) at 0ºC, followed by the addition of triethylsilane (8.0 mL; 50.20 mmol, 20 equiv.). The mixture was warmed to room temperature for 1h and to 40ºC for 4 hours. The reaction was quenched with a saturated aqueous solution of sodium

bicarbonate until reaching pH 8. The aqueous phase was extracted with ethyl acetate (50 mL x2) and the combined organic layers were washed with brine (60 mL). The organic layer was dried over anhydrous sodium sulfate, filtered and concentrated. The residue was purified by chromatography on silica gel eluting 10 – 20 % ethyl acetate in toluene to yield **8** as a solid (970 mg, 98%) ^{1}H-NMR (400 MHz; CD_3OD): δ 7.32-7.25 (m, 4H), 7.21 (m, *J* = 2.3 Hz, 1H), 7.06 (d, *J* = 8.5 Hz, 1H), 6.56 (dd, *J* = 8.4, 2.6 Hz, 1H), 6.46 (d, *J* = 2.5 Hz, 1H), 3.68 (s, 2H), 3.58 (t, *J* = 8.6 Hz, 1H), 3.07 (dd, *J* = 17.1, 4.2 Hz, 1H), 2.95-2.91 (m, 2H), 2.37-2.26 (m, 2H), 1.89-1.83 (m, 2H), 1.64 (td, *J* = 11.0, 2.2 Hz, 1H), 1.47-0.97 (m, 6H), 0.68 (s, 3H). HRMS (ESI): m/z calcd for [(M+H)+] =395.1967, found = 395.1974

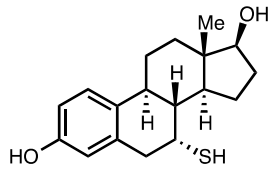

Chemical Formula: $C_{18}H_{24}O_2S$
Molecular Weight: 304.45

(7*R*,8*R*,9*S*,13*S*,14*S*,17*S*)-7-mercapto-13-methyl-7,8,9,11,12,13,14,15,16,17-decahydro-6*H*-cyclopenta[*a*]phenanthrene-3,17-diol (9): Solid lithium (66 mg, 9.52 mmol, 4 equiv.) was added to condensed ammonia (30 mL) at -78ºC and was stirred for 1.5 h resulting in a deep blue solution. A solution of **8** (940 mg, 2.38 mmol, 1 equiv.) in tetrahydrofuran (35 mL) was added via cannula to the lithium-ammonia mixture and the reaction was stirred at -78ºC for 1 min. The reaction was quenched slowly with isopropanol (5 mL) and ammonium chloride (5 mL). The reaction was warmed up to r.t. and the residual ammonia was neutralized with a 6M HCl solution until reaching pH 1-3. Sodium chloride was added until saturating the aqueous phase and the organic phase was extracted with ethyl acetate (50 mL x 3). The combined organics were washed with brine (60 mL). The residue was purified by chromatography on silica gel eluting 15 – 30 % ethyl acetate in toluene to yield **9** (681 mg, 94%) as a foam. ^{1}H-NMR (400 MHz; CD_3OD): δ 7.32-7.25 (m, 4H), 7.21 (m, *J* = 2.3 Hz, 1H), 7.06 (d, *J* = 8.5 Hz, 1H), 6.56 (dd, *J* = 8.4, 2.6 Hz, 1H),

6.46 (d, *J* = 2.5 Hz, 1H), 3.68 (s, 2H), 3.58 (t, *J* = 8.6 Hz, 1H), 3.07 (dd, *J* = 17.1, 4.2 Hz, 1H), 2.95-2.91 (m, 2H), 2.37-2.26 (m, 2H), 1.89-1.83 (m, 2H), 1.64 (td, *J* = 11.0, 2.2 Hz, 1H), 1.47-0.97 (m, 6H), 0.68 (s, 3H). 13-C NMR (126 MHz; cd3od): δ 154.8, 133.9, 129.6, 126.4, 115.4, 113.1, 81.0, 46.9, 42.9, 42.3, 40.0, 37.1, 36.58, 36.49, 29.2, 26.3, 21.7, 10.6. HRMS (ESI): m/z calcd for [(M+H)+] =305.1497, found = 305.1484

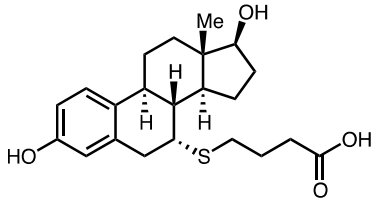

Chemical Formula: $C_{22}H_{30}O_4S$
Molecular Weight: 390.54

4-(((7*R*,8*R*,9*S*,13*S*,14*S*,17*S*)-3,17-dihydroxy-13-methyl-7,8,9,11,12,13,14,15,16,17-decahydro-6*H*-cyclopenta[*a*]phenanthren-7-yl)thio)butanoic acid (11). K_2CO_3 (315 mg, 2.28 mmol, 6 equiv.) was added to a mixture of **9** (116 mg, 0.38 mmol, 1.0 equiv.) and **10** (190 mg, 1.14 mmol, 3.0 equiv.) in deoxygenated acetonitrile (5.0 mL) and stirred for 36 hours at room temperature. The reaction mixture was concentrated and was dissolved in a 1:1 mixture of MeOH/THF (10 mL). A 1 M solution of LiOH (3.8 mL, 3.8 mmol, 10.0equiv.) was added to the solution and stirred at room temperature for 6 hours. The reaction mixture was concentrated and washed with 0.1 M HCl until pH 1 -3 was reached followed by saturation of the aqueous portion with NaCl. The organics were extracted with ethyl acetate (15 mL x2). The combined organic fractions were dried over sodium sulfate and concentrated. The residue was purified by chromatography on silica gel eluting 15 - 30 % ethyl acetate in toluene with 1 % AcOH to yield **11** as foam (108 mg, 73%). 1H-NMR (500 MHz; CD3OD): δ 7.08 (d, *J* = 8.6 Hz, 1H), 6.56 (dd, *J* = 8.4, 2.6 Hz, 1H), 6.48 (d, *J* = 2.6 Hz, 1H), 3.67 (t, *J* = 8.6 Hz, 1H), 3.17 (m, 2H), 2.96 (d, *J* = 16.8 Hz, 1H), 2.56-2.27 (m, 5H), 1.93-1.90 (m, 2H), 1.76-1.24 (m, 9H), 0.77 (s, 3H). 13-C NMR

(126 MHz; CD3OD): δ 175.5, 154.7, 135.1, 130.2, 126.3, 115.3, 112.7, 80.2, 46.5, 43.0, 42.8, 37.9, 36.5, 36.1, 32.4, 31.3, 29.6, 28.4, 28.2, 24.7, 22.0, 11.4. HRMS (ESI): m/z calcd for [(M-H)-] = 389.1865, found = 389.1873

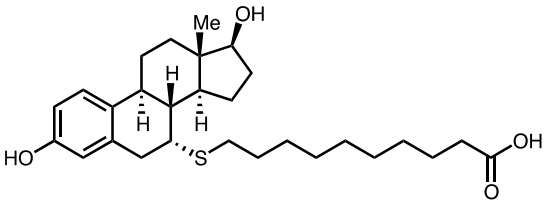

Chemical Formula: $C_{28}H_{42}O_4S$
Molecular Weight: 474.70

10-(((7*R*,8*R*,9*S*,13*S*,14*S*,17*S*)-3,17-dihydroxy-13-methyl-7,8,9,11,12,13,14,15,16,17-decahydro-6*H*-cyclopenta[*a*]phenanthren-7-yl)thio)decanoic acid (13). K_2CO_3 (203 mg, 1.48 mmol, 3 equiv.) was added to a mixture of **9** (150 mg, 0.492 mmol, 1 equiv.) and **10** (370 mg, 1.48 mmol, 3 equiv.) in deoxygenated methanol (10 mL) and stirred for 36 hours at room temperature. The reaction mixture was concentrated and washed with 0.1 M HCl until pH 1 -3 was reached, followed by saturation of the aqueous portion with NaCl. The organics were extracted with ethyl acetate (25 mL x 2). The combined organic fractions were dried over sodium sulfate and concentrated. The residue was purified by chromatography on silica gel eluting 15 - 30 % ethyl acetate in toluene with 1 % AcOH to yield **11** as foam (182 mg, 78%). 1H-NMR (500 MHz; CD3OD): δ 7.08 (d, *J* = 8.6 Hz, 1H), 6.56 (dd, *J* = 8.4, 2.6 Hz, 1H), 6.48 (d, *J* = 2.6 Hz, 1H), 3.67 (t, *J* = 8.6 Hz, 1H), 3.17 (dd, *J* = 17.3, 4.3 Hz, 1H), 3.11-3.10 (m, 1H), 2.96 (d, *J* = 16.8 Hz, 1H), 2.56-2.41 (m, 4H), 2.27 (t, *J* = 7.4 Hz, 2H), 1.92-1.24 (m, 23H), 0.77 (s, 3H). 13-C NMR (126 MHz; cd3od): δ 176.5, 154.7, 135.1, 130.2, 126.3, 115.3, 112.7, 81.0, 46.6, 43.07, 42.91, 42.6, 38.6, 36.9, 36.5, 33.7, 30.5, 29.6, 29.20, 29.06, 28.93, 28.80, 28.4, 26.7, 24.7, 22.0, 10.4. HRMS (ESI): m/z calcd for [(M-H)-] = 473.2804, found = 473.2791

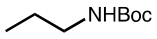

Chemical Formula: $C_8H_{17}NO_2$
Molecular Weight: 159.23

***tert*-butyl propylcarbamate (16).** Prepared according to general procedure A. Propyl amine (2.0 mL, 24.33 mmol, 1equiv.), Boc_2O (6.1 mL, 26.76 mmol, 1.1equiv.), $LiClO_4$ (518 mmg, 4.87 mmol, 0.2 equiv.). **16** was obtained an oil (3.5 g, 90%). 1H-NMR (400 MHz; CDCl3): δ 4.58 (s (br), 1H), 3.10 (q, J = 6.5 Hz, 2H), 1.45-1.41 (m, 11H), 0.91 (t, J = 7.1 Hz, 3H).

Chemical Formula: $C_9H_{19}NO_2$
Molecular Weight: 173.25

***tert*-butyl butylcarbamate (17).** Prepared according to general procedure A. Butylamine (2.5 mL, 25.19 mmol, 1.0 equiv.), Boc_2O (6.4 mL, 27.71 mmol, 1.1 equiv.), $LiClO_4$ (536 mg, 5.04 mmol, 0.2 equiv.). **17** was obtained an oil (4.2 g, 96%). 1H-NMR (400 MHz; CDCl3): δ 4.55 (s (br), 1H), 3.08 (q, J = 6.5 Hz, 2H), 1.45-1.40 (m, 11H), 1.30 (m, 2H), 0.88 (t, J = 7.3 Hz, 3H).

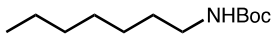

Chemical Formula: $C_{12}H_{25}NO_2$
Molecular Weight: 215.33

***tert*-butyl heptylcarbamate (22).** Prepared according to general procedure A. heptylamine (4.0 mL, 26.97 mmol, 1 equiv.), Boc_2O (6.7 mL, 29.67 mmol, 1.1 equiv.), LiClO4 (573 mg, 5.39 mmol, 0.2 equiv.). **22** was obtained an oil (4.9 g, 85%). 1H-NMR (400 MHz; CDCl3): δ 4.48 (br s, 1H), 3.10 (q, J = 6.4 Hz, 2H), 1.44 – 1.40 (m, 11H), 1.28-1.24 (m, 8H), 0.87 (t, J = 6.8 Hz, 3H).

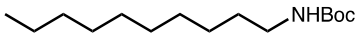

Chemical Formula: $C_{15}H_{31}NO_2$
Molecular Weight: 257.41

***tert*-butyl decylcarbamate (23).** Prepared according to general procedure A. Decyl amine (2.0 mL, 10.0 mmol, 1.0 equiv.), Boc_2O (2.52 mL, 11.0 mmol, 1.1 equiv.), $LiClO_4$ (213 mg, 2.0 mmol, 0.2 equiv.). **23** was obtained as an oil (2.5 g, 97%). 1H-NMR (400 MHz; CDCl3): δ 4.51 (br s, 1H), 3.11 (q, *J* = 6.1 Hz, 2H), 1.45 – 1.39 (m, 11H), 1.28-1.25 (m, 14H), 0.88 (t, *J* = 6.5 Hz, 3H).

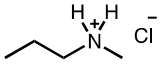

Chemical Formula: $C_4H_{12}ClN$
Molecular Weight: 109.60

***N*-methylpropan-1-aminium chloride (18).** NaH (1.9 g, 77.46 mmol, 3 equiv.) was added to a solution of **16** (4.3 g, 25.82 mmol, 1.0 equiv.) in dimethylformamide (25 mL) at 0ºC and the solution was stirred for 30 min. Methyl iodide (5.o mL, 78.54 mmol, 3.1 equiv.) was added to the reaction mixture and was stirred for 1 h at r.t. The reaction was cooled to 0ºC and quenched slowly with H_2O (5 mL). The organic phase was extracted with ethyl acetate (45 mL x 2) and washed with water (25 mL x 5) and brine (25 mL). The organic phase was dried over sodium sulfate and concentrated. A 6 M HCl solution in dry diethyl ether (45 mL) was added to the reaction mixture and was allowed to recrystallize as the hydrochloride salt overnight in a -20ºC freezer. The solid was filtrated and washed with diethyl ether and dried under vacuum. **18** was obtained as a crystalline solid (1.2 g, 53%). 1H NMR (500MHZ; $CDCl_3$), δ 2.81 (t, *J* = 7.8 Hz, 2H), 2.57 (s, 3H), 1.63 (t, *J* = 7.6 Hz, 2H), 1.31-1.24 (m, 9H), 0.84 (t, *J* = 6.9 Hz, 3H).

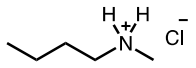

Chemical Formula: $C_5H_{14}ClN$
Molecular Weight: 123.62

***N*-methylbutan-1-aminium chloride (19).** NaH (1.9 g, 77.46 mmol, 3 equiv.) was added to a solution of **17** (4.3 g, 25.82, 1.0 equiv.) in dimethylformamide (25 mL) at 0ºC and the solution was stirred for 30 min. Methyl iodide (5.0 mL, 78.54, 3.1 equiv.) was added to the reaction mixture and was stirred for 1 h at r.t. The reaction was cooled to 0ºC and quenched slowly with H_2O (5 mL). The organic phase were extracted with ethyl acetate (45 mL x 2) and washed with water (45 mL x 2)) and brine (25 mL). The organic phase was dried over sodium sulfate and concentrated. A 6 M HCl solution in dry diethyl ether (45 mL) was added to the reaction mixture and was allowed to recrystallize as the hydrochloride salt overnight in a -20ºC freezer. The solid was filtrated and washed with diethyl ether and dried under vacuum. **19** was obtained as a crystalline solid (2.2 g, 70%). 1H-NMR (400 MHz; CDCl3): δ 9.43 (s, 2H), 2.91 (s, 2H), 2.66 (s, 3H), 1.82 (dt, *J* = 15.7, 7.8 Hz, 2H), 1.41 (sextet, *J* = 7.5 Hz, 2H), 0.94 (t, *J* = 7.4 Hz, 3H).

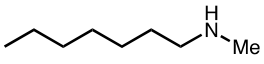

Chemical Formula: $C_8H_{19}N$
Molecular Weight: 129.24

***N*-methylheptan-1-amine (24).** LAH (710 mg, 18.6 mmol, 2.0 equiv.) was added in small portions to a solution of **22** (2.0 g, 9.30 mmol, 1.0 equiv.) in tetrahydrofuran (50 mL) at 0ºC. Upon the addition, the mixture was refluxed overnight and was quenched following the Fieser procedure. The mixture was filtered and evaporated under reduced pressure to yield **24** as an oil (1.0 g, 85%). 1H-NMR (500 MHz; CDCl3): δ 2.81 (t, *J* = 7.8 Hz, 2H), 2.57 (s, 3H), 1.63 (t, *J* = 7.6 Hz, 2H), 1.31-1.24 (m, 9H), 0.84 (t, *J* = 6.9 Hz, 3H).

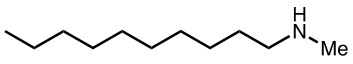

Chemical Formula: $C_{11}H_{25}N$
Molecular Weight: 171.32

***N*-methyldecan-1-amine (25).** LAH (441 mg, 11.64 mmol, 2.0 equiv.) was added in small portions to a solution of **23** (1.5 g, 5.82 mmol, 1.0 equiv.) in tetrahydrofuran at 0ºC. Upon the addition, the mixture was refluxed overnight and was quenched following the Fieser procedure. The mixture was filtered and evaporated under reduced pressure to yield **25** as an oil (965 mg, 97%). 1H-NMR (500 MHz; CDCl3): δ 2.78 (t, *J* = 7.9 Hz, 2H), 2.61 (s, 3H), 1.60 (t, *J* = 7.5 Hz, 2H), 1.29-1.25 (m, 15H), 0.86 (t, *J* = 6.5 Hz, 3H).

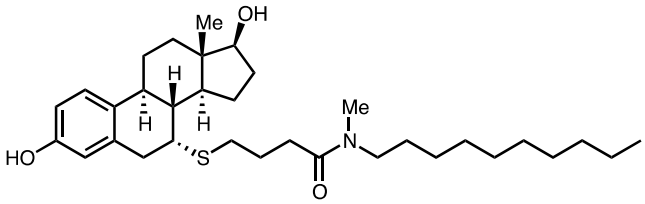

Chemical Formula: $C_{33}H_{53}NO_3S$
Molecular Weight: 543.84

***N*-decyl-4-(((7*R*,8*R*,9*S*,13*S*,14*S*,17*S*)-3,17-dihydroxy-13-methyl-7,8,9,11,12,13,14,15,16,17-decahydro-6*H*-cyclopenta[*a*]phenanthren-7-yl)thio)-*N*-methylbutanamide (26-RMS851-16).** Prepared according to general procedure B using acid **11** and amine **25. 26** was obtained as an oil (39 mg, 72%). 1H-NMR (500 MHz; CD3OD): δ 7.09-7.07 (m, 1H), 6.56 (dd, *J* = 8.4, 2.5 Hz, 1H), 6.47 (d, *J* = 2.4 Hz, 1H), 3.67 (t, *J* = 8.6 Hz, 1H), 3.20-3.14 (m, 3H), 2.98-2.95 (m, 3H), 2.88 (s, 1H), 2.65-2.32 (m, 8H), 1.94-1.24 (m, 24H), 0.89 (m, 3H), 0.78 (s, 3H). 13-C NMR (126 MHz; $CDCl_3$): δ

173.3, 154.3, 135.1, 130.7, 127.0, 116.3, 113.7, 81.7, 50.1, 47.9, 46.7, 43.55, 43.54, 43.42, 43.33, 42.8, 38.9, 37.2, 36.5, 33.71, 33.71, 33.51, 33.50, 33.0, 30.96, 30.94, 30.47, 30.28, 30.27, 29.70, 29.69, 29.00, 28.96, 28.89, 28.86, 28.5, 28.2, 26.96, 26.94, 26.83, 26.0, 25.4, 25.1, 22.46, 22.42, 14.02, 13.97, 11.2. HRMS (ESI): m/z calcd for [(M+H)+] =544.3746, found = 544.3756

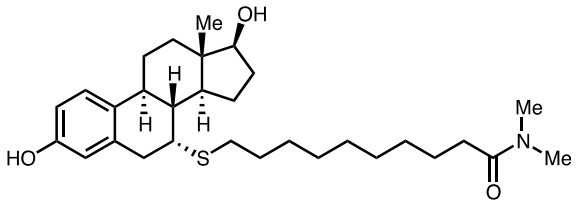

Chemical Formula: $C_{30}H_{47}NO_3S$
Molecular Weight: 501.76

10-(((7*R*,8*R*,9*S*,13*S*,14*S*,17*S*)-3,17-dihydroxy-13-methyl-7,8,9,11,12,13,14,15,16,17-decahydro-6*H*-cyclopenta[*a*]phenanthren-7-yl)thio)-*N*,*N*-dimethyldecanamide (27-RMS760-13) Prepared according to general procedure C, using acid **13** and dimethylamine hydrochloride**. 27** was obtained as an oil (18 mg, 87%). 1H-NMR (500 MHz; CDCl3): δ 7.15-7.13 (m, 1H), 6.67 (dd, *J* = 8.4, 2.6 Hz, 1H), 6.62 (d, *J* = 2.6 Hz, 1H), 3.78 (t, *J* = 8.5 Hz, 1H), 3.25-3.20 (m, 1H), 3.09-2.96 (m, 8H), 2.58-2.47 (m, 3H), 2.33 (t, *J* = 7.6 Hz, 3H), 2.17-2.13 (m, 2H), 1.91-1.26 (m, 25H), 0.78 (s, 3H). 13-C NMR (126 MHz; cdcl3): δ 173.3, 154.3, 135.1, 130.74, 130.73, 127.0, 116.3, 113.7, 81.7, 49.9, 47.7, 46.7, 43.52, 43.51, 43.32, 42.8, 38.9, 37.2, 36.5, 35.4, 33.67, 33.55, 33.0, 31.0, 30.58, 30.46, 30.23, 30.22, 29.4, 28.96, 28.89, 28.47, 28.46, 26.8, 25.4, 25.1, 22.4, 20.05, 19.95, 13.86, 13.82, 11.2. HRMS (ESI): m/z calcd for [(M+H)+] = 502.3277, found = 502.3285.

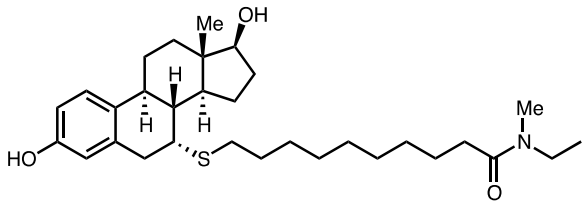

Chemical Formula: $C_{31}H_{49}NO_3S$
Molecular Weight: 515.79

10-(((7*R*,8*R*,9*S*,13*S*,14*S*,17*S*)-3,17-dihydroxy-13-methyl-7,8,9,11,12,13,14,15,16,17-decahydro-6*H*-cyclopenta[*a*]phenanthren-7-yl)thio)-*N*-ethyl-*N*-methyldecanamide (28-RMS854-14). Prepared according to general procedure B using acid **13** and N-ethylmethylamine. **28** was obtained as an oil (11 mg, 68%). 1H-NMR (500 MHz; CD3OD): δ 7.08 (d, *J* = 8.4 Hz, 1H), 6.56 (dd, *J* = 8.5, 2.6 Hz, 1H), 6.47 (d, *J* = 2.6 Hz, 1H), 3.67 (t, *J* = 8.6 Hz, 1H), 3.41-3.37 (m, 2H), 3.16-2.89 (m, 8H), 2.56-2.31 (m, 6H), 1.93-1.07 (m, 24H), 0.77 (s, 3H). 13-C NMR (126 MHz; cdcl3): δ 174.3, 154.3, 135.1, 130.7, 127.0, 116.3, 113.7, 81.7, 50.1, 47.9, 46.7, 43.55, 43.54, 43.42, 43.33, 42.8, 38.9, 37.2, 36.5, 33.71, 33.71, 33.51, 33.50, 33.0, 30.96, 30.94, 30.47, 30.28, 30.27, 29.70, 29.69, 29.00, 28.96, 28.89, 28.86, 28.5, 28.2, 26.96, 26.94, 26.83, 26.0, 25.4, 25.1, 22.46, 22.42, 14.02, 13.97, 11.2. HRMS (ESI): m/z calcd for [(M+Na)+] = 538.3331, found = 538.3318.

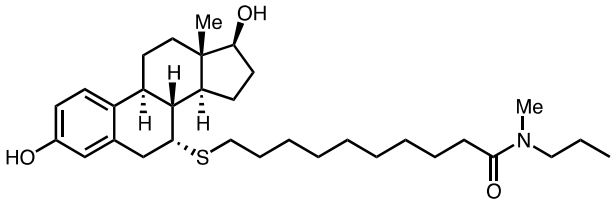

Chemical Formula: $C_{32}H_{51}NO_3S$
Molecular Weight: 529.82

10-(((7*R*,8*R*,9*S*,13*S*,14*S*,17*S*)-3,17-dihydroxy-13-methyl-7,8,9,11,12,13,14,15,16,17-decahydro-6*H*-cyclopenta[*a*]phenanthren-7-yl)thio)-*N*-methyl-*N*-propyldecanamide (29-RMS855-15). Prepared according to general procedure C using acid **13** and amine hydrochloride **18. 29** was obtained as an oil (29 mg 76%). 1H-NMR (500 MHz; CD3OD): δ 7.08 (d, *J* = 8.5 Hz, 1H), 6.56 (dd, *J* = 8.4, 2.6 Hz, 1H), 6.47

(d, *J* = 2.5 Hz, 1H), 3.67 (t, *J* = 8.6 Hz, 1H), 3.15-2.89 (m, 6H), 2.56-2.33 (m, 6H), 1.93-1.32 (m, 26H), 0.90 (dt, *J* = 21.6, 7.4 Hz, 3H), 0.77 (s, 3H). HRMS (ESI): m/z calcd for [(M+H)+] = 530.3590, found = 530.3588.

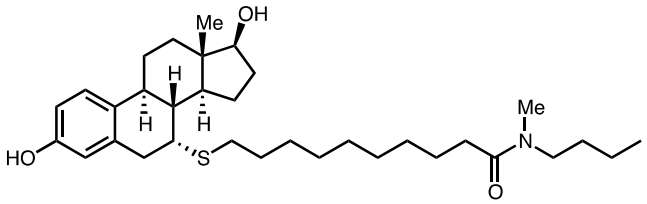

Chemical Formula: $C_{33}H_{53}NO_3S$
Molecular Weight: 543.84

***N*-butyl-10-(((7*R*,8*R*,9*S*,13*S*,14*S*,17*S*)-3,17-dihydroxy-13-methyl-7,8,9,11,12,13,14,15,16,17-decahydro-6*H*-cyclopenta[*a*]phenanthren-7-yl)thio)-*N*-methyldecanamide (30-RMS276-16).** Prepared according to general procedure C using acid **13** and amine hydrochloride **19. 30** was obtained as an oil (11 mg, 81%). 1H-NMR (500 MHz; CDCl3): δ 7.15 (d, *J* = 8.5 Hz, 1H), 6.68 (d, *J* = 8.7 Hz, 1H), 6.63 (t, *J* = 3.4 Hz, 1H), 3.78 (t, *J* = 8.5 Hz, 1H), 3.39-3.25 (m, 4H), 3.09-2.94 (m, 5H), 2.56-2.41 (m, 4H), 2.33 (m, 5H), 1.91-1.25 (m, 23H), 0.94 (dt, *J* = 15.9, 7.4 Hz, 3H), 0.78 (s, 3H). 13-C NMR (126 MHz; CDCl3): δ 154.5, 135.1, 126.9, 115.94, 115.92, 113.6, 81.7, 50.0, 47.7, 46.7, 43.73, 43.67, 43.3, 42.7, 38.7, 37.6, 36.5, 35.5, 33.67, 33.64, 32.9, 31.45, 31.40, 30.59, 30.47, 29.63, 29.61, 29.36, 29.31, 29.27, 29.21, 29.20, 28.81, 28.75, 28.63, 28.61, 28.03, 28.00, 26.9, 25.4, 25.0, 22.5, 20.04, 19.96, 13.89, 13.84, 11.2. HRMS (ESI): m/z calcd for [(M+H)+] = 544.3746, found = 544.3732 .

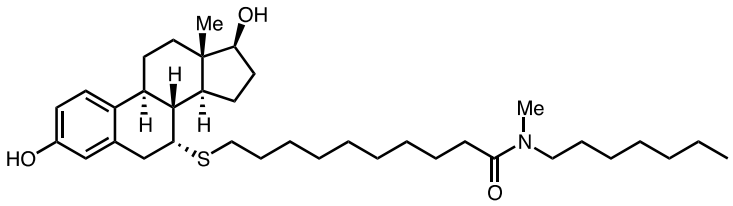

Chemical Formula: $C_{36}H_{59}NO_3S$
Molecular Weight: 585.92

10-(((7*R*,8*R*,9*S*,13*S*,14*S*,17*S*)-3,17-dihydroxy-13-methyl-7,8,9,11,12,13,14,15,16,17-decahydro-6*H*-cyclopenta[*a*]phenanthren-7-yl)thio)-*N*-heptyl-*N*-methyldecanamide (31). Prepared according to general procedure B using acid **13** and amine **24**. **31** was obtained as an oil (14 mg, 74%). 1H-NMR (500 MHz; CDCl3): δ 7.15 (d, *J* = 8.5 Hz, 1H), 6.68 (dt, *J* = 8.4, 2.3 Hz, 1H), 6.63 (dd, *J* = 5.2, 2.7 Hz, 1H), 3.78 (t, *J* = 8.5 Hz, 1H), 3.38-2.94 (m, 9H), 2.57-2.48 (m, 3H), 2.36-2.14 (m, 5H), 1.91-1.24 (m, 30H), 0.88 (dt, *J* = 9.8, 7.0 Hz, 3H), 0.78 (s, 3H). 13-C NMR (126 MHz; cdcl3): δ 173.6, 154.5, 135.1, 130.6, 126.9, 115.9, 113.6, 81.7, 50.2, 48.0, 46.7, 43.71, 43.65, 43.3, 42.7, 38.7, 37.56, 37.51, 36.5, 35.5, 33.66, 33.64, 32.9, 31.78, 31.72, 31.43, 31.39, 30.5, 29.63, 29.62, 29.32, 29.28, 29.21, 29.20, 29.09, 29.01, 28.83, 28.77, 28.65, 28.63, 28.49, 28.07, 28.03, 27.3, 26.87, 26.80, 26.69, 25.4, 25.0, 22.59, 22.56, 22.51, 14.09, 14.06, 11.2. HRMS (ESI): m/z calcd for [(M+H)+] = 586.4216, found = 586.4232 .

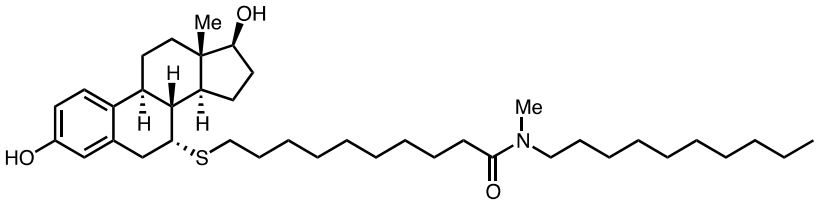

Chemical Formula: $C_{39}H_{65}NO_3S$
Molecular Weight: 628.00

***N*-decyl-10-(((7*R*,8*R*,9*S*,13*S*,14*S*,17*S*)-3,17-dihydroxy-13-methyl-7,8,9,11,12,13,14,15,16,17-decahydro-6*H*-cyclopenta[*a*]phenanthren-7-yl)thio)-*N*-methyldecanamide (32).** Prepared according to general procedure B using acid **13** and

amine **25**. **32** was obtained as an oil (15 mg, 83%). 1H-NMR (500 MHz; CD3OD): δ 7.08 (d, *J* = 8.5 Hz, 1H), 6.56 (dd, *J* = 8.5, 2.6 Hz, 1H), 6.47 (d, *J* = 2.5 Hz, 1H), 3.67 (t, *J* = 8.6 Hz, 1H), 3.36-3.31 (m, 2H), 2.88 (m, 5H), 2.56-2.31 (m, 5H), 2.06-1.24 (m, 41H), 0.89 (t, *J* = 6.9 Hz, 3H), 0.77 (s, 3H). 13-C NMR (126 MHz; cdcl3): δ 173.8, 155.2, 135.4, 130.6, 126.9, 116.2, 113.5, 81.4, 50.2, 48.0, 46.7, 43.73, 43.65, 43.3, 42.7, 38.7, 37.56, 37.51, 36.5, 35.5, 33.66, 33.64, 32.9, 31.78, 31.72, 31.43, 31.39, 30.5, 29.63, 29.62, 29.32, 29.28, 29.21, 29.20, 29.12, 29.15, 29.09, 29.01, 28.83, 28.79 28.77, 28.65, 28.64, 28.63, 28.49, 28.07, 28.03, 27.3, 26.87, 26.80, 26.69, 25.4, 25.0, 22.59, 22.56, 22.51, 14.09, 14.06, 11.2. HRMS (ESI): m/z calcd for [(M+H)+] = 628.4685, found = 628.4682.

SUPPLEMENTARY REFERENCES

1. Spera D, Cabrera G, Fiaschi R, Carlson KE, Katzenellenbogen JA, Napolitano E. 2004. Estradiol derivatives bearing sulfur-containing substituents at the 11beta or 7alpha positions: versatile reagents for the preparation of estrogen conjugates. Bioorg Med Chem **12**:4393-4401.

2 eme Article : Full antiestrogen Fulvestrant induces SUMO-dependent recruitment of the chromatin remodeling complex ACF to estrogen receptor α

Full antiestrogen Fulvestrant induces SUMO-dependent recruitment of the chromatin remodeling complex ACF to estrogen receptor α

Nader Hussein[1,2,*], Khalid Hilmi[1,2,*], Laurence Fleury[1,2,], Pierre Thibault[2,3] and Sylvie Mader[1,2,#]

* co-first authors.

[1] Biochemistry Department, Université de Montréal, Montréal, Québec, H3C 3J7 Canada.

[2] Institute for Research in Immunology and Cancer, Université de Montréal, Montréal, Québec, H3C 3J7 Canada.

[3] Chemistry Department, Université de Montréal, Montréal, Québec, H3C 3J7 Canada.

SUMMARY

Selective estrogen receptor downregulators (SERDs) such as ICI182,780 (Fulvestrant) are competitive inhibitors of estrogen receptor (ERα). Fulvestrant is currently used as a second line therapy for advanced breast tumors in postmenopausal women after treatment with tamoxifen, a selective estrogen receptor modulator (SERM). ICI182,780 downregulation of estrogen target genes was shown to be mediated by polyubiquitylation followed by an accelerated ERα turnover. We have also reported that full antiestrogens induce rapid SUMOylation of ERα. Here we show that treatment with SERDs but not SERMs induces a rapid interaction between ERα and the human ATP-utilizing chromatin assembly and remodeling factor (ACF) in transfected ER-negative cells and in ER-positive cell lines. Related ISWI complexes including RSF1, WSTF and NURF were not similarly recruited in the presence of fulvestrant. In contrast, the SWI-SNF complex was recruited both in the presence of agonists and full antiestrogens. Deletion of helix 12 of the ERα ligand binding domain or mutation of hydrophobic amino acids in H12 abrogates both SUMOylation and ACF recruitment. Further, suppression of SUMOylation by overexpression of the deSUMOylase SENP1 prevented recruitment of ACF. ACF recruitment was not necessary for induction of ERα degradation by full antiestrogens in ERα-positive MCF7 cells. Using chromatin immunoprecipitation, we observed an increase in the association of the ACF1 subunit of ACF with the proximal promoter of the estrogen target gene pS2 in the presence of Fulvestrant, suggesting that ACF plays a role in the transcriptional inactivation of ERα target genes in the presence of SERDs.

INTRODUCTION

Estrogen receptor alpha (ERα), expressed in approximately 70% breast tumors, mediates the proliferative effects of estrogens in breast epithelial cells. It belongs to the nuclear receptor superfamily of ligand-inducible transcription factors (1). Receptors of this family have a modular organization with a central DNA binding domain flanked by two transcriptional activation functions. The C-terminal activation function 2 is ligand-dependent and the activation function 1 in the N-terminal region acts in a ligand-independent manner when the receptor is bound to DNA (2, 3).

In the absence of estrogens, ERα is associated with a heat shock protein-immunophilin chaperone complex. Ligand binding induces conformational changes that decrease surface hydrophobicity of the LBD and release ERα from interaction with HSP90 interaction. Binding of ERα to estrogen response elements present in the vicinity of target genes is then followed by the sequential recruitment of histone-acetyltransferase factors, the basal transcriptional machinery and the SWI-SNF chromatin remodeling factor (4-7).

The importance of ERα in breast tumorigenesis has led to the development of antiestrogens, which are competitive inhibitors of ERα. Tamoxifen, the gold standard in ER+ breast tumor treatment, is a selective estrogen receptor modulator (SERM) (8, 9). Compounds of this class exhibit a tissue- and promoter-specific partial agonistic activity (10, 11). Unlike SERMs, full antiestrogens, also called selective estrogen receptor downregulators (SERDs) due to their capacity to accelerate receptor turnover, are devoid from any transcriptional activity and can be used as a second line therapy in post-menopausal women with hormone receptor-positive advanced breast tumors (12). Fulvestrant (ICI182,780) is the only clinically-approved SERD. Doses of 500 mg/month administered by intramuscular injections are currently suggested with an improved benefit risk profile over the previously approved 250 mg/month (13), but the limited ERα degradation observed within tumors suggests that the drug is poorly bioavailable. This has led to renewed efforts to synthesize improved full antiestrogens. However, the mechanisms of action of SERDs remains poorly understood.

Transcriptional inhibition by antiestrogens arises from their ability to displace helix H12 in the ligand binding domain of ERα and thus disrupt the primary coactivator binding surface (14, 15). In addition, SERDs like ICI182,780 induce ERα polyubiquitylation and degradation by the 26S proteasome (16). However, it was shown recently that increased degradation and transcriptional inhibition of ERα in the presence of full AEs can be uncoupled (17, 18), suggesting the involvement of additional mechanisms for transcriptional inhibition by SERDs. SERDs are also more potent than SERMs in promoting ERα binding to the corepressor NCoR (19), and can also recruit CBP but not p160 coactivators (20). Finally, SERDs have been reported to immobilize ERα in the nucleus in fluorescence after photobleaching (FRAP) experiments (17, 21), to increase association with the nuclear matrix (22, 23) and to induce interaction with nuclear matrix components cytokeratins 8 and 18 (24). We have observed recently that SERDs specifically induce SUMOylation of ERα and that inhibition of SUMOylation partially derepresses transcriptional inhibition by SERDs (23). SUMOylation of ERα may in turn lead to recruitment of specific corepressors, as observed for a variety of other transcription factors (25, 26).

Here we show that full antiestrogens specifically induce interaction of ERα with the ACF complex, a member of the ISWI group of chromatin remodeling complexes (27) that contains SNF2H, also known as SMARCA5 (28), as a catalytic subunit. ACF1, also known as BAZ1A, which contains a bromodomain, 2 PHD fingers and a putative heterochromatin targeting domain, is the non-catalytic subunit in the ACF complex (29). *In vitro,* ACF catalyzes the deposition of histones into extended periodic nucleosome arrays (30). In addition, ACF has been shown to play a role in the organization and replication of heterochromatin in the S phase of cell cycle (31). In *Drosophila*, the loss of ACF1 resulted in a decrease in the periodicity of nucleosome arrays and ACF1 was shown to contribute to chromatin-dependent transcriptional silencing by Polycomb group genes (32). In addition, ACF1 is recruited by the nuclear matrix scaffolding protein SATB1, which correlated with the inhibition of the *IL2Rα* gene in thymocytes (33). Recently, it has been shown that ACF interacts with the nuclear corepressor NCoR and associated histone deacetylase (HDAC) activity, and is co-recruited with NCoR to the unliganded Vitamin D3

receptor, contributing to chromatin inactivation (34). Thus, the interaction between ERα and the ACF complex in the presence of full antiestrogens suggests the importance of chromatin remodeling in the pharmacological properties of these compounds in addition to their SERD properties.

MATERIALS AND METHODS:

Reagents and antibodies:

17β-estradiol (E2), 4-hydroxytamoxifen (OHT), Raloxifene (Ral), ICI182,780 and mouse monoclonal anti-M2 Flag affinity gel were from Sigma-Aldrich. ICI164,384 and RMS234 were a gift from Dr. James Gleason (McGill University, Canada). The transfection reagent polyethylenimine PEI was from Polsciences, Inc. SiLentFect Lipid Reagent was from Bio-Rad and siRNAs against GAPDH, SNF2H and ACF1 were purchased from Thermo Scientific Dharmacon (sequences available upon request). Goat polyclonal anti-ACF1 and goat polyclonal anti-BPTF were from Santa Cruz. Rabbit polyclonal anti-SNF2H was from purchased from Abcam. Mouse anti RSF-1 was purchased from Upstate, and rabbit polyclonal anti-WSTF was purchased from Cell Signaling. Rabbit anti-Brg1 was a gift from Dr. Julie Lessard (IRIC, Université de Montréal, Canada). Horseradish peroxidase-conjudated secondary antibodies were purchased from Jackson. Polyvinylidene difluoride (PVDF) membranes were from Millipore and the ECL detection reagent was from PerkinElmer.

Constructs and expression vectors:

The pCDNA3-EGFP-Flag vector was kindly provided from Dr Sylvain Meloche (IRIC, Université de Montréal, Canada). pcDNA3-GFP-SENP1 was a kind gift from Dr Matunis (Johns Hopkins University, Baltimore, USA). Mutations L536A, L539A, Y537A and L540A were generated by site-directed mutagenesis of the ERα cDNA (the sequence of oligonucleotides used for mutagenesis is available upon request). To construct pCDNA3-ERα-Flag, or H12 mutants, PCR-amplified ERα was exchanged for EGFP using the Pac I and Pme I restriction sites in pCDNA3-EGFP-Flag. pSG5-ERαΔH12 was generated by deleting amino acids 535 to 545 in pSG5-ERα.

Cell culture and transfection

HEK 293 cells were maintained at 37ºC in Dulbecco's modified Eagle's medium Red (Wisent) supplemented with 10% fetal bovine serum (Sigma), and 100 U/ml penicillin-streptomycin (Wisent). MCF7 cells were maintained in α-MEM supplemented with 10% FBS, 2 mM L-glutamine and 100 U/ml penicillin-streptomycin. Three days before experiments, cells were switched to phenol red-free DMEM containing 10% charcoal-stripped serum (FBS-T).

HEK 293 cells were seeded at a density of 11 x10 ^{6} cells per 15 cm petri dish. 24 h later, cells were transfected using PEI (10 µg PEI for µg DNA). 24 h postransfection, medium was changed and the cells were incubated for another 24 h. Cells were treated with E2 (25 nM), ICI182,780 (100nM) or vehicle (ethanol) for the indicated times. MCF7 cells ($5x10^{6}$ cells) were transfected by electroporation (DNA mix containing 6 µg pCDNA3-ERα-Flag or pCDNA3-EGFP-Flag and 34 µg salmon sperm DNA) using a Gene Pulser (BioRad). 24 h postransfection, medium was replaced with fresh phenol-red free DMEM supplemented with 10% FBST. Cells were incubated for another 24 h and treated with ICI182,780 (100 nM) or vehicle for 1 h. For siRNA transfection, MCF7 cells were seeded at a density of 4 x10 ^{6} in phenol-red free DMEM supplemented with 10% FBST without penicillin-streptomycin. Transfections were performed twice using 20 nM siGAPDH, siSNF2H or siACF1 and SiLenFect Lipid Reagent.

Co-immunupreciptation and western blotting.

Cells were washed and harvested with ice-cold PBS. After centrifugation at 1,000xg for 5 min, cell pellets were resuspended in lysis buffer (20 mM Tris-HCl pH7.5, 150 mM NaCl, 2 mM EDTA, 1% NP40, completed with a cocktail of protease and phosphatase inhibitors). Cell lysis was performed at 4 ºC for 20 min. Whole cell lysates were collected after centrifugation at 11,000xg for 15 min. Following protein quantification using the DC protein assay (Bio-Rad), immunoprecipitation was performed overnight at 4ºC using equal amounts of proteins with mouse monoclonal anti M2-Flag affinity gel. The following day, beads were washed three times with IP buffer supplemented with protease and phosphatase inhibitors. Samples were denatured in Laemmli sample buffer (60 mM Tris-HCl pH 6.8, 100 mM DTT, 2% SDS, 10% glycerol,

0,01% bromophenol blue) for 5 min at 95 ºC and resolved by 7% SDS-PAGE. After electrotransfer, the PVDF membrane was blocked by incubation at room temperature for 1h in PBS supplemented with 0.2% Tween 20 and 5% nonfat dry milk. ERα and chromatin remodeling proteins were detected with the indicated antibodies and HRP-conjugated secondary antibodies. Finally, complexes were revealed by enhanced chemiluminescence as recommended by the manufacturer (PerkinElmer).

Silver staining and mass spectrometry

All solutions were prepared in MilliQ water. Proteins were fixed by incubating the gel for 1 h in 50% ethanol and 5% acetic acid. The gel was then washed three times with 50% ethanol for 20 min, followed by washes with water and sensitization with Na2S2O3 0,02% for 1 min. The gel was stained for 20 min with 0.1% AgNO3. Destaining was performed using 3% Na2CO3, 0,05% formaldehyde and stopped with 5% acetic acid.

Bands of interest were excised, reduced and alkylated prior to tryptic digestion and peptide extraction. Peptide digests were analyzed by nanoLC-MS/MS on a LTQ-Orbitrap XL mass spectrometer (Thermo Fischer Scientific) The mass spectrometer was operated in data-dependent mode, alternatively acquiring MS and MS/MS scans. MS spectra (survey scan) were acquired with a resolution of 60,000 in FTMS using lock mass. CID MS/MS spectra were acquired in data-dependent mode for the three most abundant multiply charged ions with intensity above 10,000 counts. A dynamic exclusion window was set to 90s. MS/MS spectra peak lists were extracted from Xcalibur raw data files and preprocessed using Mascot Distiller v2.1.1 (Matrix Science) using the configuration file for low resolution MS/MS for the LTQ-Orbitrap. MGF peak lists were searched with Mascot 2.1 on a concatenated target/decoy IPI human database (IPI version 3.24 november 2006) using the following parameters: peptide mass tolerance ± 10 ppm, fragment mass tolerance ± 0.5 Da, trypsin with 2 missed cleavages, and the variable modifications carbamidomethyl (C), deamidation (NQ), oxidation (M), phosphorylation (STY).

Luciferase reporter assays

HepG2 cells (10^6 cells) were transiently transfected by electroporation with the expression vector for ERα (400 ng), the reporter vector ERE3-TATA-Luc (200 ng) and a CMV-β-galactosidase internal control expression vector (400 ng), supplemented with salmon sperm DNA to 8 µg total DNA. Electroporated cells were seeded in 6-well plates (10^6 cells per well). 16 h after transfection, cells were treated with E2 (25 nM), ICI182,780 (100 nM) or vehicle (ethanol). Cells were lysed after another 24 h and aliquots of whole cell extracts were assayed for luciferase activity in the presence of luciferin with a Veritas Microplate luminometer (Turner Biosystems).

Results were normalized for β-galactosidase activity revealed with ortho-nitrophenyl-β-D-galactopyranoside (ONPG) and measured at 420 nm with a Spectramax 190 plate reader (Molecular Devices).

Chromatin immunoprecipitation (ChIP)

ChIP experiments were performed as described by Bourdeau et al. (35). Briefly cells were fixed for 10 min at room temperature with 1% formaldehyde. Cell pellets were resuspended in cell lysis buffer containing 5 mM Pipes pH 8.0, 10 mM KCl, 0,5 % NP-40, supplemented with protease and phosphatase inhibitors. Following centrifugation at 1,000xg, nuclei were resuspended in nuclear lysis buffer (50 mM Tris-HCl pH 8.1, 10 mM EDTA pH 8.0 and 1% SDS, supplemented with protease and phosphatase inhibitors). Nuclear extracts were subjected to sonication using an ice-water bath Bioruptor (Diagenode) to obtain DNA fragments of 500 pb. Following DNA quantification, samples were diluted to 0.1% SDS and immunoprecipitation was performed O/N at 4°C using equal amounts of DNA and a (1:1) mix of Sepharose A and G beads (GE). After washes, cross-linking was reversed using Chelex 100 resin (BioRad) and DNA was eluted by centrifugation at 12,000xg for 1 min. The immunoprecipitated pS2 fragments were quantified by real time qPCR using the following primers: pS2 promoter forward 5'-ctagacggaatgggcttcat-3' ; pS2 promoter reverse 5'-ctccctcctcttagggctga-3'. The amplification ratios of immunoprecipitated samples over the input were calculated using the ΔCT method.

RESULTS

ICI182,780 induces the recruitment of the ACF complex, but not other ISWI chromatin remodeling complexes by ERα in transfected HEK 293 and MCF7 cells

The full antiestrogen ICI182,780 (fulvestrant) induces inactivation and degradation of ERα. To identify new cofactors contributing to the full antiestrogenicity of ICI182,780, an immunoprecipitation experiment was performed from extracts of HEK 293 cells transfected with an ERα-flag expression vector and treated with 17-β-estradiol (E2), ICI182,780 (ICI) or vehicle (ethanol) for 1 h. After SDS PAGE, silver staining revealed two high molecular weight bands that co-purify with ERα specifically in the presence of ICI182,780 (Fig 1A). Mass spectroscopy analysis revealed 43 and 34 peptides belonging respectively to ACF1 and SNF2H (supplementary Fig. 1). The interaction between ERα and the ACF complex was validated in HEK 293 cells using specific antibodies for ACF1 and SNF2H (Fig 1B). On the other hand the association of Brg1, a cofactor of ERα recruited in the presence of E2 (36), was shown to be constitutive and enhanced by E2 and ICI182,780. Finally, we further verified that ICI182,780-dependent recruitment of ACF also takes place in MCF7 cells transiently transfected with the ERα-Flag construct (Fig. 1C).

SNF2H is the catalytic subunit in many ISWI remodeling complexes (28, 37). To assess if other members of ISWI complexes are recruited in the presence of ICI182,780, we performed immunoprecipitation of ERα-Flag and western blotting for different ISWI complex subunits. No interaction was observed with Rsf-1 and WSTF, which are respectively the non catalytic subunits of the RSF and WICH complexes (Fig. 2). We also investigated the presence of the NURF complex, which is the only human ISWI remodeler reported to contain SNF2L. Although BPTF contains four LXXLL motifs, which are usually involved in the interaction with nuclear hormone receptors (38), our results show that E2 and ICI182,780 abolish the constitutive recruitment of BPTF.

ACF recruitment is a specific property of full antiestrogens and is dependent on H12 integrity

Full antiestrogens differ from SERMs by their capacity to induce a unique conformation of the activation function 2 in the ligand binding domain of ERα in which the AE side chain binds in the coactivator binding groove while H12 is conformationally flexible (15). To investigate if recruitment of ACF can occur when ERα is liganded by other antiestrogens, we performed immunoprecipitation experiments from HEK293 cells or HeLa cells transfected with flagged-ERα (Fig. 3 and Supplementary Fig. 2). Full antiestrogens ICI182,780 and ICI164,384 were able to induce the recruitment of ACF while SERMs OHT and Ral were not. Our results thus suggest that ACF recruitment is dependent on the AF-2 conformation induced by SERDs.

Helix 12 in the ligand binding domain is a critical surface for coactivator recruitment and the main structural determinant that differs in ERα bound to agonists, SERMs or SERDs (39-41). Crystal structures and modeling studies have shown that the side chain of full antiestrogens causes steric hindrance with long hydrophobic amino acids in helix 12 (17, 40). In order to ascertain more precisely the role of helix 12 in the recruitment of the ACF complex, we performed immunoprecipitation experiments with wild-type ERα, a mutant with a deletion of H12 or mutants with single point mutations in this helix replacing long hydrophobic amino acids by alanines. Recruitment of ACF was not observed in the presence of ICI182,780 when H12 is deleted; however, weak recruitment was observed in the absence or presence of E2, suggesting a contribution of non-H12 determinants in interaction with ACF (Fig 4A). Interaction was also lost when H12 leucines L536, L539 and L540 were mutated to alanines, while the interaction was detected with the Y537A mutation (Fig 4B). Of note, mutants L536A, L539A and L540A have increased transcriptional activity in the presence of ICI182,780, while mutant Y537A does not (Fig. 4C). In addition, the same correlation was observed with SUMOylation. Taken together, our results indicate a role of the integrity of H12 in the recruitment of ACF as well as in full suppression of transcriptional activity in the presence of SERDs.

ACF is recruited to ERα in a SUMO-dependent manner in the presence of SERDs, but does not contribute to increased receptor turn-over

We have recently shown that SERDs induce rapid SUMOylation of several residues of ERα. SUMOylation contributes to ICI182,780-induced inactivation of ERα even in the absence of increased receptor turnover as observed in HepG2 cells (23), and depends on integrity of H12. Next, we examined how rapidly the interaction with ACF occurs in transiently transfected HEK293 cells after treatment with ICI182,780. The interaction was detected after 5 min treatment, reached a peak at 30 min but was persistent after 8h treatment with ICI182,780 (Fig 5). Our results thus indicate that ACF1 recruitment, like SUMOylation, is an early event after exposure to full antiestrogens. To address whether the recruitment of ACF is dependent on SUMO marks, we performed an immunoprecipitation experiment in control cells or HEK 293 cells transfected with the deSUMOylase SENP1. Overexpression of SENP1 abolished SUMOylation and strongly reduced ACF complex recruitment in the presence of ICI182,780 (Fig 6), consistent with a SUMOylation-dependent recruitment of ACF in the presence of ICI182,780.

We then examined whether the recruitment of ACF, which appears before receptor degradation is detectable, can contribute to the subsequent decrease in ERα protein levels. Transfection of siRNAs against ACF subunit ACF1 led to a marked reduction in the levels of the corresponding protein and also affected ERα expression levels irrespective of treatment; however ERα levels were still depleted in the presence of ICI182,780 compared to mock-treatment (supplementary Fig. 3). The effect of ICI182,780 on ERα levels, but not that of siACF1, was abolished by proteasome inhibitors. Transfection of siRNAs against SNF2H had more modest effects on SNF2H expression levels and did not noticeably affect ERα protein levels under any treatment condition in MCF7 cells (supplementary Fig. 3). We conclude that ACF is unlikely to play a major role in the control of ERα turnover rate in the presence of full antiestrogens.

The observation that ICI182,780 induces inactivation of ERα in the absence of an accelerated turnover (17, 18) indicates the contribution of other mechanisms in addition to ERα degradation in gene repression by ICI182,780. Recruitment of ACF, which is located in the

chromatin in cell fractionation experiments (supplementary Fig. 4), to ER binding sites may contribute to gene inactivation due to chromatin remodeling. We therefore analyzed the presence of ERα and ACF1 on the proximal promoter of the estrogen target gene pS2 after 3 hours of exposure to E2, ICI182,780 or vehicle. E2 induces recruitment of ERα to this promoter while ICI182,780 treatment only weakly increased basal recruitment at this time point where ERα degradation is detectable (data not shown). On the other hand, basal ACF1 recruitment in the absence of ligand was enhanced in the presence of ICI182,780 and completely abrogated with the agonist. Our results are consistent with a role of ligands in modulating ACF recruitment to promoters of hormone target genes and suggest a potential role of ACF in transcription inhibition in the presence of ICI182,780, as observed with unliganded VDR (34).

DISCUSSION

Full antiestrogens are antagonists that mediate complete inactivation of ERα, contrary to SERMs, which display cell- and gene-specific partial agonist activity. The basis of full anti-estrogenicity is thought to arise from their capacity to enhance ERα turnover in addition to blocking co-activator recruitment. However, full antiestrogens maintain the capacity to prevent ERα transcriptional activity using a sensitive ERE3-TATA-Luc reporter in HepG2 cells ((17) and Fig. 4C). ERα was recently shown by our group to be highly SUMOylated in the presence of full antiestrogens, but not SERMs (23). SUMOylation can modulate several properties of transcription factors, including subcellular location, turn-over, transcriptional activity, and protein-protein interactions (25, 26, 42). In this study, we examined using a proteomic approach whether the full antiestrogen ICI182,780 (fulvestrant) can induce recruitment of specific cofactors to ERα. We identified endogenous ACF as an ERα-interacting protein in the presence of full antiestrogens, but not SERMs or agonists, in transfected ER-negative and in ER-positive cells.

The interaction between ACF and ERα could be direct since the ACF1 subunit harbors one putative receptor interaction motif LXXII, also found in corepressors NCoR and SMRT, reported to interact with ERα with increased efficacy in the presence of full antiestrogens compared to SERMs (43). However, while these motifs mediate interaction of NCoR with unliganded nuclear receptors, they do not appear to interact with ERα in the presence of full antiestrogens (our unpublished results using bioluminescence resonance energy transfer between RAR or ER fused to luciferase and the nuclear receptor interaction domain or isolated corepressors motifs of NCoR). NCoR could however mediate the interaction via another surface and contribute to formation of a larger complex, as suggested for ACF/NCoR interaction with the unliganded VDR (34).

In addition, ACF recruitment in the presence of ICI182,780 was abrogated by mutations in helix 12 that prevent SUMOylation, and by SENP1 over-expression, suggesting dependence on

SUMOylation. Both SNF2H and ACF1 harbor putative SUMO interacting motifs, and it will be interesting to test whether regions containing these domains can interact with ERα in the presence of full antiestrogens. On the other hand, SUMOylation of ACF may also be important for the interaction. SUMOylation controls the activity of many transcriptional cofactors, such as the nuclear receptor corepressor NCoR, whose function is enhanced (44), or the coactivator p300 whose capacity to repress transcription is dependent on SUMOylation (42). In addition, it was shown that the PHD module of the KAP1 corepressor can exhibit an intramolecular E3 SUMO ligase activity for the adjacent bromodomain (45). As ACF1 also contains both PHD and bromodomains, it would be of interest to investigate the ability of ACF to exhibit an E3 SUMO ligase activity, with itself, ERα and NCoR as potential targets in the presence of ICI182,780.

The recruitment of ACF within 5 min exposure to ICI182,780 takes place before efficient degradation, but does not appear to be necessary for increased turnover, which is likely dependent on increased ubiquitylation of the receptor. Whether SUMOylation and ubiquitylation represent competitive modifications on an overlapping set of Lys residues in ERα remains to be determined as the target residues for ubiquitylation in full AE-complexed ERα have yet to be identified. In addition, while we identified 4 Lys residues in ERα that are modified by SUMOylation *in vivo*, more sites are likely modified as mutations of all four lysines did not abrogate full antiestrogen-induced SUMOylation.

An early property of ERα in the presence of full antiestrogens is its association with an insoluble nuclear compartment and slower mobility in FRAP experiments (17, 46, 47). H12 deletion abrogated immobilization of the receptor in FRAP experiments and interaction with cytokeratins 8 and 18 (21, 24). Notably, ACF recruitment was also abrogated when H12 was deleted. As ACF was shown to interact with the nuclear matrix scaffold protein SATB1 (33), the importance of interaction of ERα with ACF in its immobilization and association with the nuclear matrix should be further investigated.

We have shown that mutations of leucines 536, 539 and 540 to alanines lead to a gain of transcriptional activity in the presence of ICI182,780 whereas mutation of tyrosine 537 did not (17). Interestingly, these mutants correlate the lack of ACF recruitment and transcriptional de-

repression, consistent with the proposed role of ACF in transcriptional silencing. Previous studies have shown that SNF2H is associated both with the chromatin and nuclear matrix (48, 49). In our fractionation studies ACF1 and SNF2H were found in the chromatin with a subpopulation of SNF2H in the nuclear matrix. This indicates that ACF is likely to interact with ERα in the chromatin compartment in the presence of ICI182,780 and be recruited to estrogen response elements in the presence of full antiestrogens, where it may lead to chromatin remodeling. It has been shown that one third of ERα binding sites bound in the presence of E2 are also bound in the presence of ICI182,780 after 1h treatment (50). These observations agree with footprinting studies indicating that ICI182,780 recruits multiple proteins to the pS2 promoter in a pattern distinct from that of E2 (51). We verified that ICI182,780 enhanced ACF1 recruitment to the proximal promoter of pS2. Therefore it is tempting to speculate that ACF contributes to rapid gene silencing prior to and independently from ERα degradation by achieving chromatin remodeling in the presence of ICI182,780. Experiments to determine whether ACF recruitment results in increased histone density and accumulation of marks of heterochromatin on the promoters of E2 target genes are currently ongoing.

ACKNOWLEDGMENTS

This work was supported by grants from the Canadian Breast Cancer Alliance and the Cancer Research Society, Inc. S.M. holds the CIBC Breast Cancer Research Chair at Université de Montréal. K.H. has been recipient of awards from the Faculté des Études Supérieures de l'Université de Montréal, and N.H. was the recipient of a fellowship from the Montreal Center for Experimental Therapeutics in Cancer. The Institute for Research in Immunology and Cancer is supported in part by the Canadian Center of Excellence in Commercialization and Research, the Canada Foundation for Innovation, and the Fonds de la Recherche en Santé du Québec

FIGURE LEGENDS

Fig 1. Recruitment of ACF by ERα in the presence of ICI182, 780.

A. HEK 293 cells were transiently transfected with the expression vectors for ERα-Flag or EGFP-Flag for 48 h and treated with vehicle or ligands 17-β-estradiol (E2, 25 nM), ICI182,780 (ICI, 100 nM) for 1 h. ERα-Flag and associated proteins were immunoprecipitated from extracts. Following SDS–PAGE, proteins were revealed by silver staining and bands of interest were excised and analyzed by LC-MS/MS. **B-C**. The presence of the ACF complex components ACF1 and SNF2H in anti-Flag immunoprecipitates from transiently transfected HEK 293 (B) or MCF7 (C) cells were revealed by western blotting. Experiments were performed at a least three times with similar results.

Fig 2. Other ISWI remodelers are not recruited in the presence of ICI182,780.

HEK 293 were transiently transfected with expression vectors for ERα-Flag or EGFP-Flag for 48 h and treated for 1 h with E2 (25 nM), ICI182,780 (ICI, 100 nM) or vehicle. Following immunoprecipitation, the presence of the ACF complex and of subunits of other ISWI complexes were assessed by western blotting. A representative result is shown.

Fig 3. ACF recruitment is a specific property of full antiestrogens.

HEK 293 were transiently transfected with expression vectors for ERα-Flag or EGFP-Flag for 48 h and treated for 1 h with vehicle, E2 (25 nM) or the antiestrogens 4-hydroxytamoxifen (OHT), raloxifene (Ral), ICI182,780 (ICI182) and ICI164,384 (ICI164), 100 nM each. Following immunoprecipitation the presence of ACF1 and of SNF2H in immunoprecipitates was assessed by western blotting. The experiment was performed two times with similar results (see also supplementary figure 2 for similar results in HeLa cells).

Fig 4. ACF recruitment depends on H12 integrity and correlates with inhibition of transcriptional activation by full antiestrogens in ERα mutants.

HEK 293 cells were transiently transfected for 48 h with the expression vectors for ERα and ERα ΔH12 in A. or with expression vectors for ERα-Flag, Helix 12 mutants or the empty vector in B. Cells were treated with ligands of vehicle for 1h. Recruitment of ACF was assessed by immunoprecipitation followed by western blotting. The experiment was performed three times with similar results. C. HepG2 cells were transiently transfected with the expression vector for ERα, the reporter vector ERE3-TATA-Luc and the expression vector CMV-β-galactosidase. Cells were treated 24 h after transfection with 25 nM E2 or 100 nM ICI182,780. Cells were lysed after another 24 h and aliquots of whole cell extracts were assayed for luciferase activity. The experiment was performed 3 times with similar results and a representative experiment is shown (mean values +/- SD from duplicates).

Fig 5. ACF recruitment follows rapid kinetics in the presence of ICI182,780

HEK 293 cells were transiently transfected with expression vectors for ERα-Flag or EGFP-Flag for 48 h and treated for the indicated time with ICI182,780 or with vehicle for 1 h. Following immunoprecipitation, the presence of ACF1, SNF2H and ERα in the imunoprecipitates was assessed by western blotting. The experiment was performed two times with similar results.

Fig 6. DeSUMOylation by SENP1 abrogates the recruitment of ACF in the presence of ICI182,780.

HEK293 were transiently transfected with expression vectors for ERα-Flag and EGFP-Flag or ERα-Flag and SENP1 for 48 h and treated for 1 h with ICI182,780 (ICI, 100 nM) or the vehicle. Following immunoprecipitation, the ACF complex and ERα interaction was assessed by western blotting. The experiment was performed twice with similar results.

Fig 7. ICI182,780 enhances ACF1 recruitment to the pS2 proximal promoter.

MCF7 cells were treated with 0, E2 (25 nM) or ICI182,780 (100 nM) for 3 hours. Complexes were crosslinked with paraformaldehyde. Immunoprecipitation was performed using equal amounts of chromatin with anti-ERα and anti-ACF1 antibodies. After crosslinking reversal, the proximal ERE of pS2 was amplified by PCR in the input and immunopreciptated fraction and ratios of IP/input ratios of amplification were calculated. Experiment was performed three times with similar results. Results correspond to mean values +/- SD.

Supplementary figure 1. Mass spectrometry identification of the main proteins in band 1 and band 2

HEK 293 cells were transiently transfected with the expression vectors for ERα-Flag or EGFP-Flag for 48 h and treated with E2 (25 nM), ICI182,780 (100 nM) or vehicle for 1h. ERα-Flag and associated proteins were immunoprecipitated from extracts. Following SDS–PAGE, proteins were revealed by silver staining and bands of interest were excised and analyzed by LC-MS/MS. Peptides corresponding to the major proteins characterized for bands 1 and 2 are shown.

Supplementary figure 2. ACF recruitment is a specific property of full antiestrogens

HeLa cells were transiently transfected with expression vectors for ERα-Flag or EGFP-Flag for 48 h and treated for 1 h with E2 (25 nM), antiestrogens (100 nM) or vehicle. Following immunopreciptaion the presence of ACF1 and SNF2H in immunoprecipitates was assessed by western blotting.

Supplementary figure 3. Knockdown of ACF1or SNF2H does not inhibit degradation of ERα in the presence of ICI182,780 in MCF7 cells.

MCF7 were transfected twice with siRNAs against GAPDH, ACF1 or SNF2H for 72 hours. Cells were pretreated or not with the proteasome inhibitor MG132 (10 μM) for 1h and then with E2 (25 nM), ICI182,780 (100 nM) or vehicle for 16 h. Aliquots containing equal amounts of total

proteins were resolved by SDS-PAGE and levels of ERα, SNF2H and ACF1, and tubulin were analyzed by western blotting. The experiment was performed two times with similar results.

Supplementary figure 4. ACF1 and SNF2H are present in the chromatin fraction of MCF7 cells irrespective of hormonal treatment.

MCF7 were treated with E2 (25 nM), ICI182,780 (100 nM) or vehicle for 1h. Cytonuclear (CN), chromatin-bound (CB) and nuclear matrix (NM) fractions were prepared, aliquots containing equal amounts of total proteins were resolved by SDS-PAGE and ERα, SNF2H and ACF1 levels in each fraction were analyzed by western blotting. Tubulin, PolII and CK5/8 were used as markers for fractionation. The experiment was performed three times with similar results.

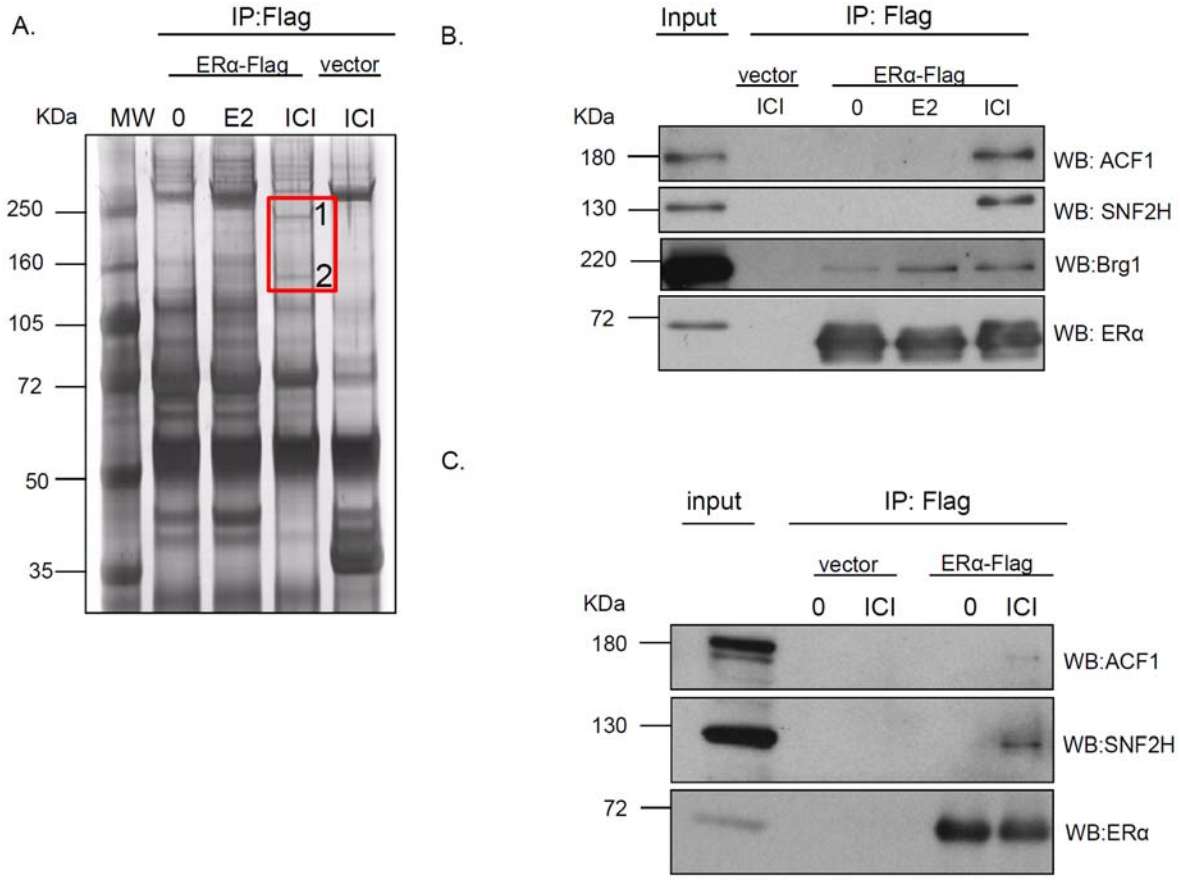

Figure 1. Identification and validation of the recruitment of ACF by ERα in the presence of ICI182,780.

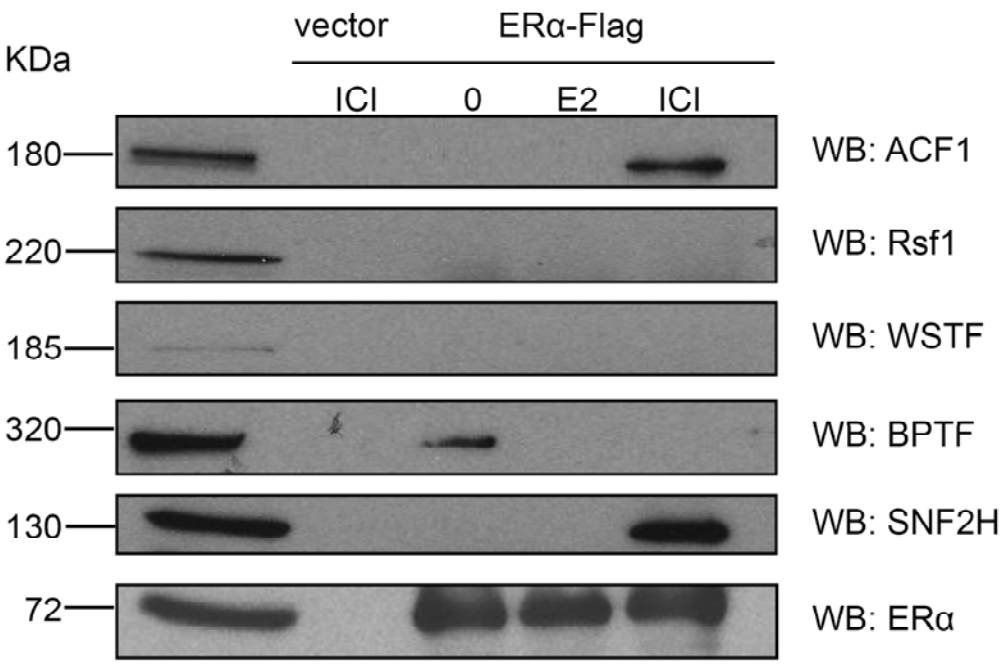

Figure 2. Other ISWI remodelers are not recruited in the presence of ICI182,780.

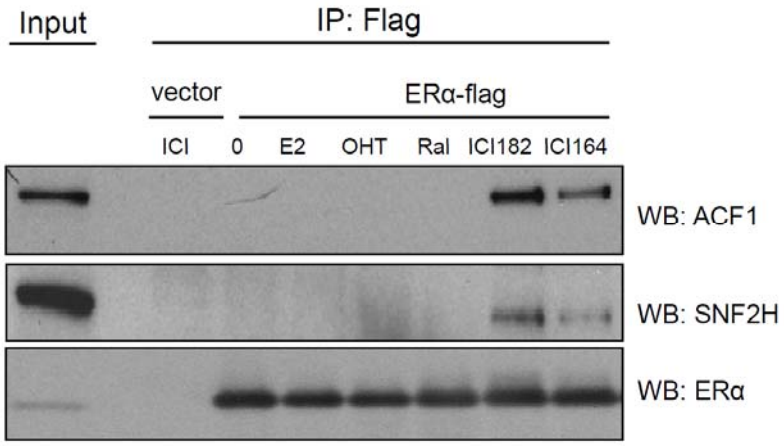

Figure 3. ACF recruitment is a specific property of full antiestrogens.

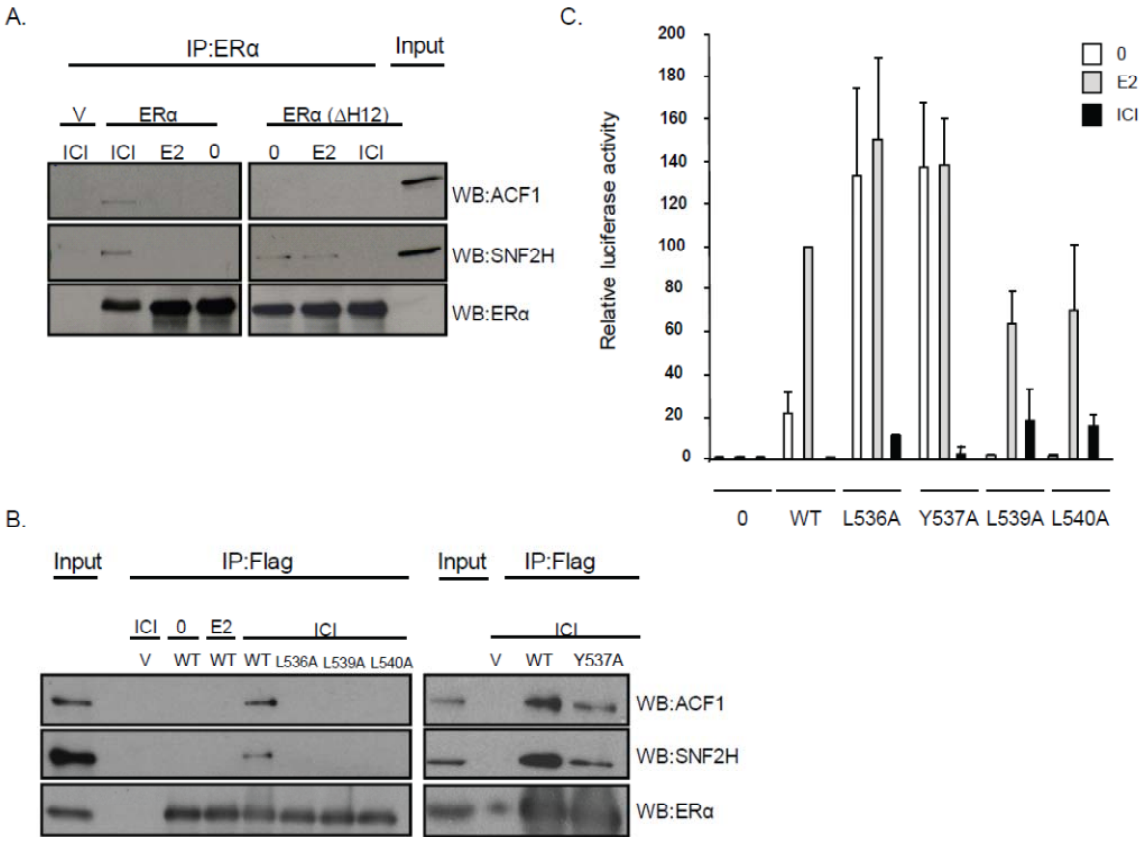

Figure 4. ACF recruitment depends on H12 integrity and correlates with inhibition of transcriptional activation by full antiestrogens in ERα mutants.

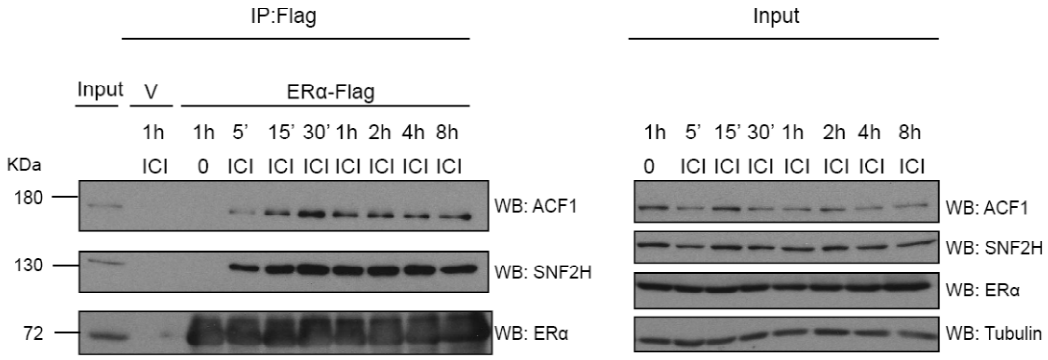

Figure 5. ACF recruitment by ERα follows rapid kinetics in the presence of ICI182,780.

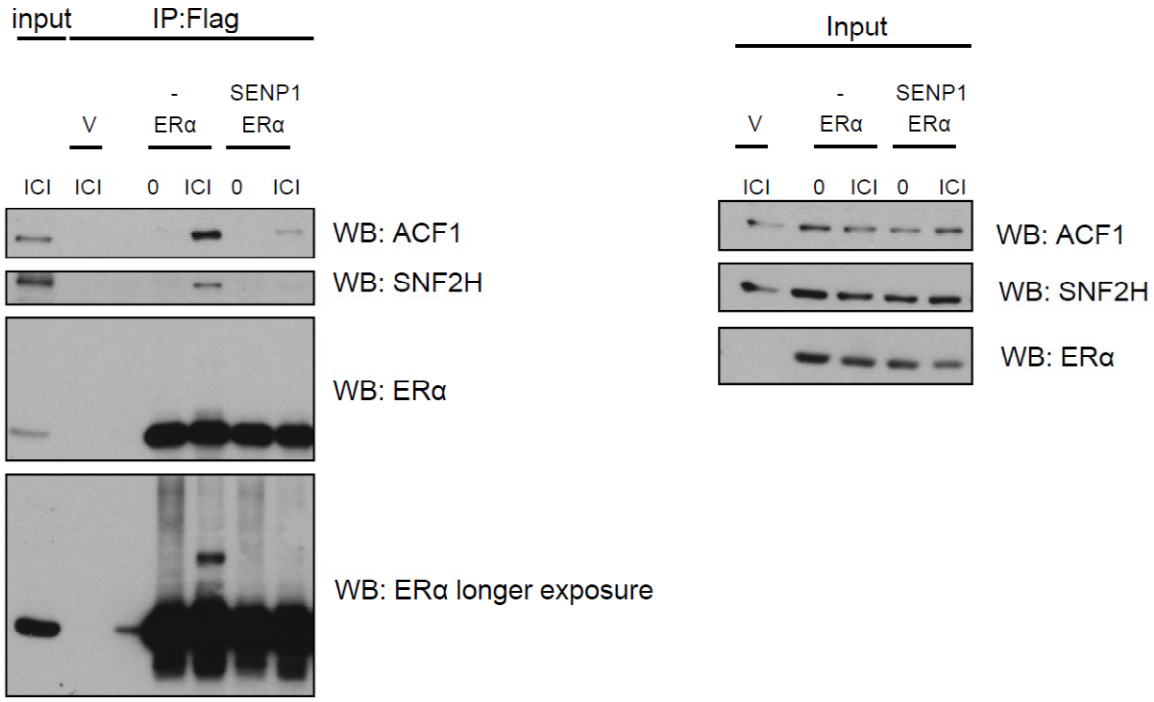

Figure 6. DeSUMOylation by SENP1 abrogates the recruitment of ACF in the presence of ICI182,780

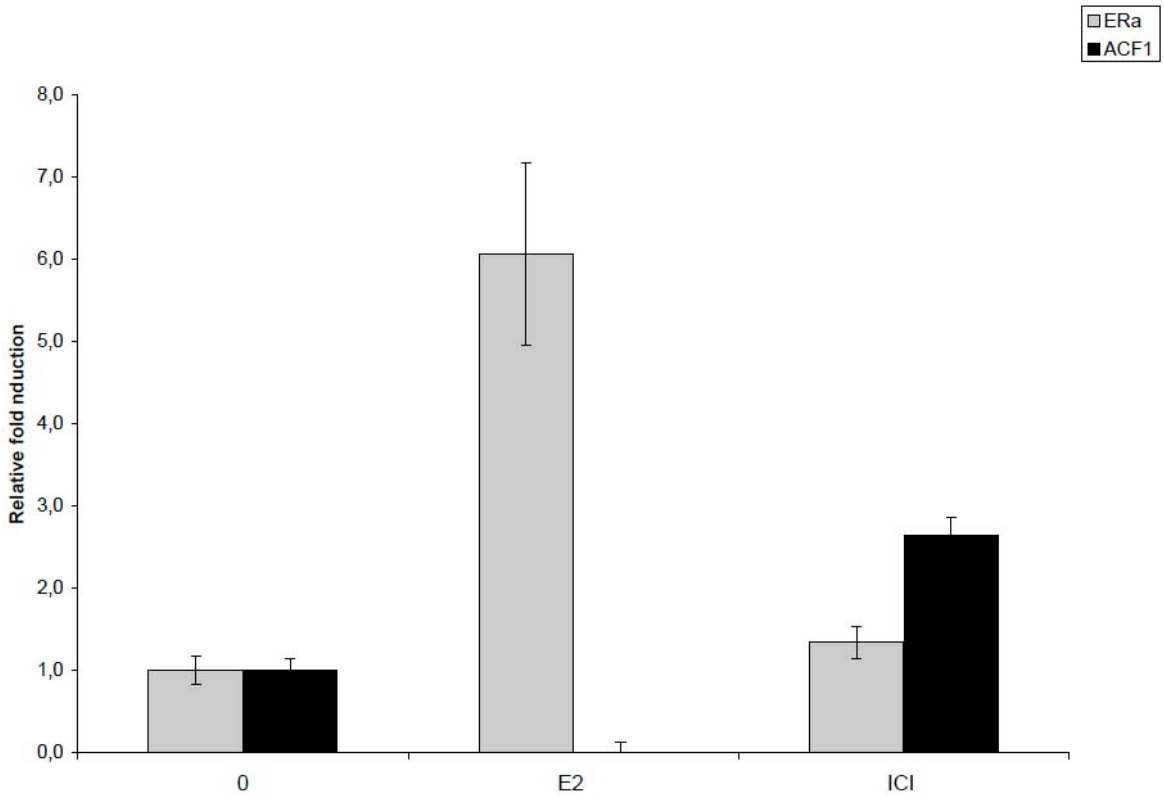

Figure 7. ICI182,780 enhances ACF1 recruitment to the pS2 proximal promoter.

SUPPLEMENTAL DATA

Band 1:

Protein ID : IPI:IPI00412415 **protein description** : Tax_Id=9606 Isoform 1 of Bromodomain adjacent to zinc finger domain protein 1A

protein mass: 180, 245 Kda **protein score**: 470,07 **protein length**: 1556 **number of peptide:** 43

peptide sequence: ICAQLAR;ETLLQEK;RGRPQVR;LSSSFSSR;VTNEIFR;ILHALCGK;APLDASDSGR;IVEEERLK;LLKQEEMK;GKLSSSFSSR;INSAPPTETK ;IYQGTLGAIK;HYDDFFER;HDDSWPFLK;QEQINCVTR;KDAIDPLLFK;GQNGFKEFTR+Deamidation (NQ)-N3; KINSAPPTETK;QSPEPSPVTLGR;QHCEPQDGVIK;FLKAPLDASDSGR;YFVEETVEVIR;ESALKETLLQEK;DFIEDYVDILR;GQQQEPGRYPSR;LRDFLLDIEDR; RIHISQEDNVANK;DLTEALDEDADPTK;GGFDATDDACMELR;LHILASGADVTSANAK;SSNAYDPSQMCAEK;SLDLDSCTLSEILR;KLSSTSVYDLTPGEK;DRYFVEETVEV IR;IQSAIACTNIFPLGR;RGGFDATDDACMELR;KGDAENMVLCDGCDR;TVNEDVEEMEIDEQTK;TGEPLMSESTSNIDQGPR;TVNEDVEEMEIDEQTK+Oxidation (M)-M9; KSANNTPENSPNFPNFR;HSHGPLQADVFVELLSPR;EPLTADEEEALKQEHQR

link: http://srs.ebi.ac.uk/cgi-bin/wgetz?-id+sessionid+-e+[IPI-acc:IPI00412415]

Band 2:

Protein ID : IPI:IPI002972115 **protein description** : Tax_Id=9606 SWI/SNF-related matrix-associated actin-dependent regulator of chromatin subfamily A member 5

protein mass: 122,512 Kda **protein score**: 310,237 **protein length**: 1052 **number of peptide**: 34

peptide sequence: IKADVEK;EILFYR;TAMELQR;SKLSEIVR;TIGYKVPR;DIDILNSAGK;HGATHVFASK;VLIFSQMTR;YLVIDEAHR;QNLLSVGDYR ;LDGQTPHDER;ANYAVDAYFR;NPELPNAAQAQK;NIPGPHMVLVPK;SVCLIGDKEQR;KANYAVDAYFR;LLTQGFTNWNK;IGKDEMLQMIR;WGRDDIENIAR; LRLDSIVIQQGR;EIQEPDPTYEEK;ILMKDIDILNSAGK;QDSINAYNEPNSTK;LGFDKENVYDELR;VLDILEDYCMWR;QPNVQDFQFFPPR;ESEITDEDIDGILER ;QKEIQEPDPTYEEK;TEQEEDEELLTESSK;TPEEVIEYSAVFWER;NPELPNAAQAQKEEQLK;RTEQEEDEELLTESSK;IDEAESLNDEELEEKEK; NFTMDTESSVYNFEGEDYREK

link : http://srs.ebi.ac.uk/cgi-bin/wgetz?-id+sessionid+-e+[IPI-acc:IPI00297211]

Supplementary figure 1. Mass spectrometry identification of the main proteins in band 1 and band 2.

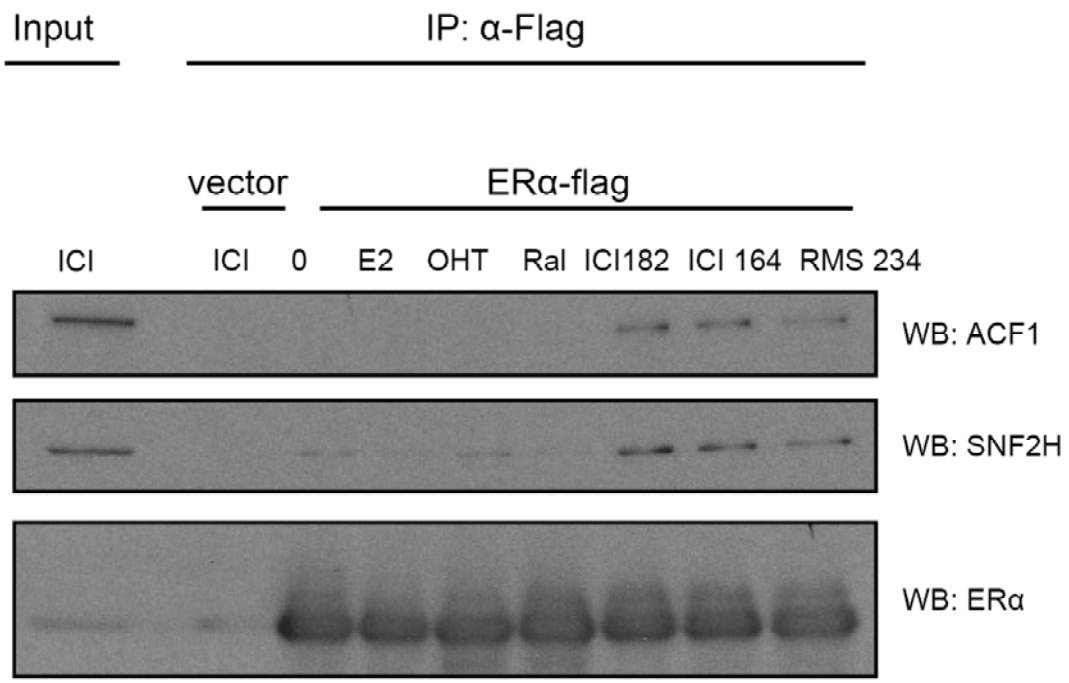

Supplementary figure 2. ACF recruitment is a specific property of full antiestrogens

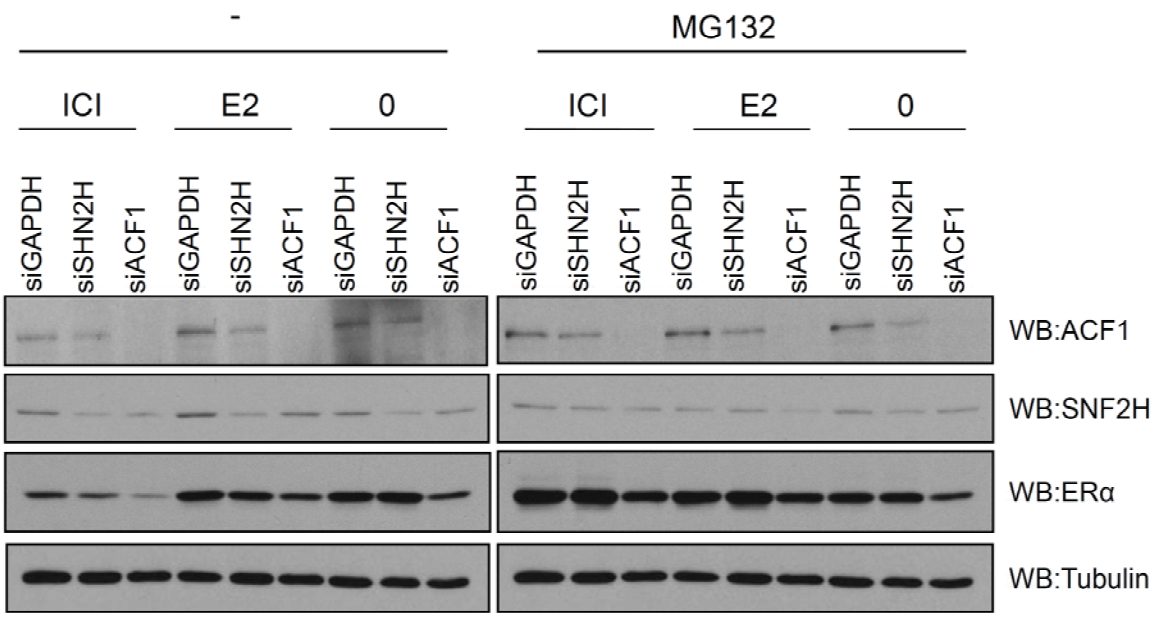

Supplementary figure 3. Knockdown of ACF1 or SNF2H does not inhibit degradation of ERα in the presence of ICI182,780 in MCF7 cells.

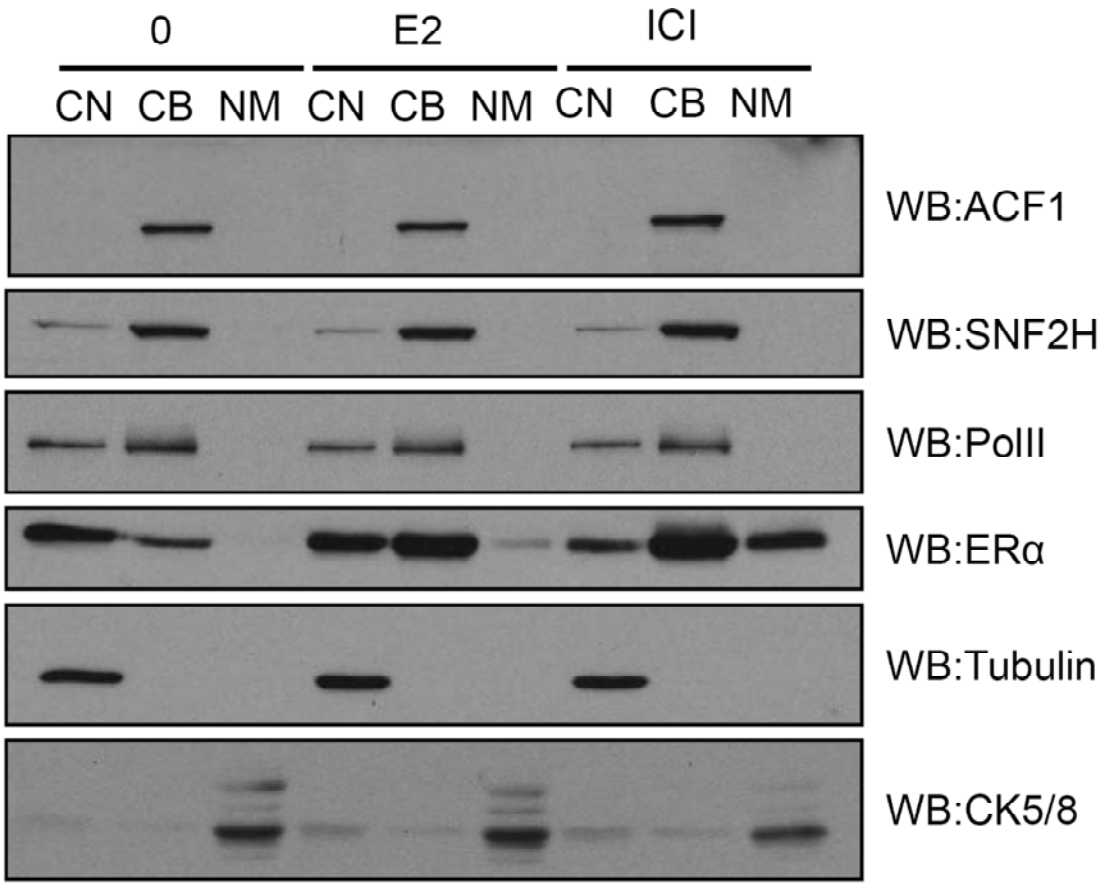

Supplementary figure 4. ACF1 and SNF2H distribution is not affected by ICI182,780 treatment in MCF7 cells.

REFERENCES

1. Mangelsdorf DJ, Thummel C, Beato M, Herrlich P, Schutz G, Umesono K, Blumberg B, Kastner P, Mark M, Chambon P, et al. 1995. The nuclear receptor superfamily: the second decade. Cell **83**:835-839.

2. Metivier R, Stark A, Flouriot G, Hubner MR, Brand H, Penot G, Manu D, Denger S, Reid G, Kos M, et al. 2002. A dynamic structural model for estrogen receptor-alpha activation by ligands, emphasizing the role of interactions between distant A and E domains. Mol Cell **10**:1019-1032.

3. Merot Y, Metivier R, Penot G, Manu D, Saligaut C, Gannon F, Pakdel F, Kah O, Flouriot G. 2004. The relative contribution exerted by AF-1 and AF-2 transactivation functions in estrogen receptor alpha transcriptional activity depends upon the differentiation stage of the cell. J Biol Chem **279**:26184-26191.

4. Freedman LP. 1999. Increasing the complexity of coactivation in nuclear receptor signaling. Cell **97**:5-8.

5. Leo C, Chen JD. 2000. The SRC family of nuclear receptor coactivators. Gene **245**:1-11.

6. Rosenfeld MG, Glass CK. 2001. Coregulator codes of transcriptional regulation by nuclear receptors. J Biol Chem **276**:36865-36868.

7. Metivier R, Penot G, Hubner MR, Reid G, Brand H, Kos M, Gannon F. 2003. Estrogen receptor-alpha directs ordered, cyclical, and combinatorial recruitment of cofactors on a natural target promoter. Cell **115**:751-763.

8. Cole H, Halnan KE. 1971. Facilitation of tumour spread in irradiated tissue after prophylactic post-operative x-ray therapy for breast cancer. Clin Radiol **22**:133-135.

9. Jordan VC. 2003. Antiestrogens and selective estrogen receptor modulators as multifunctional medicines. 2. Clinical considerations and new agents. J Med Chem **46**:1081-1111.

10. Berry M, Metzger D, Chambon P. 1990. Role of the two activating domains of the oestrogen receptor in the cell-type and promoter-context dependent agonistic activity of the anti-oestrogen 4-hydroxytamoxifen. Embo J **9**:2811-2818.

11. Metzger D, Losson R, Bornert JM, Lemoine Y, Chambon P. 1992. Promoter specificity of the two transcriptional activation functions of the human oestrogen receptor in yeast. Nucleic Acids Res **20**:2813-2817.

12. Wakeling AE, Dukes M, Bowler J. 1991. A potent specific pure antiestrogen with clinical potential. Cancer Res **51**:3867-3873.

13. Howell A, Sapunar F. 2011. Fulvestrant revisited: efficacy and safety of the 500-mg dose. Clin Breast Cancer **11**:204-210.

14. Pike AC, Brzozowski AM, Hubbard RE. 2000. A structural biologist's view of the oestrogen receptor. J Steroid Biochem Mol Biol **74**:261-268.

15. Pike AC, Brzozowski AM, Walton J, Hubbard RE, Thorsell AG, Li YL, Gustafsson JA, Carlquist M. 2001. Structural insights into the mode of action of a pure antiestrogen. Structure **9**:145-153.

16. Wijayaratne AL, McDonnell DP. 2001. The human estrogen receptor-alpha is a ubiquitinated protein whose stability is affected differentially by agonists, antagonists, and selective estrogen receptor modulators. J Biol Chem **276**:35684-35692.

17. Lupien M, Jeyakumar M, Hebert E, Hilmi K, Cotnoir-White D, Loch C, Auger A, Dayan G, Pinard GA, Wurtz JM, et al. 2007. Raloxifene and ICI182,780 increase estrogen receptor-alpha association with a nuclear compartment via overlapping sets of hydrophobic amino acids in activation function 2 helix 12. Mol Endocrinol **21**:797-816.

18. Wardell SE, Marks JR, McDonnell DP. 2011. The turnover of estrogen receptor alpha by the selective estrogen receptor degrader (SERD) fulvestrant is a saturable process that is not required for antagonist efficacy. Biochem Pharmacol **82**:122-130.

19. Webb P, Nguyen P, Kushner PJ. 2003. Differential SERM effects on corepressor binding dictate ERalpha activity in vivo. J Biol Chem **278**:6912-6920.

20. Jaber BM, Gao T, Huang L, Karmakar S, Smith CL. 2006. The pure estrogen receptor antagonist ICI 182,780 promotes a novel interaction of estrogen receptor-alpha with the 3',5'-cyclic adenosine monophosphate response element-binding protein-binding protein/p300 coactivators. Mol Endocrinol **20**:2695-2710.

21. Stenoien DL, Patel K, Mancini MG, Dutertre M, Smith CL, O'Malley BW, Mancini MA. 2001. FRAP reveals that mobility of oestrogen receptor-alpha is ligand- and proteasome-dependent. Nat Cell Biol **3**:15-23.

22. Stenoien DL, Mancini MG, Patel K, Allegretto* EA, Smith CL, Mancini MA. 2000. Subnuclear Trafficking of Estrogen Receptor-{alpha} and Steroid Receptor Coactivator-1. Mol Endocrinol **14**:518-534.

23. Hilmi K, Hussein N, Mendoza-Sanchez R, El-Ezzy M, Ismail H, Durette C, Bail M, Rozendaal MJ, Bouvier M, Thibault P, et al. 2012. Role of SUMOylation in full antiestrogenicity. Mol Cell Biol.

24. Long X, Nephew KP. 2006. Fulvestrant (ICI 182,780)-dependent interacting proteins mediate immobilization and degradation of estrogen receptor-alpha. J Biol Chem **281**:9607-9615.

25. Geoffroy MC, Hay RT. 2009. An additional role for SUMO in ubiquitin-mediated proteolysis. Nat Rev Mol Cell Biol **10**:564-568.

26. Poukka H, Karvonen U, Janne OA, Palvimo JJ. 2000. Covalent modification of the androgen receptor by small ubiquitin-like modifier 1 (SUMO-1). Proc Natl Acad Sci U S A **97**:14145-14150.

27. Dirscherl SS, Krebs JE. 2004. Functional diversity of ISWI complexes. Biochem Cell Biol **82**:482-489.

28. Hargreaves DC, Crabtree GR. 2011. ATP-dependent chromatin remodeling: genetics, genomics and mechanisms. Cell Res **21**:396-420.

29. Ito T, Levenstein ME, Fyodorov DV, Kutach AK, Kobayashi R, Kadonaga JT. 1999. ACF consists of two subunits, Acf1 and ISWI, that function cooperatively in the ATP-dependent catalysis of chromatin assembly. Genes Dev **13**:1529-1539.

30. Fyodorov DV, Kadonaga JT. 2002. Dynamics of ATP-dependent chromatin assembly by ACF. Nature **418**:897-900.

31. Collins N, Poot RA, Kukimoto I, Garcia-Jimenez C, Dellaire G, Varga-Weisz PD. 2002. An ACF1-ISWI chromatin-remodeling complex is required for DNA replication through heterochromatin. Nat Genet **32**:627-632.

32. Fyodorov DV, Blower MD, Karpen GH, Kadonaga JT. 2004. Acf1 confers unique activities to ACF/CHRAC and promotes the formation rather than disruption of chromatin in vivo. Genes Dev **18**:170-183.

33. Yasui D, Miyano M, Cai S, Varga-Weisz P, Kohwi-Shigematsu T. 2002. SATB1 targets chromatin remodelling to regulate genes over long distances. Nature **419**:641-645.

34. Ewing AK, Attner M, Chakravarti D. 2007. Novel regulatory role for human Acf1 in transcriptional repression of vitamin D3 receptor-regulated genes. Mol Endocrinol **21**:1791-1806.

35. Bourdeau V, Deschenes J, Metivier R, Nagai Y, Nguyen D, Bretschneider N, Gannon F, White JH, Mader S. 2004. Genome-wide identification of high-affinity estrogen response elements in human and mouse. Mol Endocrinol **18**:1411-1427.

36. Ichinose H, Garnier JM, Chambon P, Losson R. 1997. Ligand-dependent interaction between the estrogen receptor and the human homologues of SWI2/SNF2. Gene **188**:95-100.

37. Sheu JJ, Choi JH, Yildiz I, Tsai FJ, Shaul Y, Wang TL, Shih Ie M. 2008. The roles of human sucrose nonfermenting protein 2 homologue in the tumor-promoting functions of Rsf-1. Cancer Res **68**:4050-4057.

38. Barak O, Lazzaro MA, Lane WS, Speicher DW, Picketts DJ, Shiekhattar R. 2003. Isolation of human NURF: a regulator of Engrailed gene expression. Embo J **22**:6089-6100.

39. Shiau AK, Barstad D, Loria PM, Cheng L, Kushner PJ, Agard DA, Greene GL. 1998. The structural basis of estrogen receptor/coactivator recognition and the antagonism of this interaction by tamoxifen. Cell **95**:927-937.

40. Pike AC, Brzozowski AM, Hubbard RE, Bonn T, Thorsell AG, Engstrom O, Ljunggren J, Gustafsson JA, Carlquist M. 1999. Structure of the ligand-binding domain of oestrogen receptor beta in the presence of a partial agonist and a full antagonist. Embo J **18**:4608-4618.

41. Savkur RS, Burris TP. 2004. The coactivator LXXLL nuclear receptor recognition motif. J Pept Res **63**:207-212.

42. Girdwood D, Bumpass D, Vaughan OA, Thain A, Anderson LA, Snowden AW, Garcia-Wilson E, Perkins ND, Hay RT. 2003. P300 transcriptional repression is mediated by SUMO modification. Mol Cell **11**:1043-1054.

43. Webb P, Anderson CM, Valentine C, Nguyen P, Marimuthu A, West BL, Baxter JD, Kushner PJ. 2000. The nuclear receptor corepressor (N-CoR) contains three isoleucine motifs (I/LXXII) that serve as receptor interaction domains (IDs). Mol Endocrinol **14**:1976-1985.

44. Tiefenbach J, Novac N, Ducasse M, Eck M, Melchior F, Heinzel T. 2006. SUMOylation of the corepressor N-CoR modulates its capacity to repress transcription. Mol Biol Cell **17**:1643-1651.

45. Ivanov AV, Peng H, Yurchenko V, Yap KL, Negorev DG, Schultz DC, Psulkowski E, Fredericks WJ, White DE, Maul GG, et al. 2007. PHD domain-mediated E3 ligase activity directs intramolecular sumoylation of an adjacent bromodomain required for gene silencing. Mol Cell **28**:823-837.

46. Giamarchi C, Chailleux C, Callige M, Rochaix P, Trouche D, Richard-Foy H. 2002. Two antiestrogens affect differently chromatin remodeling of trefoil factor 1 (pS2) gene and the fate of estrogen receptor in MCF7 cells. Biochim Biophys Acta **1578**:12-20.

47. Lipfert L, Fisher JE, Wei N, Scafonas A, Su Q, Yudkovitz J, Chen F, Warrier S, Birzin ET, Kim S, et al. 2006. Antagonist-induced, activation function-2-independent estrogen receptor alpha phosphorylation. Mol Endocrinol **20**:516-533.

48. Reyes JC, Muchardt C, Yaniv M. 1997. Components of the human SWI/SNF complex are enriched in active chromatin and are associated with the nuclear matrix. J Cell Biol **137**:263-274.

49. Sugimoto N, Yugawa T, Iizuka M, Kiyono T, Fujita M. 2011. Chromatin remodeler sucrose nonfermenting 2 homolog (SNF2H) is recruited onto DNA replication origins through interaction with Cdc10 protein-dependent transcript 1 (Cdt1) and promotes pre-replication complex formation. J Biol Chem **286**:39200-39210.

50. Welboren WJ, van Driel MA, Janssen-Megens EM, van Heeringen SJ, Sweep FC, Span PN, Stunnenberg HG. 2009. ChIP-Seq of ERalpha and RNA polymerase II defines genes differentially responding to ligands. EMBO J **28**:1418-1428.

51. Kim J, Petz LN, Ziegler YS, Wood JR, Potthoff SJ, Nardulli AM. 2000. Regulation of the estrogen-responsive pS2 gene in MCF-7 human breast cancer cells. J Steroid Biochem Mol Biol **74**:157-168.

Discussion

1-La dualité de l'insolubilité et de la dégradation de ERα avec les SERD.

Notre premier objectif a été l'étude de la contribution de la dégradation dans l'inactivation de ERα. Nous avons testé les profils de transactivation dans les cellules HepG2 transfectées par ERα et un vecteur rapporteur contenant un promoteur minimal avec trois sites de fixation pour le ER. En parallèle, nous avons évalué par western blot les niveaux de ERα en utilisant un tampon d'extraction à haute concentration en sel 400 mM KCl (HSB). Les résultats démontrent qu'OHT, qui agit comme un agoniste partiel, stabilise les niveaux de ERα. A l'opposé, les niveaux de ERα sont faibles dans ces extraits en présence de Ral et ICI, qui agissent comme un agoniste inverse (Fig 1. A et B annexes 1). Ces résultats sont compatibles avec un mécanisme d'action basé sur la dégradation de ERα. Cependant, l'inhibition de la dégradation par MG132 ne permet pas de retrouver ERα dans la fraction soluble avec ICI et de Ral. Finalement, l'utilisation d'extraits totaux avec 2 % SDS confirme l'absence d'une dégradation de ERα (Fig 1. D annexes 1). Ces résultats indiquent que ICI et Ral se comportent comme des antioestrogènes totaux en absence de dégradation accélérée de ERα.

De la même manière, dans les cellules MCF7, il est possible d'observer une insolubilité dans le tampon HSB même après l'inhibition de la dégradation par MG132 (Fig1. E annexe 1). Également, à des temps très courts de traitement avec ICI le récepteur est faiblement extrait avec le tampon HSB bien avant que la dégradation ne soit amorcée. (Fig 1 A article 1). Le test de mobilité FRAP dans les cellules HepG2 montre qu'ICI et Ral diminuent la mobilité de ERα. En effet, nous avons pu observer que le temps de régénération de la fluorescence de ERα-GFP est plus long quand les cellules sont traitées par ICI ou Ral en comparaison avec le véhicule (Fig 12 annexes 1). Nos résultats concordent avec des observations précédentes [174, 175, 179] et suggèrent que ICI et Ral induisent un changement dans les propriétés d'extraction de ERα qui se traduit par une insolubilité et une diminution de la mobilité.

Afin d'établir la localisation du récepteur insoluble nous avons réalisé des expériences d'immunofluorescence au sein de cellules HepG2. Nos résultats montrent une

distribution uniforme du récepteur dans le noyau avec un faible pourcentage de cellules qui présentent des agrégats cytosoliques (Fig 2 annexes 1), contrairement à la formation d'agrégats à des degrés plus élevés dans les COS1 transfectée par ERα de l'humain ou de souris [169, 182]. Étant donné la localisation nucléaire majoritaire de ERα, nous avons utilisé le fractionnement cellulaire pour définir la fraction nucléaire où le récepteur s'accumule (Fig S1 article 1). ERα se trouve à l'état soluble dans la fraction cytonucléaire (CN) et peut s'associer avec la chromatine (CB), ce qui corrèle avec sa fonction de facteur de transcription. En présence d'ICI, il y a une augmentation de l'association de ERα avec la matrice nucléaire (NM). Globalement, ces résultats suggèrent que la force de l'interaction de ERα avec la matrice nucléaire résiste à l'extraction à haute force ionique et à la digestion avec la DNase I, qui sont les deux étapes préalables à la préparation de la matrice nucléaire. En accord avec nos résultats, il a été démontré qu'ICI induit l'interaction de ERα avec les cytokératines 8 et 18, qui forment des filaments intermédiaires de la matrice nucléaire [176]. De même, nous avons observé que les cytokératines 8 et 18 sont présentes dans la fraction matrice nucléaire.

Dans leur ensemble, nos observations indiquent que le profil d'extraction de ERα avec ICI et sa faible mobilité nucléaire reflètent une forte interaction avec la matrice nucléaire. Ce changement précoce survient avant la dégradation de ERα et corrèle avec son inactivation en absence de dégradation.

L'interaction avec la matrice nucléaire pourrait être due à une association avec des sites ADN délocalisés dans cette fraction nucléaire. En effet, il a été démontré que ERα conserve sa capacité à lier les ERE in vitro en présence d'ICI [287]. Néanmoins, nos résultats indiquent que le domaine de liaison à l'ADN de même que la région AB ne sont pas nécessaires pour l'association avec le compartiment insoluble (Fig S7 article 1 et résultats non publiés). Une explication alternative est que ERα est recruté au sein d'une fraction insoluble par des interactions protéine-protéine rendues possibles par la conformation spécifique du récepteur induite par les antioestrogènes totaux. Les données structurales suggèrent que l'absence d'une conformation bien définie de l'hélice H12 avec ICI pourrait exposer les surfaces hydrophobes du sillon de recrutement des coactivateurs [154]. Nos résultats de BRET qui indiquent une augmentation du transfert d'énergie entre

les monomères de ERα en présence d'ICI suggèrent que cette conformation pourrait résulter en une capacité de multimérisation accrue du récepteur (Fig 11 annexes 1), qui pourrait jouer un rôle dans sa localisation dans une fraction insoluble.

L'hélice H12 est de nature amphipathique. En présence d'agoniste, elle se replie sur la cavité du LBD et dirige ses résidus hydrophobes vers le ligand. En nous basant sur les données structurales, nous avons établi à l'aide de modèles moléculaires que les chaines latérales d'ICI et Ral sont en conflit stérique avec les résidus longs et hydrophobes de l'hélice H12; de plus, l'adoption d'une conformation antagoniste comme dans le cas de OHT ne permet pas de résoudre le conflit avec les acides aminés L536, L539 et L540.

Pour comprendre le rôle de l'hélice H12, nous avons caractérisé les profils de transactivation, de solubilité et de mobilité des mutants qui permettent de réduire la taille des résidus longs et hydrophobes de cette hélice. Nous avons pu observer que les mutations L536A, L539A et L540A, M543A et L544A entrainent en une augmentation de la transactivation et de la solubilité en présence d'ICI et Ral. Ce retour d'activité pourrait être attribué à l'adoption d'une conformation qui permet un recrutement des coactivateurs. Par contre, les mutations Y537A et L541A conservent le même profil que le récepteur sauvage (Fig 4. annexes 1). D'autre part, le mutant L540A permet de distinguer entre ICI et Ral car il ne permet pas de hausser les niveaux de solubilité et de l'activité en présence de Ral. Ces observations corrèlent avec les profils de mobilité de ERα dans le noyau puisque les mutants les plus actifs L536A, L539A et L540A regagnent de la mobilité en présence d'ICI et Ral. De même, le mutant L540A demeure plus immobile en présence de Ral (Fig 12. annexes 1).

En accord avec nos résultats, il a été démontré que la délétion de l'hélice H12 rend le récepteur mobile et abolit son interaction avec les cytokératines CK8 et CK18 en présence d'ICI [176, 179]. Par contre, le récepteur est dépourvu de toute activité transcriptionnelle ce qui est en accord avec le rôle de l'hélice H12 dans le recrutement des coactivateurs.

Nous avons donc pu établir que l'insolubilité est une propriété des antioestrogènes de type SERD; elle se produit avant la dégradation et corrèle avec l'inactivation de ERα et son association avec la matrice nucléaire. L'hélice H12 du LBD joue un rôle important car

des mutations ponctuelles au sein de cette hélice renversent les phénotypes de l'insolubilité et de l'inactivation.

2-Induction de la SUMOylation de ERα par les SERD

La dégradation de ERα est le résultat probable d'une augmentation de sa polyubiquitination, tel que démontré par Wijayaratne et coll. Cependant les sites d'ubiquitination et les enzymes impliquées demeurent inconnus. Au niveau des cellules MCF7, il est possible d'observer des modifications qui s'apparentent à l'ubiquitination après 10 minutes de traitement avec ICI182, 780. Il s'agit de deux bandes bien définies d'un poids moléculaire d'environ 10 kDa au dessus de ERα (Fig 1 B article 1). L'apparition de ces bandes de haut poids moléculaire survient avant le début de la dégradation. Les cinétiques de la dégradation de ERα et de ses formes modifiées sont les mêmes, ce qui suggère que la modification de ERα ne le protège pas de la dégradation. D'autre part, l'inhibition du proteasome par MG132 combinée à une extraction totale révèle une échelle de formes modifiées de ERα en absence de traitement hormonal, et une modification de ce profil de modification en réponse au traitement par un SERD. Le récepteur est donc la cible de plusieurs modifications posttraductionnelles impliquant l'ajout de peptides d'environ 10 kDa comme l'ubiquitination et la SUMOylation [173]. Nous nous sommes intéressés à la modification par SUMO pour les raisons suivantes. D'une part l'activité de ERα est inhibée en présence d'ICI, d'autre part ses propriétés d'extraction nécessitent des conditions d'extraction semblables à celles des corps PML [262]. En revanche, le récepteur ne présente pas un consensus de SUMOylation. De plus, il a été démontré que la SUMOylation est nécessaire pour son activité transcriptionnelle avec E2 et que UBC9 et PIAS 1/3 peuvent jouer le rôle de coactivateur de ERα indépendamment de leur implication dans la SUMOylation [288, 289].

Dans le but de caractériser la nature des modifications induites par ICI, nous avons effectué des expériences d'immunoprécipitation de ERα à partir d'extraits totaux contenant du N. éthylmalmeide (NEM) un inhibiteur de la déSUMOylation et de désubiquitination.

L'hybridation des membranes avec des anticorps anti-SUMO1 et anti-SUMO2 a révélé une modification de ERα dans les cellules MCF7 par SUMO1 et SUMO2/3 (Fig 2 article 1). Les mêmes observations ont pu être réalisées à partir des cellules HEK 293 transfectées et par BRET, qui est une méthode plus quantitative, dans ces mêmes cellules (Fig 3 article 1). Nos résultats de spectroscopie de masse confirment la SUMOylation de ERα au niveau des résidus K171, k180 et K299 et K472 (Fig 8 article 1). Cependant, la mutation combinée des résidus K171, K180 et K299 en arginines n'abolit pas la SUMOyaltion, ce qui suggère une possibilité de compensation par d'autres sites.

2-1-Relation entre la SUMOylation et l'insolubilité

La SUMOylation, en équilibre avec la déSUMOylation, joue un rôle dans la localisation de certaines protéines à la matrice nucléaire et plus particulièrement dans les corps PML [245]. Pour étudier le lien entre la SUMoylation et l'insolubilité nous avons étudié l'impact de la déSUMOylation sur la solubilité du récepteur en présence d'ICI. Nos résultats montrent que la surexpression de la déSUMOylase SENP1 dans les cellules HEK293 ne permet pas d'augmenter les niveaux du récepteur dans la fraction soluble (Fig S7 article 1). De plus, nous avons identifié le domaine de liaison à l'ADN comme un domaine crucial pour la SUMOylation de ERα en présence d'ICI; or l'expression de ERα sans le domaine de liaison ne permet pas d'augmenter sa répartition dans la fraction soluble (Fig S7 article 1). Également, dans les expériences de fractionnement, nous observons que le récepteur conjugué à SUMO et non-conjugé à SUMO s'associe avec la matrice nucléaire comme à la fraction chromatine. Si la SUMOylation était nécessaire pour l'association à la matrice, on s'attendrait à obtenir un enrichissement en formes SUMOylées au niveau de ce compartiment.

Une autre possibilité est que le récepteur soit SUMOylé dans la matrice nucléaire mais soit redistribué rapidement dans les autres fractions. Les résultats avec les mutants de l'hélice H12 sont en accord avec cette idée car les mutants les plus solubles et mobiles comme le mutant L539A et L540A présentent des niveaux de SUMOylation faibles alors que le mutant insoluble L541A conserve des niveaux de SUMOylation élevés et une faible solubilité. Néanmoins, le mutant L536A fait l'exception car il conserve la SUMOylation en

présence de ICI tout en étant très soluble (résultats non publiés). En conclusion, nous n'avons pas pour l'instant de données permettant de conclure à un lien entre SUMOylation et insolubilité, bien que ces deux propriétés apparaissent spécifiques des SERD (voir ci-dessous).

2-2-Relation entre la SUMOylation et l'inactivation

Nous nous sommes demandé ensuite si la SUMOylation est une propriété qui distingue ICI 182,780 des autres composés ou il s'agit d'une observation qui peut être étendue à d'autres anti-oestrogènes. Dans les cellules MCF7 et dans les cellules HEK293, nous avons testé une panoplie de composés synthétiques qui appartiennent à la classe des SERM comme OHT, Ral et RU39,411et des composés de la classe des SERDs comme ICI182,780, ICI164,384 et RU58,668. Nous avons observé que la SUMOylation est fortement induite en présence des SERD alors que Ral et RU39,411 induisent faiblement la SUMOylation. Cependant, la SUMOylation avec Ral est très faiblement observée au niveau des cellules MCF7; ceci est possiblement dû au fait qu'il s'agit d'une analyse de type western blot alors que dans le cas des HEK 293 il s'agit d'une immunoprécipitation sur une plus grande quantité d'extraits cellulaire (Fig 4 article 1). Cependant, dans les cellules HepG2, Ral induit une SUMOylation comparable à celle de ICI164,384 (Fig 9 article 1), en accord avec le fait que les effets des SERMs dépendent du contexte cellulaire.

En parallèle, l'analyse des profils de transactivation de ces composés nous révèle que les composés qui induisent la SUMOylation agissent comme des agonistes pour ERα dans les cellules HepG2 en absence de la dégradation tandis que RU39,411 et OHT agissent comme des agonistes partiels. Ces résultats suggèrent une corrélation entre la SUMOylation et l'inactivation (Fig 5C article 1). En accord avec ces résultats, l'analyse des profils de transactivation des mutants de l'hélice H12 a permis d'établir une corrélation inverse entre la capacité d'un mutant à transactiver et sa SUMOylation. De plus, la corrélation inclut le mutant L536A pour lequel nous avons une forte activité constitutive qui est réprimée en présence d'ICI (Fig 4A annexes 1).

Par ailleurs, les données structurales suggèrent que la chaine latérale des antioestrogènes de type SERD joue un rôle important dans leurs mécanismes d'action.

Nous avons vu que cette chaine impose à l'hélice H12 une conformation différente de celle adoptée en présence des composés de type SERM. De plus, malgré l'absence d'une structure cristallographique avec RU39,411 et RU58,668, le fait que ces deux antioestrogènes possèdent le même noyau stéroïdien mais une longueur différente de chaine greffée au niveau du carbone 11α est d'une longueur différente. Cette chaine étant plus courte dans le cas de RU39 411. Ceci nous suggère que la chaine latérale pourrait avoir un impact sur l'incidence de la SUMOylation.

Afin d'étudier le rôle de la chaine latérale dans l'inactivation et la SUMOylation de ERα, nous avons synthétisé une série de composés basés sur la structure de ICI164,384 avec une longueur variable et nous avons testé les profils de l'activité et de la SUMOylation du récepteur. Pour vérifier leur liaison au récepteur, nous avons évalué leur capacité à supprimer les effets transcriptionnels de E2.

Nos résultats démontrent qu'une longueur de chaine entre 15 et 19 atomes est idéale pour qu'un antioestrogène induise la SUMOylation et inactive totalement l'activité transcriptionnelle du récepteur. Également, l'emplacement de la fonction méthyle amide à 4 carbones du noyau stéroïdien ne semble pas influencer la capacité d'un composé à agir comme un SERD (Figure 5C article 1). Dans leur ensemble, ces analyses suggèrent que la longueur de la chaine latérale dicte une conformation au sein du LBD qui expose les résidus nécessaires à la SUMOylation.

Le lien entre la SUMOylation et l'inactivation peut être établi de manière indirecte en utilisant des inhibiteurs de la voie de SUMOylation. En effet, la surexpression d'une déSUMOylase ou de GAM1, un inhibiteur du complexe SAE1/SAE2, dans les cellules HepG2 permet d'augmenter les niveaux de la transactivation avec les antioestrogènes totaux mais pas avec E2 ou les SERM (Figure 12 article 1). Bien entendu, la déSUMOylase peut affecter la SUMOylation de ERα ou la SUMOylation d'un facteur dont la SUMOylation contribue à l'inactivation de ERα en présence des anti-oestrogènes totaux.

2-3-Relation entre la SUMOylation et la dégradation

Les facteurs responsables de la dégradation de ERa en présence d'anti-oestrogènes ne sont pas caractérisés. CHIP est une Ubiquitine E3 ligase impliquée dans la dégradation de ERα [290]. Parmi les candidats potentiels qui peuvent faire le lien entre l'ubiquitination et la SUMOylation, on trouve RNF4, qui peut jouer le rôle d'une ubiquitine E3 ligase grâce à son domaine RING et également interagir avec les protéines SUMO.

Nos résultats préliminaires démontrent que la surexpression de RNF4 de type sauvage induit une forte ubiquitination de ERα. Par contre, la surexpression d'un dominant négatif de RNF4 permet de stabiliser les niveaux de ERα en présence de ICI même après 16h (Fig 1 Annexe 2). De manière significative, on a pu observer que les niveaux des formes SUMOylées sont stabilisés quand le dominant négatif est surexprimé. Ces résultats suggèrent que RNF4 pourrait jouer un rôle dans l'ubiquitination de ERα en présence de ICI. En accord avec ces observations, nous avons observé que la dégradation du récepteur est fortement atténuée en présence de SENP1 (Fig 2 annexe 2). De plus, la SUMOylation semble jouer un rôle dans l'ubiquitination de ERα car le profil de migration montre une absence de toutes les formes modifiées quand SENP1 est surexprimée (Fig 2 annexe 2). Par ailleurs, les sites d'ubiquitination sont toujours inconnus. Il a été on démontré que SUMO2 est ubiquitinée par RNF4 au niveau des lysines 11, 32 et 41 et que l'ubiquitine est attachée par sa lysine 68, ce qui est une caractéristique de la présence d'une polyubiquitination [262]. Les sites d'ubiquitination pourraient donc se trouver sur les chaines de SUMOylation ou sur ERα. 4-Recrutement du complexe ACF par ERα en présence de ICI182,780. Afin d'identifier les cofacteurs impliqués dans les mécanismes d'action des anti-oestrogènes totaux, nous avons procédé à des expériences d'immunopréciptation à partir des cellules HEK 293 transfectées par ERα-Flag et traitées par le véhicule, E2 ou ICI182,780 (Fig.1A article 2, Fig S1). L'analyse par spectroscopie de masse des deux bandes qui co-purifient avec ERα en présence de ICI182,780 a révélé 34 et 43 peptides qui appartiennent à SNF2H et à ACF1, respectivement. À l'aide d'anticorps spécifiques, nous avons validé l'interaction entre le complexe ACF et ERα dans les HEK293 et dans les MCF7 (Fig.1 B et C).

L'interaction pourrait être directe via l'une des sous unités du complexe ACF ou indirecte via un partenaire inconnu; dans le cas du récepteur de la vitamine D3, le recrutement de ACF en absence du ligand se fait via le complexe N-COR-HDAC4 [215]. Le traitement par ICI augmente la titration des répresseurs par ERα [153]. Le recrutement de ACF s'effectue à des temps très courts et persiste après 8 h de traitement (Fig 2). Ceci est en accord avec les cinétiques de la SUMOylation et de l'insolubilité de ERα (Fig1 article 1). ICI n'affecte pas le profil de distribution de ACF1 et SNF2H (Fig S3 article 2). Nos résultats montrent que ACF1 et SNF2H sont fortement enrichis au sein de la fraction chromatine, ce qui est en accord avec le rôle du complexe ACF dans le remodelage de la chromatine. Cependant, ICI crée une plus forte association de ERα avec la fraction CB et NM. Le fait que le traitement par ICI n'influence pas la distribution cellulaire de ACF suggère que l'interaction avec ERα n'implique qu'une faible proportion de ce complexe.

Bien entendu, le fractionnement cellulaire ne permet pas d'identifier le compartiment dans lequel l'interaction a lieu; ERα peut interagir avec ACF dans la chromatine avant que ERα ne soit dirigé vers la matrice nucléaire. De même, l'interaction entre ERα et ACF pourrait s'effectuer dans la matrice nucléaire mais ne pas résister aux conditions de la préparation de cette fraction. Par ailleurs, les CK8 et CK18 sont des composantes de la matrice nucléaire qui interagissent avec ERα en présence d'ICI [176]. Néanmoins, nous n'avons pu observer de complexe incluant ACF, ERα et CK8 et CK18.

La sous-unité catalytique de ACF, SNF2H, est incorporée dans d'autres complexes de remodelage de la chromatine, qui compétitionnent pour cette sous unité. Il a été démontré par exemple que la surexpression de RSF1 diminue le recrutement de SNF2H par ACF1 et WSTF[291]. Cependant, nos résultats démontrent que ACF est le seul complexe recruté par ERα en présence d'ICI (Fig 3 article 2). Ceci suggère que l'interaction est effectuée par ACF1 plutôt que par SNF2H qui participe à d'autres complexes.

3-Rôle de ACF dans l'inactivation de ERα en présence des SERD

Contrairement à ICI182,780 et ICI164,384, OHT et Ral ne permettent pas le recrutement de ACF. D'autre part, les mutations L536A, L539A et L540A au sein de l'hélice H12 abolissent le recrutement du complexe, contrairement à la mutation Y537A (Fig 4 B article 2). De plus, les profils de l'interaction avec le complexe ACF sont inversement corrélés avec les profils de l'activité et de la mobilité de ces mutants. Autrement dit, les mutants actifs en présence de ICI n'interagissent pas avec le complexe ACF alors que le mutant inactif Y537A maintient une interaction. Nos résultats suggèrent que les anti-oestrogènes totaux induisent une conformation de l'hélice H12 qui favorise le recrutement de ACF. Afin de mieux comprendre le lien entre la SUMOylation et le recrutement de ACF par ERα en présence d'Anti-oestrogènes totaux, il serait utile de vérifier si les profils de SUMOylation avec les dérivés de ICI164,384 corrèlent avec le profil de recrutement de ACF.

ACF joue un rôle dans la répression et dans les interactions avec la chromatine; il a été démontré que la suppression de ACF chez la drosophile conduit à une dé répression partielle du phénotype *white* [219]. De plus, la sous unité ACF1 contient des motifs caractéristiques des facteurs qui s'associent avec la chromatine, notamment un bromodomaine qui détecte les résidus acétyle-lysines des histones ainsi que les doigts de zinc PHD connus pour leur capacité à reconnaitre les résidus méthyle-lysines des histones [292].

Afin de vérifier le rôle potentiel de ACF dans l'expression des gènes cibles des oestrogènes, nous nous sommes intéressés à pS2 qui est un des gènes cibles des oestrogènes les mieux connus. Il a été démontré que l'expression de pS2 est inhibée par un mécanisme qui implique la dégradation de ERα après une longue exposition à ICI [174]. D'autres gènes tels que p21 et P-Cadherine peuvent être réactivés suite à la dégradation de ERα en présence de ICI. De même, le ciblage de ERα par des siRNA peut modifier le profil de méthylation de certains promoteurs [157, 293]. Cependant, dans le cas de pS2, la liaison de ERα au niveau au promoteur n'est pas abolie à des temps courts de traitement avec ICI ce

qui suggère des mécanismes d'inhibition indépendants de la dégradation de ERα [294].Nous avons étudié par ChIP le recrutement de ACF au niveau du promoteur proximal de pS2 (Fig7. Article 2). Nos résultats montrent que ERα est recruté au niveau de ce promoteur en présence de E2. Par contre, le traitement avec ICI pendant 3 heures diminue le recrutement de ERα à ces rangs minimaux. ACF1 est présent de manière constitutive sur la même région du promoteur et cette interaction est supprimée par le traitement avec E2. D'autre part, le traitement par ICI augmente les niveaux de ACF1, ce qui suggère une stabilisation de l'association avec la fraction du récepteur liée à cette région. Ces observations sont en accord avec le fait qu'ICI induit un changement de l'empreinte à l'ADNase I au niveau du promoteur de pS2 [295]. De même, nos résultats sont compatibles avec le mode de recrutement du complexe ACF par le récepteur de la vitamine D3 en absence du ligand [215].

Le complexe ACF pourrait être relié à la SUMOylation pour différentes raisons. Premièrement, la surexpression d'une déSUMOylase abolit le recrutement de ce complexe, suggérant que la SUMOylation de ERα ou de ACF1 ou d'un autre facteur est nécessaire pour la formation du complexe entre ERα et ACF. Deuxièmement, des peptides de ACF1 ont été purifiés à partir des cellules HEK 293 transfectées par HIS6-SUMO3 et ERα et traitées avec ICI, ce qui suggère que ACF1 pourrait être SUMOylé. Il a été démontré dans le cas de KAP1 que le domaine PHD peut jouer le rôle d'une SUMO E3 ligase envers le bromodomain adjacent [264]. Dans leur ensemble nos résultats suggèrent que le complexe ACF joue un rôle dans l'inactivation de ERα en présence d'ICI en agissant comme un corépresseur par sa fonction de remodelage la chromatine.

4- Mise en perspective et modèles

Nos observations indiquent que le profil d'extraction de ERα avec ICI et sa faible mobilité reflètent une forte interaction avec le compartiment nucléaire. L'insolubilité récapitule une distribution de ERα dans les fractions des protéines qui lient la chromatine et la matrice nucléaire. L'insolubilité et la SUMOylation surviennent avant la dégradation de ERα.

La séquestration d'un facteur de transcription est souvent corrélée avec l'inhibition de son activité transcriptionnelle, l'insolubilité de ERα se déroule essentiellement dans le noyau des cellules HepG2 avec la formation de rares agrégats ce qui est en accord avec les résultats de Stenoien et Coll, Calligé et Coll et Giamarchi et Coll. Par opposition aux travaux de Lipfet et Coll et Davis et Coll qui montrent une forte agrégation nucléaire et cytoplasmique. Une explication plausible est que la formation d'agrégats dépend du type cellulaire et est proportionnelle aux niveaux d'expression de ERα. En effet, l'insolubilité est recrée dans les cellules MCF7 dans des conditions de surexpression du récepteur ce qui indique que la saturation la de la machinerie de la dégradation peut induire une accumulation dans la fraction insoluble. les mutants de l'hélice H12 indiquent que l'exposition des surfaces hydrophobes du LBD et le sillon de recrutement des coactivateurs sont importants pour l'agrégation.

L'insolubilité de ERα en présence des antioestrogènes totaux demeure une observation empirique qui se définit en fonction du tampon d'extraction. Cependant, Elle peut refléter la présence de plusieurs populations de ERα. Le tampon HSB à 400 mM n'extrait qu'une infime partie du récepteur avec ICI et l'extraction du récepteur augmente graduellement en présence de détergent dans le tampon de lyse et atteint son maximum dans les extraits totaux à 2% SDS. En outre, le fractionnement cellulaire indique la présence du récepteur dans les fractions cytonucléaire, chromatinienne et matricielle. Il est probable que le récepteur participe dans interactions de différents degrés qui se traduisent par une extraction différentielle. Ces interactions peuvent correspondre à des complexes de ERα avec les enzymes de l'ubiquitination et de la SUMOylation, les protéines de la chromatine comme le complexe ACF ou encore les protéines de matrice nucléaire comme

les cytokératines. Il est important de noter que le fractionnement cellulaire s'opposent à notre modèle de « compartimentalisation» car le récepteur est SUMOylé et dégradé avec des cinétiques similaires dans les trois fractions. L'importance de l'insolubilité pour la dégradation de ERα n'est pas bien établie car en l'absence du DBD, le récepteur est stable tout en étant insoluble. Ceci indique que les domaines requis pour la dégradation sont différents des domaines requis pour l'insolubilité.

Les CK8 et CK18 interagissent avec ERα en présence d'ICI dans un tampon contenant 1 % NP40 et 0,5 % Triton et se trouvent dans le matériel insoluble dans le tampon HSB. Dans les conditions d'extraction avec le tampon contenant 1 % NP40, nous n'avons pas observé un complexe incluant ACF, ERα et CK8 et CK18. Autrement dit, les conditions utilisées pour l'interaction avec ACF ne le sont pas pour les cytokératines. Il est donc nécessaire de mettre au point des conditions qui préservent les interactions lors de l'extraction des partenaires de ERα. ICI n'affecte pas le profil de distribution de ACF indiquant qu'une faible proportion de ACF qui interagit avec ERα. De plus, la délétion de ACF ne permet pas d'augmenter la solubilité ou d'inhiber la SUMOylation.

Dans le même ordre d'idée, les formes SUMOylés ont les mêmes cinétiques de dégradation que les formes non modifiées. Donc, il est probable que la SUMOylation est un état transitoire qui permet de dégrader une partie du récepteur ou à interagir avec le complexe ACF pour l'inhibition de l'activité. Les liens possibles d'ACF avec l'insolubilité découlent du fait que ACF interagit dans les lymphocytes T avec SATB1 qui est fortement associé avec la matrice nucléaire. Également, les profils de l'interaction avec le complexe ACF sont inversement corrélés avec les profils de l'activité et de la mobilité des mutants L536A, L539A et L540A. Les mutants actifs et mobiles en présence d'ICI n'interagissent pas avec le complexe ACF alors que le mutant Y537A maintient une interaction tout en étant inactif est insoluble .

Il est clair que la dégradation de ERα demeure le mécanisme d'action de Fulvestrant le mieux décrit. Bien qu'il existe une forte corrélation entre l'inactivation, la SUMOylation et le recrutement de ACF, les méthodes biochimiques utilisées demeurent insuffisantes pour établir des liens de cause à effet entre ces phénomènes dans le contexte de tumeurs mammaires ER+. Nos études se sont déroulées dans un contexte où il n'existe aucune

information qui indique un rôle de la SUMOylation et le remodelage de la chromatine par ACF dans le mécanisme de Fulvestrant. Nous avons fondé notre analyse sur des comparaisons avec d'autres récepteurs nucléaires qui interagissent avec le complexe ACF et avec la voie de la SUMOylation. De nombreuses questions se posent, Tout d'abord, existe-t-il des populations de ERα avec Fulvestrant? Nos résultats actuels nous permettent-ils de conclure quant à la spécificité de l'interaction de ACF? Les autres complexes qui ont SNF2H sont-ils en mesure d'interagir avec ERα ? existe-t-elle une sous unité accessoires non connue qui donne à ACF une spécificité d'interaction avec ERα ou c'est la sous unité non catalytique ACF1 qui détermine la spécificité? Les cellules SKOV-3 sont un modèle ER+ du cancer de l'ovaire. Dans ces cellules, RSF-1 est important pour la croissance et a une plus forte affinité pour SNF2H que les autres complexes ISWI. Est-il possible que le traitement avec Fulvestrant puisse affaiblir les effets prolifératifs de RSF-1 en favorisant la formation du complexe où ACF est séquestré dans un complexe avec ERα. Finalement, ACF, SUMO et l'insolubilité sont-ils le reflet d'un stress induit par Fulvestrant? Pour clore cette thèse nous proposons les modèles suivants.

Modèle 1 : Dans les cellules de tumeurs mammaires ER+ à des niveaux d'expression endogène. Fulvestrant induit une insolubilité précoce qui corrèle avec la SUMOylation de ERα. La SUMOylation est incompatible avec la liaison de ERα à l'ADN et permet l'interaction avec le complexe ACF. Ensuite, ACF favorise l'incorporation de nouveaux nucléosomes et le remodelage de la chromatine ce qui rend les promoteurs des gènes cibles des oestrogènes non disponibles pour l'activation de la transcription. La SUMOylation permet de recruter des ubiquitines ligases RNF4 qui induisent la polyubiquitination de ERα et la chaine SUMO et enfin la dégradation du récepteur par le proteasome 26 S. Dans les conditions phyisologiques, il y a des oestrogènes circulants ce qui permet un recrutement constitutif de ERα sur les promoteurs de gènes cibles des oestrogènes. Il est connu que les régions qui sont liées par les facteurs de transcription sont dépourvues de nucléosomes, ces régions seront probablement exposées aux dommages à l'ADN causés par doses élévées de Fulvestrant. Dans ce cas, il est probable que ERα interagit avec ACF et les facteurs de réparation des dommages à l'ADN tels que

les KU70/KU80. Une interaction entre ACF et KU70/KU80 a été récemment décrite. L'intégration de tous ces processus se manifeste par l'effet agoniste inverse de fulvestrant qui conduit à l'induction des gènes d'arrêt du cycle cellulaire $p21^{waf}$ et les gènes proapoptotiques en l'occurrence bcl2.

Modèle 2 : Dans les cellules HepG2 et dans les cellules MCF7 dans des conditions de sur expression du récepteur, l'agrégation d'ERα en présence d'ICI est le résultat de l'exposition des surfaces hydrophobes du sillon de recrutement des coactivateurs. L'accumulation de ERα est perçue comme un stress protéique. Faute d'une dégradation efficace, HDAC6, connue pour son rôle dans la formation des aggrésomes, interagit avec ERα conjugué à l'ubiquitine et l'achemine aux aggrésomes formés de filaments intermédiaires CK8 et CK18. Ceci se traduit par une immobilisation de ERα dans un compartiment où il n'est plus accessible aux déSUMOylases, l'équilibre est déplacé vers l'accumulation de la SUMOylation. Dans ce contexte, des ligases de SUMO (E3) associées à la matrice nucléaire comme PIASy jouent un rôle. L'activité agoniste inverse des antioestrogènes totaux est le résultat d'une conformation défavorable pour la transactivation et à la séquestration de ERα dans un compartiment insoluble.

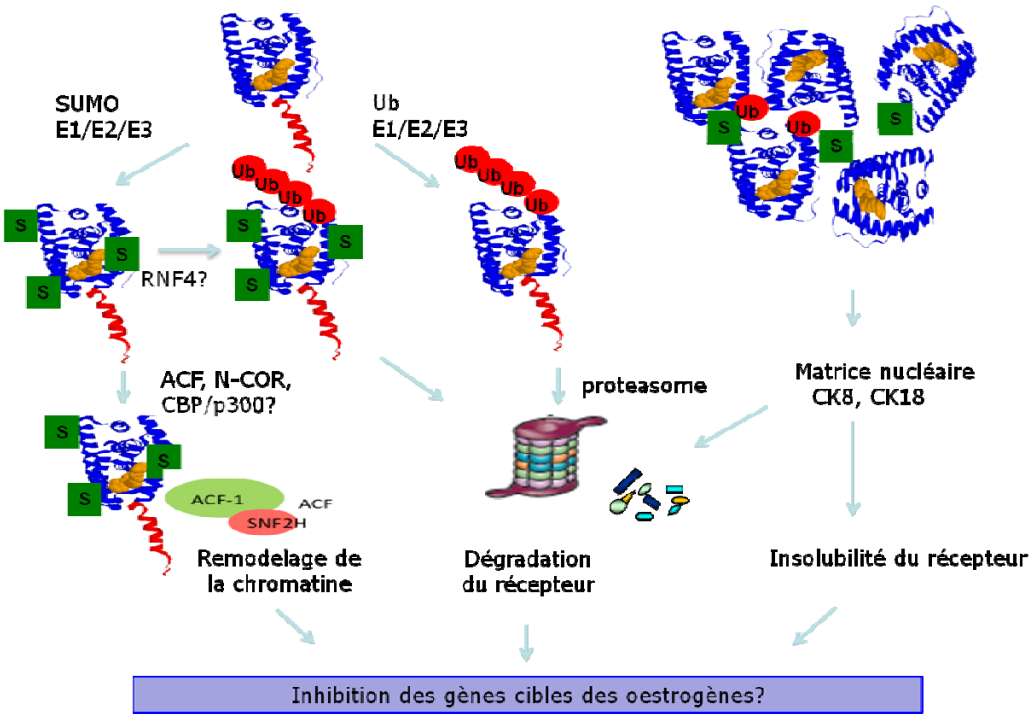
SUMO
E1/E2/E3
Ub
E1/E2/E3
RNF4?
ACF, N-COR,
CBP/p300?
proteasome
Matrice nucléaire
CK8, CK18
ACF-1
ACF
SNF2H
Remodelage de
la chromatine
Dégradation
du récepteur
Insolubilité du récepteur
Inhibition des gènes cibles des oestrogènes?

5- Travaux futures

1- Identifier les partenaires de ERα en présence des antioestrogènes totaux et leurs rôles dans l'insolubilité.

a) En assumant la formation de différentes populations de ERα avec des propriétés différentes en présence des antioestrogènes totaux, on propose la purification de ERα à partir des fractions CN, CB et NM et l'identification des protéines qui co-purifient avec le récepteur dans chacune de ces fractions. On propose d'utiliser un agent réticulant pour préserver les interactions lors du fractionnement. Les complexes protéiques seront également isolés en fonction de leur densité par centrifugation sur gradient de sucrose et les composantes protéiques de chaque fraction seront identifiées par spectroscopie de masse.

b) La réversibilité de l'association de ERα avec le compartiment insoluble et son inactivation sera testée dans les cellules HepG2 transfectées. Premièrement, l'insolubilité sera induite par un traitement à ICI 182, 780 suivie d'un traitement avec E2. Les niveaux de ERα dans la fraction soluble et son activité seront mesurés. Deuxièmement, les facteurs impliqués dans l'immobilisation, les cytokératines CK8 et CK18 et HDAC6 seront ciblés par des siRNAs. Le rôle de HDAC6 impliquée dans la formation des agrégats sera testé par les inhibiteurs des HDAC.

2- Caractériser le rôle de la SUMOylation et le recrutement ACF dans l'inactivation de ERα avec les antioestrogènes totaux

a) La SUMOylation est un événement précoce qui précède la dégradation de ERα et corrèle avec une très faible liaison aux promoteurs des gènes cibles des oestrogènes, il est probable que la SUMOylation soit incompatible avec la liaison de ERα à ses ERE. Par Chip, nous allons vérifier si l'inhibition de la SUMOylation stabilise le recrutement du récepteur à l'ADN en présence de ICI182, 780. Alternativement, nous allons mettre au point les conditions d'extraction des formes SUMOylées de ERα et tester leur capacité à lier des ERE *in vitro* par retard sur gel, des mutants son SUMOylables seront utilisés pour compléter cette analyse.

b) Définir le domaine minimal de l'interaction entre ACF et ERα en utilisant des domaines de délétions du récepteur et de ACF par immunoprécipitation et par BRET. Pour bien caractériser l'interaction entre ACF et ERα, on propose des tests d'interaction *in vitro* entre ERα produit chez la bactérie et ACF traduit *in vitro* en présence ou en absence d'extraits cellulaires traitées avec ICI182, 780. Pour vérifier la contribution de ACF aux effets répressifs des antioestrogènes, il serait utile de tester si ICI 182, 780 influence le positionnement des nucléosomes. De plus, Étant donné la colocalisation de ACF avec HP1β, L'induction des marques de la chromatine répressive au niveau des promoteurs des gènes cibles des oestrogènes sera testée par immunopréciptation de l'histone H3trimethylée à la lysine 27.

c) Le complexe ACF continent de nombreux motifs SIM potentiels, si le recrutement d'ACF par ERα nécessite une interaction directe de type SIM-SUMO; il est probable que la surexpression d'une forme de SUMO avec des mutations dans les résidus clés pour l'interaction SIM-SUMO abolisse l'interaction avec ACF en présence des antioestrogènes totaux. Les mutants de SUMO1 F36A, K37et K45A seront testés par co-immunoprécipitation. Le rôle de la SUMOylation dans le recrutement de ACF à la chromatine sera testé par ChIP. À l'aide d'une lignée inductible pour la DéSUMOylase SENP1 ou des shRNAs dirigés contre les enzymes SAE1/SAE2 ou UBC9 nous allons vérifier si la déSUMOylation est corrélée avec la perte de recrutement de ACF aux régions régulatrices des gènes cibles des oestrogènes en présence de ICI182, 780.

Conclusion

Les antioestrogènes totaux sont des composés intéressants de par leur mécanisme d'action et constituent une alternative thérapeutique pour les tumeurs mammaires ER+. Dans cette étude, nous montrons que les antioestrogènes totaux ont des propriétés qui les distinguent des antioestrogènes partiels. L'inactivation de ERα avec les antioestrogènes totaux est corrélée non seulement avec une dégradation du récepteur mais aussi avec son accumulation dans une fraction insoluble et avec la SUMOylation et le recrutement du complexe ACF.

L'impact de la liaison des antioestrogènes sur la conformation de l'hélice H12 du LBD est important pour ces trois événements. Les mutations qui réduisent la taille des résidus longs et hydrophobes de l'hélice H12 augmentent la solubilité et la transactivation de ERα en présence de ICI182,780. En même temps, elles inhibent le recrutement du complexe ACF. D'autre part, la taille de la chaine latérale des antioestrogènes totaux joue un rôle crucial dans la SUMOylation et l'inactivation. Nos résultats démontrent également que la SUMOylation joue un rôle dans l'inactivation de ERα.

La SUMOylation d'ERα et le recrutement d'ACF sont des propriétés spécifiques aux antioestrogènes totaux. Elles peuvent être utilisées dans des criblages afin d'identifier de nouveaux composés avec de meilleures propriétés pharmacologiques. Une modulation de l'expression ou de l'activité des facteurs qui gouvernent ces phénomènes peuvent affecter la réponse des tumeurs ER+ aux antioestrogènes totaux.

Bibliographie

1. Jin J.Z. and Lin S.X. (1999). Human estrogenic 17beta-hydroxysteroid dehydrogenase: predominance of estrone reduction and its induction by NADPH. *Biochem Biophys Res Commun* **259**(2) p. 489-93.

2. Simpson E.R. and Davis S.R. (2001). Minireview: aromatase and the regulation of estrogen biosynthesis--some new perspectives. *Endocrinology* **142**(11) p. 4589-94.

3. Riggs B.L., Khosla S., and Melton L.J., 3rd (2002). Sex steroids and the construction and conservation of the adult skeleton. *Endocr Rev* **23**(3) p. 279-302.

4. Simpson E., Rubin G., Clyne C., Robertson K., O'Donnell L., Jones M., and Davis S. (2000). The role of local estrogen biosynthesis in males and females. *Trends Endocrinol Metab* **11**(5) p. 184-8.

5. Ruggiero R.J. and Likis F.E. (2002). Estrogen: physiology, pharmacology, and formulations for replacement therapy. *J Midwifery Womens Health* **47**(3) p. 130-8.

6. Buzdar A.U. and Robertson J.F. (2006). Fulvestrant: pharmacologic profile versus existing endocrine agents for the treatment of breast cancer. *Ann Pharmacother* **40**(9) p. 1572-83.

7. Lubahn D.B., Moyer J.S., Golding T.S., Couse J.F., Korach K.S., and Smithies O. (1993). Alteration of reproductive function but not prenatal sexual development after insertional disruption of the mouse estrogen receptor gene. *Proc Natl Acad Sci U S A* **90**(23) p. 11162-6.

8. Ali S., Buluwela L., and Coombes R.C. (2011). Antiestrogens and their therapeutic applications in breast cancer and other diseases. *Annu Rev Med* **62** p. 217-32.

9. Maggi A., Ciana P., Belcredito S., and Vegeto E. (2004). Estrogens in the nervous system: mechanisms and nonreproductive functions. *Annu Rev Physiol* **66** p. 291-313.

10. Woolley C.S. (2007). Acute effects of estrogen on neuronal physiology. *Annu Rev Pharmacol Toxicol* **47** p. 657-80.

11. Naftolin F., Ryan K.J., and Petro Z. (1971). Aromatization of androstenedione by the diencephalon. *J Clin Endocrinol Metab* **33**(2) p. 368-70.

12. Yague J.G., Wang A.C., Janssen W.G., Hof P.R., Garcia-Segura L.M., Azcoitia I., and Morrison J.H. (2008). Aromatase distribution in the monkey temporal neocortex and hippocampus. *Brain Res* **1209** p. 115-27.

13. Fillit H., Weinreb H., Cholst I., Luine V., McEwen B., Amador R., and Zabriskie J. (1986). Observations in a preliminary open trial of estradiol therapy for senile dementia-Alzheimer's type. *Psychoneuroendocrinology* **11**(3) p. 337-45.

14. Sherwin B.B. (1997). Estrogen effects on cognition in menopausal women. *Neurology* **48**(5 Suppl 7) p. S21-6.

15. Green P.S. and Simpkins J.W. (2000). Neuroprotective effects of estrogens: potential mechanisms of action. *Int J Dev Neurosci* **18**(4-5) p. 347-58.

16. Caulin-Glaser T., Garcia-Cardena G., Sarrel P., Sessa W.C., and Bender J.R. (1997). 17 beta-estradiol regulation of human endothelial cell basal nitric oxide release, independent of cytosolic Ca2+ mobilization. *Circ Res* **81**(5) p. 885-92.

17. Lantin-Hermoso R.L., Rosenfeld C.R., Yuhanna I.S., German Z., Chen Z., and Shaul P.W. (1997). Estrogen acutely stimulates nitric oxide synthase activity in fetal pulmonary artery endothelium. *Am J Physiol* **273**(1 Pt 1) p. L119-26.

18. Klouche M. (2006). Estrogens in human vascular diseases. *Ann N Y Acad Sci* **1089** p. 431-43.

19. Parfitt A.M., Travers R., Rauch F., and Glorieux F.H. (2000). Structural and cellular changes during bone growth in healthy children. *Bone* **27**(4) p. 487-94.

20. Khosla S., Melton L.J., 3rd, Atkinson E.J., O'Fallon W.M., Klee G.G., and Riggs B.L. (1998). Relationship of serum sex steroid levels and bone turnover markers with bone mineral density in men and women: a key role for bioavailable estrogen. *J Clin Endocrinol Metab* **83**(7) p. 2266-74.

21. Imai Y., Kondoh S., Kouzmenko A., and Kato S. (2010). Minireview: osteoprotective action of estrogens is mediated by osteoclastic estrogen receptor-alpha. *Mol Endocrinol* **24**(5) p. 877-85.

22. Shang Y. (2007). Hormones and cancer. *Cell Res* **17**(4) p. 277-9.

23. Bernstein L. and Ross R.K. (1993). Endogenous hormones and breast cancer risk. *Epidemiol Rev* **15**(1) p. 48-65.

24. Feigelson H.S. and Henderson B.E. (1996). Estrogens and breast cancer. *Carcinogenesis* **17**(11) p. 2279-84.

25. Toniolo P.G., Levitz M., Zeleniuch-Jacquotte A., Banerjee S., Koenig K.L., Shore R.E., Strax P., and Pasternack B.S. (1995). A prospective study of endogenous estrogens and breast cancer in postmenopausal women. *J Natl Cancer Inst* **87**(3) p. 190-7.

26. Dorgan J.F., Longcope C., Stephenson H.E., Jr., Falk R.T., Miller R., Franz C., Kahle L., Campbell W.S., Tangrea J.A., and Schatzkin A. (1997). Serum sex hormone levels are related to breast cancer risk in postmenopausal women. *Environ Health Perspect* **105 Suppl 3** p. 583-5.

27. Foidart J.M., Desreux J., Pintiaux A., and Gompel A. (2007). Hormone therapy and breast cancer risk. *Climacteric* **10 Suppl 2** p. 54-61.

28. Bernstein L., Ross R.K., Pike M.C., Brown J.B., and Henderson B.E. (1990). Hormone levels in older women: a study of post-menopausal breast cancer patients and healthy population controls. *Br J Cancer* **61**(2) p. 298-302.

29. Miller W.R. and O'Neill J. (1987). The importance of local synthesis of estrogen within the breast. *Steroids* **50**(4-6) p. 537-48.

30. O'Neill J.S. and Miller W.R. (1987). Aromatase activity in breast adipose tissue from women with benign and malignant breast diseases. *Br J Cancer* **56**(5) p. 601-4.

31. Santen R.J., Santner S.J., Pauley R.J., Tait L., Kaseta J., Demers L.M., Hamilton C., Yue W., and Wang J.P. (1997). Estrogen production via the aromatase enzyme in breast carcinoma: which cell type is responsible? *J Steroid Biochem Mol Biol* **61**(3-6) p. 267-71.

32. Simpson E.R., Clyne C., Speed C., Rubin G., and Bulun S. (2001). Tissue-specific estrogen biosynthesis and metabolism. *Ann N Y Acad Sci* **949** p. 58-67.

33. Gupta P.B. and Kuperwasser C. (2006). Contributions of estrogen to ER-negative breast tumor growth. *J Steroid Biochem Mol Biol* **102**(1-5) p. 71-8.

34. Holst F., Stahl P.R., Ruiz C., Hellwinkel O., Jehan Z., Wendland M., Lebeau A., Terracciano L., Al-Kuraya K., Janicke F., Sauter G., and Simon R. (2007). Estrogen receptor alpha (ESR1) gene amplification is frequent in breast cancer. *Nat Genet* **39**(5) p. 655-60.

35. Jefcoate C.R., Liehr J.G., Santen R.J., Sutter T.R., Yager J.D., Yue W., Santner S.J., Tekmal R., Demers L., Pauley R., Naftolin F., Mor G., and Berstein L. (2000). Tissue-specific synthesis and oxidative metabolism of estrogens. *J Natl Cancer Inst Monogr* (27) p. 95-112.

36. Bocchinfuso W.P. and Korach K.S. (1997). Mammary gland development and tumorigenesis in estrogen receptor knockout mice. *J Mammary Gland Biol Neoplasia* **2**(4) p. 323-34.

37. Russo I.H. and Russo J. (1996). Mammary gland neoplasia in long-term rodent studies. *Environ Health Perspect* **104**(9) p. 938-67.

38. Russo J. and Russo I.H. (2006). The role of estrogen in the initiation of breast cancer. *J Steroid Biochem Mol Biol* **102**(1-5) p. 89-96.

39. Bolton J.L. and Thatcher G.R. (2008). Potential mechanisms of estrogen quinone carcinogenesis. *Chem Res Toxicol* **21**(1) p. 93-101.

40. Yager J.D. and Davidson N.E. (2006). Estrogen carcinogenesis in breast cancer. *N Engl J Med* **354**(3) p. 270-82.

41. Singh S., Chakravarti D., Edney J.A., Hollins R.R., Johnson P.J., West W.W., Higginbotham S.M., Cavalieri E.L., and Rogan E.G. (2005). Relative imbalances in the expression of estrogen-metabolizing enzymes in the breast tissue of women with breast carcinoma. *Oncol Rep* **14**(4) p. 1091-6.

42. Greene G.L., Gilna P., Waterfield M., Baker A., Hort Y., and Shine J. (1986). Sequence and expression of human estrogen receptor complementary DNA. *Science* **231**(4742) p. 1150-4.

43. Green S., Walter P., Kumar V., Krust A., Bornert J.M., Argos P., and Chambon P. (1986). Human oestrogen receptor cDNA: sequence, expression and homology to v-erb-A. *Nature* **320**(6058) p. 134-9.

44. Kuiper G.G., Enmark E., Pelto-Huikko M., Nilsson S., and Gustafsson J.A. (1996). Cloning of a novel receptor expressed in rat prostate and ovary. *Proc Natl Acad Sci U S A* **93**(12) p. 5925-30.

45. Mangelsdorf D.J., Thummel C., Beato M., Herrlich P., Schutz G., Umesono K., Blumberg B., Kastner P., Mark M., Chambon P., and Evans R.M. (1995). The nuclear receptor superfamily: the second decade. *Cell* **83**(6) p. 835-9.

46. Stunnenberg H.G. (1993). Mechanisms of transactivation by retinoic acid receptors. *Bioessays* **15**(5) p. 309-15.

47. Enmark E., Pelto-Huikko M., Grandien K., Lagercrantz S., Lagercrantz J., Fried G., Nordenskjold M., and Gustafsson J.A. (1997). Human estrogen receptor beta-gene structure, chromosomal localization, and expression pattern. *J Clin Endocrinol Metab* **82**(12) p. 4258-65.

48. Barkhem T., Carlsson B., Nilsson Y., Enmark E., Gustafsson J., and Nilsson S. (1998). Differential response of estrogen receptor alpha and estrogen receptor beta to partial estrogen agonists/antagonists. *Mol Pharmacol* **54**(1) p. 105-12.

49. Berry M., Metzger D., and Chambon P. (1990). Role of the two activating domains of the oestrogen receptor in the cell-type and promoter-context dependent agonistic activity of the anti-oestrogen 4-hydroxytamoxifen. *Embo J* **9**(9) p. 2811-8.

50. Metzger D., Losson R., Bornert J.M., Lemoine Y., and Chambon P. (1992). Promoter specificity of the two transcriptional activation functions of the human oestrogen receptor in yeast. *Nucleic Acids Res* **20**(11) p. 2813-7.

51. Klein-Hitpass L., Kaling M., and Ryffel G.U. (1988). Synergism of closely adjacent estrogen-responsive elements increases their regulatory potential. *J Mol Biol* **201**(3) p. 537-44.

52. Bourdeau V., Deschenes J., Metivier R., Nagai Y., Nguyen D., Bretschneider N., Gannon F., White J.H., and Mader S. (2004). Genome-wide identification of high-affinity estrogen response elements in human and mouse. *Mol Endocrinol* **18**(6) p. 1411-27.

53. Nilsson S., Makela S., Treuter E., Tujague M., Thomsen J., Andersson G., Enmark E., Pettersson K., Warner M., and Gustafsson J.A. (2001). Mechanisms of estrogen action. *Physiol Rev* **81**(4) p. 1535-65.

54. Hart L.L. and Davie J.R. (2002). The estrogen receptor: more than the average transcription factor. *Biochem Cell Biol* **80**(3) p. 335-41.

55. Le Romancer M., Poulard C., Cohen P., Sentis S., Renoir J.M., and Corbo L. (2011). Cracking the estrogen receptor's posttranslational code in breast tumors. *Endocr Rev* **32**(5) p. 597-622.

56. Pappas T.C., Gametchu B., and Watson C.S. (1995). Membrane estrogen receptors identified by multiple antibody labeling and impeded-ligand binding. *FASEB J* **9**(5) p. 404-10.

57. Pratt W.B. and Toft D.O. (1997). Steroid receptor interactions with heat shock protein and immunophilin chaperones. *Endocr Rev* **18**(3) p. 306-60.

58. Weigel N.L. and Zhang Y. (1998). Ligand-independent activation of steroid hormone receptors. *J Mol Med* **76**(7) p. 469-79.

59. Anstead G.M., Carlson K.E., and Katzenellenbogen J.A. (1997). The estradiol pharmacophore: ligand structure-estrogen receptor binding affinity relationships and a model for the receptor binding site. *Steroids* **62**(3) p. 268-303.

60. Toran-Allerand C.D., Tinnikov A.A., Singh R.J., and Nethrapalli I.S. (2005). 17alpha-estradiol: a brain-active estrogen? *Endocrinology* **146**(9) p. 3843-50.

61. Pace P., Taylor J., Suntharalingam S., Coombes R.C., and Ali S. (1997). Human estrogen receptor beta binds DNA in a manner similar to and dimerizes with estrogen receptor alpha. *J Biol Chem* **272**(41) p. 25832-8.

62. Wood J.R., Greene G.L., and Nardulli A.M. (1998). Estrogen response elements function as allosteric modulators of estrogen receptor conformation. *Mol Cell Biol* **18**(4) p. 1927-34.

63. Fryer C.J. and Archer T.K. (1998). Chromatin remodelling by the glucocorticoid receptor requires the BRG1 complex. *Nature* **393**(6680) p. 88-91.

64. Kamei Y., Xu L., Heinzel T., Torchia J., Kurokawa R., Gloss B., Lin S.C., Heyman R.A., Rose D.W., Glass C.K., and Rosenfeld M.G. (1996). A CBP integrator complex mediates transcriptional activation and AP-1 inhibition by nuclear receptors. *Cell* **85**(3) p. 403-14.

65. Fondell J.D., Ge H., and Roeder R.G. (1996). Ligand induction of a transcriptionally active thyroid hormone receptor coactivator complex. *Proc Natl Acad Sci U S A* **93**(16) p. 8329-33.

66. Kato S. (2001). Estrogen receptor-mediated cross-talk with growth factor signaling pathways. *Breast Cancer* **8**(1) p. 3-9.

67. Joel P.B., Traish A.M., and Lannigan D.A. (1995). Estradiol and phorbol ester cause phosphorylation of serine 118 in the human estrogen receptor. *Mol Endocrinol* **9**(8) p. 1041-52.

68. Campbell R.A., Bhat-Nakshatri P., Patel N.M., Constantinidou D., Ali S., and Nakshatri H. (2001). Phosphatidylinositol 3-kinase/AKT-mediated activation of estrogen receptor alpha: a new model for anti-estrogen resistance. *J Biol Chem* **276**(13) p. 9817-24.

69. Rogatsky I., Trowbridge J.M., and Garabedian M.J. (1999). Potentiation of human estrogen receptor alpha transcriptional activation through phosphorylation of serines 104 and 106 by the cyclin A-CDK2 complex. *J Biol Chem* **274**(32) p. 22296-302.

70. Rochette-Egly C. (2003). Nuclear receptors: integration of multiple signalling pathways through phosphorylation. *Cell Signal* **15**(4) p. 355-66.

71. Gaub M.P., Bellard M., Scheuer I., Chambon P., and Sassone-Corsi P. (1990). Activation of the ovalbumin gene by the estrogen receptor involves the fos-jun complex. *Cell* **63**(6) p. 1267-76.

72. Webb P., Lopez G.N., Uht R.M., and Kushner P.J. (1995). Tamoxifen activation of the estrogen receptor/AP-1 pathway: potential origin for the cell-specific estrogen-like effects of antiestrogens. *Mol Endocrinol* **9**(4) p. 443-56.

73. Umayahara Y., Kawamori R., Watada H., Imano E., Iwama N., Morishima T., Yamasaki Y., Kajimoto Y., and Kamada T. (1994). Estrogen regulation of the insulin-like growth factor I gene transcription involves an AP-1 enhancer. *J Biol Chem* **269**(23) p. 16433-42.

74. Webb P., Nguyen P., Valentine C., Lopez G.N., Kwok G.R., McInerney E., Katzenellenbogen B.S., Enmark E., Gustafsson J.A., Nilsson S., and Kushner P.J. (1999). The estrogen receptor enhances AP-1 activity by two distinct mechanisms with different requirements for receptor transactivation functions. *Mol Endocrinol* **13**(10) p. 1672-85.

75. Kushner P.J., Agard D.A., Greene G.L., Scanlan T.S., Shiau A.K., Uht R.M., and Webb P. (2000). Estrogen receptor pathways to AP-1. *J Steroid Biochem Mol Biol* **74**(5) p. 311-7.

76. Porter W., Saville B., Hoivik D., and Safe S. (1997). Functional synergy between the transcription factor Sp1 and the estrogen receptor. *Mol Endocrinol* **11**(11) p. 1569-80.

77. Safe S. and Kim K. (2008). Non-classical genomic estrogen receptor (ER)/specificity protein and ER/activating protein-1 signaling pathways. *J Mol Endocrinol* **41**(5) p. 263-75.

78. Ray A., Prefontaine K.E., and Ray P. (1994). Down-modulation of interleukin-6 gene expression by 17 beta-estradiol in the absence of high affinity DNA binding by the estrogen receptor. *J Biol Chem* **269**(17) p. 12940-6.

79. Stein B. and Yang M.X. (1995). Repression of the interleukin-6 promoter by estrogen receptor is mediated by NF-kappa B and C/EBP beta. *Mol Cell Biol* **15**(9) p. 4971-9.

80. Blobel G.A., Sieff C.A., and Orkin S.H. (1995). Ligand-dependent repression of the erythroid transcription factor GATA-1 by the estrogen receptor. *Mol Cell Biol* **15**(6) p. 3147-53.

81. Stoecklin E., Wissler M., Schaetzle D., Pfitzner E., and Groner B. (1999). Interactions in the transcriptional regulation exerted by Stat5 and by members of the steroid hormone receptor family. *J Steroid Biochem Mol Biol* **69**(1-6) p. 195-204.

82. Stender J.D., Kim K., Charn T.H., Komm B., Chang K.C., Kraus W.L., Benner C., Glass C.K., and Katzenellenbogen B.S. (2010). Genome-wide analysis of estrogen receptor alpha DNA binding and tethering mechanisms identifies Runx1 as a novel tethering factor in receptor-mediated transcriptional activation. *Mol Cell Biol* **30**(16) p. 3943-55.

83. Improta-Brears T., Whorton A.R., Codazzi F., York J.D., Meyer T., and McDonnell D.P. (1999). Estrogen-induced activation of mitogen-activated protein kinase requires mobilization of intracellular calcium. *Proc Natl Acad Sci U S A* **96**(8) p. 4686-91.

84. Aronica S.M., Kraus W.L., and Katzenellenbogen B.S. (1994). Estrogen action via the cAMP signaling pathway: stimulation of adenylate cyclase and cAMP-regulated gene transcription. *Proc Natl Acad Sci U S A* **91**(18) p. 8517-21.

85. Migliaccio A., Di Domenico M., Castoria G., de Falco A., Bontempo P., Nola E., and Auricchio F. (1996). Tyrosine kinase/p21ras/MAP-kinase pathway activation by estradiol-receptor complex in MCF-7 cells. *EMBO J* **15**(6) p. 1292-300.

86. Pietras R.J. and Szego C.M. (1977). Specific binding sites for oestrogen at the outer surfaces of isolated endometrial cells. *Nature* **265**(5589) p. 69-72.

87. Parikh I., Anderson W.L., and Neame P. (1980). Identification of high affinity estrogen binding sites in calf uterine microsomal membranes. *J Biol Chem* **255**(21) p. 10266-70.

88. Monje P. and Boland R. (1999). Characterization of membrane estrogen binding proteins from rabbit uterus. *Mol Cell Endocrinol* **147**(1-2) p. 75-84.

89. Li L., Haynes M.P., and Bender J.R. (2003). Plasma membrane localization and function of the estrogen receptor alpha variant (ER46) in human endothelial cells. *Proc Natl Acad Sci U S A* **100**(8) p. 4807-12.

90. Acconcia F., Ascenzi P., Fabozzi G., Visca P., and Marino M. (2004). S-palmitoylation modulates human estrogen receptor-alpha functions. *Biochem Biophys Res Commun* **316**(3) p. 878-83.

91. Gilligan D.M., Quyyumi A.A., and Cannon R.O., 3rd (1994). Effects of physiological levels of estrogen on coronary vasomotor function in postmenopausal women. *Circulation* **89**(6) p. 2545-51.

92. Migliaccio A., Pagano M., and Auricchio F. (1993). Immediate and transient stimulation of protein tyrosine phosphorylation by estradiol in MCF-7 cells. *Oncogene* **8**(8) p. 2183-91.

93. Monje P., Zanello S., Holick M., and Boland R. (2001). Differential cellular localization of estrogen receptor alpha in uterine and mammary cells. *Mol Cell Endocrinol* **181**(1-2) p. 117-29.

94. Castoria G., Migliaccio A., Bilancio A., Di Domenico M., de Falco A., Lombardi M., Fiorentino R., Varricchio L., Barone M.V., and Auricchio F. (2001). PI3-kinase in concert with Src promotes the S-phase entry of oestradiol-stimulated MCF-7 cells. *EMBO J* **20**(21) p. 6050-9.

95. Chung Y.L., Sheu M.L., Yang S.C., Lin C.H., and Yen S.H. (2002). Resistance to tamoxifen-induced apoptosis is associated with direct interaction between Her2/neu and cell membrane estrogen receptor in breast cancer. *Int J Cancer* **97**(3) p. 306-12.

96. Kahlert S., Nuedling S., van Eickels M., Vetter H., Meyer R., and Grohe C. (2000). Estrogen receptor alpha rapidly activates the IGF-1 receptor pathway. *J Biol Chem* **275**(24) p. 18447-53.

97. Marino M., Acconcia F., Bresciani F., Weisz A., and Trentalance A. (2002). Distinct nongenomic signal transduction pathways controlled by 17beta-estradiol regulate DNA synthesis and cyclin D(1) gene transcription in HepG2 cells. *Mol Biol Cell* **13**(10) p. 3720-9.

98. Brzozowski A.M., Pike A.C., Dauter Z., Hubbard R.E., Bonn T., Engstrom O., Ohman L., Greene G.L., Gustafsson J.A., and Carlquist M. (1997). Molecular basis of agonism and antagonism in the oestrogen receptor. *Nature* **389**(6652) p. 753-8.

99. Pike A.C., Brzozowski A.M., and Hubbard R.E. (2000). A structural biologist's view of the oestrogen receptor. *J Steroid Biochem Mol Biol* **74**(5) p. 261-8.

100. Savkur R.S. and Burris T.P. (2004). The coactivator LXXLL nuclear receptor recognition motif. *J Pept Res* **63**(3) p. 207-12.

101. Halachmi S., Marden E., Martin G., MacKay H., Abbondanza C., and Brown M. (1994). Estrogen receptor-associated proteins: possible mediators of hormone-induced transcription. *Science* **264**(5164) p. 1455-8.

102. Onate S.A., Tsai S.Y., Tsai M.J., and O'Malley B.W. (1995). Sequence and characterization of a coactivator for the steroid hormone receptor superfamily. *Science* **270**(5240) p. 1354-7.

103. Metivier R., Penot G., Flouriot G., and Pakdel F. (2001). Synergism between ERalpha transactivation function 1 (AF-1) and AF-2 mediated by steroid receptor coactivator protein-1: requirement for the AF-1 alpha-helical core and for a direct interaction between the N- and C-terminal domains. *Mol Endocrinol* **15**(11) p. 1953-70.

104. Heery D.M., Kalkhoven E., Hoare S., and Parker M.G. (1997). A signature motif in transcriptional co-activators mediates binding to nuclear receptors. *Nature* **387**(6634) p. 733-6.

105. McInerney E.M., Rose D.W., Flynn S.E., Westin S., Mullen T.M., Krones A., Inostroza J., Torchia J., Nolte R.T., Assa-Munt N., Milburn M.V., Glass C.K., and Rosenfeld M.G. (1998). Determinants of coactivator LXXLL motif specificity in nuclear receptor transcriptional activation. *Genes Dev* **12**(21) p. 3357-68.

106. Voegel J.J., Heine M.J., Tini M., Vivat V., Chambon P., and Gronemeyer H. (1998). The coactivator TIF2 contains three nuclear receptor-binding motifs and mediates transactivation through CBP binding-dependent and -independent pathways. *Embo J* **17**(2) p. 507-19.

107. Ito T., Levenstein M.E., Fyodorov D.V., Kutach A.K., Kobayashi R., and Kadonaga J.T. (1999). ACF consists of two subunits, Acf1 and ISWI, that function cooperatively in the ATP-dependent catalysis of chromatin assembly. *Genes Dev* **13**(12) p. 1529-39.

108. Freedman L.P. (1999). Increasing the complexity of coactivation in nuclear receptor signaling. *Cell* **97**(1) p. 5-8.

109. Yuan C.X., Ito M., Fondell J.D., Fu Z.Y., and Roeder R.G. (1998). The TRAP220 component of a thyroid hormone receptor- associated protein (TRAP) coactivator complex interacts directly with nuclear receptors in a ligand-dependent fashion. *Proc Natl Acad Sci U S A* **95**(14) p. 7939-44.

110. Warnmark A., Almlof T., Leers J., Gustafsson J.A., and Treuter E. (2001). Differential recruitment of the mammalian mediator subunit TRAP220 by estrogen receptors ERalpha and ERbeta. *J Biol Chem* **276**(26) p. 23397-404.

111. Chen H., Lin R.J., Xie W., Wilpitz D., and Evans R.M. (1999). Regulation of hormone-induced histone hyperacetylation and gene activation via acetylation of an acetylase. *Cell* **98**(5) p. 675-86.

112. Bardou V.J., Arpino G., Elledge R.M., Osborne C.K., and Clark G.M. (2003). Progesterone receptor status significantly improves outcome prediction over estrogen receptor status alone for adjuvant endocrine therapy in two large breast cancer databases. *J Clin Oncol* **21**(10) p. 1973-9.

113. Bertos N.R. and Park M. (2011). Breast cancer - one term, many entities? *J Clin Invest* **121**(10) p. 3789-96.

114. Sotiriou C. and Pusztai L. (2009). Gene-expression signatures in breast cancer. *N Engl J Med* **360**(8) p. 790-800.

115. Jensen E.V., Block G.E., Smith S., Kyser K., and DeSombre E.R. (1971). Estrogen receptors and breast cancer response to adrenalectomy. *Natl Cancer Inst Monogr* **34** p. 55-70.

116. Jensen E.V. and DeSombre E.R. (1971). Effects of ovarian hormones at the subcellular level. *Curr Top Exp Endocrinol* **1** p. 229-69.

117. Jensen E.V., Numata M., Brecher P.I., and Desombre E.R. (1971). Hormone-receptor interaction as a guide to biochemical mechanism. *Biochem Soc Symp* **32** p. 133-59.

118. Anderson E. (2002). The role of oestrogen and progesterone receptors in human mammary development and tumorigenesis. *Breast Cancer Res* **4**(5) p. 197-201.

119. Stierer M., Rosen H., Weber R., Hanak H., Spona J., and Tuchler H. (1993). Immunohistochemical and biochemical measurement of estrogen and progesterone receptors in primary breast cancer. Correlation of histopathology and prognostic factors. *Ann Surg* **218**(1) p. 13-21.

120. Khan S.A., Rogers M.A., Obando J.A., and Tamsen A. (1994). Estrogen receptor expression of benign breast epithelium and its association with breast cancer. *Cancer Res* **54**(4) p. 993-7.

121. Holtkamp D.E., Greslin J.G., Root C.A., and Lerner L.J. (1960). Gonadotrophin inhibiting and anti-fecundity effects of chloramiphene. *Proc Soc Exp Biol Med* **105** p. 197-201.

122. Herbst A.L., Griffiths C.T., and Kistner R.W. (1964). Clomiphene Citrate (Nsc-35770) in Disseminated Mammary Carcinoma. *Cancer Chemother Rep* **43** p. 39-41.

123. Kistner R.W. and Smith O.W. (1960). Observations on the use of a non-steroidal estrogen antagonist: MER-25. *Surg Forum* **10** p. 725-9.

124. Cole M.P., Jones C.T., and Todd I.D. (1971). A new anti-oestrogenic agent in late breast cancer. An early clinical appraisal of ICI46474. *Br J Cancer* **25**(2) p. 270-5.

125. Jordan V.C. (2003). Tamoxifen: a most unlikely pioneering medicine. *Nat Rev Drug Discov* **2**(3) p. 205-13.

126. Prentice R.L. (1990). Tamoxifen as a potential preventive agent in healthy postmenopausal women. *J Natl Cancer Inst* **82**(16) p. 1310-1.

127. Fisher B., Costantino J.P., Wickerham D.L., Redmond C.K., Kavanah M., Cronin W.M., Vogel V., Robidoux A., Dimitrov N., Atkins J., Daly M., Wieand S., Tan-Chiu E., Ford L., and Wolmark N. (1998). Tamoxifen for prevention of breast cancer: report of the National Surgical Adjuvant Breast and Bowel Project P-1 Study. *J Natl Cancer Inst* **90**(18) p. 1371-88.

128. Harper M.J. and Walpole A.L. (1966). Contrasting endocrine activities of cis and trans isomers in a series of substituted triphenylethylenes. *Nature* **212**(5057) p. 87.

129. Terenius L. (1971). Structure-activity relationships of anti-oestrogens with regard to interaction with 17-beta-oestradiol in the mouse uterus and vagina. *Acta Endocrinol (Copenh)* **66**(3) p. 431-47.

130. Harper M.J. and Walpole A.L. (1967). A new derivative of triphenylethylene: effect on implantation and mode of action in rats. *J Reprod Fertil* **13**(1) p. 101-19.

131. Wolf D.M. and Jordan V.C. (1994). The estrogen receptor from a tamoxifen stimulated MCF-7 tumor variant contains a point mutation in the ligand binding domain. *Breast Cancer Res Treat* **31**(1) p. 129-38.

132. Assikis V.J., Neven P., Jordan V.C., and Vergote I. (1996). A realistic clinical perspective of tamoxifen and endometrial carcinogenesis. *Eur J Cancer* **32A**(9) p. 1464-76.

133. Shang Y. and Brown M. (2002). Molecular determinants for the tissue specificity of SERMs. *Science* **295**(5564) p. 2465-8.

134. Smith C.L., Nawaz Z., and O'Malley B.W. (1997). Coactivator and corepressor regulation of the agonist/antagonist activity of the mixed antiestrogen, 4-hydroxytamoxifen. *Mol Endocrinol* **11**(6) p. 657-66.

135. Bunone G., Briand P.A., Miksicek R.J., and Picard D. (1996). Activation of the unliganded estrogen receptor by EGF involves the MAP kinase pathway and direct phosphorylation. *EMBO J* **15**(9) p. 2174-83.

136. Castano E., Chen C.W., Vorojeikina D.P., and Notides A.C. (1998). The role of phosphorylation in human estrogen receptor function. *J Steroid Biochem Mol Biol* **65**(1-6) p. 101-10.

137. Metivier R., Petit F.G., Valotaire Y., and Pakdel F. (2000). Function of N-terminal transactivation domain of the estrogen receptor requires a potential alpha-helical structure and is negatively regulated by the A domain. *Mol Endocrinol* **14**(11) p. 1849-71.

138. O'Regan R.M., Osipo C., Ariazi E., Lee E.S., Meeke K., Morris C., Bertucci A., Sarker M.A., Grigg R., and Jordan V.C. (2006). Development and therapeutic options for the treatment of raloxifene-stimulated breast cancer in athymic mice. *Clin Cancer Res* **12**(7 Pt 1) p. 2255-63.

139. Gottardis M.M. and Jordan V.C. (1988). Development of tamoxifen-stimulated growth of MCF-7 tumors in athymic mice after long-term antiestrogen administration. *Cancer Res* **48**(18) p. 5183-7.

140. Stearns V., Johnson M.D., Rae J.M., Morocho A., Novielli A., Bhargava P., Hayes D.F., Desta Z., and Flockhart D.A. (2003). Active tamoxifen metabolite plasma concentrations after coadministration of tamoxifen and the selective serotonin reuptake inhibitor paroxetine. *J Natl Cancer Inst* **95**(23) p. 1758-64.

141. Jin Y., Desta Z., Stearns V., Ward B., Ho H., Lee K.H., Skaar T., Storniolo A.M., Li L., Araba A., Blanchard R., Nguyen A., Ullmer L., Hayden J., Lemler S., Weinshilboum R.M., Rae J.M., Hayes D.F., and Flockhart D.A. (2005). CYP2D6 genotype, antidepressant use, and tamoxifen metabolism during adjuvant breast cancer treatment. *J Natl Cancer Inst* **97**(1) p. 30-9.

142. McClelland R.A., Barrow D., Madden T.A., Dutkowski C.M., Pamment J., Knowlden J.M., Gee J.M., and Nicholson R.I. (2001). Enhanced epidermal growth factor receptor signaling in MCF7 breast cancer cells after long-term culture in the presence of the pure antiestrogen ICI 182,780 (Faslodex). *Endocrinology* **142**(7) p. 2776-88.

143. Johnston S.R. (1997). Acquired tamoxifen resistance in human breast cancer--potential mechanisms and clinical implications. *Anticancer Drugs* **8**(10) p. 911-30.

144. Zwart W., Griekspoor A., Berno V., Lakeman K., Jalink K., Mancini M., Neefjes J., and Michalides R. (2007). PKA-induced resistance to tamoxifen is associated with an altered orientation of ERalpha towards co-activator SRC-1. *EMBO J* **26**(15) p. 3534-44.

145. Jordan V.C. and Gosden B. (1982). Importance of the alkylaminoethoxy side-chain for the estrogenic and antiestrogenic actions of tamoxifen and trioxifene in the immature rat uterus. *Mol Cell Endocrinol* **27**(3) p. 291-306.

146. Robertson D.W., Katzenellenbogen J.A., Hayes J.R., and Katzenellenbogen B.S. (1982). Antiestrogen basicity--activity relationships: a comparison of the estrogen receptor binding and antiuterotrophic potencies of several analogues of (Z)-1,2-diphenyl-1-[4-[2-(dimethylamino)ethoxy]phenyl]-1-butene (tamoxifen, Nolvadex) having altered basicity. *J Med Chem* **25**(2) p. 167-71.

147. Shiau A.K., Barstad D., Loria P.M., Cheng L., Kushner P.J., Agard D.A., and Greene G.L. (1998). The structural basis of estrogen receptor/coactivator recognition and the antagonism of this interaction by tamoxifen. *Cell* **95**(7) p. 927-37.

148. Pike A.C., Brzozowski A.M., Hubbard R.E., Bonn T., Thorsell A.G., Engstrom O., Ljunggren J., Gustafsson J.A., and Carlquist M. (1999). Structure of the ligand-

binding domain of oestrogen receptor beta in the presence of a partial agonist and a full antagonist. *Embo J* **18**(17) p. 4608-18.

149. Darimont B.D., Wagner R.L., Apriletti J.W., Stallcup M.R., Kushner P.J., Baxter J.D., Fletterick R.J., and Yamamoto K.R. (1998). Structure and specificity of nuclear receptor-coactivator interactions. *Genes Dev* **12**(21) p. 3343-56.

150. Lavinsky R.M., Jepsen K., Heinzel T., Torchia J., Mullen T.M., Schiff R., Del-Rio A.L., Ricote M., Ngo S., Gemsch J., Hilsenbeck S.G., Osborne C.K., Glass C.K., Rosenfeld M.G., and Rose D.W. (1998). Diverse signaling pathways modulate nuclear receptor recruitment of N-CoR and SMRT complexes. *Proc Natl Acad Sci U S A* **95**(6) p. 2920-5.

151. Shang Y., Hu X., DiRenzo J., Lazar M.A., and Brown M. (2000). Cofactor dynamics and sufficiency in estrogen receptor-regulated transcription. *Cell* **103**(6) p. 843-52.

152. Xu H.E., Stanley T.B., Montana V.G., Lambert M.H., Shearer B.G., Cobb J.E., McKee D.D., Galardi C.M., Plunket K.D., Nolte R.T., Parks D.J., Moore J.T., Kliewer S.A., Willson T.M., and Stimmel J.B. (2002). Structural basis for antagonist-mediated recruitment of nuclear co-repressors by PPARalpha. *Nature* **415**(6873) p. 813-7.

153. Webb P., Nguyen P., and Kushner P.J. (2003). Differential SERM effects on corepressor binding dictate ERalpha activity in vivo. *J Biol Chem* **278**(9) p. 6912-20.

154. Pike A.C., Brzozowski A.M., Walton J., Hubbard R.E., Thorsell A.G., Li Y.L., Gustafsson J.A., and Carlquist M. (2001). Structural insights into the mode of action of a pure antiestrogen. *Structure* **9**(2) p. 145-53.

155. Wakeling A.E. and Bowler J. (1987). Steroidal pure antioestrogens. *J Endocrinol* **112**(3) p. R7-10.

156. Fawell S.E., Lees J.A., White R., and Parker M.G. (1990). Characterization and colocalization of steroid binding and dimerization activities in the mouse estrogen receptor. *Cell* **60**(6) p. 953-62.

157. Varshochi R., Halim F., Sunters A., Alao J.P., Madureira P.A., Hart S.M., Ali S., Vigushin D.M., Coombes R.C., and Lam E.W. (2005). ICI182,780 induces p21Waf1 gene transcription through releasing histone deacetylase 1 and estrogen receptor alpha from Sp1 sites to induce cell cycle arrest in MCF-7 breast cancer cell line. *J Biol Chem* **280**(5) p. 3185-96.

158. Wakeling A.E., Dukes M., and Bowler J. (1991). A potent specific pure antiestrogen with clinical potential. *Cancer Res* **51**(15) p. 3867-73.

159. Osborne C.K., Wakeling A., and Nicholson R.I. (2004). Fulvestrant: an oestrogen receptor antagonist with a novel mechanism of action. *Br J Cancer* **90 Suppl 1** p. S2-6.

160. Howell A. (2006). Fulvestrant ('Faslodex'): current and future role in breast cancer management. *Crit Rev Oncol Hematol* **57**(3) p. 265-73.

161. Mahfoudi A., Roulet E., Dauvois S., Parker M.G., and Wahli W. (1995). Specific mutations in the estrogen receptor change the properties of antiestrogens to full agonists. *Proc Natl Acad Sci U S A* **92**(10) p. 4206-10.

162. Montano M.M., Muller V., Trobaugh A., and Katzenellenbogen B.S. (1995). The carboxy-terminal F domain of the human estrogen receptor: role in the transcriptional activity of the receptor and the effectiveness of antiestrogens as estrogen antagonists. *Mol Endocrinol* **9**(7) p. 814-25.

163. Van Den Bemd G.J., Kuiper G.G., Pols H.A., and Van Leeuwen J.P. (1999). Distinct effects on the conformation of estrogen receptor alpha and beta by both the antiestrogens ICI 164,384 and ICI 182,780 leading to opposite effects on receptor stability. *Biochem Biophys Res Commun* **261**(1) p. 1-5.

164. Wu Y.L., Yang X., Ren Z., McDonnell D.P., Norris J.D., Willson T.M., and Greene G.L. (2005). Structural basis for an unexpected mode of SERM-mediated ER antagonism. *Mol Cell* **18**(4) p. 413-24.

165. Wakeling A.E. (1995). Use of pure antioestrogens to elucidate the mode of action of oestrogens. *Biochem Pharmacol* **49**(11) p. 1545-9.

166. Osborne C.K., Coronado-Heinsohn E.B., Hilsenbeck S.G., McCue B.L., Wakeling A.E., McClelland R.A., Manning D.L., and Nicholson R.I. (1995). Comparison of the effects of a pure steroidal antiestrogen with those of tamoxifen in a model of human breast cancer. *J Natl Cancer Inst* **87**(10) p. 746-50.

167. McClelland R.A., Gee J.M., Francis A.B., Robertson J.F., Blamey R.W., Wakeling A.E., and Nicholson R.I. (1996). Short-term effects of pure anti-oestrogen ICI 182780 treatment on oestrogen receptor, epidermal growth factor receptor and transforming growth factor-alpha protein expression in human breast cancer. *Eur J Cancer* **32A**(3) p. 413-6.

168. Dauvois S., Danielian P.S., White R., and Parker M.G. (1992). Antiestrogen ICI 164,384 reduces cellular estrogen receptor content by increasing its turnover. *Proc Natl Acad Sci U S A* **89**(9) p. 4037-41.

169. Dauvois S., White R., and Parker M.G. (1993). The antiestrogen ICI 182780 disrupts estrogen receptor nucleocytoplasmic shuttling. *J Cell Sci* **106 (Pt 4)** p. 1377-88.

170. Parker M.G. (1993). Action of "pure" antiestrogens in inhibiting estrogen receptor action. *Breast Cancer Res Treat* **26**(2) p. 131-7.

171. Peekhaus N.T., Chang T., Hayes E.C., Wilkinson H.A., Mitra S.W., Schaeffer J.M., and Rohrer S.P. (2004). Distinct effects of the antiestrogen Faslodex on the stability of estrogen receptors-alpha and -beta in the breast cancer cell line MCF-7. *J Mol Endocrinol* **32**(3) p. 987-95.

172. Berry N.B., Fan M., and Nephew K.P. (2008). Estrogen receptor-alpha hinge-region lysines 302 and 303 regulate receptor degradation by the proteasome. *Mol Endocrinol* **22**(7) p. 1535-51.

173. Wijayaratne A.L. and McDonnell D.P. (2001). The human estrogen receptor-alpha is a ubiquitinated protein whose stability is affected differentially by agonists, antagonists, and selective estrogen receptor modulators. *J Biol Chem* **276**(38) p. 35684-92.

174. Giamarchi C., Chailleux C., Callige M., Rochaix P., Trouche D., and Richard-Foy H. (2002). Two antiestrogens affect differently chromatin remodeling of trefoil factor 1 (pS2) gene and the fate of estrogen receptor in MCF7 cells. *Biochim Biophys Acta* **1578**(1-3) p. 12-20.

175. Callige M., Kieffer I., and Richard-Foy H. (2005). CSN5/Jab1 is involved in ligand-dependent degradation of estrogen receptor {alpha} by the proteasome. *Mol Cell Biol* **25**(11) p. 4349-58.

176. Long X. and Nephew K.P. (2006). Fulvestrant (ICI 182,780)-dependent interacting proteins mediate immobilization and degradation of estrogen receptor-alpha. *J Biol Chem* **281**(14) p. 9607-15.

177. Htun H., Holth L.T., Walker D., Davie J.R., and Hager G.L. (1999). Direct visualization of the human estrogen receptor alpha reveals a role for ligand in the nuclear distribution of the receptor. *Mol Biol Cell* **10**(2) p. 471-86.

178. Stenoien D.L., Mancini M.G., Patel K., Allegretto* E.A., Smith C.L., and Mancini M.A. (2000). Subnuclear Trafficking of Estrogen Receptor-{alpha} and Steroid Receptor Coactivator-1. *Mol Endocrinol* **14**(4) p. 518-534.

179. Stenoien D.L., Patel K., Mancini M.G., Dutertre M., Smith C.L., O'Malley B.W., and Mancini M.A. (2001). FRAP reveals that mobility of oestrogen receptor-alpha is ligand- and proteasome-dependent. *Nat Cell Biol* **3**(1) p. 15-23.

180. Matsuda K., Nishi M., Takaya H., Kaku N., and Kawata M. (2008). Intranuclear mobility of estrogen receptor alpha and progesterone receptors in association with nuclear matrix dynamics. *J Cell Biochem* **103**(1) p. 136-48.

181. Marsaud V., Gougelet A., Maillard S., and Renoir J.M. (2003). Various phosphorylation pathways, depending on agonist and antagonist binding to endogenous estrogen receptor alpha (ERalpha), differentially affect ERalpha extractability, proteasome-mediated stability, and transcriptional activity in human breast cancer cells. *Mol Endocrinol* **17**(10) p. 2013-27.

182. Lipfert L., Fisher J.E., Wei N., Scafonas A., Su Q., Yudkovitz J., Chen F., Warrier S., Birzin E.T., Kim S., Chen H.Y., Tan Q., Schmidt A., Dininno F., Rohrer S.P., Hammond M.L., Rodan G.A., Freedman L.P., and Reszka A.A. (2006). Antagonist-induced, activation function-2-independent estrogen receptor alpha phosphorylation. *Mol Endocrinol* **20**(3) p. 516-33.

183. Lupien M., Jeyakumar M., Hebert E., Hilmi K., Cotnoir-White D., Loch C., Auger A., Dayan G., Pinard G.A., Wurtz J.M., Moras D., Katzenellenbogen J., and Mader S. (2007). Raloxifene and ICI182,780 increase estrogen receptor-alpha association with a nuclear compartment via overlapping sets of hydrophobic amino acids in activation function 2 helix 12. *Mol Endocrinol* **21**(4) p. 797-816.

184. Henikoff S., Furuyama T., and Ahmad K. (2004). Histone variants, nucleosome assembly and epigenetic inheritance. *Trends Genet* **20**(7) p. 320-6.

185. Luger K., Mader A.W., Richmond R.K., Sargent D.F., and Richmond T.J. (1997). Crystal structure of the nucleosome core particle at 2.8 A resolution. *Nature* **389**(6648) p. 251-60.

186. Sarma K. and Reinberg D. (2005). Histone variants meet their match. *Nat Rev Mol Cell Biol* **6**(2) p. 139-49.

187. Gevry N., Hardy S., Jacques P.E., Laflamme L., Svotelis A., Robert F., and Gaudreau L. (2009). Histone H2A.Z is essential for estrogen receptor signaling. *Genes Dev* **23**(13) p. 1522-33.

188. Bradbury E.M. (1992). Reversible histone modifications and the chromosome cell cycle. *Bioessays* **14**(1) p. 9-16.

189. Steger D.J. and Workman J.L. (1999). Transcriptional analysis of purified histone acetyltransferase complexes. *Methods* **19**(3) p. 410-6.

190. Carlson M., Osmond B.C., and Botstein D. (1981). SUC genes of yeast: a dispersed gene family. *Cold Spring Harb Symp Quant Biol* **45 Pt 2** p. 799-803.

191. Winston F. and Carlson M. (1992). Yeast SNF/SWI transcriptional activators and the SPT/SIN chromatin connection. *Trends Genet* **8**(11) p. 387-91.

192. Hill D.A. (2001). Influence of linker histone H1 on chromatin remodeling. *Biochem Cell Biol* **79**(3) p. 317-24.

193. Lusser A. and Kadonaga J.T. (2003). Chromatin remodeling by ATP-dependent molecular machines. *Bioessays* **25**(12) p. 1192-200.

194. Aalfs J.D. and Kingston R.E. (2000). What does 'chromatin remodeling' mean? *Trends Biochem Sci* **25**(11) p. 548-55.

195. Kingston R.E. and Narlikar G.J. (1999). ATP-dependent remodeling and acetylation as regulators of chromatin fluidity. *Genes Dev* **13**(18) p. 2339-52.

196. Becker P.B., Tsukiyama T., and Wu C. (1994). Chromatin assembly extracts from Drosophila embryos. *Methods Cell Biol* **44** p. 207-23.

197. Sudarsanam P. and Winston F. (2000). The Swi/Snf family nucleosome-remodeling complexes and transcriptional control. *Trends Genet* **16**(8) p. 345-51.

198. Cote J., Quinn J., Workman J.L., and Peterson C.L. (1994). Stimulation of GAL4 derivative binding to nucleosomal DNA by the yeast SWI/SNF complex. *Science* **265**(5168) p. 53-60.

199. Boyer L.A., Latek R.R., and Peterson C.L. (2004). The SANT domain: a unique histone-tail-binding module? *Nat Rev Mol Cell Biol* **5**(2) p. 158-63.

200. Dirscherl S.S. and Krebs J.E. (2004). Functional diversity of ISWI complexes. *Biochem Cell Biol* **82**(4) p. 482-9.

201. Johnson C.N., Adkins N.L., and Georgel P. (2005). Chromatin remodeling complexes: ATP-dependent machines in action. *Biochem Cell Biol* **83**(4) p. 405-17.

202. Fyodorov D.V. and Kadonaga J.T. (2002). Binding of Acf1 to DNA involves a WAC motif and is important for ACF-mediated chromatin assembly. *Mol Cell Biol* **22**(18) p. 6344-53.

203. Fyodorov D.V. and Kadonaga J.T. (2002). Dynamics of ATP-dependent chromatin assembly by ACF. *Nature* **418**(6900) p. 897-900.

204. Becker P.B. and Horz W. (2002). ATP-dependent nucleosome remodeling. *Annu Rev Biochem* **71** p. 247-73.

205. Gavin I., Horn P.J., and Peterson C.L. (2001). SWI/SNF chromatin remodeling requires changes in DNA topology. *Mol Cell* **7**(1) p. 97-104.

206. Barak O., Lazzaro M.A., Lane W.S., Speicher D.W., Picketts D.J., and Shiekhattar R. (2003). Isolation of human NURF: a regulator of Engrailed gene expression. *Embo J* **22**(22) p. 6089-100.

207. Georgel P.T., Tsukiyama T., and Wu C. (1997). Role of histone tails in nucleosome remodeling by Drosophila NURF. *Embo J* **16**(15) p. 4717-26.

208. Aalfs J.D., Narlikar G.J., and Kingston R.E. (2001). Functional differences between the human ATP-dependent nucleosome remodeling proteins BRG1 and SNF2H. *J Biol Chem* **276**(36) p. 34270-8.

209. Clapier C.R., Nightingale K.P., and Becker P.B. (2002). A critical epitope for substrate recognition by the nucleosome remodeling ATPase ISWI. *Nucleic Acids Res* **30**(3) p. 649-55.

210. Grune T., Brzeski J., Eberharter A., Clapier C.R., Corona D.F., Becker P.B., and Muller C.W. (2003). Crystal structure and functional analysis of a nucleosome recognition module of the remodeling factor ISWI. *Mol Cell* **12**(2) p. 449-60.

211. Aasland R., Gibson T.J., and Stewart A.F. (1995). The PHD finger: implications for chromatin-mediated transcriptional regulation. *Trends Biochem Sci* **20**(2) p. 56-9.

212. Clapier C.R., Langst G., Corona D.F., Becker P.B., and Nightingale K.P. (2001). Critical role for the histone H4 N terminus in nucleosome remodeling by ISWI. *Mol Cell Biol* **21**(3) p. 875-83.

213. Eberharter A., Vetter I., Ferreira R., and Becker P.B. (2004). ACF1 improves the effectiveness of nucleosome mobilization by ISWI through PHD-histone contacts. *EMBO J* **23**(20) p. 4029-39.

214. Eberharter A., Ferrari S., Langst G., Straub T., Imhof A., Varga-Weisz P., Wilm M., and Becker P.B. (2001). Acf1, the largest subunit of CHRAC, regulates ISWI-induced nucleosome remodelling. *Embo J* **20**(14) p. 3781-8.

215. Ewing A.K., Attner M., and Chakravarti D. (2007). Novel regulatory role for human Acf1 in transcriptional repression of vitamin D3 receptor-regulated genes. *Mol Endocrinol* **21**(8) p. 1791-806.

216. Stopka T. and Skoultchi A.I. (2003). The ISWI ATPase Snf2h is required for early mouse development. *Proc Natl Acad Sci U S A* **100**(24) p. 14097-102.

217. Collins N., Poot R.A., Kukimoto I., Garcia-Jimenez C., Dellaire G., and Varga-Weisz P.D. (2002). An ACF1-ISWI chromatin-remodeling complex is required for DNA replication through heterochromatin. *Nat Genet* **32**(4) p. 627-32.

218. Weinmann A.S., Yan P.S., Oberley M.J., Huang T.H., and Farnham P.J. (2002). Isolating human transcription factor targets by coupling chromatin immunoprecipitation and CpG island microarray analysis. *Genes Dev* **16**(2) p. 235-44.

219. Fyodorov D.V., Blower M.D., Karpen G.H., and Kadonaga J.T. (2004). Acf1 confers unique activities to ACF/CHRAC and promotes the formation rather than disruption of chromatin in vivo. *Genes Dev* **18**(2) p. 170-83.

220. Yasui D., Miyano M., Cai S., Varga-Weisz P., and Kohwi-Shigematsu T. (2002). SATB1 targets chromatin remodelling to regulate genes over long distances. *Nature* **419**(6907) p. 641-5.

221. Alenghat T., Yu J., and Lazar M.A. (2006). The N-CoR complex enables chromatin remodeler SNF2H to enhance repression by thyroid hormone receptor. *EMBO J* **25**(17) p. 3966-74.

222. . st.

223. Lan L., Ui A., Nakajima S., Hatakeyama K., Hoshi M., Watanabe R., Janicki S.M., Ogiwara H., Kohno T., Kanno S., and Yasui A. (2010). The ACF1 complex is required for DNA double-strand break repair in human cells. *Mol Cell* **40**(6) p. 976-87.

224. Sanchez-Molina S., Mortusewicz O., Bieber B., Auer S., Eckey M., Leonhardt H., Friedl A.A., and Becker P.B. (2011). Role for hACF1 in the G2/M damage checkpoint. *Nucleic Acids Res* **39**(19) p. 8445-56.

225. Boddy M.N., Howe K., Etkin L.D., Solomon E., and Freemont P.S. (1996). PIC 1, a novel ubiquitin-like protein which interacts with the PML component of a multiprotein complex that is disrupted in acute promyelocytic leukaemia. *Oncogene* **13**(5) p. 971-82.

226. Saitoh H. and Hinchey J. (2000). Functional heterogeneity of small ubiquitin-related protein modifiers SUMO-1 versus SUMO-2/3. *J Biol Chem* **275**(9) p. 6252-8.

227. Ayaydin F. and Dasso M. (2004). Distinct in vivo dynamics of vertebrate SUMO paralogues. *Mol Biol Cell* **15**(12) p. 5208-18.

228. Bohren K.M., Nadkarni V., Song J.H., Gabbay K.H., and Owerbach D. (2004). A M55V polymorphism in a novel SUMO gene (SUMO-4) differentially activates heat shock transcription factors and is associated with susceptibility to type I diabetes mellitus. *J Biol Chem* **279**(26) p. 27233-8.

229. Rodriguez M.S., Dargemont C., and Hay R.T. (2001). SUMO-1 conjugation in vivo requires both a consensus modification motif and nuclear targeting. *J Biol Chem* **276**(16) p. 12654-9.

230. Tremblay A.M., Wilson B.J., Yang X.J., and Giguere V. (2008). Phosphorylation-dependent sumoylation regulates estrogen-related receptor-alpha and -gamma transcriptional activity through a synergy control motif. *Mol Endocrinol* **22**(3) p. 570-84.

231. Yang S.H., Galanis A., Witty J., and Sharrocks A.D. (2006). An extended consensus motif enhances the specificity of substrate modification by SUMO. *EMBO J* **25**(21) p. 5083-93.

232. Hay R.T. (2005). SUMO: a history of modification. *Mol Cell* **18**(1) p. 1-12.

233. Desterro J.M., Rodriguez M.S., Kemp G.D., and Hay R.T. (1999). Identification of the enzyme required for activation of the small ubiquitin-like protein SUMO-1. *J Biol Chem* **274**(15) p. 10618-24.

234. Desterro J.M., Thomson J., and Hay R.T. (1997). Ubch9 conjugates SUMO but not ubiquitin. *FEBS Lett* **417**(3) p. 297-300.

235. Nacerddine K., Lehembre F., Bhaumik M., Artus J., Cohen-Tannoudji M., Babinet C., Pandolfi P.P., and Dejean A. (2005). The SUMO pathway is essential for nuclear integrity and chromosome segregation in mice. *Dev Cell* **9**(6) p. 769-79.

236. Chung C.D., Liao J., Liu B., Rao X., Jay P., Berta P., and Shuai K. (1997). Specific inhibition of Stat3 signal transduction by PIAS3. *Science* **278**(5344) p. 1803-5.

237. Rytinki M.M., Kaikkonen S., Pehkonen P., Jaaskelainen T., and Palvimo J.J. (2009). PIAS proteins: pleiotropic interactors associated with SUMO. *Cell Mol Life Sci* **66**(18) p. 3029-41.

238. Wilkinson K.A. and Henley J.M. (2010). Mechanisms, regulation and consequences of protein SUMOylation. *Biochem J* **428**(2) p. 133-45.

239. Bawa-Khalfe T. and Yeh E.T. (2010). SUMO Losing Balance: SUMO Proteases Disrupt SUMO Homeostasis to Facilitate Cancer Development and Progression. *Genes Cancer* **1**(7) p. 748-752.

240. Song J., Durrin L.K., Wilkinson T.A., Krontiris T.G., and Chen Y. (2004). Identification of a SUMO-binding motif that recognizes SUMO-modified proteins. *Proc Natl Acad Sci U S A* **101**(40) p. 14373-8.

241. Hannich J.T., Lewis A., Kroetz M.B., Li S.J., Heide H., Emili A., and Hochstrasser M. (2005). Defining the SUMO-modified proteome by multiple approaches in Saccharomyces cerevisiae. *J Biol Chem* **280**(6) p. 4102-10.

242. Hecker C.M., Rabiller M., Haglund K., Bayer P., and Dikic I. (2006). Specification of SUMO1- and SUMO2-interacting motifs. *J Biol Chem* **281**(23) p. 16117-27.

243. Kuo H.Y., Chang C.C., Jeng J.C., Hu H.M., Lin D.Y., Maul G.G., Kwok R.P., and Shih H.M. (2005). SUMO modification negatively modulates the transcriptional activity of CREB-binding protein via the recruitment of Daxx. *Proc Natl Acad Sci U S A* **102**(47) p. 16973-8.

244. Geoffroy M.C. and Hay R.T. (2009). An additional role for SUMO in ubiquitin-mediated proteolysis. *Nat Rev Mol Cell Biol* **10**(8) p. 564-8.

245. Lallemand-Breitenbach V. and de The H. (2010). PML nuclear bodies. *Cold Spring Harb Perspect Biol* **2**(5) p. a000661.

246. Swanson K.A., Kang R.S., Stamenova S.D., Hicke L., and Radhakrishnan I. (2003). Solution structure of Vps27 UIM-ubiquitin complex important for endosomal sorting and receptor downregulation. *EMBO J* **22**(18) p. 4597-606.

247. Reverter D. and Lima C.D. (2005). Insights into E3 ligase activity revealed by a SUMO-RanGAP1-Ubc9-Nup358 complex. *Nature* **435**(7042) p. 687-92.

248. Song J., Zhang Z., Hu W., and Chen Y. (2005). Small ubiquitin-like modifier (SUMO) recognition of a SUMO binding motif: a reversal of the bound orientation. *J Biol Chem* **280**(48) p. 40122-9.

249. de T.H.E., Riviere M., and Bernhard W. (1960). [Examination by electron microscope of the VX2 tumor of the domestic rabbit derived from the Shope papilloma]. *Bull Assoc Fr Etud Cancer* **47** p. 570-84.

250. Stuurman N., de Graaf A., Floore A., Josso A., Humbel B., de Jong L., and van Driel R. (1992). A monoclonal antibody recognizing nuclear matrix-associated nuclear bodies. *J Cell Sci* **101 (Pt 4)** p. 773-84.

251. Jensen K., Shiels C., and Freemont P.S. (2001). PML protein isoforms and the RBCC/TRIM motif. *Oncogene* **20**(49) p. 7223-33.

252. Saitoh H., Uchimura Y., Mishiro T., and Uwada J. (2006). [Studying the SUMO modification pathway: from molecular structure to regulation of epigenome]. *Tanpakushitsu Kakusan Koso* **51**(10 Suppl) p. 1195-200.

253. Duprez E., Saurin A.J., Desterro J.M., Lallemand-Breitenbach V., Howe K., Boddy M.N., Solomon E., de The H., Hay R.T., and Freemont P.S. (1999). SUMO-1 modification of the acute promyelocytic leukaemia protein PML: implications for nuclear localisation. *J Cell Sci* **112 (Pt 3)** p. 381-93.

254. Kamitani T., Kito K., Nguyen H.P., Wada H., Fukuda-Kamitani T., and Yeh E.T. (1998). Identification of three major sentrinization sites in PML. *J Biol Chem* **273**(41) p. 26675-82.

255. Percherancier Y., Germain-Desprez D., Galisson F., Mascle X.H., Dianoux L., Estephan P., Chelbi-Alix M.K., and Aubry M. (2009). Role of SUMO in RNF4-mediated promyelocytic leukemia protein (PML) degradation: sumoylation of PML and phospho-switch control of its SUMO binding domain dissected in living cells. *J Biol Chem* **284**(24) p. 16595-608.

256. Shen T.H., Lin H.K., Scaglioni P.P., Yung T.M., and Pandolfi P.P. (2006). The mechanisms of PML-nuclear body formation. *Mol Cell* **24**(3) p. 331-9.

257. Zhong S., Muller S., Ronchetti S., Freemont P.S., Dejean A., and Pandolfi P.P. (2000). Role of SUMO-1-modified PML in nuclear body formation. *Blood* **95**(9) p. 2748-52.

258. Quimby B.B., Yong-Gonzalez V., Anan T., Strunnikov A.V., and Dasso M. (2006). The promyelocytic leukemia protein stimulates SUMO conjugation in yeast. *Oncogene* **25**(21) p. 2999-3005.

259. Moilanen A.M., Poukka H., Karvonen U., Hakli M., Janne O.A., and Palvimo J.J. (1998). Identification of a novel RING finger protein as a coregulator in steroid receptor-mediated gene transcription. *Mol Cell Biol* **18**(9) p. 5128-39.

260. Hakli M., Karvonen U., Janne O.A., and Palvimo J.J. (2005). SUMO-1 promotes association of SNURF (RNF4) with PML nuclear bodies. *Exp Cell Res* **304**(1) p. 224-33.

261. Sun H., Leverson J.D., and Hunter T. (2007). Conserved function of RNF4 family proteins in eukaryotes: targeting a ubiquitin ligase to SUMOylated proteins. *EMBO J* **26**(18) p. 4102-12.

262. Tatham M.H., Geoffroy M.C., Shen L., Plechanovova A., Hattersley N., Jaffray E.G., Palvimo J.J., and Hay R.T. (2008). RNF4 is a poly-SUMO-specific E3 ubiquitin ligase required for arsenic-induced PML degradation. *Nat Cell Biol* **10**(5) p. 538-46.

263. Lallemand-Breitenbach V., Jeanne M., Benhenda S., Nasr R., Lei M., Peres L., Zhou J., Zhu J., Raught B., and de The H. (2008). Arsenic degrades PML or PML-RARalpha through a SUMO-triggered RNF4/ubiquitin-mediated pathway. *Nat Cell Biol* **10**(5) p. 547-55.

264. Ivanov A.V., Peng H., Yurchenko V., Yap K.L., Negorev D.G., Schultz D.C., Psulkowski E., Fredericks W.J., White D.E., Maul G.G., Sadofsky M.J., Zhou M.M., and Rauscher F.J., 3rd (2007). PHD domain-mediated E3 ligase activity directs intramolecular sumoylation of an adjacent bromodomain required for gene silencing. *Mol Cell* **28**(5) p. 823-37.

265. Stielow B., Sapetschnig A., Kruger I., Kunert N., Brehm A., Boutros M., and Suske G. (2008). Identification of SUMO-dependent chromatin-associated transcriptional repression components by a genome-wide RNAi screen. *Mol Cell* **29**(6) p. 742-54.

266. Yang S.H. and Sharrocks A.D. (2004). SUMO promotes HDAC-mediated transcriptional repression. *Mol Cell* **13**(4) p. 611-7.

267. Ahn J.W., Lee Y.A., Ahn J.H., and Choi C.Y. (2009). Covalent conjugation of Groucho with SUMO-1 modulates its corepressor activity. *Biochem Biophys Res Commun* **379**(1) p. 160-5.

268. Stielow B., Sapetschnig A., Wink C., Kruger I., and Suske G. (2008). SUMO-modified Sp3 represses transcription by provoking local heterochromatic gene silencing. *EMBO Rep* **9**(9) p. 899-906.

269. Ouyang J., Shi Y., Valin A., Xuan Y., and Gill G. (2009). Direct binding of CoREST1 to SUMO-2/3 contributes to gene-specific repression by the LSD1/CoREST1/HDAC complex. *Mol Cell* **34**(2) p. 145-54.

270. Gostissa M., Hengstermann A., Fogal V., Sandy P., Schwarz S.E., Scheffner M., and Del Sal G. (1999). Activation of p53 by conjugation to the ubiquitin-like protein SUMO-1. *EMBO J* **18**(22) p. 6462-71.

271. Rodriguez M.S., Desterro J.M., Lain S., Midgley C.A., Lane D.P., and Hay R.T. (1999). SUMO-1 modification activates the transcriptional response of p53. *EMBO J* **18**(22) p. 6455-61.

272. Ling Y., Sankpal U.T., Robertson A.K., McNally J.G., Karpova T., and Robertson K.D. (2004). Modification of de novo DNA methyltransferase 3a (Dnmt3a) by SUMO-1 modulates its interaction with histone deacetylases (HDACs) and its capacity to repress transcription. *Nucleic Acids Res* **32**(2) p. 598-610.

273. Gomez-del Arco P., Koipally J., and Georgopoulos K. (2005). Ikaros SUMOylation: switching out of repression. *Mol Cell Biol* **25**(7) p. 2688-97.

274. Kaikkonen S., Jaaskelainen T., Karvonen U., Rytinki M.M., Makkonen H., Gioeli D., Paschal B.M., and Palvimo J.J. (2009). SUMO-specific protease 1 (SENP1)

reverses the hormone-augmented SUMOylation of androgen receptor and modulates gene responses in prostate cancer cells. *Mol Endocrinol* **23**(3) p. 292-307.

275. Poukka H., Karvonen U., Janne O.A., and Palvimo J.J. (2000). Covalent modification of the androgen receptor by small ubiquitin-like modifier 1 (SUMO-1). *Proc Natl Acad Sci U S A* **97**(26) p. 14145-50.

276. Lin D.Y., Fang H.I., Ma A.H., Huang Y.S., Pu Y.S., Jenster G., Kung H.J., and Shih H.M. (2004). Negative modulation of androgen receptor transcriptional activity by Daxx. *Mol Cell Biol* **24**(24) p. 10529-41.

277. Yang Y., Tse A.K., Li P., Ma Q., Xiang S., Nicosia S.V., Seto E., Zhang X., and Bai W. (2011). Inhibition of androgen receptor activity by histone deacetylase 4 through receptor SUMOylation. *Oncogene* **30**(19) p. 2207-18.

278. Tian S., Poukka H., Palvimo J.J., and Janne O.A. (2002). Small ubiquitin-related modifier-1 (SUMO-1) modification of the glucocorticoid receptor. *Biochem J* **367**(Pt 3) p. 907-11.

279. Holmstrom S., Van Antwerp M.E., and Iniguez-Lluhi J.A. (2003). Direct and distinguishable inhibitory roles for SUMO isoforms in the control of transcriptional synergy. *Proc Natl Acad Sci U S A* **100**(26) p. 15758-63.

280. Holmstrom S.R., Chupreta S., So A.Y., and Iniguez-Lluhi J.A. (2008). SUMO-mediated inhibition of glucocorticoid receptor synergistic activity depends on stable assembly at the promoter but not on DAXX. *Mol Endocrinol* **22**(9) p. 2061-75.

281. Lin D.Y., Huang Y.S., Jeng J.C., Kuo H.Y., Chang C.C., Chao T.T., Ho C.C., Chen Y.C., Lin T.P., Fang H.I., Hung C.C., Suen C.S., Hwang M.J., Chang K.S., Maul G.G., and Shih H.M. (2006). Role of SUMO-interacting motif in Daxx SUMO modification, subnuclear localization, and repression of sumoylated transcription factors. *Mol Cell* **24**(3) p. 341-54.

282. Abdel-Hafiz H., Dudevoir M.L., and Horwitz K.B. (2009). Mechanisms underlying the control of progesterone receptor transcriptional activity by SUMOylation. *J Biol Chem* **284**(14) p. 9099-108.

283. Abdel-Hafiz H., Takimoto G.S., Tung L., and Horwitz K.B. (2002). The inhibitory function in human progesterone receptor N termini binds SUMO-1 protein to regulate autoinhibition and transrepression. *J Biol Chem* **277**(37) p. 33950-6.

284. Daniel A.R., Faivre E.J., and Lange C.A. (2007). Phosphorylation-dependent antagonism of sumoylation derepresses progesterone receptor action in breast cancer cells. *Mol Endocrinol* **21**(12) p. 2890-906.

285. Tallec L.P., Kirsh O., Lecomte M.C., Viengchareun S., Zennaro M.C., Dejean A., and Lombes M. (2003). Protein inhibitor of activated signal transducer and activator of transcription 1 interacts with the N-terminal domain of mineralocorticoid receptor and represses its transcriptional activity: implication of small ubiquitin-related modifier 1 modification. *Mol Endocrinol* **17**(12) p. 2529-42.

286. Tirard M., Almeida O.F., Hutzler P., Melchior F., and Michaelidis T.M. (2007). Sumoylation and proteasomal activity determine the transactivation properties of the mineralocorticoid receptor. *Mol Cell Endocrinol* **268**(1-2) p. 20-9.

287. Barsalou A., Gao W., Anghel S.I., Carriere J., and Mader S. (1998). Estrogen response elements can mediate agonist activity of anti-estrogens in human endometrial Ishikawa cells. *J Biol Chem* **273**(27) p. 17138-46.

288. Sentis S., Le Romancer M., Bianchin C., Rostan M.C., and Corbo L. (2005). Sumoylation of the estrogen receptor alpha hinge region regulates its transcriptional activity. *Mol Endocrinol* **19**(11) p. 2671-84.

289. Kobayashi S., Shibata H., Yokota K., Suda N., Murai A., Kurihara I., Saito I., and Saruta T. (2004). FHL2, UBC9, and PIAS1 are novel estrogen receptor alpha-interacting proteins. *Endocr Res* **30**(4) p. 617-21.

290. Fan M., Park A., and Nephew K.P. (2005). CHIP (carboxyl terminus of Hsc70-interacting protein) promotes basal and geldanamycin-induced degradation of estrogen receptor-alpha. *Mol Endocrinol* **19**(12) p. 2901-14.

291. Sheu J.J., Choi J.H., Yildiz I., Tsai F.J., Shaul Y., Wang T.L., and Shih Ie M. (2008). The roles of human sucrose nonfermenting protein 2 homologue in the tumor-promoting functions of Rsf-1. *Cancer Res* **68**(11) p. 4050-7.

292. Peng J. and Wysocka J. (2008). It takes a PHD to SUMO. *Trends Biochem Sci* **33**(5) p. 191-4.

293. Albergaria A., Ribeiro A.S., Pinho S., Milanezi F., Carneiro V., Sousa B., Sousa S., Oliveira C., Machado J.C., Seruca R., Paredes J., and Schmitt F. (2010). ICI 182,780 induces P-cadherin overexpression in breast cancer cells through chromatin remodelling at the promoter level: a role for C/EBPbeta in CDH3 gene activation. *Hum Mol Genet* **19**(13) p. 2554-66.

294. Welboren W.J., van Driel M.A., Janssen-Megens E.M., van Heeringen S.J., Sweep F.C., Span P.N., and Stunnenberg H.G. (2009). ChIP-Seq of ERalpha and RNA polymerase II defines genes differentially responding to ligands. *EMBO J* **28**(10) p. 1418-28.

295. Kim J., Petz L.N., Ziegler Y.S., Wood J.R., Potthoff S.J., and Nardulli A.M. (2000). Regulation of the estrogen-responsive pS2 gene in MCF-7 human breast cancer cells. *J Steroid Biochem Mol Biol* **74**(4) p. 157-68.

Annexes

Annexe 1 : Raloxifene and ICI182,780 Increase Estrogen Receptor- Association with a Nuclear Compartment via Overlapping Sets of Hydrophobic Amino Acids in Activation Function 2 Helix 12

0888-8809/07/$15.00/0
Printed in U.S.A.

Molecular Endocrinology 21(4):797–816

doi: 10.1210/me.2006-0074

Raloxifene and ICI182,780 Increase Estrogen Receptor-α Association with a Nuclear Compartment via Overlapping Sets of Hydrophobic Amino Acids in Activation Function 2 Helix 12

Mathieu Lupien, M. Jeyakumar, Elise Hébert, Khalid Hilmi, David Cotnoir-White, Caroline Loch, Anick Auger, Guila Dayan, Geneviève-Anne Pinard, Jean-Marie Wurtz, Dino Moras, John Katzenellenbogen, and Sylvie Mader

Department of Medicine (M.L., S.M.), Division of Experimental Medicine, McGill University, Montreal, Québec, Canada H3A 1A3; Department of Chemistry (M.J., J.K.), University of Illinois, Urbana, Illinois 61801; Department of Biochemistry (E.H., K.H., A.A., G.D., G-A.P., S.M.) and Institute for Research in Immunology and Cancer (K.H., D.C.-W., S.M.), Université de Montréal, Montréal, Québec, Canada H3C 3J7; and Institut de Génétique et de Biologie Moléculaire et Cellulaire (C.L., J.-M.W., D.M.), 67 404 Illkirch Cédex, France

The basis for the differential repressive effects of antiestrogens on transactivation by estrogen receptor-α (ERα) remains incompletely understood. Here, we show that the full antiestrogen ICI182,780 and, to a lesser extent, the selective ER modulator raloxifene (Ral), induce accumulation of exogenous ERα in a poorly soluble fraction in transiently transfected HepG2 or stably transfected MDA-MB231 cells and of endogenous receptor in MCF7 cells. ERα remained nuclear in HepG2 cells treated with either compound. Replacement of selected hydrophobic residues of ERα ligand-binding domain helix 12 (H12) enhanced receptor solubility in the presence of ICI182,780 or Ral. These mutations also increased transcriptional activity with Ral or ICI182,780 on reporter genes or on the endogenous estrogen target gene TFF1 in a manner requiring the integrity of the N-terminal AF-1 domain. The antiestrogen-specific effects of single mutations suggest that they affect receptor function by mechanisms other than a simple decrease in hydrophobicity of H12, possibly due to relief from local steric hindrance between these residues and the antiestrogen side chains. Fluorescence anisotropy experiments indicated an enhanced regional stabilization of mutant ligand-binding domains in the presence of antiestrogens. H12 mutations also prevent the increase in bioluminescence resonance energy transfer between ERα monomers induced by Ral or ICI182,780 and increase intranuclear receptor mobility in correlation with transcriptional activity in the presence of these antiestrogens. Our data indicate that ICI182,780 and Ral locally alter the ERα ligand binding structure via specific hydrophobic residues of H12 and decrease its transcriptional activity through tighter association with an insoluble nuclear structure. (*Molecular Endocrinology* 21: 797–816, 2007)

ESTROGENS, SUCH AS 17β-estradiol (E2), have pleiotropic actions on a number of target tissues in the skeletal, reproductive, cardiovascular, and central nervous systems (1–4). These actions are mediated by two estrogen receptors, ERα and ERβ (4, 5), members of the nuclear receptor superfamily of ligand-inducible transcription factors (6–9). Like other unliganded steroid hormone receptors, ERs are thought to interact in the absence of hormone with molecular chaperone complexes including the heat shock protein hsp90, the cochaperone p23, and immunophilins (10, 11). Hormone binding induces conformational changes resulting in binding to DNA (12–15) and in the ordered recruitment of a series of coactivator complexes responsible for histone acetylation, chromatin remodeling, and enhanced recruitment of the basal transcription machinery (16–21). Binding to DNA is achieved through specific interactions between the central DNA-binding domain, corresponding to homology region C (22, 23), and palindromic estrogen response elements [EREs (24–27)]. Two transcriptional activation functions are localized on either side of the DNA-binding domain. The activa-

First Published Online February 13, 2007

Abbreviations: AF-1, Activation function 1; AF-2, activation function 2; BRET, bioluminescence resonance energy transfer; E2, 17β-estradiol; ER, estrogen receptor; ERE, estrogen response element; FBS, fetal bovine serum; FRAP: fluorescence recovery after photobleaching; H12, helix 12; HEK, human embryonic kidney; HSB, high salt buffer; LBD, ligand-binding domain; LSM, laser scanning microscopy; MTMR, tetramethylrhodamine-5-maleimide; OHT, hydroxytamoxifen; PDB, protein database; Ral, Raloxifene; ROI, region of interest; RFU, relative fluorescence units; SERM, selective estrogen receptor modulator; TIF2, transcriptional intermediary factor 2; wt, wild type; YFP, yellow fluorescent protein.

***Molecular Endocrinology* is published monthly by The Endocrine Society (http://www.endo-society.org), the foremost professional society serving the endocrine community.**

tion function AF-2 is located in the C-terminal ligand-binding domain (LBD, region E), and recruits coactivators in a ligand-dependent manner. The activation function AF-1, in the N-terminal A/B region, can function in a ligand-independent manner and is very variable both in length and sequence in the nuclear receptor superfamily (5, 6, 28, 29).

The observation that estrogen induces proliferation of mammary epithelial cells and of ERα-positive breast tumor cells has led to the development of antiestrogens for the treatment and prevention of breast cancer (30–32). Antiestrogens are competitive antagonists of estrogen and block the transcriptional activation properties of ERs. However, some antiestrogens display partial estrogenic activity in a tissue- and gene-dependent manner, hence their description as selective estrogen receptor modulators (SERMs). In animal models, both 4-hydroxytamoxifen (OHT) and raloxifene (Ral) have a favorable, estrogen-like action in bone (33). However, OHT has marked estrogenic activity on the rodent uterus, whereas Ral has only low activity in this model (33, 34). On the other hand, full antiestrogens such as ICI164,384, ICI182,780, and RU58,668 (35–37) completely block transcriptional activity of ERs in breast and uterine tissues.

Transcriptional activity of ERs in the presence of OHT has been observed in different cellular models and correlates with activity of the AF-1 region (38, 39). Recruitment of corepressors nuclear receptor corepressor (N-CoR) and silencing mediator of retinoid and thyroid hormone receptor (SMRT) in the presence of antiestrogens has been demonstrated (40–42), and it has been proposed that a higher degree of interaction with corepressors in the presence of full antiestrogens explains their more complete antagonist activity compared with OHT (43). However, effects on ERα protein turnover also provide another explanation for the different pharmacological properties of antiestrogens. OHT stabilizes the ERα protein (44, 45), whereas full antiestrogens induce a rapid loss of nuclear ERα, resulting in depletion of the receptor from estrogen-responsive promoters (15). Clearance of nuclear ERα correlates with proteasome-dependent degradation in ERα-positive cells (46–49). In addition, ERα was reported to accumulate in insoluble complexes in MCF7 cells in the presence of full antiestrogens and proteasome inhibitors (49). Formation of cytosolic aggregates was reported in transfected cells (44, 45, 50), whereas fluorescence recovery after photobleaching (FRAP) experiments performed in transfected HeLa cells have indicated slower intranuclear dynamics of ERα in the presence of ICI182,780 (51). These observations indicate a variety of potential mechanisms of receptor inactivation by full antiestrogens. Moreover, Ral has often more limited agonist activity than OHT in ERα-expressing cells or in transiently transfected cell lines (43, 52–56), but the mechanisms of its stronger repressive effects remain poorly characterized to date.

Antiestrogens have been shown by crystallography studies to bind to ERs in a manner similar to that of estrogens, but to prevent folding of the LBD into its agonist conformation due to steric hindrance of the antiestrogen side chain (57–59). In particular, helix 12 (H12), which is crucial for AF-2 activity, is displaced by the antiestrogen side chain from its position in the agonist conformation on top of the ligand binding cavity. The crystal structures of ERα complexed to antiestrogens OHT or Ral are similar, with H12 associating with the coactivator binding groove formed by helices H3–H5, thus preventing coactivator recruitment by AF-2 (57, 58). On the other hand, in the crystal structure of rat ERβ complexed to ICI164,384, the longer side chain characteristic of full antiestrogens (35–37) interacts directly with the coactivator binding groove (59). The position of H12 is undefined, suggesting conformational flexibility.

Specific mutations in H12 have been shown to convert the full antiestrogen ICI164,384 into an agonist in some experimental cell systems (44, 60–62), indicating the importance of H12 in the antagonist activity of antiestrogens. However, it remains unclear which residues of H12 contribute to the antagonist activity of full antiestrogens and which properties of the receptor are altered by these residues. In addition, it is currently unknown why Ral, which induces a structure of the ERα LBD similar to that observed with OHT, displays a degree of antagonist activity comparable to that of full antiestrogens in transfected cells. In this study, we have sought to analyze the molecular basis and mechanisms of the more pronounced antiestrogenic action of Ral and ICI182,780 *vs.* OHT using different cell models expressing the wt receptor or a series of point mutants affected in H12 residues.

RESULTS

Ral and Full Antiestrogens Decrease Extractability of ERα from a Nuclear Compartment in HepG2 Cells

HepG2 cells are a well-established model system for studying the differential activity of antiestrogens (14, 62–65). In these cells, cotransfected with an expression vector for human ERα and the ERE3-TATA-Luc reporter vector, transcriptional activity was observed in the absence of hormone, due to basal activity of the receptor, and was induced approximately 5-fold in the presence of estradiol. Saturating concentrations of OHT [sufficient to fully displace estradiol in competition experiments (data not shown)] were partially permissive for transcriptional activity of the reporter vector, whereas either the full antiestrogen ICI182,780 or the SERM Ral fully repressed the receptor transcriptional activation properties (Fig. 1A). Thus, in this model system, Ral behaves more like a full than a partial antiestrogen. In addition, similar results were obtained in transiently transfected HeLa cells, except that the degree of transcriptional activity obtained with OHT was smaller (data not shown).

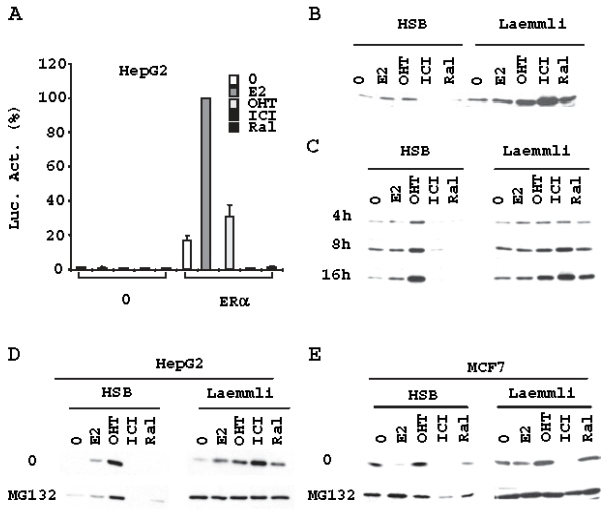

Fig. 1. The SERM Ral and the Full Antiestrogen ICI182,780 Both Efficiently Repress ERα Transcription and Decrease Soluble Receptor Levels in HepG2 Cells

A, Transient transfection experiments were performed in HepG2 cells by electroporation with an ERE3-TATA-Luc reporter, the internal control plasmid CMV-β-gal, and expression vectors for wt ERα or mutant ΔH12, as indicated. Cells were treated with vehicle (0), E2 (25 nM), OHT (100 nM), ICI 182,780 (ICI, 100 nM) or Ral (100 nM), for 48 h. Luciferase activity and β-galactosidase activity were quantified, and relative luciferase activity was calculated. Results from at least three experiments performed in triplicate are shown; *error bars* reflect the SD between independent experiments. B, After transient transfection with an expression vector for wt ERα, HepG2 cells were cultured in steroid-free medium for 36 h and subsequently treated with vehicle (0), E2, OHT, ICI182,780 (ICI), or Ral for 16 h. Extracts in HSB or Laemmli sample buffer (Laemmli) corresponding to one tenth of a plate in both cases were analyzed by SDS-PAGE and Western analysis using the anti-ERα antibody B10. C, A time course study of ERα protein levels after ligand treatment was performed by Western analysis as described in panel B. D, Receptor levels were evaluated in HepG2 cells transiently transfected with an expression vector for wt ERα and treated with hormones as in panel B. Treatment with the proteasome inhibitor MG132 (10 μM) was initiated 1 h before hormonal treatment. Extracts in HSB (50 μg) or Laemmli sample buffer were analyzed by SDS-PAGE and Western analysis using anti-ERα antibody B10. E, MCF7 cells were cultured in steroid-free medium for 36 h and subsequently treated with hormones and proteasome inhibitor as in panel D. Extracts in HSB (50 μg) or Laemmli sample buffer were analyzed by SDS-PAGE and Western analysis also as in panel D. Luc. Act., Luciferase activity.

To determine whether Ral and ICI182,780 induce receptor degradation in HepG2 cells, we performed a Western analysis of receptor levels in whole-cell extracts of HepG2 cells prepared using high-salt buffer (HSB). As reported before in a variety of cell systems (47–49, 66–69), OHT increased receptor levels compared with vehicle controls (Fig. 1B, *left panel*); estradiol also led to increased receptor content in the HSB fraction in HepG2 cells, but to lower levels than OHT (Fig. 1B, *left panel*). On the other hand, ICI182,780 induced disappearance of the receptor from the HSB-soluble fraction (Fig. 1B, *left panel*). In contrast to OHT, Ral did not lead to stabilization of the receptor but like ICI182,780 decreased receptor content in HSB extracts (Fig. 1B, *left panel*).

Because formation of cytoplasmic aggregates of ERα was observed in the presence of full antiestrogens in some cell systems (45, 50), we also examined receptor levels in Laemmli buffer, which extracts not only high-salt soluble receptor but also insoluble receptor aggregates. Western analysis performed with the same number of cells extracted either with HSB or Laemmli extract reveals that higher levels of receptor were extracted from cells with Laemmli buffer under all conditions, but that there was a marked accumulation of the receptor in the presence of ICI182,780 and, to a lesser extent, OHT or Ral (Fig. 1B, *right panel*). Comparison of profiles obtained with HSB and Laemmli extracts suggest therefore that disappearance of ERα from HSB extracts with ICI182,780 or Ral results from accumulation of the receptor in an insoluble form rather than from increased degradation. To determine whether insolubility of the receptor was due to formation of cytosolic aggregates in HepG2 cells, we performed an immunocytochemical analysis of ERα distribution on cells treated with vehicle, ICI182,780, or Ral for 16 h. Although cytosolic aggregates could be detected in some of the transfected cells treated with

ICI182,780 or Ral, this represented only a minority of the transfected cells (8% for ICI182,780 and 2.5% for Ral). Nuclear staining was observed in the majority of the transfected cells treated with antiestrogens as in cells exposed to vehicle only (Fig. 2).

To examine the kinetics of receptor insolubility in HepG2 cells, its distribution in the HSB-soluble and total (Laemmli buffer-soluble) fractions was determined at different times after exposure to antiestrogens. Poor extraction of the receptor in HSB was already observed at 4 h in the presence of ICI182,780 or Ral (Fig. 1C). Receptor levels gradually increased as a function of time in the presence of all antiestrogens in Laemmli extracts (Fig. 1C, *right panel*), but only in the presence of OHT in the HSB-soluble fraction (Fig. 1C, *left panel*). Together, these results suggest that all three antiestrogens stabilize the receptor against degradation in HepG2 cells, leading to a time-dependent accumulation reflecting *de novo* synthesis. However, these antiestrogens have markedly different effects on receptor solubility.

To verify that the variable levels of receptor observed both in HSB and Laemmli extracts from cells treated with the various ligands reflect different rates of degradation, we examined whether treatment of cells with the proteasome inhibitor MG132 would equalize levels of receptors under all treatment conditions. This was indeed the case in Laemmli extracts (Fig. 1D, *right panel*), confirming that all antiestrogens protect the receptor from degradation compared with no treatment or treatment with E2, but that ICI182,780 and Ral prevent extraction of the receptor in HSB.

Although these findings suggest different biophysical properties of the receptor in the presence of different antiestrogens, they contrast with reports that full antiestrogens induce receptor degradation in ER+ cells (47–49, 66–69). Indeed, under similar experimental conditions, treatment of MCF7 cells with ICI182,780 induced a depletion of receptor levels both in HSB and Laemmli extracts, although slightly higher levels of receptor were detected in Laemmli extracts (Fig. 1E, *upper panels*). Treatment of cells with MG132 fully restored receptor levels to amounts observed in the absence of treatment in Laemmli extracts (Fig. 1E, *lower right panel*), indicating that the receptor is indeed degraded in the presence of ICI182,780. However, receptor levels were still reduced by treatment with ICI182,780 in HSB even in the presence of MG132, indicating that the endogenous receptor in MCF7 cells is insoluble in the presence of ICI182,780 as well as in HepG2 cells. This property may explain the observation that treatment with proteasome inhibitors does not increase transcriptional activity of the receptor in the presence of ICI182,780 (data not shown). In MCF7 cells, receptor levels in the presence of Ral in the HSB fraction were intermediate between those with OHT and ICI182,780 and were increased either by extraction in Laemmli or by treatment with MG132, suggesting that both degradation and insolubility of the receptor contribute to reduced levels in the presence of Ral. In addition, ERα accumulated in an insoluble fraction in MCF7 treated with ICI182,780 or Ral at early time points (20 min) before degradation is initiated (data not shown). In conclusion, the overall patterns of receptor levels in the presence of antiestrogens are similar in HepG2 and MCF7 cells, and insolubility of the receptor in the presence of full antiestrogens is not restricted to transiently transfected cells.

Specific Long Hydrophobic Amino Acids of H12 Play a Role in Transcriptional Repression and Insolubility of the Receptor in the Presence of Ral or ICI182,780

A major difference in the structures of the receptor complexed to SERMs and full antiestrogens is the position of H12, which is present at the C terminus of the LBDs of all nuclear receptors (Fig. 3, A and B). H12 is amphipathic (Fig. 3C) and its hydrophobic face is buried against the rest of the LBD in the presence of agonists or of SERMs. Indeed, H12 acts as a lid to the ligand binding cavity in the presence of agonists. On the other hand, it binds to the coactivator binding groove in the presence of OHT or Ral, residues 540, 543, and 544 mimicking the critical leucine residues in the coactivator LXXLL motifs (57, 58). In contrast, the coactivator binding groove position is occupied by the long side chain of the full antiestrogen ICI164,384, and the position of H12 is not defined in the crystal structure with ERβ, suggesting conformational flexibility (59).

Although the positioning of helix 12 is similar in the presence of OHT and Ral (57, 58), we decided to investigate the role of this helix in antiestrogen-induced insolubility of the receptor based on previous studies reporting that combined mutation to alanines of two hydrophobic amino acids (L539-L540 and M543-L544), or the single L540Q mutation in H12 can lead to receptors with an inversion in their patterns of transcriptional activity with agonists and antagonists in transfected cells (44, 60–62). To investigate whether amino acids of H12 play a role in accumulation of the receptor in an insoluble fraction in the presence of Ral and/or ICI182,780 in HepG2 cells, and clarify the relationship between this property and transcriptional repression, we performed an alanine scanning mutagenesis of all hydrophobic amino acids in H12. Note that although amino acids 536–537 are not part of H12 in the agonist conformation, they are incorporated into H12 in the presence of SERMs (57, 58) and therefore were included in this analysis.

The activity of the different mutants was tested in HepG2 cells in the presence of agonists and antagonists (Fig. 4A). Contrary to the wt receptor, several mutants (at positions 536, 539, 540, 543, and 544) were transcriptionally active in the presence of ICI182,780. Note that titration curves performed with mutant L536A, which had a higher degree of activity in

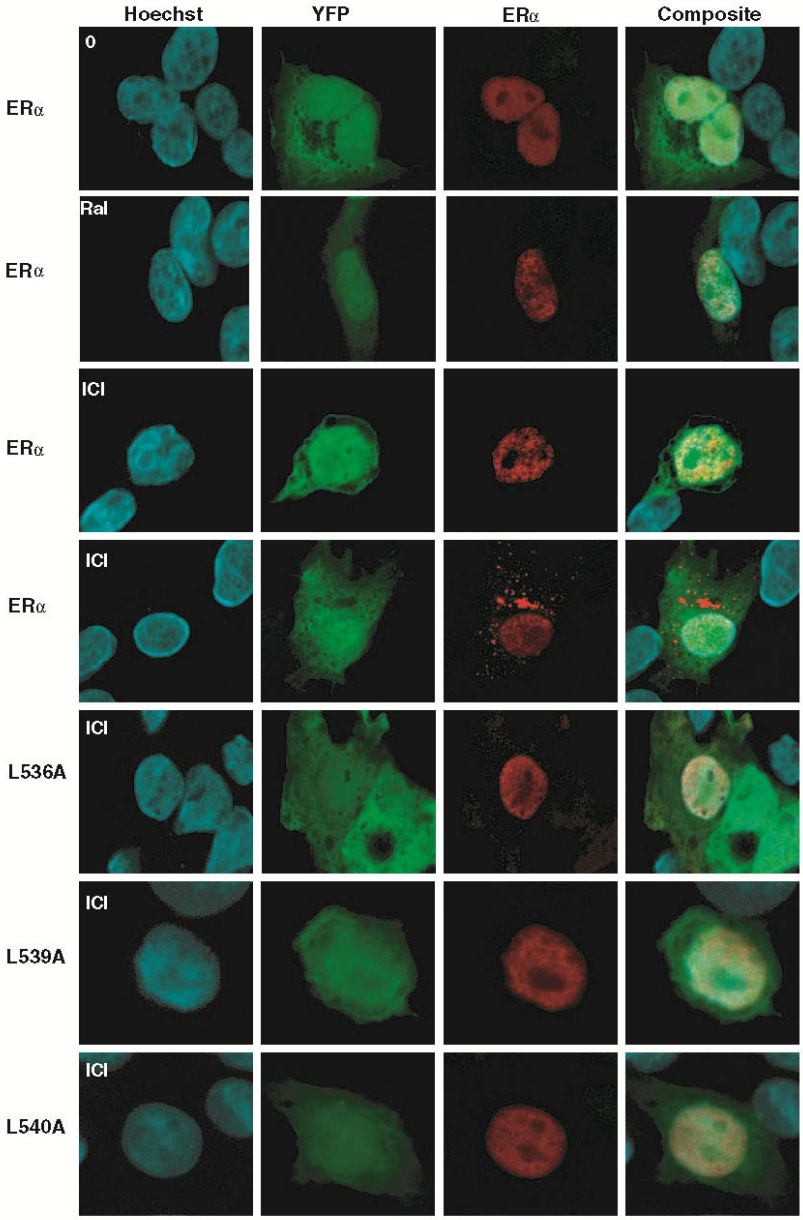

Fig. 2. Nuclear Localization of wt ERα and of H12 Mutant Receptors in HepG2 Cells

HepG2 cells were cotransfected with expression vectors for wt ERα or mutants affected in H12 (as indicated) and for YFP, and were treated with vehicle or ligands for 16 h before fixation, permeabilization, and antibody staining with a mouse anti-ERα (B10) and an Alexa Fluor® 595 dye-labeled goat antimouse secondary antibody. Images are from *left* to *right*: nuclear staining (Hoechst 33342), YFP, ERα, and composite images. ICI, ICI182,780.

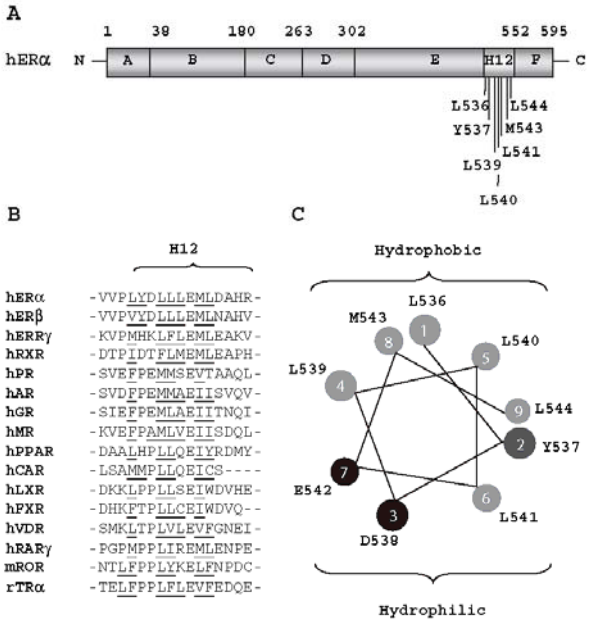

Fig. 3. Conservation of Hydrophobic Amino Acids in H12 in the Nuclear Receptor Superfamily

A, The domain organization characteristic of nuclear receptors is shown, and amino acids at the interdomain boundaries in ERα are indicated. The hydrophobic amino acids in helix H12 of the LBD are also highlighted. B, Alignment of H12 and flanking sequences (residues 535–545 in ERα) in the nuclear receptor superfamily. Conserved hydrophobic amino acids are *underlined* (h, human; r, rat; m, murine). C, Positioning of the hydrophobic residues in H12. Nonpolar (*light gray*), polar and uncharged (*medium gray*), or acidic (*black*) residues are placed on an α-helical wheel (generated using software at http://cti.itc.virginia.edu/~cmg/Demo/contents.html). AR, Androgen receptor; CAR, constitutive androstane receptor; ERR, estrogen-related receptor; GR, glucocorticoid receptor; LXR, liver X receptor; MR, mineralocorticoid receptor; PR, progesterone receptor; RAR, retinoic acid receptor; RXR, retinoic X receptor; VDR, vitamin D receptor.

the absence of ligand than in the presence of ICI182,780, confirmed that the increased activity in the presence of ICI182,780 was not due to lack of saturation of the receptor (data not shown). Activity in the presence of ICI182,780 was significantly increased with mutants L536A, L539A, L540A, M543A, and L544A compared with the response of the wt ERα ($P <$ 0.01 in Student's *t* test). A subset of these mutations also increased activity in the presence of Ral (536, 539, and to a lesser extent 544; $P < 0.01$). Interestingly, whereas mutants at positions 536 and 539 were more active with Ral than ICI182,780, mutant L540A had the opposite activity profile. Increased activity in the presence of antiestrogens was observed with mutants that had normal as well as reduced levels of estrogen-induced transcription. Similarly, there was no correlation between levels of basal activity, which were either reduced or increased by these mutations, and levels of activity in the presence of antiestrogens. This suggests that molecular determinants of activity in the presence of antiestrogens differ from those controlling transcriptional activity in the absence of ligand or in the presence of agonists. Finally, note that not all mutations in long hydrophobic residues generated increased activity of the receptor in the presence of Ral or ICI182,780, because mutants Y537A and L541A had an activity profile similar to that of wt receptor.

To assess whether mutations that increased activity in the presence of antiestrogens have altered solubility profiles, we performed Western analyses on all above described ERα mutants. Receptor levels in the soluble fraction in the presence of ICI182,780 or Ral correlated well with transcriptional activity of the receptors (Fig. 4B). All mutants with increased activity in the presence of Ral (L536A, L539A, and, to a lesser extent, L544A) were present at markedly increased levels in high-salt extracts. In particular, protein levels and transcriptional activity were both as high in the presence of Ral as of OHT for the L536A and L539A mutants (Fig. 4, A and B). In addition, mutants with increased activity in the presence of ICI182,780 (L536A, L539A, L540A, M543A, and L544A) were all detected at higher levels

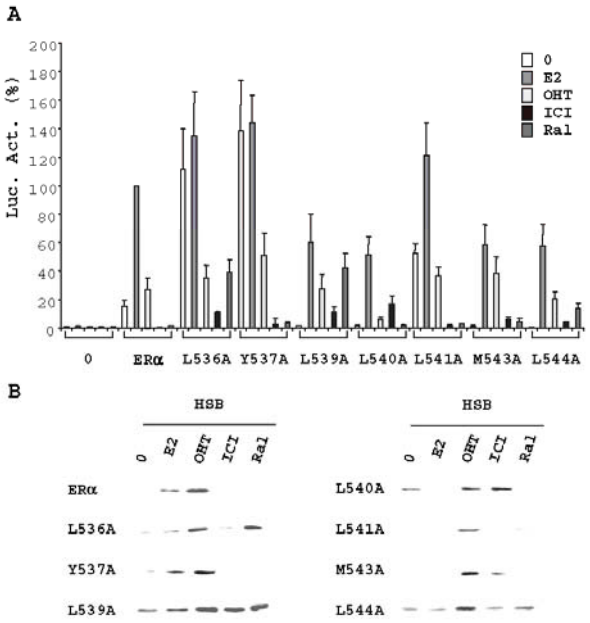

Fig. 4. The Long Hydrophobic Amino Acids of H12 Modulate Receptor Solubility and Activity in an Antiestrogen-Specific Manner

A, HepG2 cells were electroporated with the ERE3-TATA-Luc reporter, the internal control plasmid CMV-β-gal, and expression vectors for wt ERα or mutants affected in H12 hydrophobic residues. Cells were treated with hormones and harvested as described in Fig. 1A. Relative luciferase activity is shown. B, After transient transfection with expression vectors for wt or mutant ERα, HepG2 cells were cultured in steroid-free medium for 36 h and subsequently treated with hormones as in Fig. 1B. HSB extracts (HSB) (50 μg) were analyzed by SDS-PAGE and Western analysis using anti-ERα antibody B10 as described in Fig. 1B. ICI, ICI182,780.

in HSB extracts than the wt receptor in the presence of this antiestrogen (Fig. 4B). Notably, mutant L540A had higher solubility in the presence of ICI182,780 than Ral (Fig. 4B), correlating with the transcriptional profiles in the presence of these antiestrogens (Fig. 4A). Finally, mutants Y537A and L541A had similar patterns of extraction in HSB as the wt receptor, as well as similar patterns of transcriptional activation, in the presence of OHT, Ral, and ICI182,780.

Together, these observations suggest that mutations in H12 affect simultaneously receptor extractability from the nuclear compartment and transcriptional activity in the presence of antiestrogens ICI182,780 or Ral.

Partial Agonist Activity of Antiestrogens on the TFF1 Target Gene in MDA-MB-231 Cells Stably Transfected with the L539A Mutant

Although profiles of receptor levels in the presence of antiestrogens were similar in MCF7 and transiently transfected HepG2 cells, it remains possible that high expression levels generated in transfected HepG2 cells may lead to artifactual insolubility and not reflect the functional properties of receptors expressed at lower levels. To exclude this possibility, we generated stable cell lines expressing the wt ERα or mutant L539A in ERα-negative MDA-MB-231 cells. Hygromycin-resistant clones were analyzed for receptor expression by RT-PCR, and two clones with comparable expression levels were selected as well as a negative control clone propagating the empty parental vector (data not shown). Western analysis indicated that the expression levels of the wt receptor in the absence of hormone were lower than that of the endogenous receptor in MCF7 cells and that the pattern of ER levels in the presence of various antiestrogens after extraction in HSB was similar to those observed in MCF7 cells and HepG2 cells (Fig. 5A). The patterns of mutant L539A expression in HSB extracts were also comparable to those observed in HepG2 cells, with a relative increase in receptor levels in the presence of ICI182,780 and Ral compared with the wt receptor (Fig. 5B). Transient transfection of the ERE3-TATA-Luc reporter vector in the stable clones also indicated that

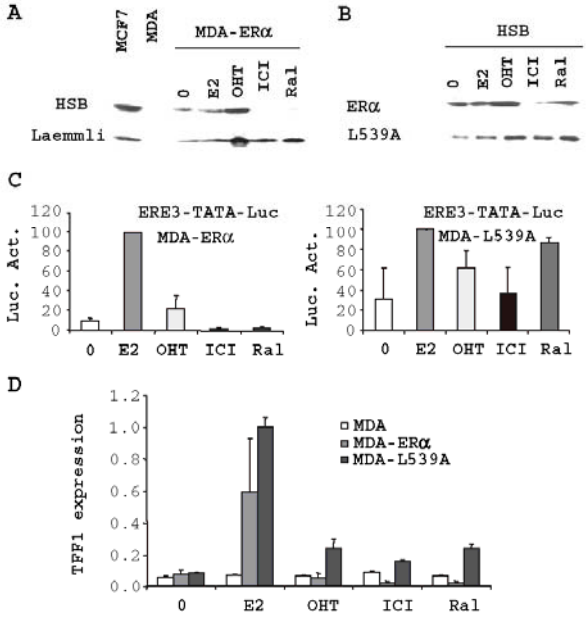

Fig. 5. The L539A Mutant Has Increased Transcriptional Activity in the Presence of Antiestrogens on the Endogenous pS2 Target Gene

A, Receptor levels in a stably transfected MDA-MB-231 clone expressing ERα (clone 22A) were determined both in HSB and Laemmli extracts using the B10 monoclonal antibody. Cells were treated with vehicle (0), E2, OHT, ICI182,780 (ICI), or Ral for 16 h and whole-protein extracts were prepared in either extraction buffer. Extracts from MCF7 or MDA-MB-231 cells were loaded for comparison. B, Western analysis of receptor levels in stably transfected MDA-MB-231 clones expressing ERα (clone 22A) or L539A (clone 4A) after hormonal treatment for 16 h and extraction in HSB. C, Transcriptional activity of the wt ERα or the L539A mutant was analyzed in stable clones (clone 22A and 4A, respectively) by transient transfection of the ERE3-TATA-Luc reporter construct. D, Transcription levels of the endogenous pS2/TFF1 gene in MDA-MB-231 stable clones were measured by quantitative-PCR amplification of reverse transcribed RNAs and standardized on expression of the housekeeping p36b4 gene, the mRNA levels of which are not affected by hormonal treatment. Luc. Act. Luciferase activity.

the patterns of transcriptional activity of the wt and mutant receptors were comparable to those observed in HepG2 cells. Indeed, ICI182,780 and Ral fully repressed activity of the reporter vector in the clone expressing the wt receptor, whereas they were partially permissive for transcription in the L539A clone, resulting in similar levels of activity with OHT and Ral, and slightly lower activity with ICI182,780 (Fig. 5C). Thus, results obtained in HepG2 cells are reproducible in cells that express receptors at near-endogenous levels.

Next, we investigated whether the L539A mutation could increase activity on endogenous receptor target genes. The pS2/TFF1 gene is a well-characterized estrogen target gene that contains a classical estrogen response element (70). Transcription of the TFF1 gene is returned to basal levels by OHT but further repressed by ICI182,780 and Ral (Fig. 5D; compare levels of activity obtained in the control and wt ERα-expressing clones). Basal levels of expression were similar in the clone expressing the L539A mutant and in the two other clones. On the other hand, levels of transcription of the TFF1 gene in the presence of ICI182,780 and Ral were significantly higher in the L539A clone than in the wt ERα-expressing clone ($P < 0.01$ in a *t* test). These results indicate that mutations in amino acids of H12 can lead to a gain in transcriptional activity in the presence of antiestrogens on endogenous estrogen target genes as well as with a reporter containing a minimal ERE3-TATA promoter.

Mutations in Long Hydrophobic Amino Acids of H12 Relieve Local Steric Hindrance with the Antiestrogen Side Chains

Because some mutations in hydrophobic residues (Y537A, L541A) had no effect on receptor solubility/activity and others had antiestrogen-selective effects, our results suggest a specific role of individual H12 residues on receptor conformation in the presence of

Ral or ICI182,780. To investigate this hypothesis, we superimposed complexes obtained in the presence of OHT (58), Ral (57), or ICI164,384, a compound closely related to ICI182,780 (59), to the ERα-E2 complex (71) and assessed the impact of antiestrogen binding on the agonist structure of the receptor. The side chains of antiestrogens created steric clashes with H12 in the agonist position at amino acids L536 (OHT; Fig. 6B), L540 (OHT, Ral, and, to a lesser extent, ICI164,384; Fig. 6, B–D) and/or M543 (ICI164,384; Fig. 6D). Depending on the extent of the clash, replacement of these residues by alanines may directly relieve steric hindrance. For instance, steric conflict between L540 and the side chain of ICI164,384, but not the more extensive overlap with the side chain of Ral, can be relieved by mutation to alanine (Fig. 6, C and D), correlating with a gain in transcriptional activity in the presence of ICI182,780, but not Ral, for this mutant. Replacement of L536 by alanine was also insufficient to relieve the steric clash with the OHT side chain and did not generate increased levels of transcriptional activity in the presence of this antiestrogen. Note that mutations removing the long hydrophobic side chains of amino acids close to those in direct steric conflict may result in rearrangement of the side chain of Ral or ICI182,780 in a manner that allows positioning of H12 in an agonist-like conformation.

We also examined the effect of the Ral or ICI164,384 side chains on positioning of H12 in the coactivator binding groove by superimposing the corresponding structures (57, 59) with that of OHT-bound ERα (Fig. 7, A and B) (57). The side chain of Ral was not found to generate important steric conflicts with H12, because the closest amino acids, L536 and L539, could form van der Waals contacts (Fig. 7C) as observed in the crystal structure of ERα with Ral (57). The ICI164,384 side chain, on the other hand, led to steric clash with L536, and less critical hindrance with L540 (Fig. 7D), amino acids the replacement of which by alanine residues increases agonist activity of ICI182,780.

In conclusion, many of the alanine mutations studied here reduce, either directly or indirectly, steric hindrance between antiestrogen side chains and H12 positioned either on top of the ligand binding cavity or in the coactivator binding groove and may thus increase LBD stability.

Increased Transcriptional Activity in the Presence of Ral or ICI182,780 Does Not Correlate with Increased Recruitment of an LXXLL Motif and Necessitates the Presence of the AF-1 Region

To examine whether mutations in several long hydrophobic amino acids of H12 result in gain in AF-2 activity in the presence of Ral or ICI182,780, we assessed recruitment of an LXXLL peptide in a mammalian two-hybrid assay (72). As expected, the α/βI peptide was recruited to the wt receptor only in

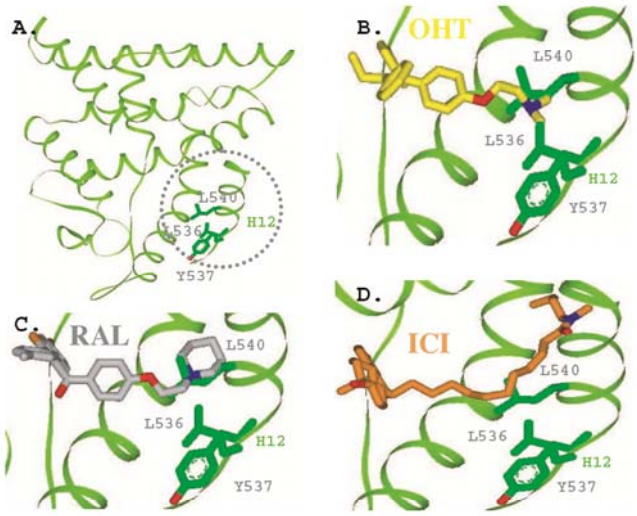

Fig. 6. Structural Constraints Exerted by the Side Chains of Antiestrogens on Positioning of H12 on Top of the Ligand Binding Pocket

The ERα-E2 complex (71) (A), was superimposed with that obtained in the presence of OHT (58) (B), Ral (57) (C) or ICI164,384 (59) (D) using the Lsq-man module of the O package. The side chain of Y537 does not result in steric hindrance with the antiestrogen side chains, whereas that of amino acid L536 or L540 result in steric clash with the side chain of OHT or Ral/ICI164,384 (ICI), respectively.

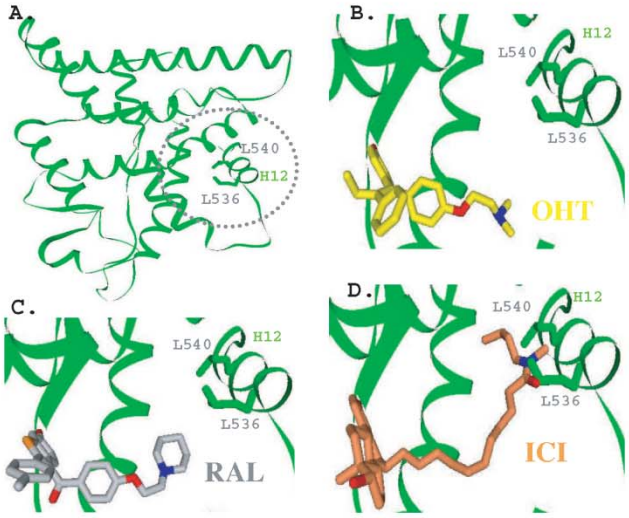

Fig. 7. Structural Constraints Exerted by the Side Chains of Antiestrogens on Positioning of H12 in the Coactivator Binding Groove

The structure of the ERα-OHT complex (58) (A and B) was superimposed with that obtained in the presence of Ral (57) (C) or ICI164,384 (59) (D) as in Fig. 6. The side chains of L536 and L540, which generate steric hindrance with the ICI164,384 (ICI) side chain, are shown.

the absence of ligand or the presence of E2, but not in the presence of any antiestrogen (Fig. 8). Recruitment in the presence of E2 was not drastically affected by the L536A, Y537A and L541A mutants, all of which transactivated an ERE3-TATA-Luc reporter vector at least as well as the wt receptor. Decreased E2-dependent recruitment was observed with the mutants affecting amino acids 539, 540, 543, and 544, which are known to be involved in stabilization of H12 in the agonist position and/or in interactions with the coactivator LXXLL motif (57, 58). This effect is consistent with the decrease in transactivation capacity observed with these mutants (Fig. 4). No recruitment of the LXXLL peptide was observed in the presence of either Ral or ICI182,780 with any of the mutants that had increased transcriptional activity with these antiestrogens, *i.e.* L536A, L539A, L540A, M543A, and L544A (Fig. 8). Similar results were obtained using a bioluminescence resonance energy transfer assay (data not shown). These observations indicate that the conformation of ERα mutants with increased agonist activity in the presence of Ral or ICI182,780 does not result in detectable AF-2 activity in this assay and suggest involvement of additional functional determinants in the observed gains in transcriptional activity.

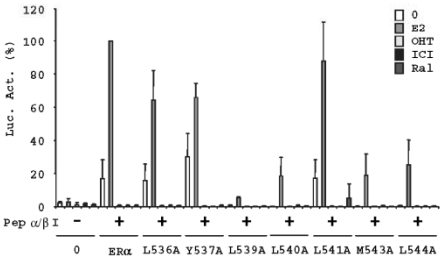

Fig. 8. Lack of Detectable Recruitment of an LXXLL Motif by Receptor Mutants with Increased Transcriptional Activity in the Presence of Ral or ICI182,780

HeLa cells were electroporated with the 5×GAL4-TATA-Luc reporter, the internal control plasmid CMV-β-gal, and expression vectors for the GAL4-pep α/β I fusion protein and for full-length wt ERα or mutants of H12 fused to VP16. Cells were treated with hormones and harvested as described in Fig. 1. Relative luciferase activity is shown. Luc.Act., Luciferase activity; Pep, peptide.

Because transcriptional activity in the presence of the partial antiestrogen OHT has been correlated with activity of the AF-1 region (38, 39), we have assessed whether this is also the case for activity of ERα mutants in the presence of full antiestrogens. In HepG2 cells, removal of the AF-1-containing AB region (ΔAB construct) practically inactivates the wt receptor, with residual activity detectable only in the presence of E2 on the minimal ERE3-TATA promoter. This is likely due to the loss of cooperativity between AF-1 and AF-2 for

coactivator recruitment (73). Transactivation in the presence of E2, but not in the presence of OHT, can be rescued by cotransfection of the core domain of coactivator TIF2 [transcriptional intermediary factor 2 (core domain TIF2.1)], member of the p160 family of coactivators (74, 75). Removal of the AF-1 activation function in mutant L536A, which displays increased levels of transcriptional activity in the presence of both ICI182,780 and Ral as well as in the absence of ligand, also led to loss of detectable activity in the presence of all ligands except for residual transcription in the presence of E2 (Fig. 9). Although TIF2.1 expression could restore activity in the presence of E2 and the absence of ligand, it did not enhance the activity of the truncated receptor ΔAB/L536A in the presence of OHT, ICI182,780, or Ral. Overexpression of the full-length steroid receptor coactivator 1 (SRC1), another member of the p160 family, also led to a partial rescue of activity in the presence of E2 or the absence of ligand, but failed to rescue activity in the presence of antiestrogens (data not shown). Similar results were obtained with ΔAB/L539A (data not shown). Together, these results strongly suggest that the AF-1 region is required for cofactor recruitment mediating the agonist activity of Ral and ICI182,780 with mutant receptors as well as for that of OHT with the wt receptor.

Mutations L536A and L539A Lead to a Selective Local Stabilization of the Receptor LBD in the Presence of Antiestrogens

To better investigate the molecular basis of the increase in ERα activity in the presence of antiestrogens resulting from mutations in long hydrophobic amino acids of H12, we examined regional LBD dynamics in two of these mutants, L536A and L539A, using a fluorescence polarization assay. By attaching an appropriate fluorophore, such as tetramethylrhodamine-5-maleimide, site-specifically at C530, we were able to develop a sensitive method for evaluating, in a rapid and quantitative manner, distinctive changes in the regional dynamics of the ERα LBD induced by the binding of ligands of a different pharmacological nature (76). Indeed, C530 is part of H11 in the LBD of ERα complexed to E2, but the alternative positioning of H12 induced by antiestrogens results in a different degree of helicity at this position, H11 terminating at position 530 in the presence of E_2, 529 for ICI182,780, 528 for Ral, and 526 for OHT. In the case of OHT or Ral, which have the shortest H11, this partial unwinding of H11 is necessary to allow repositioning of H12 in the coactivator binding groove (57, 58). The fluorescence signal shows higher anisotropy values when the local protein environment is rigid or α-helical (as in the agonist or ICI182,780 complexes) and lower anisotropy values when it is more dynamic or in a loop structure (as in the OHT complex).

As reported previously and also shown in Fig. 10, there are very significant differences ($P < 0.001$) between the anisotropy value of wt ERα complexed with E2 and the values with the Ral and OHT complexes, reflecting differences in the local conformation in the C530 region for these complexes (76). Interestingly, whereas the anisotropy values for unliganded and E2-bound L536A and L539A mutants were not markedly different from those of wt ERα, these mutations had a large effect on the anisotropy of the OHT, ICI182,780, and Ral complexes compared with those with wt ERα ($P < 0.001$). The anisotropy values for the Ral and ICI182,780 complexes with these mutants rise to the point that they are comparable to or greater than those of the corresponding E2-bound complexes, respectively; the anisotropy values for the two ERα mutants bound to OHT also increased significantly ($P < 0.01$). Thus, the mutational changes in L536A and L539A reduced conformational mobility of the C530 position

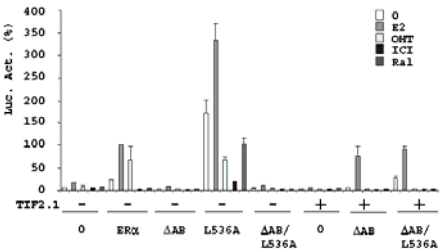

Fig. 9. Transcriptional Activity of ERα in the Presence of Ral or ICI182,780 Requires AF-1 Activity

Transient transfection analysis of the transcriptional activity of the wt ERα, or the mutant L536A and of derivatives thereof carrying deletions of the AB region in the presence or not of overexpressed TIF2.1 (4 μg) was performed as in Fig. 1. Relative luciferase activity is shown. Luc. Act., Luciferase activity.

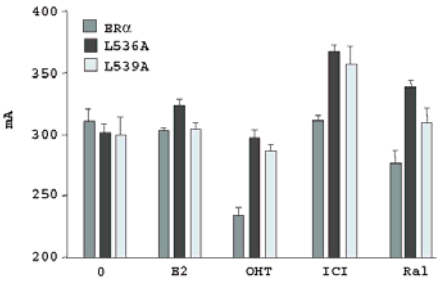

Fig. 10. Mutations L536A and L539A Selectively Stabilize Receptor Conformation in the Vicinity of C530 in the Presence of Antiestrogens

The ligand-induced regional dynamics of the LBDs of wt ERα, or of the L536A or L539A mutants were determined through fluorescence anisotropy assays (mA = anisotropy × 1000). Each fluorescence anisotropy value represents the mean ± SEM obtained from four independent experiments. ICI, ICI182,780.

considerably in the presence of all three antiestrogens, consistent with a more agonist-like conformation, although the conformational dynamics of each complex remained different.

ICI182,780 and Ral Induce Increases in Bioluminescence Resonance Energy Transfer between wt, but Not H12 Mutant Receptors in Live HepG2 Cells

To assess whether the different properties of the receptor in the presence of ICI182,780 and Ral *vs.* other ligands could be detected *in vivo* as well as through differential extraction or *in vitro* assays, we constructed fusion proteins between wt or mutant receptors and either *Renilla* luciferase or yellow fluorescent protein (YFP) and performed bioluminescence resonance energy transfer (BRET) assays between two wt or mutant ER monomers to determine whether antiestrogens affected receptor association and/or conformation. Titration curves performed with varying concentrations of the YFP fusion protein indicated a saturable autoassociation of the receptor in the presence of estradiol, ICI182,780, or Ral, with apparent affinities that were comparable for ICI182,780 and E2, and slightly lower for Ral (Fig. 11A; compare the slopes of the linear parts of the curves). These results indicate that the two antiestrogens do not have a destabilizing effect on the whole LBD structure. However, the maxima reached in the presence of the two antiestrogens were much higher than with E2 (Fig. 11A) or vehicle (data not shown; see also Fig. 11B), indicating a more efficient transfer of energy at saturation. Of interest, OHT did not induce an increase in energy transfer between wt receptors, and ICI182,780 or Ral did not increase energy transfer between mutant receptors that have increased solubility in the presence of these antiestrogens (Fig. 11B). These results suggest that the differential properties of antiestrogens in this BRET assay are linked to their different effects on receptor extractability. The increased energy transfer observed between wt but not mutant receptors could reflect a different conformation of the receptors bringing the YFP and luciferase moieties in closer proximity, and/or a higher local concentration of receptors, allowing exchange between one luciferase and several YFP molecules.

Mutations in H12 Increase Intranuclear Mobility of ERα in the Presence of ICI182,780 and Ral

It has previously been observed that the full antiestrogen ICI182,780 reduces the intranuclear mobility of ERα in transiently transfected HeLa cells (51). Because we also observe insolubility of ERα in HSB buffer in ICI182,780-treated HeLa cells (data not shown), we assessed whether insolubility of the receptor in HepG2 cells in the presence of ICI182,780 or Ral correlates with lower receptor mobility. FRAP experiments were performed with HepG2 cells transiently transfected

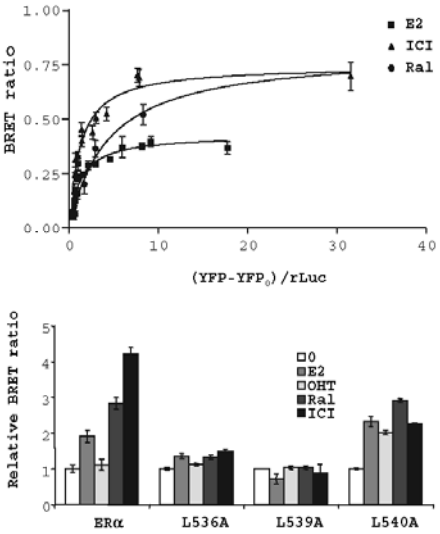

Fig. 11. Mutations Increasing ERα Solubility in the Presence of ICI182,780 or Ral Prevent Induction by These Antiestrogens of BRET between ER Monomers

HEK293 cells were transfected by expression vectors for fusion proteins between wt or mutant ERα and C-terminally fused rLuc or YFP proteins and treated for 40 min with different ligands. BRET ratios were calculated as described in *Materials and Methods*. A, Energy transfer between wt ERα monomers was measured using increasing concentrations of ERα-YFP fusion protein in the presence of E2, ICI182,780, or Ral. The x-axis value represents the ratio of ER-YFP fusion protein to ER-Luc fusion proteins, calculated as described in *Materials and Methods*. B, Effect of mutations in long hydrophobic amino acids of H12 on BRET ratios at saturating ratios of YFP *vs.* rLuc (*Renilla* luciferase) fusion proteins.

with an expression vector for the wt receptor fused to yellow fluorescent protein (YFP). The results indicate that treatment of cells with ICI182,780 or Ral prevents recovery of the fluorescence in the bleached zone over the course of the experiment (210 sec), with only a small fraction of the fluorescence being reconstituted (Fig. 12, *middle* and *bottom panels*). In contrast, fluorescence is nearly completely recovered with the unliganded receptor (Fig. 12, *top panel*). These observations are consistent with the immobilization of the receptor observed in HeLa cells in the presence of ICI182,780 and extend these observations to another cell context and to Ral.

To determine the impact of mutations in H12 on receptor mobility, we measured fluorescence recovery after bleaching in cells expressing fusion proteins with mutants L536A, L539A, and L540A (Fig. 12, *middle* and *bottom panels*). Note that mutations in long hydrophobic amino acids of H12 did not alter the nuclear distribution of the receptor in the presence of anties-

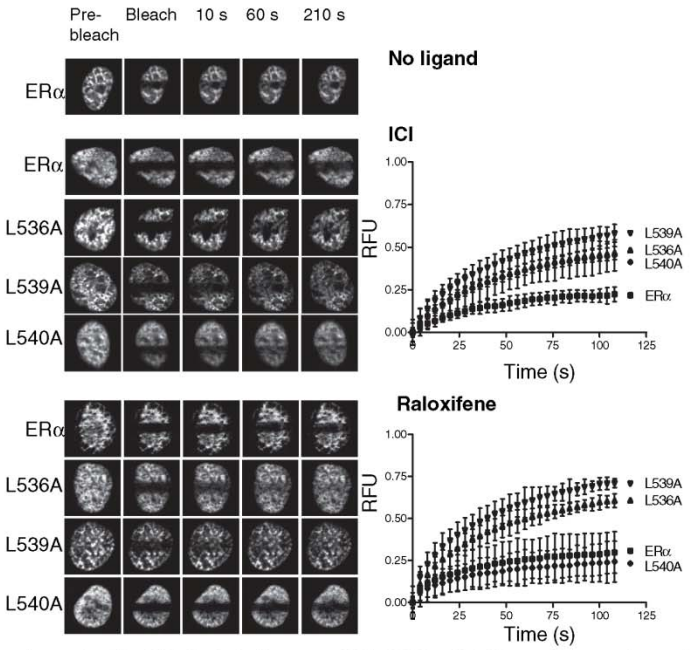

Fig. 12. Mutations Increasing ERα Solubility in the Presence of ICI182,780 or Ral Enhance Receptor Intranuclear Mobility

HepG2 cells transiently transfected with expression vectors for wt or mutant ERα fused to YFP were treated with vehicle or ligands for 16 h. A single region of interest was bleached with an Ar 488 laser. Images were captured at time intervals of 4 sec and analyzed for fluorescence intensities in the region of interest and in the whole cell by Meta Imaging Series 6.1 software. Fluorescence is represented in RFUs where 0 is the fluorescence after bleaching (time 0) and 1.00 is the expected fluorescence at homogeneity. *Error bars* represent the SD between three independent measurements. s, Seconds.

trogens ICI182,780 or Ral (data not shown). Strikingly, all mutations led to an increase in the fraction of the receptor that is mobile in the presence of ICI182,780. In addition, mutations L536A and L539A, but not L540A, similarly increased mobility of the Ral-bound receptor. These results correlate well with the gains in receptor solubility in HSB extracts and of transcriptional activity of all mutants in the presence of ICI182,780, as well as of mutants L536A and L539A, but not L540A, with Ral. Together, these observations suggest that activity of the receptor in the presence of these antiestrogens is limited by its stable association with a nuclear component that results in poor extractability in HSB.

DISCUSSION

Our goals in this study were to analyze the molecular basis of the more complete transcriptional repression of ERα by the antiestrogens Ral and ICI182,780 than by OHT in cell line models. Our results show that despite the similar structures of the receptor LBD in the presence of OHT and Ral (57, 58), Ral, like ICI182,780, leads to a marked reduction in the levels of ERα extractable in HSB in HepG2 cells. These observations are not specific to HepG2 cells, as receptor levels in the presence of Ral were also intermediate between those observed with OHT and full antiestrogens in transfected HeLa and human embryonic kidney HEK293 cells (data not shown) or in native MCF7 cells. In HepG2 cells, the observed reduction in receptor levels in HSB extracts in the presence of Ral or ICI182,780 did not correspond to a proteasome-mediated degradation of ERα as described for full antiestrogen ICI182,780 in MCF7 cells (47–49), but to insolubility in HSB. In MCF7 cells, accumulation of the endogenous receptor in an insoluble fraction in the presence of ICI182,780 was also observed in the presence of the proteasome inhibitor MG132, consistent with previous observations (49). In addition, the wt receptor was insoluble in HSB extracts when stably expressed in MDA-MB-231 cells at levels similar to those of the endogenous receptor in MCF7 cells, dem-

onstrating that receptor insolubility is not due to expression of large amounts of receptor.

Previous reports have described accumulation of ERα in aggregates in the cytoplasm of transfected COS cells (45, 50) and suggested that this was due to lack of nuclear import of the receptor (50). However, ERα remained nuclear in the vast majority of HepG2 cells in the presence of ICI182,780 or Ral. In addition, a large fraction of the receptor was immobile in the presence of Ral or ICI182,780 in FRAP experiments in HepG2 cells, contrasting with the near total mobility of unliganded receptors. Thus, it appears that not only degradation but also tighter association with a nuclear compartment can account for the reduced levels of receptor in HSB extracts in the presence of full antiestrogens or Ral.

Taken together, these observations suggest that the dramatically reduced transcriptional activity of ERα in the presence of Ral *vs.* OHT in HepG2 cells results from much lower levels of functional nuclear receptors even in the absence of degradation or relocalization to the cytosol. In support of this hypothesis, our results indicate that all H12 mutants with increased agonist activity in the presence of Ral had increased solubility in HSB in HepG2 cells. The same correlation was established in the presence of ICI182,780. Similar results were obtained in transiently transfected HeLa cells, although transcriptional activity in the presence of all antiestrogens was weaker in HeLa cells (data not shown). Note also that gains in transcriptional activation were not limited to our synthetic reporter vector, because increased transcription of the endogenous estrogen target gene TFF1 in the presence of Ral or ICI182,780 was observed in MDA-MB-231 cells stably transfected with the L539A mutant. Together, these results suggest that the decreased concentration of high-salt extractable receptor contributes to the transcriptional inhibition observed in HepG2 cells in the presence of either Ral or of ICI182,780. The increase in the fraction of mobile receptors observed in FRAP experiments with mutant receptors that have increased solubility and transcriptional activity further suggests that immobilization of the receptor is due to tighter interaction with a nuclear component responsible for poor extraction in HSB and inactivity of the receptor.

The observation that Ral and ICI182,780 share functional properties in this experimental system may seem surprising in view of the fact that the crystal structure of Ral resembles closely that obtained with OHT, with H12 positioned in both cases in the coactivator binding groove (57, 58), whereas H12 is unresolved in the crystal structure of rat ERβ with the full antiestrogen ICI164,384 (59), a close relative of ICI182,780 (35, 36). Note, however, that H12 is also highly disordered in Ral-bound rat ERβ (77). Furthermore, crystal structures may trap H12 in one of several possible conformations, as suggested by the observation that H12 can be found in the coactivator binding groove, even in the presence of agonists in a transcriptionally active ERα LBD mutant (78), or in the rat ERβ LBD in the presence of the partial agonist genistein (77). Thus, Ral and OHT have differential effects on conformational equilibrium of H12 in solution and potentially also play different roles in the conformational stabilization of the whole ER LBD observed with agonists (79).

Lack of stable association of H12 with the LBD in the presence of antiestrogens may play an important role in accumulation of ERα in an insoluble fraction and/or in its degradation. Receptors with unstable H12 would expose hydrophobic regions to the surface of the protein, such as the hydrophobic face of H12 itself or the coactivator binding groove, which is normally protected by protein-protein interactions with coactivators or H12. While this article was in preparation, Wu *et al.* (80) published the structure of the ERα LBD complexed to the antiestrogen GW5638, which induces degradation of the receptor. This study concluded that binding of GW5638 leads to increased exposure of hydrophobic regions and that reducing surface hydrophobicity of H12 by the combined mutation of three hydrophobic amino acids (leucines 536, 539, and 540) to glutamine residues stabilized the receptor. Accumulation of the receptor in an insoluble fraction in HepG2 cells in the presence of Ral or ICI182,780 may also be caused by increased exposure of hydrophobic regions, because mutations reducing the hydrophobic character of H12 were found to restore receptor levels in the HSB fraction. Nonetheless, our results indicate that replacement of two other H12 hydrophobic residues (Y537 and L541) had little effect. This observation together with the differential effect of mutations on receptor solubility/activity in the presence of Ral *vs.* ICI182,780 demonstrates the importance of specific hydrophobic amino acids rather than of global H12 hydrophobicity.

Our modeling studies from available crystal structures indicate that the side chains of Ral and ICI164,384 create steric clashes with H12 in the agonist or antagonist position at the level of amino acids L536 (ICI164,384 with H12 in the coactivator binding groove), L540 (Ral and ICI164,384 with H12 in the agonist position and ICI164,384 with H12 in the coactivator binding groove), and M543 (ICI164,384 with H12 in the agonist position). Of interest, the capacity of mutation L540 to relieve local steric hindrance with the side chain of ICI182,780, but not Ral, correlates with gains in receptor solubility/activity only in the presence of ICI182,780. Mutation of residues not directly involved in steric clashes with the antiestrogen side chain may also increase space available for rearrangement of the antiestrogen side chain or of neighboring bulky amino acids. In addition, L544 points toward the Ral backbone in the ligand binding cavity when H12 is in the agonist position, and its mutation may allow for a better accommodation of Ral, which is bulkier than steroid derivatives or OHT in this region. Overall, replacement of long hydrophobic amino acids of H12 by alanine residues may facilitate burial of the hydropho-

bic side of H12 by reducing structural constraints due to the antiestrogen side chains in a residue- and ligand-specific manner. It is also possible, however, that specific hydrophobic amino acids of H12 mediate recognition of uncharacterized protein(s) important for accumulation of the receptor in an insoluble form.

Although increasing solubility of the receptor in the presence of ICI182,780 or Ral correlates with partial agonist activity in HepG2 cells, it is not necessarily sufficient because levels of pS2/TFF1 transcriptional activity were low in the presence of OHT with wt ERα in spite of high levels of soluble receptor. Also, complete deletion of H12 increased solubility in the presence of either ICI182,780 or Ral but, contrary to single mutations in long hydrophobic residues, did not lead to significant gains of transcriptional activity with the minimal ERE3-TATA promoter used in this study (data not shown). Similarly, the double mutation L539–540A was very weakly active under our experimental conditions, although soluble receptor levels were increased in the presence of ICI182,780 or Ral (data not shown). Activity of the latter mutant with ICI164,384 or ICI182,780 has been reported in HepG2 cells cotransfected with the glucocorticoid receptor interacting protein 1 (GRIP1) coactivator or in COS-1 cells with an ERE-tk-CAT reporter vector (60, 62), suggesting promoter and cell specificity in transcriptional activity of this mutant in the presence of antiestrogens. Transcriptional activity in the presence of antiestrogens appears thus to require additional functional determinants compared with those responsible for receptor solubility.

We found that the presence of the AF-1 region was important for partial transcriptional activity, both of the wt receptor with OHT and of stabilized mutant receptors with Ral or ICI182,780. We did not observe recruitment of LXXLL motifs in a two-hybrid assay, suggestive of an inactive AF-2 function, either with OHT-bound wt receptor or with mutants with increased activity in the presence of Ral or ICI182,780. Nevertheless, we cannot exclude that antiestrogens allow weak AF-2 activity, requiring cooperativity with AF-1 to be detected. Alternatively, the LBD surface formed in the presence of partial antiestrogens, or of full antiestrogens in permissive ERα mutants, may recruit specific coactivators through different motifs. Finally, recruitment of corepressors, leading to suppression of AF-1 activity, may be affected in a differential manner depending on effects of ligands or mutations on LBD conformation. Corepressor recruitment was found to be stronger with ICI182,780 and Ral than with OHT (43). Corepressor interaction with the LBD involves amino acids buried by H12 both in the agonist (on top of the ligand cavity) or antagonist (in the coactivator binding groove) positions (81), and thus mutations increasing association of H12 in either position would be expected to reduce corepressor recruitment.

Fluorescence anisotropy data measuring conformational flexibility in the vicinity of C530 indicate that the antiestrogen-bound L536A/L539A ERα-LBDs showed significantly higher anisotropy values ($P < 0.01$) than their corresponding wt ERα complexes, reaching values even greater than that of the ERα-E2 complex for some complexes. This may result from an increased degree of α-helicity of the end of H11 and/or from conformational stabilization of this region of the LBD. We speculate that this effect may result from facilitated positioning of H12 in a manner that decreases receptor insolubility in the presence of ICI182,780 or Ral and opens up the LBD surface for interactions with coactivators or with the AF-1 transcriptional activation function, or inhibits recruitment of corepressors in the ERα-antagonist complexes. In addition, the higher levels of bioluminescence energy transfer obtained in the presence of Ral or ICI182,780 in live HEK293 cells is compatible with a different conformation of the C-terminal end of the receptors, although it could also directly reflect a higher local concentration of receptors within multimers or aggregates. However, the similar association rates of the receptor in the presence of the antiestrogens or of E2 indicates that conformational alterations are likely local and do not affect the whole LBD.

In conclusion, results presented in this paper demonstrate that both Ral and ICI182,780 induce tighter association of the receptor with a nuclear compartment in HepG2 cells, that long hydrophobic amino acids of LBD H12 play a role in decreasing receptor mobility, extractability, and activity in an antiestrogen-specific manner, likely through differences in local conformation of the receptor LBD, without affecting some of its properties such as dimerization efficiency. Future experiments will be required to characterize the molecular interactions underlying the tighter association of the receptor with the nuclear compartment. While this article was under preparation, ICI182,780-specific interaction between ERα and cytokeratins 8 and 18 has been described, but this interaction appears to mediate receptor degradation rather than insolubility because the latter takes place in CK8-CK18-negative HeLa cells (82). Mutant receptors characterized here will be useful to identify proteins playing a role in receptor association with the nuclear compartment in the presence of Ral or ICI182,780, on the basis of their interaction with wt but not mutant receptors. Characterizing the patterns of mutant receptor association with corepressors should also clarify the respective roles of corepressor recruitment and association with a nuclear compartment in the full antagonist activity of antiestrogens.

MATERIALS AND METHODS

Plasmids and Reagents

E2 and OHT were purchased from Sigma (Sigma, Oakville, Ontario, Canada); ICI182,780 and Ral were purchased from Tocris Cookson Ltd. (Ellisville, MO) and Sigma, respectively.

Radioactive E2 ([^{3}H]E_2, 54 Ci/mmol) was from Amersham Pharmacia Biotech (Piscataway, NJ) and tetramethylrhodamine-5-maleimide (MTMR) from Molecular Probes (Eugene, OR). MG132 was purchased from EMD Biosciences (La Jolla, CA). pSG5-ERα and pSG5-HEG19 (ER$\alpha\Delta$AB) and pSG5-TIF2.1 were kind gifts from Professor P. Chambon (38, 83). Mutations at positions 531, 536, 537, 539, 540, 541, 543, and 544 were introduced by site-directed mutagenesis using PCR amplification of the ERα cDNA (the sequence of oligonucleotides used for mutagenesis is available upon request). Expression plasmids for ERα mutants were generated by subcloning the digested PCR fragments into the pSG5-ERα expression vector (792-bp *Hin*dIII/*Bam*HI fragment). Clones for each mutant were characterized by restriction digest and sequencing. The ΔAB/L536A mutant was generated by subcloning a 834-bp *Xba*I fragment from pSG5-L536A into the pSG5-ER$\alpha\Delta$AB expression vector. Vectors pVP16-ERα, pM-peptide α/βI, and 5$\times$ GAL4-TATA-Luc were generous gifts from Dr. D. P. McDonnell (72). Mutations L536A, L539A, L540A, L541A, M543A, and L544A were introduced in the pVP16-ERα by exchanging a 1611-bp *Not*I-*Bam*HI fragment. The pcDNA3-Hygro (ERα) and (L539A) were generated by inserting 1819-bp *Eco*RI blunted fragments derived from pSG5-ERα and pSG5-L539A, respectively. To create pCMV-ERα-rLuc and mutant derivatives (L536A, Y537A, L539A, and L540A), the coding sequences of the receptors without the stop codons were amplified by PCR from the corresponding pSG5 expression vectors. The amplified cDNA fragments were then subcloned into the *Eco*RI and *Xho*I sites of pRL-CMV-rLuc (Promega BioSciences, San Luis Obispo, CA). The same approach was used to create pCMV-ERα(WT, L536A, Y537A, L539A, and L540A)-YFP using the pGFP-N1-Topaz vector (PerkinElmer Corp., Wellesley, MA) instead of pRL.

Cell Culture

HepG2 cells were maintained in DMEM supplemented with 10% fetal bovine serum (FBS), MCF7 cells in α-MEM supplemented with 10% FBS, and MDA-MB-231 cells in DMEM supplemented with 5% FBS. Three days before experiments, MDA-MB-231 cells were switched to phenol red-free DMEM containing 5% charcoal-stripped serum, whereas HepG2 and MCF7 cells were switched to phenol red-free DMEM containing 10% charcoal-stripped serum.

Stable clones in MDA-MB-231 cells were selected for in the presence of hygromycin (0.25 mg/ml; Invitrogen, Burlington, Ontario, Canada) following electroporation (0.25 kV, 975 μF in a Bio-Rad Gene Pulser II apparatus) with 5 μg pCDNA3-hygro, pCDNA3-hygro-ERα, or pCDNA3-hygro-L539A together with 35 μg carrier salmon sperm DNA (Invitrogen).

Luciferase Assays

For luciferase assays, electroporation was carried out (Bio-Rad Gene Pulser II apparatus; Bio-Rad Laboratories, Hercules, CA) in HepG2 cells (0.24 kV, 950 μF) or in MDA-MB-231 cells (0.25 kV, 975 μF). Cells were plated in six-well plates (8×10^5 cells per well for HepG2 cells, 1×10^6 cells per well for MDA-MB-231 cells). Typically, DNA mixes contained 1 μg expression vector, 2 μg ERE3-TATA-Luc reporter vector, 2 μg internal control pCMV-βGal, and 35 μg carrier salmon sperm DNA (Invitrogen); in addition, 4 μg of the pSG5-TIF2.1 vector was used in experiments described in Fig. 8. E2 (25 nM), OHT (100 nM), ICI182,780 (100 nM), or Ral (100 nM) or vehicle (ethanol) were added immediately after electroporation. Cells were harvested 48 h later in lysis buffer (100 mM Tris-HCl, pH 7.9; 0.5% Nonidet P-40, 1 mM dithiothreitol). For proteasome inhibition, HepG2 cells were pretreated for 1 h with MG132 (10 μM) the day after transfection and subsequently treated with E2 (25 nM), OHT (100 nM), ICI182,780 (100 nM) or Ral (100 nM) for 6 h. Luciferase activity was measured in the presence of luciferin with a Fusion Universal Microplate Analyser (PerkinElmer, Woodbridge, Ontario, Canada) and was normalized for β-galactosidase activity, measured at 420 nm with a Spectramax 190 plate reader (Molecular Devices, Sunnyvale, CA). Each transfection was carried out in triplicate and repeated at least three times. Statistical analysis was performed using Student's *t* test analysis.

Two-Hybrid Assays

HeLa cells were electroporated (0.24 kV, 950 μF in a Bio-Rad Gene Pulser II apparatus) and plated in six-well plates (8×10^5 cells per well). The DNA mix contained 1 μg of the expression vector for the Gal4-pep α/β I fusion protein, 1 μg expression vector for full-length wt ERα or mutants of H12 fused to VP16, 1 μg 5$\times$ GAL4-TATA-Luc reporter, 1 μg internal control plasmid CMV-β-gal, and 36 μg carrier salmon sperm DNA (Invitrogen). E2 (25 nM), OHT (100 nM), ICI182,780 (100 nM) or Ral (100 nM) or vehicle (ethanol) was added immediately after electroporation. Cells were harvested 48 h later in lysis buffer (100 mM Tris-HCl, pH 7.9; 0.5% Nonidet P-40; 1 mM dithiothreitol). Luciferase activity was measured and normalized for β-galactosidase activity as described above. All transfections were carried out in triplicate and performed a minimum of three times.

RT-PCR Assays of Receptor and TFF1 Expression Levels

Stable clones of MDA-MB-231 cells carrying the empty pCDNA3-hygro vector (0, clone 10A), or expressing the wt ERα (clone 22A) or mutant L539A (clone 4A) were kept in white DMEM supplemented with 5% treated-FBS for 72 h. Twenty four hours after plating (5×10^6 cells per 10-cm petri dish), cells were treated with vehicle, E2 (25 nM), OHT (100 nM), ICI182,780 (100 nM), or Ral (100 nM) for 48 h. RNA was extracted using TRIzol (GIBCO, from Invitrogen) according to the manufacturer's instructions. After quantification (Spectramax; Molecular Devices, Sunnyvale, CA), cDNAs were generated using 2 μg of RNA and the RevertAid H minus direct strand cDNA synthesis kit with M-MuLV reverse transcriptase (Fermentas; Burlington, Ontario, Canada).

Quantitative PCR

For quantitative PCR amplification of reverse transcribed mRNAs, the following specific oligonucleotides were used

TFF1: 5′-ACCATGGAGAACAAGGTGAT-3′, 3′-AAATTCA CACTCCTCTTCTG-5′;

p36B4: 5′-TGAAGTCACTGTGCCAGCCCA-3′, 3′-AGAAG GGGGAGATGTTGAGCA-5′

The reaction mix contained 250 nM of primers, 1/100th of the RT-PCR, Jump Start Taq DNA polymerase (Sigma, St. Louis, MO), 0.625$\times$ SybrGreen solution (Molecular Probes, from Invitrogen), 0.4 mM NTP, and $MgCl_2$ (4.0 mM for TFF1, 4.5 mM for p36B4). Samples were run on a Rotor-Gene Q-PCR machine (Corbett Research, Sydney, Australia). Similar results were obtained with three independent mRNA preparations.

Western Analysis of Receptor Levels

For Western blotting, HepG2 cells were transiently transfected by electroporation (5×10^6 cells) with 10 μg of pSG5 expression vectors containing wt or mutant ERα cDNAs and 30 μg carrier salmon sperm DNA (Invitrogen), and were plated in 10-cm plates. Stable clones derived from MDA-MB-231 cells (2.5×10^6 cells) or transfected HepG2 cells were treated with E2 (25 nM), OHT (100 nM), ICI182,780 (100 nM), Ral (100 nM) or vehicle overnight before protein extraction.

Cells were harvested in ice-cold PBS, and whole-cell extracts were prepared from half the cells by three freeze-thaw cycles in HSB as previously described (84). The other half of cells harvested was resuspended in Laemmli sample buffer (85) and incubated at 100 C for 5 min.

For western blotting of endogenous ERα in MCF7 cells, cells were plated in six-well plates (5×10^5 cells per well). The following day, cells were pretreated for 1 h with MG132 (10 μM) or vehicle (dimethylsulfoxide). E2 (25 nM), OHT (100 nM), ICI182,780 (100 nM), or Ral (100 nM) were then added for 16 h. Cells were harvested in ice-cold PBS, and whole-cell extracts were prepared as described for HepG2 cells or by resuspension in Laemmli sample buffer and incubation at 100 C for 5 min.

Whole-cell extracts from ERα-expressing cells were analyzed by electrophoresis on a sodium dodecyl sulfate-polyacrylamide gel (7.5% acrylamide) and transferred onto nitrocellulose. Membranes were incubated with an anti-ERα mouse monoclonal antibody (B10, kind gift from Professor P. Chambon). Complexes were revealed by enhanced chemiluminescence (PerkinElmer Corp.) as recommended by the manufacturer.

Confocal Fluorescence Microscopy and FRAP Analyses

HepG2 cells were plated on 35-mm γ-irradiated Corning Petri dishes (MaTek, Ashland, MA) at a density of 3000 cells/cm^2 in 2 ml white DMEM supplemented with 10% FBS and 1% penicillin/streptomycin. After 2 d, cells were transfected with wt or mutant ERα and treated 24 h later with vehicle or ligands (E2, 2.5×10^{-5} M; OHT, ICI182,780, or Ral, 10^{-7} M) for an additional 16 h. Petri dishes were washed twice with PBS and fixed with PBS 3% paraformaldehyde for 15 min. After fixation, cells were permeabilized and blocked with PBS containing 0.2% BSA and 0.3% Triton X-100 for 10 min at room temperature. The antibody against ERα (B10, a kind gift from Professor Pierre Chambon, Strasbourg, France) and the Alexa Fluor 595 dye-labeled secondary antibody (Invitrogen) were diluted 1:800 and 1:2000, respectively, in PBS-0.2% BSA. Nuclei were stained for 5 min with 50 ng/ml Hoechst 33342 (Sigma) in PBS-0.2% BSA. Petri dishes were washed twice with PBS and once with water and were mounted using ProLong Gold antifade reagent (Invitrogen). Cells were visualized using a laser scanning microscopy (LSM) 510 META ^{MK4} confocal microscope (Carl Zeiss, Jena, Germany). Images were analyzed using LSM 3.2 software.

FRAP analysis was performed on HepG2 cells transiently transfected with expression vectors for wt or mutant ERα fused to YFP. Cells were treated as described above, except that a single region of interest (ROI) of about 25% of the nuclear volume was bleached using an Ar 488-nm laser at maximum power for 200 iterations. Emission corresponding to YFP fluorescence was captured at time intervals of 4 sec using a 505-nm LP (long pass) filter and a PMT (photomultiplicator) detector. LSM images were exported as 12 bit TIF files (256 × 256 pixels), and fluorescence intensities in the ROI and the whole cell were quantified by Meta Imaging Series 6.1. Data were analyzed using Prism Graph Pad (GraphPad Software, Inc., San Diego, CA). Fluorescence is represented in relative fluorescence units (RFU) where 0 is the fluorescence after photobleaching (time 0) and 1.00 is the expected fluorescence at homogeneity taking into account the total loss of fluorescence in the cell after photobleaching according to the formula

$$RFU = \frac{(Z_i - Z_0)/Z_{0i}}{(C_i - C_0)/C_{0i}}$$

where Z_i is the average intensity in the ROI at time i, Z_0 the average intensity after bleaching in the ROI, Z_{0i} the intensity before bleaching in the ROI, C_i the average intensity in the whole cell, C_0 the estimated fluorescence background obtained after bleaching of the whole cell, and C_{0i} the average intensity of the whole cell before bleaching. Only cells displaying low to medium fluorescence intensities were analyzed (at least six cells were analyzed for each treatment).

Modeling

To compare the structural effects of the various mutations on the agonist and antagonist conformations of ERα, the crystal structures of ERα complexed with E2 [protein database (PDB) code 1GWR (71)], OHT [PDB code 3ERT (58)], Ral [PDB code 1ERR (57)], and ICI164,384 [PDB code 1HJ1, (59)] were first superimposed using the Lsq-man module of the O package [version 6 (86)]. Mutations were introduced in each crystal structure using the O package.

Expression, Purification, and Site-Specific MTMR Labeling of ERα-LBD Constructs

The expression of wt ER-LBDα(303–554) containing the single reactive cysteine at position 530 (*C530* having C381S and C417S mutations) and the L536A and L539A ER-LBDα mutants in the *C530* background and their site-specific labeling with MTMR were performed as described previously (76).

Fluorescence Anisotropy Experiments

Fluorescent anisotropy analysis of the different ER-LBD constructs labeled with MTMR was performed essentially as described previously (76). Briefly, a sample of 2 nM MTMR-labeled wt or L536A or L539A mutant was incubated with 100 nM of the respective unlabeled LBDs in Tris-glycerol (pH 8.0) buffer containing 0.3 mg/ml chicken ovalbumin for 5–7 h at room temperature in the dark. Excess unlabeled LBD was added to minimize homo-FRET artifacts by ensuring, after dimer equilibration, that only one member of the LBD dimer contained the fluorophore (76). A 700-μl sample was placed in separate tubes, and 5 μl of vehicle (dimethylsulfoxide) or 700 μM ligand stock was added, resulting in 5 μM final ligand concentrations. After equilibration for 1 h at room temperature in the dark, samples were individually analyzed at 25 C in a Spex Fluorolog II (model IIIc) cuvette-based fluorometer, with an L-configuration polarization unit using Data Max 2.2 software (Spex Industries, Edison, NJ). Excitation was at 541 nm, and MTMR fluorescence anisotropy was monitored at 580 nm. Results were analyzed using Prism 3.00 (GraphPad Software). Each fluorescent anisotropy value represents the mean ± SEM obtained from four independent experiments. All significant differences have $P < 0.05$ by one-way ANOVA.

Bioluminescence Resonance Energy Transfer Assays

For BRET assays, HEK293 cells were plated in 10-cm dishes (2.5 million cells per dish) and transfected with ERα-RLuc (1 μg) and ERα-YFP (6 μg) by the calcium phosphate method. Cells were washed twice in PBS 48 h later and harvested with 1.5 ml of PBS-5 mM EDTA. containing E2 (25 nM), OHT (100 nM), ICI182,780 (100 nM), or vehicle (ethanol). Aliquots containing 100,000 cells were distributed in a 96-well microplate (white Optiplate, Packard Instruments), and cells were treated with vehicle (EtOH), 25 nM E2, 100 nM OHT, 100 nM Ral, or ICI182,780 (100 nM) for 40 min at room temperature. Coelenterazine (Sigma) was added to a final concentration of 5 μM, and readings were immediately collected on a Mithras LB 940 (Berthold Technologies, Bad Wildbad, Germany), with sequential integration of signals detected at 485 nm (*Renilla* luciferase emission) and 530 nm (YFP emission). The BRET ratio was defined as described in Ref. 87. ERα-YFP to ERα-Luc ratios were calculated for each amount of transfected ERα-YFP expression vector in the presence of a fixed amount of the ERα-rLuc vector as the total YFP signal measured by direct YFP stimulation [YFP] minus the basal signal from cells

transfected with only ERα-rLuc [YFP_0] divided by the rLuc signal [rLuc] in the cotransfected cells.

Acknowledgments

We thank Professor Pierre Chambon for the kind gift of anti-hERα B10 antibody and of hERα expression vectors and Dr. Donald McDonnell for the pVP16-ERα, pM-peptide α/βI, and 5× GAL4-TATA-Luc vectors. We are grateful to Dr. Genevieve Morinville for critical comments on the manuscript and Samuel Chagnon for excellent technical assistance.

Received February 10, 2006. Accepted February 5, 2007.

Address all correspondence and requests for reprints to: Sylvie Mader, Institute for Research in Immunology and Cancer, Université de Montréal, CP 6128 Succursale Centre-Ville, Montréal, Québec, Canada H3C 3J7. E-mail: sylvie.mader@umontreal.ca.

This work was supported by Grant IC1-70246 from the Cancer Institute of the Canadian Institutes for Health Research and Grant 017503 from the Canadian Breast Cancer Research Alliance (to S.M.) and from the National Institutes of Health (Grant PHS 5R37 DK15556 to J.A.K.). M. L. is recipient of an award from the Montréal Centre for Experimental Therapeutics in Cancer-Canadian Institutes for Health Research training program, and S.M. holds the Canadian Imperial Bank of Commerce Breast Cancer Research Chair at Université de Montréal.

None of the authors have anything to declare.

REFERENCES

1. Couse JF, Korach KS 1999 Estrogen receptor null mice: what have we learned and where will they lead us. Endocr Rev 20:358–417
2. McEwen BS, Alves SE 1999 Estrogen actions in the central nervous system. Endocr Rev 20:279–307
3. Jordan VC 2001 Estrogen, selective estrogen receptor modulation, and coronary heart disease: something or nothing. J Natl Canc Inst 93:2–4
4. Nilsson S, Makela S, Treuter E, Tujague M, Thomsen J, Andersson G, Enmark E, Pettersson K, Warner M, Gustafsson JA 2001 Mechanisms of estrogen action. Physiol Rev 81:1535–1565
5. Green S, Chambon P 1988 Nuclear receptors enhance our understanding of transcription regulation. Trends Genet 4:309–314
6. Beato M, Herrlich P, Schutz G 1995 Steroid hormone receptors: many actors in search of a plot. Cell 83:851–857
7. Mangelsdorf DJ, Thummel C, Beato M, Herrlich P, Schutz G, Umesono K, Blumberg B, Kastner P, Mark M, Chambon P, Evans, RM 1995 The nuclear receptor superfamily: the second decade. Cell 83:835–839
8. Chawla A, Repa JJ, Evans RM, Mangelsdorf DJ 2001 Nuclear receptors and lipid physiology: opening the X-files. Science 294:1866–1870
9. Robinson-Rechavi M, Escriva Garcia H, Laudet V 2003 The nuclear receptor superfamily. J Cell Sci 116:585–586
10. Pratt WB, Toft DO 1997 Steroid receptor interactions with heat shock protein and immunophilin chaperones. Endocr Rev 18:306–360
11. Ylikomi T, Wurtz JM, Syvala H, Passinen S, Pekki A, Haverinen M, Blauer M, Tuohimaa P, Gronemeyer H 1998 Reappraisal of the role of heat shock proteins as regulators of steroid receptor activity. Crit Rev Biochem Mol Biol 33:437–466
12. Burakov D, Crofts LA, Chang CP, Freedman LP 2002 Reciprocal recruitment of DRIP/mediator and p160 coactivator complexes in vivo by estrogen receptor. J Biol Chem 277:14359–14362
13. Shang Y, Hu X, DiRenzo J, Lazar MA, Brown M 2000 Cofactor dynamics and sufficiency in estrogen receptor-regulated transcription. Cell 103:843–852
14. Metivier R, Stark A, Flouriot G, Hubner MR, Brand H, Penot G, Manu D, Denger S, Reid G, Kos M, Russell RB, Kah O, Pakdel F, Gannon F 2002 A dynamic structural model for estrogen receptor-α activation by ligands, emphasizing the role of interactions between distant A and E domains. Mol Cell 10:1019–1032
15. Reid G, Hubner MR, Metivier R, Brand H, Denger S, Manu D, Beaudouin J, Ellenberg J, Gannon F 2003 Cyclic, proteasome-mediated turnover of unliganded and liganded ERα on responsive promoters is an integral feature of estrogen signaling. Mol Cell 11:695–707
16. Leo C, Chen JD 2000 The SRC family of nuclear receptor coactivators. Gene 245:1–11
17. Rosenfeld MG, Glass CK 2001 Coregulator codes of transcriptional regulation by nuclear receptors. J Biol Chem 276:36865–36868
18. Rachez C, Freedman LP 2001 Mediator complexes and transcription. Curr Opin Cell Biol 13:274–280
19. Dilworth FJ, Chambon P 2001 Nuclear receptors coordinate the activities of chromatin remodeling complexes and coactivators to facilitate initiation of transcription. Oncogene 20:3047–3054
20. McDonnell DP, Norris JD 2002 Connections and regulation of the human estrogen receptor. Science 296:1642–1644
21. Belandia B, Parker MG 2003 Nuclear receptors: a rendezvous for chromatin remodeling factors. Cell 114:277–280
22. Krust A, Green S, Argos P, Kumar V, Walter P, Bornert JM, Chambon P 1986 The chicken oestrogen receptor sequence: homology with v-erbA and the human oestrogen and glucocorticoid receptors. EMBO J 5:891–897
23. Mader S, Chambon P, White JH 1993 Defining a minimal estrogen receptor DNA binding domain. Nucleic Acids Res 21:1125–1132
24. Klein-Hitpass L, Schorpp M, Wagner U, Ryffel GU 1986 An estrogen-responsive element derived from the 5′ flanking region of the *Xenopus* vitellogenin A2 gene functions in transfected human cells. Cell 46:1053–1061
25. Klinge CM 2001 Estrogen receptor interaction with estrogen response elements. Nucleic Acids Res 29:2905–2919
26. Sanchez R, Nguyen D, Rocha W, White JH, Mader S 2002 Diversity in the mechanisms of gene regulation by estrogen receptors. Bioessays 24:244–254
27. Bourdeau V, Deschenes J, Metivier R, Nagai Y, Nguyen D, Bretschneider N, Gannon F, White JH, Mader S 2004 Genome-wide identification of high-affinity estrogen response elements in human and mouse. Mol Endocrinol 18:1411–1427
28. Leid M, Kastner P, Chambon P 1992 Multiplicity generates diversity in the retinoic acid signalling pathways. Trends Biochem Sci 17:427–433
29. Gustafsson J-A 1999 Estrogen receptor β—a new dimension in estrogen mechanism of action. J Endocrinol 163:379–383
30. Dunn BK, Ford LG 2001 From adjuvant therapy to breast cancer prevention: bcpt and star. Breast J 7:144–147
31. O'Regan RM, Jordan VC 2001 Chemoprevention of breast cancer. Cancer Treat Res 106:137–154
32. Jordan VC 2003 Tamoxifen: a most unlikely pioneering medicine. Nat Rev Drug Discov 2:205–213
33. Black LJ, Sato M, Rowley ER, Magee DE, Bekele A, Williams DC, Cullinan GJ, Bendele R, Kauffman RF, Bensch WR, Frolik CA, Termine JD, Bryant HU 1994 Raloxifene (LY139481 HCl) prevents bone loss and reduces serum cholesterol without causing uterine hypertrophy in ovariectomized rats. J Clin Invest 93:63–69

34. Grese TA, Sluka JP, Bryant HU, Cullinan GJ, Glasebrook AL, Jones CD, Matsumoto K, Palkowitz AD, Sato M, Termine JD, Winter MA, Yang NN, Dodge JA 1997 Molecular determinants of tissue selectivity in estrogen receptor modulators. Proc Natl Acad Sci USA 94: 14105–14110
35. Bowler J, Lilley TJ, Pittam JD, Wakeling AE 1989 Novel steroidal pure antiestrogens. Steroids 54:71–99
36. Wakeling AE, Dukes M, Bowler J 1991 A potent specific pure antiestrogen with clinical potential. Cancer Res 51: 3867–3873
37. Van de Velde P, Nique F, Bouchoux F, Bremaud J, Hameau MC, Lucas D, Moratille C, Viet S, Philibert D, Teutsch G 1994 RU 58,668, a new pure antiestrogen inducing a regression of human mammary carcinoma implanted in nude mice. J Steroid Biochem Mol Biol 48:187–196
38. Berry M, Metzger D, Chambon P 1990 Role of the two activating domains of the oestrogen receptor in the cell-type and promoter-context dependent agonistic activity of the anti-oestrogen 4-hydroxytamoxifen. EMBO J 9:2811–2818
39. Tzukerman MT, Esty A, Santiso-Mere D, Danielian P, Parker MG, Stein RB, Pike JW, McDonnell DP 1994 Human estrogen receptor transactivational capacity is determined by both cellular and promoter context and mediated by two functionally distinct intramolecular regions. Mol Endocrinol 8:21–30
40. Jackson TA, Richer JK, Bain DL, Takimoto GS, Tung L, Horwitz KB 1997 The partial agonist activity of antagonist-occupied steroid receptors is controlled by a novel hinge domain-binding coactivator L7/SPA and the corepressors N-CoR or SMRT. Mol Endocrinol 11:693–705
41. Smith CL, Nawaz Z, O'Malley BW 1997 Coactivator and corepressor regulation of the agonist/antagonist activity of the mixed antiestrogen, 4-hydroxytamoxifen. Mol Endocrinol 11:657–666
42. Keeton EK, Brown M 2005 Cell cycle progression stimulated by tamoxifen-bound estrogen receptor-α and promoter-specific effects in breast cancer cells deficient in N-CoR and SMRT. Mol Endocrinol 19:1543–1554
43. Webb P, Nguyen P, Kushner PJ 2003 Differential SERM effects on corepressor binding dictate ERα activity in vivo. J Biol Chem 278:6912–6920
44. Dauvois S, Danielian PS, White R, Parker MG 1992 Antiestrogen ICI 164,384 reduces cellular estrogen receptor content by increasing its turnover. Proc Natl Acad Sci USA 89:4037–4041
45. Devin-Leclerc J, Meng X, Delahaye F, Leclerc P, Baulieu EE, Catelli MG 1998 Interaction and dissociation by ligands of estrogen receptor and Hsp90: the antiestrogen RU 58668 induces a protein synthesis-dependent clustering of the receptor in the cytoplasm. Mol Endocrinol 12:842–854
46. Borras M, Laios I, el Khissiin A, Seo HS, Lempereur F, Legros N, Leclercq G 1996 Estrogenic and antiestrogenic regulation of the half-life of covalently labeled estrogen receptor in MCF-7 breast cancer cells. J Steroid Biochem Mol Biol 57:203–213
47. Nawaz Z, Lonard DM, Dennis AP, Smith CL, O'Malley BW 1999 Proteasome-dependent degradation of the human estrogen receptor. Proc Natl Acad Sci USA 96: 1858–1862
48. Wijayaratne AL, McDonnell DP 2001 The human estrogen receptor-α is a ubiquitinated protein whose stability is affected differentially by agonists, antagonists, and selective estrogen receptor modulators. J Biol Chem 276:35684–35692
49. Marsaud V, Gougelet A, Maillard S, Renoir JM 2003 Various phosphorylation pathways, depending on agonist and antagonist binding to endogenous estrogen receptor α (ERα), differentially affect ERα extractability, proteasome-mediated stability, and transcriptional activity in human breast cancer cells. Mol Endocrinol 17: 2013–2027
50. Dauvois S, White R, Parker MG 1993 The antiestrogen ICI 182780 disrupts estrogen receptor nucleocytoplasmic shuttling. J Cell Sci 106:1377–1388
51. Stenoien DL, Patel K, Mancini MG, Dutertre M, Smith CL, O'Malley BW, Mancini MA 2001 FRAP reveals that mobility of oestrogen receptor-α is ligand- and proteasome-dependent. Nat Cell Biol 3:15–23
52. Simard J, Sanchez R, Poirier D, Gauthier S, Singh SM, Merand Y, Belanger A, Labrie C, Labrie F 1997 Blockade of the stimulatory effect of estrogens, OH-tamoxifen, OH-toremifene, droloxifene, and raloxifene on alkaline phosphatase activity by the antiestrogen EM-800 in human endometrial adenocarcinoma Ishikawa cells. Cancer Res 57:3494–3497
53. Levenson AS, Jordan VC 1998 The key to the antiestrogenic mechanism of raloxifene is amino acid 351 (aspartate) in the estrogen receptor. Cancer Res 58:1872–1875
54. Barsalou A, Dayan G, Anghel SI, Alaoui-Jamali M, Van de Velde P, Mader S 2002 Growth-stimulatory and transcriptional activation properties of raloxifene in human endometrial Ishikawa cells. Mol Cell Endocrinol 190: 65–73
55. Wijayaratne AL, Nagel SC, Paige LA, Christensen DJ, Norris JD, Fowlkes DM, McDonnell DP 1999 Comparative analyses of mechanistic differences among antiestrogens. Endocrinology 140:5828–5840
56. Shang Y, Brown M 2002 Molecular determinants for the tissue specificity of SERMs. Science 295:2465–2468
57. Brzozowski AM, Pike AC, Dauter Z, Hubbard RE, Bonn T, Engstrom O, Ohman L, Greene GL, Gustafsson JA, Carlquist M 1997 Molecular basis of agonism and antagonism in the oestrogen receptor. Nature 389:753–758
58. Shiau AK, Barstad D, Loria PM, Cheng L, Kushner PJ, Agard DA, Greene GL 1998 The structural basis of estrogen receptor/coactivator recognition and the antagonism of this interaction by tamoxifen. Cell 95:927–937
59. Pike AC, Brzozowski AM, Walton J, Hubbard RE, Thorsell AG, Li YL, Gustafsson JA, Carlquist M 2001 Structural insights into the mode of action of a pure antiestrogen. Structure (Camb) 9:145–153
60. Mahfoudi A, Roulet E, Dauvois S, Parker MG, Wahli W 1995 Specific mutations in the estrogen receptor change the properties of antiestrogens to full agonists. Proc Natl Acad Sci USA 92:4206–4210
61. Montano MM, Ekena K, Krueger KD, Keller AL, Katzenellenbogen BS 1996 Human estrogen receptor ligand activity inversion mutants: receptors that interpret antiestrogens as estrogens and estrogens as antiestrogens and discriminate among different antiestrogens. Mol Endocrinol 10:230–242
62. Norris JD, Fan D, Stallcup MR, McDonnell DP 1998 Enhancement of estrogen receptor transcriptional activity by the coactivator GRIP-1 highlights the role of activation function 2 in determining estrogen receptor pharmacology. J Biol Chem 273:6679–6688
63. Fan JD, Wagner BL, McDonnell DP 1996 Identification of the sequences within the human complement 3 promoter required for estrogen responsiveness provides insight into the mechanism of tamoxifen mixed agonist activity. Mol Endocrinol 10:1605–1616
64. Metivier R, Penot G, Flouriot G, Pakdel F 2001 Synergism between ERα transactivation function 1 (AF-1) and AF-2 mediated by steroid receptor coactivator protein-1: requirement for the AF-1 α-helical core and for a direct interaction between the N- and C-terminal domains. Mol Endocrinol 15:1953–1970
65. Castro-Rivera E, Safe S 2003 17β-Estradiol- and 4-hydroxytamoxifen-induced transactivation in breast, endometrial and liver cancer cells is dependent on ER-subtype, cell and promoter context. J Steroid Biochem Mol Biol 84:23–31

66. Gibson MK, Nemmers LA, Beckman Jr WC, Davis VL, Curtis SW, Korach KS 1991 The mechanism of ICI 164,384 antiestrogenicity involves rapid loss of estrogen receptor in uterine tissue. Endocrinology 129:2000–2010
67. Seo HS, Larsimont D, Querton G, El Khissiin A, Laios I, Legros N, Leclercq G 1998 Estrogenic and anti-estrogenic regulation of estrogen receptor in MCF-7 breast-cancer cells: comparison of immunocytochemical data with biochemical measurements. Int J Cancer 78: 760–765
68. Alarid ET, Bakopoulos N, Solodin N 1999 Proteasome-mediated proteolysis of estrogen receptor: a novel component in autologous down-regulation. Mol Endocrinol 13:1522–1534
69. El Khissiin A, Leclercq G 1999 Implication of proteasome in estrogen receptor degradation. FEBS Lett 448: 160–166
70. Berry M, Nunez A-M, Chambon P 1989 Estrogen-responsive element of the human pS2 gene is an imperfectly palindromic sequence. Proc Natl Acad Sci USA 86:1218–1222
71. Wanmark A, Treuter E, Gustafsson JA, Hubbard RE, Brzozowski AM, Pike AC 2002 Interaction of transcriptional intermediary factor 2 nuclear receptor box peptides with the coactivator binding site of estrogen receptor α. J Biol Chem 277:21862–21868
72. Norris JD, Paige LA, Christensen DJ, Chang CY, Huacani MR, Fan D, Hamilton PT, Fowlkes DM, McDonnell DP 1999 Peptide antagonists of the human estrogen receptor. Science 285:744–746
73. Benecke A, Chambon P, Gronemeyer H 2000 Synergy between estrogen receptor α activation functions AF-1 and AF2 mediated by transcription intermediary factor TIF2. EMBO Rep 1:151–157
74. Voegel JJ, Heine M, Zechel C, Chambon P, Gronemeyer H 1996 Tif2, a 160 kda transcriptional mediator for the ligand-dependent activation function AF-2 of nuclear receptors. EMBO J 15:3667–3675
75. Voegel JJ, Heine MJ, Tini M, Vivat V, Chambon P, Gronemeyer H 1998 The coactivator TIF2 contains three nuclear receptor-binding motifs and mediates transactivation through CBP binding-dependent and -independent pathways. EMBO J 17:507–519
76. Tamrazi A, Carlson KE, Katzenellenbogen JA 2003 Molecular sensors of estrogen receptor conformations and dynamics. Mol Endocrinol 17:2593–2602
77. Pike AC, Brzozowski AM, Hubbard RE, Bonn T, Thorsell AG, Engstrom O, Ljunggren J, Gustafsson JA, Carlquist M 1999 Structure of the ligand-binding domain of oestrogen receptor β in the presence of a partial agonist and a full antagonist. EMBO J 18:4608–4618
78. Gangloff M, Ruff M, Eiler S, Duclaud S, Wurtz JM, Moras D 2001 Crystal structure of a mutant hERα ligand-binding domain reveals key structural features for the mechanism of partial agonism. J Biol Chem 276:15059–15065
79. Johnson BA, Wilson EM, Li Y, Moller DE, Smith RG, Zhou G 2000 Ligand-induced stabilization of PPARγ monitored by NMR spectroscopy: implications for nuclear receptor activation. J Mol Biol 298:187–194
80. Wu YL, Yang X, Ren Z, McDonnell DP, Norris JD, Willson TM, Greene GL 2005 Structural basis for an unexpected mode of SERM-mediated ER antagonism. Mol Cell 18: 413–424
81. Marimuthu A, Feng W, Tagami T, Nguyen H, Jameson JL, Fletterick RJ, Baxter JD, West BL 2002 TR surfaces and conformations required to bind nuclear receptor corepressor. Mol Endocrinol 16:271–286
82. Long X, Nephew KP 2006 Fulvestrant (ICI 182,780)-dependent interacting proteins mediate immobilization and degradation of estrogen receptor-α. J Biol Chem 281: 9607–9615
83. Green S, Issemann I, Sheer E 1988 A versatile in vivo and in vitro eukaryotic expression vector for protein engineering. Nucleic Acids Res 16:369
84. Nguyen D, Steinberg SV, Rouault E, Chagnon S, Gottlieb B, Pinsky L, Trifiro M, Mader S 2001 A G577R mutation in the human AR P box results in selective decreases in DNA binding and in partial androgen insensitivity syndrome. Mol Endocrinol 15:1790–1802
85. Laemmli UK 1970 Cleavage of structural proteins during the assembly of the head of bacteriophage T4. Nature 227:680–685
86. Jones TA, Zou JY, Cowan SW, Kjeldgaard 1991 Improved methods for building protein models in electron density maps and the location of errors in these models. Acta Crystallogr A 47:110–119
87. Angers S, Salahpour A, Joly E, Hilairet S, Chelsky D, Dennis M, Bouvier M 2000 Detection of β 2-adrenergic receptor dimerization in living cells using bioluminescence resonance energy transfer (BRET). Proc Natl Acad Sci USA 97:3684–3689

Molecular Endocrinology **is published monthly by The Endocrine Society (http://www.endo-society.org), the foremost professional society serving the endocrine community.**

Annexe 2 :Relation entre l'ubiquitination et la SUMOylation

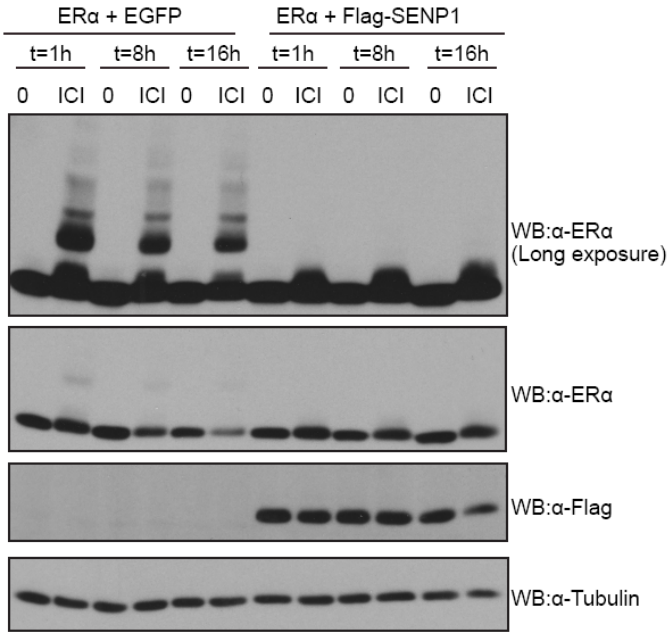

Fig. 1. Rôle de la SUMOylation dans la stabilité de ERα en présence de ICI 182, 780

Les cellules HEK 293 ont été transfectées transitoirement par les vecteurs d'expression de ERα en combinaison avec le vecteur d'expression de EGFP ou de SENP1. Les cellules ont été traitées par le véhicule ou ICI 182, 780 pendant 1h, 8h ou 16h. Les niveaux de ERα, de SENP1et de la tubuline ont été analysés par western blot.

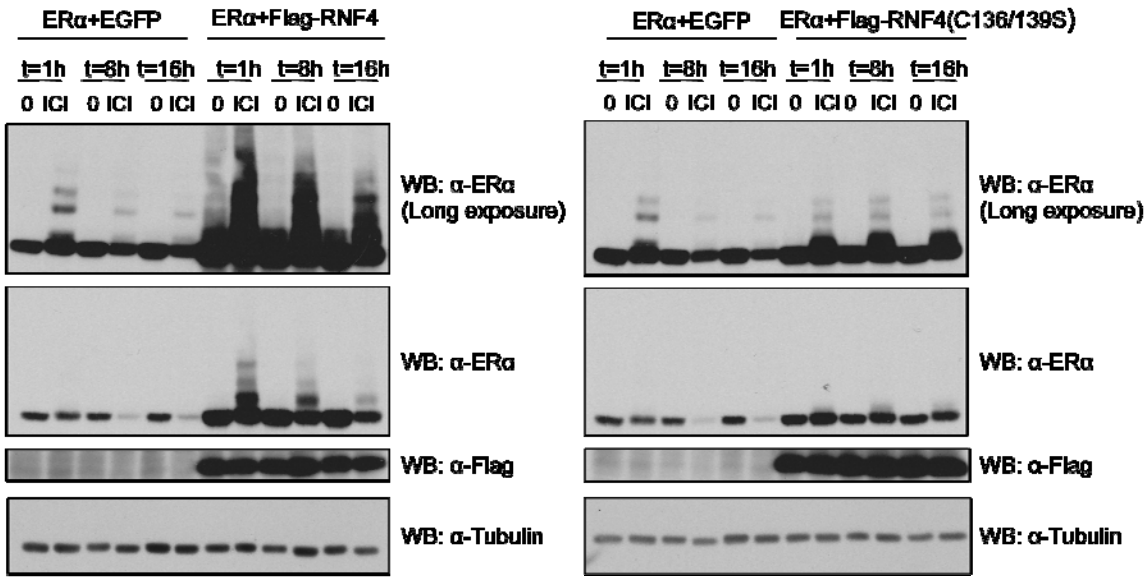

Fig. 2. Rôle de RNF4 dans la stabilité de ERα en présence de ICI 182, 780

Les cellules HEK 293 ont été transfectées transitoirement par les vecteurs d'expression de ERα en combinaison avec le vecteur d'expression de EGFP, de RNF4 ou de sans dominant négatif (RNF4 136/139S). Les cellules ont été traitées par le véhicule ou ICI 182, 780 pendant 1h, 8h ou 16h. Les niveaux de ERα, de RNF4 et de la tubuline ont été analysés par western blot.